Chronology, Paleoecology and Stratigraphy of Late Pleistocene Sediments from the Hudson Bay Lowlands, Canada

by

April Sue Rogers Dalton

A thesis submitted in conformity with the requirements
for the degree of Doctor of Philosophy in Earth Sciences

Department of Earth Sciences
University of Toronto

Chronology, Paleoecology and Stratigraphy of Late Pleistocene Sediments from the Hudson Bay Lowlands, Canada

April Sue Rogers Dalton

Doctor of Philosophy in Earth Sciences

Department of Earth Sciences
University of Toronto

2017

Abstract

Stratigraphic records in the Hudson Bay Lowlands (HBL), Canada, offer rare insight into local paleoenvironments and the Late Pleistocene climate system over North America. Age determinations on sub-till non-glacial materials suggest that the HBL, lying near the centre of the Last Glacial Maximum (LGM) extent of the Laurentide Ice Sheet (LIS), was ice-free for parts of Marine Isotope Stage 3 (MIS 3; 57,000 to 29,000 yr BP), MIS 5 (130,000 to 71,000 yr BP) and MIS 7 (243,000 to 190,000 yr BP). The MIS 3 age assignment is notable since it suggests the possibility of significant retreat of the LIS and a relatively high global sea level, both of which are a contrast to assumptions that North America was moderately glaciated, and that global sea level was relatively low during that time interval. Paleoecological proxies, including pollen and plant macrofossils, suggest that the HBL contained peatland and boreal vegetation during all previous non-glacial intervals, and pollen-based quantitative reconstructions of sites which are hypothesized to be MIS 3 and MIS 5a (~80,000 yr BP) in age suggest that climate during MIS 3 may have had less annual precipitation than during MIS 5a and present day. Stratigraphic analyses of these glacial and non-glacial sediments provide insight into the dynamicity of Late Pleistocene ice sheets; multiproxy analyses of three stratigraphic successions along the Albany River resulted in the recognition of at least three glacial advances from shifting ice centers within

the Québec sector of the Laurentide Ice Sheet during the Late Pleistocene. This dissertation contributes a chronological dataset for reconstructing the movement, timing and dynamics of Late Pleistocene ice sheets over North America, as well as paleoecological data for understanding the character and distribution of boreal peatlands during previous interstadial and interglacial periods.

Acknowledgments

First and foremost, I would like to sincerely thank my supervisor Sarah Finkelstein for providing me with this research opportunity, offering constant guidance and support, and for being an outstanding mentor. Thank you for setting deadlines and making me stick to them!

I would also like to thank the members of my advisory committee, Martin Head, Joe Desloges and Peter Barnett, who provided invaluable guidance and insight for this project. In particular, this project would not have been possible without the enthusiasm and expertise of Peter Barnett, who provided limitless mentorship and guidance from his work in the Hudson Bay Lowlands.

Countless other people have helped me along the way. In particular, thank you to Steve Forman for hosting me in his optically stimulated luminescence lab, his keen interest in HBL research and providing invaluable insights and guidance on Quaternary dating and stratigraphy. Thank you also to Minna Väliranta for macrofossil expertise and guidance. Additional thanks to Karin Helmens for mentorship and helpful conversations about interstadial deposits; Tamara Pico and Jerry Mitrovica for helpful sea level discussions; Art Dyke for sharing radiocarbon datasets; Martin Roy for attempting U-Th dates on wood samples; Anna Soleski, Tina Hui and Jason Davison for lab assistance; Siobhan Williams and Maurice Nguyen for fieldwork assistance, and; Carley Crann and the A.E. Lalonde AMS Laboratory for hosting my visit in 2015.

Funding for this research was provided by the Ontario Geological Survey, the Natural Sciences and Engineering Research Council (Canada) and the Northern Scientific Training Program (NSTP). My experience as a graduate student was enriched by additional funding from the University of Toronto Centre for Global Change Science; scholarship funding provided by the Ontario Graduate Scholarship; the University of Toronto School of Graduate Studies (SGS) Conference Grant; the 2016 Connaught Summer Institute in Arctic Science, and conference funding from Past Global Changes (PAGES).

Finally, this journey would not have been possible without the love and support of my family and friends. In particular to Daniel– thank you for your patience and understanding!

Table of Contents

List of Tables

List of Figures

List of Appendices

Chapter 1
Introduction

The temporal focus of this dissertation is the Late Pleistocene, beginning at the penultimate interglaciation and ending with the onset of the Holocene (130,000 years before present (yr BP) to 11,700 yr BP; Head and Gibbard, 2015). Although there is some variation in estimates, most global proxies suggest that this interval spans a time period of implied interglaciation (Marine Isotope Stage 5; MIS 5; 130,000 to 71,000 yr BP), glacial growth (MIS 4; 71,000 to 57,000 yr BP), glacial recession (MIS 3; 57,000 to 29,000 yr BP) and subsequent ice build-up and retreat (MIS 2; 29,000 to 11,700 yr BP). These global proxy records include the benthic foraminifera $\delta^{18}O$ record, which is a proxy for the volume of ice stored on continents (Lisiecki and Raymo, 2005); CH_4 and CO_2 concentrations preserved in ice cores that reflect the relative expansion and contraction of the biosphere (Loulergue et al., 2008; Lüthi et al., 2008); oxygen isotopes from gases trapped in ice cores that can be used to infer past temperatures, and; estimates of past global mean sea level (GMSL) that relate to estimates of continental ice storage (Grant et al., 2014). Glaciations had significant impacts on processes in the atmosphere (Ullman et al., 2014), the biosphere (Brovkin et al., 2016), sea level (Grant et al., 2014) and lithosphere (Peltier et al., 2015). However, few stratigraphic records survive glacial erosion. Thus, most research from previously glaciated regions is limited to the Holocene (11,700 yr BP to present-day) and the last glacial (MIS 2; 29,000 to 11,700 yr BP) and comparatively little is known about the remainder of the Late Pleistocene from land-based records.

1.1 Late Pleistocene terminology and the use of climatostratigraphic records

There are inconsistencies with the terminology for the Late Pleistocene in the literature which require clarification. Notably, the term “Late Pleistocene”, a subseries widely recognized in the literature, has not yet been officially recognized by the International Commission on Stratigraphy (ICS), thus it often appears in the literature as “late Pleistocene” with inconsistent capitalization. Following a recent proposition to formally recognize the Late Pleistocene as a subepoch (Head et al., 2017), and in recognition of its inherent chronostratigraphic properties, the upper-case is used in this dissertation. Further, this dissertation does not distinguish between the chronostratigraphic

"Upper" and geochronologic "Late" modifiers for the Pleistocene Series/Epoch; the latter is chosen owing to its common use in Quaternary literature.

There are also inconsistencies related to the terminology of Late Pleistocene glacial stages over North America, in particular the time interval comprising ~71,000 to ~24,000 yr BP. This interval of glacial build-up prior to the Last Glacial Maximum (LGM) is referred to in various publications as *Wisconsin glaciation, Wisconsinan glaciation, Wisconsinian glaciation* or *Wisconsin episode* (Lamoureux and England, 2000; Ó'Cofaigh et al., 2000; Young and Burr, 2006; Colgan et al., 2015). Since no formal definition exists, the term Wisconsinan Stage is used in this dissertation to describe this glacial episode. This convention follows the rules governing the naming of chronostratigraphic stages by using the "adjectival form of the geographic term" (Salvador, 1994). This is a regional stage, not to be confused with stages of the International Chronostratigraphic Chart. In addition, the naming of Late Pleistocene ice sheets is also inconsistent in the literature. The Laurentide Ice Sheet was originally defined as the ice sheet that comprised the entire Wisconsinan Stage, culminating at the LGM (Flint, 1943). This is the definition that is used in this dissertation. However, the Laurentide Ice Sheet has also been taken to represent any Pleistocene-aged ice mass housed over central Canada, sometimes extending back to Early Pleistocene glaciations (Balco and Rovey, 2010). The term "*geographic* center" of the Laurentide Ice Sheet is used in this dissertation to reflect field-based evidence for multiple ice spreading centers (domes) in the region (Shilts, 1980; Parent et al., 1995), as opposed to the "single ice dome" hypothesis put forward by Flint (1943). Finally, in this dissertation, the term "previously glaciated region" refers to the area contained within the envelope of the Laurentide Ice Sheet at the LGM.

Climatostratigraphic records - climatic changes that are detected in proxy records - are often used as a stratigraphic tool to facilitate discussion and correlation of Quaternary-aged deposits. The most widely cited climatostratigraphic record is the marine isotope record, where relative glacial and interglacial intervals are inferred from changes to the $\delta^{18}O$ values of benthic foraminifera in marine sediment records (Lisiecki and Raymo, 2005). The resultant MIS stages and substages (Railsback et al., 2015) are commonly used to correlate Pleistocene records on a global scale owing to the lack of geochronological method that spans the entire Quaternary Period. However, using climatostratigraphy to link records is sometimes problematic because climate events are not always recognized, nor synchronous on the global scale. For example, the onset of fully

interglacial conditions for the most recent interglacial varies by several thousand years depending on which terrestrial and marine records are compared (Head and Gibbard, 2015). The use of climatostratigraphic records (especially MIS stages) is adopted in this dissertation, although effort has been made to use chronological data whenever possible. The use of MIS stages is appropriate here since the focus of this dissertation is a coastal plain that is highly influenced by changes in global mean sea level and ice volume.

1.2 Summary of Late Pleistocene paleoclimate in North America

1.2.1 Penultimate interglaciation (MIS 5; 130,000 to 71,000 yr BP)

The beginning of MIS 5, MIS 5e (ca. 123,000 yr BP) was the warmest part of the penultimate interglacial period, when oxygen isotope derived temperature values from ice cores suggest that temperature may have been 5 to 8 °C warmer than today (North Greenland Ice Core Project members, 2004; NEEM community members, 2013); inferred GMSL was higher than present-day (Grant et al., 2014), and there was a strong reduction in continental ice (Lisiecki and Raymo, 2005). Owing to difficulties in dating, few continental records have been constrained to this time interval, although some deposits from Eastern Canada (Fig. 1-1) have been assigned to MIS 5e on the basis of stratigraphic analyses and the recognition of a warm temperature signal in the biostratigraphic record (de Vernal et al., 1986; Fréchette and de Vernal, 2013). Similarly, warmer-than-present-day conditions were inferred from a pollen record contained in a paleo-wetland deposit in Idaho (Herring and Gavin, 2015). In that case, the MIS 5 age assignment was made by correlating the organic content of the paleo-record to fluctuations in the $\delta^{18}O$ record as well as alignment of pollen-based climate interpretations and sedimentological data (Herring and Gavin, 2015).

Following the temperature peak at ca. 123,000 yr BP (MIS 5e), the MIS 5 climate alternated between relative stadial (MIS 5d, c; 109,000 yr BP, 87,000 yr BP) and interstadial (MIS 5a, c; 96,000, 82,000 yr BP) intervals (Lisiecki and Raymo, 2005). The growth and recession of ice sheets corresponding to these late MIS 5 climatic fluctuations are documented in glacial landforms (striations, regional flow, lineations) in the glaciated region (Kleman et al., 2010), and the MIS 5a glacial recession is documented as a sea level high stand at ~81,000 yr BP, which suggests that continental ice was largely absent at that time (Dorale et al., 2010).

1.2.2 Stadial event (MIS 4; 71,000 to 57,000 yr BP)

Global proxy records for ice volume and sea level suggest the growth of continental ice during MIS 4 (Lisiecki and Raymo, 2005; Grant et al., 2014). However, very little land-based evidence has been chronologically constrained to this interval owing to difficulties in dating. Evidence from the previously glaciated region is from glacial landform analyses, which suggest that the ice sheet may have grown to almost LGM extent over Eastern Canada (Fig. 1-1) during that time (Kleman et al., 2010). Outside the glaciated region, pedothems, which are calcite deposits dated via U/Th dating, from the mid-western United States also show an anomaly in the $\delta^{18}O$ record for that time (Oerter et al., 2016). A comparison to the modern-day climate system suggests that isotope values in this region are controlled in part by shifts in moisture transport between Pacific and Gulf of Mexico sources, therefore the anomaly during MIS 4 was interpreted as a shift in atmospheric circulation caused by glacial growth in northeastern North America (Oerter et al., 2016). Paleoecological data from MIS 4 are scarce, but a speleothem record from the mid-continental United States (Fig. 1-1) suggests that grassland conditions existed just beyond the inferred ice margin at that time (Dorale et al., 1998). This MIS 4 shift towards cooler conditions is noted in several pollen records preserved beyond the boundary of the ice sheet, but the dating on these records is sometimes inferential or based on comparison to other records (Jiménez-Moreno et al., 2010; Herring and Gavin, 2015).

1.2.3 Interstadial event (MIS 3; 57,000 to 29,000 yr BP)

Most global proxy records suggest a relative interstadial during MIS 3, notably an increase in global sea level as well as decreased continental ice volume relative to MIS 4 (Lisiecki and Raymo, 2005; Grant et al., 2014). Perhaps the most well-dated land-based sites within the LGM margin dating to this time period are the Zorra Quarry, southern Ontario (Fig. 1-1), constrained to ca. 40,000 to 50,000 yr BP by means of multiple radiocarbon dates on wood, where pollen data were used to infer a boreal forest in this region (Bajc et al., 2015). A boreal and/or tundra environment is recognized at several other sites in this peripheral region during MIS 3 (Cong et al., 1996; Karig and Miller, 2013). Boreal conditions in the Prairies and Eastern Canada have also been noted during MIS 3, although chronology for the latter records is reliant on inferential and stratigraphic correlation (de Vernal et al., 1986; Fréchette and de Vernal, 2013; Bélanger et al., 2014). Outside of the previously glaciated region, pollen records from the northwestern and

continental United States document a shift towards boreal-type conditions (Herring and Gavin, 2015) and a prolonged period of temperature rise and a shift towards warmer-temperature biomes during MIS 3 relative to MIS 4 and MIS 2 (Jiménez-Moreno et al., 2010). Further, a speleothem record from the mid-continental United States suggests forested conditions during that time (Dorale et al., 1998).

Heinrich and Dansgaard-Oeschger events occurred during MIS 3, suggesting that this interstadial was a time of at least partial continental glaciation and of abrupt climatic change (Dansgaard et al., 1993; Hemming, 2004). While some models assume a relatively static ice sheet of moderate size during MIS 3, land-based evidence has long been used to support the hypothesis of a more dynamic glaciation at that time. Loess records from the upper continental United States, which document advance of the ice margin into the Mississippi River watershed, suggest that the ice sheet advanced into this region several times between 55,000 and 45,000 yr BP (Forman, 1992). These glacial advances may be the cause for land-based shifts between *Pinus* and grassland-dominated regimes noted in the pollen record from Lake Tulane, Florida during this time period (Grimm et al., 2006; Jiménez-Moreno et al., 2010). Near the end of MIS 3, there is evidence for ice sheet growth at ~40,000 yr BP owing to the presence of proglacial lake sediments and other ice-marginal evidence in the peripheral regions of the ice sheet (Berger and Eyles, 1994; Wood et al., 2010; Karig and Miller, 2013).

1.2.4 Widespread glaciation (MIS 2; 29,000 to 14,000 yr BP)

The final event in the Late Pleistocene was glacial growth, which began at ~29,000 yr BP and is recognized in most global proxy records. Flint (1943) hypothesized that a single large ice dome formed over the Hudson Bay region (Fig. 1-1) and expanded radially, however field-based evidence has suggested that multiple ice growth centers (domes) contributed towards ice growth at this time (Shilts, 1980; Parent et al., 1995). Pollen data from outside the glaciated region suggest that glacial growth promoted a shift towards cooler-temperature biomes during MIS 2 compared to any other point during the Late Pleistocene (Jiménez-Moreno et al., 2010). The ice sheet reached its peak extent at ~24,000 yr BP (LGM), followed by gradual recession beginning at ~21,000 yr BP. Some areas in the peripheral region of the ice sheet were ice-free by 14,000 yr BP (Dyke, 2004).

1.3 Late Pleistocene records in the Hudson Bay Lowlands, Canada

The focus of this dissertation is extensive Pleistocene-aged sediments preserved in the Hudson Bay Lowlands (HBL), Canada (Fig. 1-1). Stratigraphic records in this region have escaped glacial erosion, and therefore provide rare insight into Late Pleistocene paleo-history in the glaciated region of North America. The HBL is largely accepted to have been the geographic center for many Pleistocene ice sheets, consequently the glacial sediments in this region document the interlobate dynamics of former ice sheets, whereas non-glacial intervals record the paleoecological setting of periglacial environments. The non-glacial units typically consist of fluvial, organic-bearing and/or lacustrine sediments and have been termed the "Missinaibi Formation" (Skinner, 1973).

Stratigraphic records in the HBL were the focus of government and academic study in the 1970s and 1980s, but little work has been published since that time (McNeely, 2002; Allard et al., 2012; Dubé-Loubert et al., 2013). Thus the overarching objective of this dissertation is to use a suite of geochronological techniques, quantitative analyses of biostratigraphic data and multivariate statistics to resolve the age of these deposits and the paleoenvironments in which they developed. Much of the previous work from the region is also summarized, critically evaluated and placed in context of new results. These stratigraphic records may be among the most extensive occurrences of Pleistocene-aged deposits within the bounds of the ice sheet in eastern North America. These deposits are therefore important for reconstructing the movement, timing and dynamics of Late Pleistocene ice sheets as well as understanding the character and distribution of vegetation biomes during previous interglacial periods.

1.4 Regional setting

The HBL is a coastal plain covering an area of >325 000 km^2 lying adjacent to James and Hudson bays (Riley, 2011). Bedrock in this area is composed of Palaeozoic and Mesozoic carbonate and clastic rocks, which is overlain by a cover (10–50 m in thickness) of Pleistocene-aged glacial and non-glacial sediments. At the LGM, this region was covered by glacial ice of ~3–4 km in thickness (Andrews and Dyke, 2007; Peltier et al., 2015), thus present-day isostatic rebound rates are among the highest in the world (~10 mm per year; Sella et al., 2007). This isostatic rebound played an important role in shaping the Holocene landscape in this region:

upon deglaciation was the development of a proglacial lake (Lake Agassiz/Ojibway; Roy et al., 2011), marine incursion at ~8000 yr BP (Tyrell Sea; Lee, 1960), landscape drainage, and the development of peatlands beginning at ~8000 yr BP and continuing to present-day (Packalen et al., 2014). Holocene peat accumulation is up to 4 m in thickness, and is promoted by a low regional gradient (generally less than 1 m per km) and poor drainage ability of underlying strata. The HBL is presently one of North America's largest wetlands, comprised of a combination of ombrotrophic bogs (36%), minerotrophic fens (24%), permafrost wetlands (22%), swamps (13%) and marshland (5%) (Riley, 2003).

The HBL is largely located in the boreal biome, with a transition to tundra occurring in northern coastal areas where permafrost is present (MacDonald and Gajewski, 1992). In the southeastern HBL, mean annual temperatures average 0°C and annual precipitation is 850 mm, which transitions to -7°C and 400 mm at the northwestern region of the HBL (Natural Resources Canada, 2014). Hudson and James bays freeze each winter owing to significant freshwater input from rivers, as well as their relatively shallow depth. Thus, these water bodies do not effectively moderate climate in the region, resulting in strong continentality. Modern-day vegetation in the HBL has a relatively low diversity, consisting largely of boreal-peatland taxa, including *Picea*, *Betula*, *Larix*, Poaceae, Cyperaceae, and *Sphagnum*. Modern pollen records from this region reflect in part long-distance transport and differential representation based on variability in pollen production. For example, *Pinus* pollen is often a significant component of the modern assemblage (e.g. Lichti-Federovich and Ritchie, 1968; Farley-Wilson, 1975; Farley-Gill, 1980), despite the fact that *Pinus* is rarely found in the region (Riley, 2003). Contrastingly, *Abies* and *Larix*, are significantly under-represented in modern pollen assemblages (Farley-Gill, 1980).

Eight main rivers dissect the low-gradient wetlands in the HBL, including the Nottaway, Harricana, Moose, Albany, Attawapiskat, Winisk, Severn and Nelson. Main river channels can be upwards of 1 km in width and incise 30–50 m into the Holocene and Pleistocene deposits, sometimes eroding to bedrock. These rivers form the terminus of the Hudson Bay watershed, which covers ~4,000,000 km^2 of Canada. Tributaries of these rivers are heavily meandering and form a dendritic drainage network. River regimes in this region are largely nival with peak discharge observed in May (King and Martini, 1983), and can range from < 500 m^3/s in the winter months to peaks of 2000–10,000 m^3/s during spring discharge (Government of Canada, 2017). The widespread peatlands have an important influence on the river networks; runoff from

peatlands contributes 50–60% of the stream flow in the region (Orlova and Branfireun, 2014) and tannins from adjacent peatlands commonly cause the river water to be brown during summer months. These rivers are of importance for this dissertation because they expose Pleistocene-aged sediments for study, and fluvial deposits comprise many of the paleoenvironmental contexts analyzed in this dissertation. It has been hypothesized that shelter from paleo-riverbanks may have contributed toward the preservation of many of these Pleistocene-aged deposits from subsequent glacial erosion (Barnett and Finkelstein, 2013).

1.5 Research objectives

1.5.1 Chronology

The age of the Missinaibi Formation has been debated since its discovery in the late 1800s (Bell, 1879, 1886). At first, it was believed that the organic-bearing units were compressed lignite of pre-Quaternary age, until McLearn (1927) made the distinction between Mesozoic lignite and what were hypothesized to be Pleistocene-aged organics. The advent of radiocarbon dating in the 1950s provided a promising opportunity to resolve the age of these deposits. However, many attempts yielded infinite age determinations, leading to the hypothesis that these deposits dated to the last interglacial (ca. 130,000 to ca. 71,000 yr BP) or perhaps older. Further work using amino acid, radiocarbon and thermoluminescence (TL) techniques suggested that this region may have been ice-free several times during the Wisconsinan Stage (e.g. ~70,000 to ~11,700 yr BP; Andrews et al., 1983; Forman et al., 1987; Berger and Nielsen, 1990; McNeely, 2002). However, these ages were largely dismissed on the basis of errors and uncertainties inherent to the dating methods, and also because long-standing estimates of ice volume show a fully glaciated HBL region during the entire Wisconsinan Stage (Andrews and Dyke, 2007; Peltier et al., 2015). Thus, there is no consensus on the age(s) of the Missinaibi Formation, nor on whether strata correlative to the Missinaibi Formation are contemporaneous.

The first objective of this dissertation is to refine age estimates for the Missinaibi Formation. This is accomplished by attempting radiocarbon and optically stimulated luminescence (OSL) techniques on several new sites, along with synthesizing previously published chronology data into a regional dataset, and applying a critical evaluation of all age determinations based on new analytical considerations. Understanding the age of these deposits provides important land-based evidence for validating models of ice sheet extent and paleo-geography, and permits comparison

to contemporaneous records from more peripheral regions of the glaciated region, thus providing insight into the complex record of Late Pleistocene paleoenvironments in North America.

Main research questions: What are the age(s) of the Missinaibi Formation? Can OSL and radiocarbon methods be used to refine previous estimates based mainly on bulk radiocarbon, amino acid and thermoluminescence dates? Are numerous non-glacial Late Pleistocene events preserved in the HBL?

1.5.2 Paleoecology

Pollen is well-preserved at many of the Pleistocene-aged sites in the HBL. While pollen has long been recognized as a key proxy with potential to help corroborate age determinations, its potential as an inferential dating tool and paleoclimate proxy has yet to be fully maximized. It has been argued for some time that fossil pollen assemblages may be able to differentiate between interglacial and interstadial deposits in the HBL; Terasmae and Hughes (1960) hypothesized that some deposits in the HBL were interstadial on the basis of sub-arctic pollen taxa, while Skinner (1973) and Mott and DiLabio (1990) suggested that others may be interglacial on the basis of pollen assemblages similar to present-day. However, the vegetation-climate relationship in northern peatlands is complex owing to large climate gradients, low species diversity and extensive geographic ranges of many taxa (Riley, 2003). Thus, it is not known whether vegetation in this region is sufficiently sensitive to respond to climate differences between interstadial and interglacial conditions, which may be subtle.

In addition to its potential as an inferential dating technique, pollen is helpful for characterizing the paleoenvironments of non-glacial intervals. Previous pollen-based work in the HBL has shown that this region was a wetland environment during all non-glaciated times during the Quaternary (Nielsen et al., 1986; Gao et al., 2012). However, thus far, pollen has largely been used as a qualitative tool on these deposits, with papers describing only general shifts in vegetation and comparisons to present-day conditions (Terasmae and Hughes, 1960; Nielsen et al., 1986; Dredge et al., 1990; Allard et al., 2012). Several methods exist whereby pollen data can be quantitatively used to reconstruct paleoclimate variables such as precipitation and temperature. However, no quantitative palynological work has been undertaken on these deposits.

The second objective of this dissertation is to use quantitative techniques on fossil pollen data to characterize the paleoenvironment of Pleistocene-aged ice-free intervals in the HBL. The method presented here is the modern analogue technique (Overpeck et al., 1985) to reconstruct paleo-temperature and paleo-precipitation. These quantitative reconstructions provide insight into Late Pleistocene climate variability from the glaciated region, provide important insight into vegetation adaptation under conditions of climate change, and facilitate comparison to other local, regional and global Pleistocene-aged records. Macrofossils are also examined at key sites to support the pollen-based paleoclimate inferences. The potential for pollen to be used as an inferential dating tool is tested via comparison of interstadial (MIS 3) and interglacial (MIS 5) pollen records; if strong climatic distinctions can be made between interglacial and interstadial sites, then this pollen-based inference technique may be extended to assign interstadial or interglacial ages to sites which are not well constrained chronologically.

Main research questions: What type(s) of vegetation assemblages were present in the HBL during previous ice-free periods? How do these assemblages compare to the Holocene and present day? Can pollen effectively be used as an inferential dating tool in the Hudson Bay Lowlands? How do the paleo-environments in the HBL relate to other records from more peripheral areas of the glaciated region?

1.5.3 Stratigraphy

The stratigraphic record in the HBL has been repeatedly identified as critical for understanding the pre-LGM ice configuration owing to its position at the geographic center of many Pleistocene ice sheets (Dredge and Thorleifson, 1987; Kleman et al., 2010). Because stratigraphic records in the HBL are highly fragmented and discontinuous, the first studies were limited to small geographic areas; Skinner (1973) mapped and correlated various units in the Moose River Basin and hypothesized that at least two pre-LGM ice-free intervals were preserved there, separated by glacial intervals. Similar efforts were made to correlate units along the Nelson River, at the western end of the HBL (Nielsen et al., 1986). In both cases, records were aligned using stratigraphic position, amino acid data, texture and lithology, while non-glacial intervals were correlated on the basis of inferred paleoenvironments, chronological data (where available) and position relative to till units. More recent efforts have focused on developing a stratigraphic framework for the entire HBL. Thorleifson et al. (1992) incorporated research from the Moose

River Basin, Nelson River and other locales to infer at least four glacial movements across the region separated by at least one non-glacial interval. Efforts have also been made to examine and interpret regional landform features (Boulton and Clark, 1990; Kleman et al., 2010) to reconstruct the movement and extent of past ice sheets. However, the fragmentary nature of records in this region, paired with the lack of chronological constraints on many of the non-glacial intervals, means that much of these stratigraphic frameworks are presented in the form of several hypotheses.

The third objective of this dissertation is to examine the stratigraphic record in two field areas, the Ridge River and Albany River. Previous stratigraphic work has been conducted in the Ridge River area (Nguyen et al., 2012; Nguyen, 2014), but little work has been conducted in the vicinity of the Albany River owing to its remote location. The stratigraphic record along the Albany River is fragmented owing to glacial erosion, but our use of elemental, sedimentological and geomorphological analyses of the till units, along with comparison of geochronological age attempts and paleoecological analyses of the non-glacial intervals, permits reconstruction of Late Pleistocene history at the centre of the previously glaciated region. Stratigraphic analyses of the non-glacial units will also take place via loss-on-ignition, particle size and carbon content analysis to characterize the paleo-environment and local setting. This research is complementary to other efforts to reconstruct the pre-LGM history of ice sheets using glacial and geomorphological records (Kleman et al., 2010).

Main research questions: How well can elemental, sedimentological, paleoecological and chronological data be used to amalgamate fragmented stratigraphic records along the Albany and Ridge rivers? How many glacial and non-glacial events are preserved in this region?

1.5.4 Use of land-based data to infer past ice extents

The most recent synthesis of records from the glaciated region was by Dyke et al. (2002), where ~200 radiocarbon dates from the peripheral regions of the glaciated area were used to delimit the ice sheet boundary between 30,000 and 27,000 yr BP. The moderate continental glaciation implied by this land-based evidence aligns well with generally-accepted models of ice volume (Peltier et al., 2015), records of sea level (Grant et al., 2014), and the oceanic $\delta^{18}O$ record (Lisiecki and Raymo, 2005). Although Dyke et al. (2002) clearly states that this hypothesized ice configuration is only for the 30-27 ka interval, it is often taken to represent the position of the

Laurentide Ice Sheet during the latter half of the Wisconsinan Stage. However, since 2002, additional chronology data have been published which extend the spatial and temporal extent of glacial recession for the pre-LGM ice sheet over what was proposed by Dyke et al. (2002). There is a need to examine terrestrial data from the previously glaciated region to resolve the position of the Laurentide Ice Sheet for this time period.

The fourth objective of this dissertation is to synthesize a dataset of MIS 3 sites in the previously glaciated region. The location and age of these sites can be used to develop hypotheses on the position of the MIS 3 ice sheet, which is then discussed in context of global proxy records including records of sea level. This synthesis provides important empirical data to test models of ice volume as well as refine emerging data on global mean sea level and ice sheet constraints during the Late Pleistocene.

Main research questions: Is evidence for glacial recession present in other areas in the previously glaciated region? Is it possible to use this evidence to delineate a revised hypothesis of ice sheet configuration through the Wisconsinan Stage? Does the proposed reduced ice extent fit with constraints imposed by proxy records of global mean sea level and constraints on glacial isostatic adjustment?

1.6 Publication status of thesis chapters

1.6.1 Chapter 2: Constraining the Late Pleistocene history of the Laurentide Ice Sheet by dating the Missinaibi Formation, Hudson Bay Lowlands, Canada

Chapter 2 summarizes and critically evaluates chronology data from the Missinaibi Formation. Previously published chronology data (n = 88) as well as newly contributed data (n = 39) are synthesized and interpreted. This Chapter was published in *Quaternary Science Reviews* (v. 146, p. 288–299, 2016), with an author list of April S Dalton, Sarah A Finkelstein, Peter J Barnett and Steven L Forman, and is reprinted here with permission from Elsevier (RightsLink® license no. 4118350201231). Chronological data were collected, synthesized and interpreted by ASD. The manuscript was written by ASD under the supervision of SAF with feedback from PJB and SLF. Further, OSL data were provided by SLF, and PJB identified field sites and interpreted glacial stratigraphy.

1.6.2 Chapter 3: Pollen and macrofossil-inferred palaeoclimate at the Ridge Site, Hudson Bay Lowlands, Canada: evidence for a dry climate and significant recession of the Laurentide Ice Sheet during Marine Isotope Stage 3

Chapter 3 is an investigation of the paleoenvironments at a purported MIS 3 site in the HBL. Pollen and macrofossil assemblages are used to reconstruct vegetation assemblages. Quantitative pollen techniques were used to infer past temperature and precipitation regimes for this paleo-wetland, while macrofossils and sedimentological data were also used to strengthen this interpretation. This chapter was published in *Boreas* (v. 46 (3), p. 388–401, 2017) with an author list of April S Dalton, Minna Väliranta, Peter J Barnett and Sarah A Finkelstein, and is reprinted here with permission from John Wiley and Sons (RightsLink® license no. 4118350724833). ASD contributed modern pollen counts from the HBL, compiled the modern pollen dataset, performed all statistical analyses, interpreted the data and wrote the manuscript under the supervision of SAF with feedback from PJB and MV. All fossil pollen was counted by SAF; macrofossil data were contributed by MV; field site identification and glacial stratigraphic interpretations were contributed by PJB.

1.6.3 Chapter 4: Late Pleistocene chronology, paleoecology and stratigraphy at a suite of sites along the Albany River, Hudson Bay Lowlands, Canada

Chapter 4 is an investigation into the paleoclimate, age and sedimentology of three Pleistocene-aged sites along the Albany River, HBL. The organic-bearing units were dated by OSL and radiocarbon techniques, whereas the paleoecology was examined using biological proxies (pollen, macrofossils) along with sedimentological data. Stratigraphic records at the three sites were amalgamated using elemental, particle size and geomorphological analyses of the till units, along with comparison of geochronological age attempts and paleoecological analyses of the non-glacial intervals. This manuscript is in preparation for submission to a paleoenvironment-themed journal with an author list of April S Dalton, Sarah A Finkelstein, Peter J Barnett, Minna Väliranta, and Steven L Forman. Pollen identification, sedimentological data analyses, statistical analyses, interpretations and manuscript writing was performed by ASD under the supervision of SAF with feedback from PJB, SLF and MV. Macrofossil identification was performed by MV;

OSL dating and interpretation was contributed by SLF; identification of field areas and interpretation of glacial stratigraphy was contributed by PJB.

1.6.4 Chapter 5: Land-based evidence suggests a significantly reduced Laurentide Ice Sheet during Marine Isotope Stage 3

Chapter 5 is a synthesis of land-based evidence from the previously glaciated region that is used to infer the position of the ice sheet during the Wisconsinan Stage. Chronology data from 671 sites are synthesized and compared to hypothesized Wisconsinan ice extents and global sea level data from previously published sources. This manuscript is currently under development for submission to a geosciences journal of broad interest with an author list of April S Dalton, Sarah A Finkelstein, Steven L Forman and Peter J Barnett. Data synthesis, interpretation and manuscript writing was performed by ASD under the supervision of SAF with feedback from PJB and SLF. OSL ages were developed by SLF.

1.7 Figures

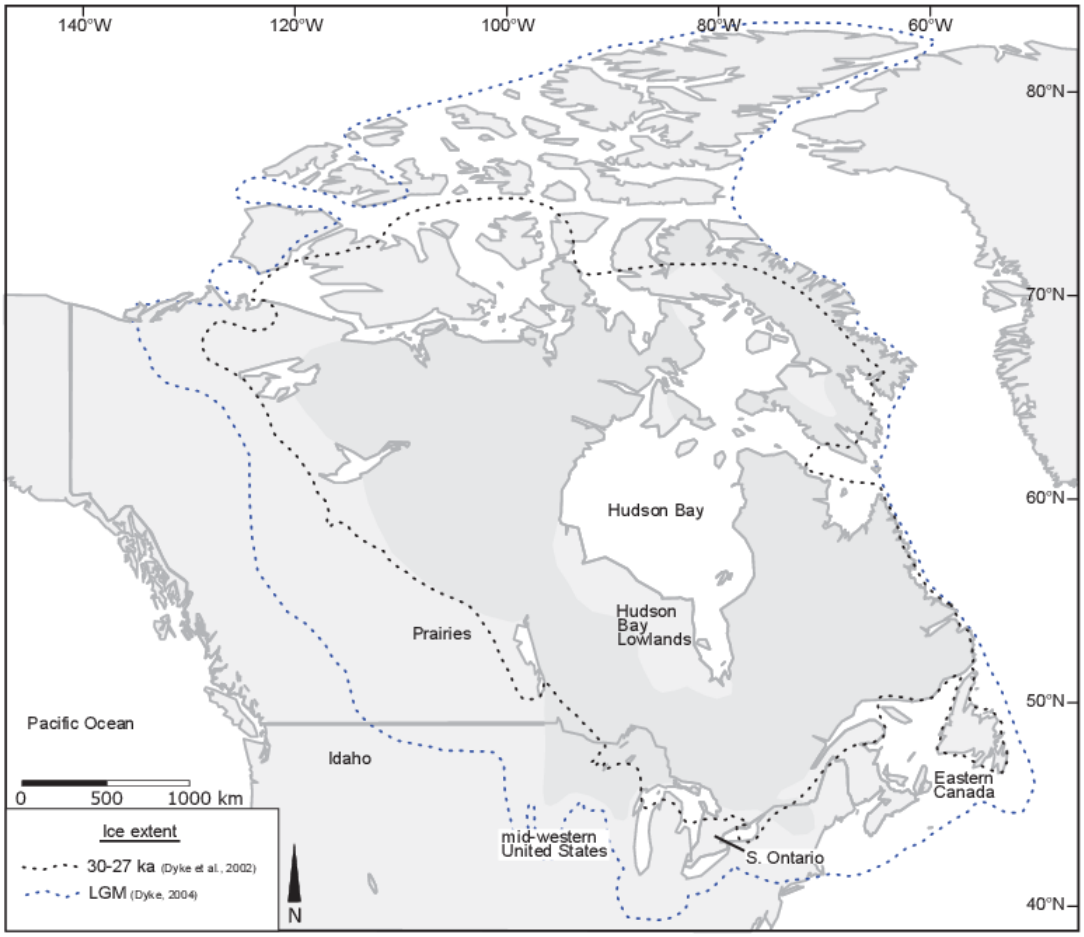

Fig. 1-1. Map of North America showing the location of sites mentioned in Chapter 1. Shaded region shows the extent of the Canadian Shield.

Chapter 2
Constraining the Late Pleistocene history of the Laurentide Ice Sheet by dating the Missinaibi Formation, Hudson Bay Lowlands, Canada

2.1 Abstract

Well-dated paleorecords from periods prior to the Last Glacial Maximum (LGM) are important for validating models of ice-sheet build-up and growth. However, owing to glacial erosion, most Late Pleistocene records lie outside of the previously glaciated region, which limits their ability to inform about the dynamics of paleo-ice sheets. Here, we evaluate new and previously published chronology data from the Missinaibi Formation, a Pleistocene-aged deposit in the Hudson Bay Lowlands (HBL), Canada, located near the geographic center of the Laurentide Ice Sheet (LIS). Available radiocarbon (accelerator mass spectrometry = 44, conventional = 36), amino acid (n = 13), uranium-thorium (U-Th, n = 14), thermoluminescence (TL, n = 15) and optically stimulated luminescence (OSL, n = 5) data suggest that an ice-free HBL may have been possible during parts of Marine Isotope Stage 7 (MIS 7; ca. 243,000 to ca. 190,000 yr BP), MIS 5 (ca. 130,000 to ca. 71,000 yr BP) and MIS 3 (ca. 29,000 to ca. 57,000). While MIS 7 and MIS 5 are well-documented interglacial periods, the development of peat, forest bed and fluvial deposits dating to MIS 3 (n = 20 radiocarbon dates; 4 TL dates, 3 OSL dates), suggests that the LIS retreated and remained beyond, or somewhere within, the boundaries of the HBL during this interstadial. Ice sheet models approximate the margin of the LIS to Southern Ontario during this time, which is 700 km south of the HBL. Therefore, if correct, our data help constrain a significantly different configuration and dynamicity for the LIS than previously modelled. We can find no chronological basis to discount the MIS 3 age assignments. However, since most data originate from radiocarbon dates lying close to the reliable limit of this geochronometer, future work on dating the Missinaibi Formation using other geochronological methods (e.g. U-Th, OSL) is necessary in order to confirm the age estimates and strengthen the boundaries of the LIS during this period.

2.2 Introduction

Understanding the quantitative relations amongst the biosphere, cryosphere and atmosphere is critically important towards formulating accurate predictions for future climates; and the growth and decay of ice sheets in the Late Pleistocene provides boundary conditions for testing Earth System Models (Loutre and Berger, 2003; Kleinen et al., 2015). To make such climate predictions, these models require empirically derived boundary conditions including the duration and dynamics of previous glaciations. To that end, the recent deglaciation sequence of the Laurentide Ice Sheet (LIS) from the Last Glacial Maximum (LGM) to the present-day is well understood owing to well constrained models of isostatic rebound (Peltier et al., 2015) and a plethora of radiocarbon ages (Dyke, 2004). However, because of glacial erosion, we have a highly incomplete understanding of the period prior to the LGM (Kleman et al., 2010).

Records of relative sea level (RSL) and the $\delta^{18}O$ from benthic foraminifera are important tools for approximating the volume of continental ice during the Pleistocene. For example, a decrease in RSL to -100 m (compared to present-day) (Grant et al., 2014), paired with an increase in the $\delta^{18}O$ from benthic foraminifera (Lisiecki and Raymo, 2005) from ca. 68,000 to 63,000 years before present (yr BP), implies moderate glaciation over North America at that time (Fig. 2-1). Immediately following this stadial was a partial deglaciation of the continent as shown by a rapid rise in RSL, maintaining a level between -70 m and -80 m until 40,000 yr BP (Grant et al., 2014), and a slight decrease in the $\delta^{18}O$ from benthic foraminifera (Lisiecki and Raymo, 2005). This period of implied partial continental glaciation corresponds broadly to the early part of Marine Isotope Stage 3 (MIS 3; ca. 57,000 to ca. 29,000 yr BP; Lisiecki and Raymo (2005)), where summer insolation was stable and higher than today at 60° N (Berger and Loutre, 1991). Understanding the configuration of North American ice sheets during MIS 3 is important because it will help validate models which approximate ice-sheet build-up and growth for that time (e.g. Ganopolski et al., 2010; Kleman et al., 2010; Ganopolski and Calov, 2011; Stokes et al., 2012).

Although rare and spatially discontinuous, available paleorecords from North America suggest a dynamic and lobed margin of the LIS during MIS 3. For example, the Roxana Silt, a loess deposit dating to ca. 60,000 to ca. 30,000 yr BP, suggests that glacial activity reached the Mississippi watershed during that time (Forman and Pierson, 2002). Furthermore, several

corroborative studies on sedimentological and biological records suggest that the LIS advanced into the continental United States at ca. 45,000 to ca. 42,000 yr BP, resulting in drainage southward toward the Gulf of Mexico (Hill et al., 2006; Tripsanas et al., 2007; Sionneau et al., 2013). Contrastingly, studies suggest an ice-free MIS 3 in Southern Ontario (Karrow and Warner, 1984; Warner et al., 1988; Karrow et al., 2001; Bajc et al., 2015), Atlantic Canada (Fréchette and de Vernal, 2013; Rémillard et al., 2013) and Repulse Bay (McMartin et al., 2015). These datasets indicate the possibility for a dynamic and regionally varied response of the ice sheet margin to MIS 3 paleoclimates. Additional terrestrial records, especially those from the previously glaciated region, are needed to further constrain the boundaries of the LIS during MIS 3.

2.2.1 Missinaibi Formation, Canada

The Late Pleistocene history of the Hudson Bay Lowlands (HBL), Canada (Fig. 2-2), has been identified as an important archive for constraining the history of glaciations over North America (Dredge and Thorleifson, 1987; Kleman et al., 2010). Importantly, the HBL contains the Missinaibi Formation, a non-glacial deposit underlying till. Since the HBL is located near the geographic center of many Pleistocene ice sheets, the age of this non-glacial deposit can be used to infer the absence of regional ice sheets (e.g. Helmens et al., 2007; Bos et al., 2009; Helmens and Engels, 2010), therefore improving our understanding of the timing and spatial extent of ice-free regions during Late Pleistocene glaciations over North America. Furthermore, since this region is likely to have been a peatland for other ice-free periods in the Pleistocene (Terasmae and Hughes, 1960; Allard et al., 2012), constraining the age of this deposit will permit empirical validation of models which simulate carbon storage and potential methane release during that time (Kleinen et al., 2015).

Despite the importance of the Missinaibi Formation as a Pleistocene archive, there is no consensus on its age or whether the deposits are penecontemporaneous or span much of the Late Pleistocene. The inability to constrain the age of these deposits reflects that radiocarbon dating has mostly yielded infinite results and there is a scarcity of suitable material for geochronological methods such as optically stimulated luminescence (OSL) and uranium-thorium (U-Th) dating. Despite these issues, previous attempts to constrain the age of the Missinaibi Formation have resulted in the recognition of at least one MIS 5 (ca. 130,000 to 71,000 yr BP) site via U-Th and OSL dating (Allard et al., 2012; Dubé-Loubert et al., 2013), which is correlative to the

penultimate interglacial period. Given the substantial glacial retreat during the MIS 5 period (Andrews and Dyke, 2007; NEEM community members, 2013), such deposits can be expected.

There are, however, several sites in the HBL which have yielded MIS 3 ages (Wyatt, 1989; Berger and Nielsen, 1990; McNeely, 2002). These results have ignited considerable debate, since an ice-free HBL during that time would imply a significantly different configuration of the LIS than predicted by glacial models (e.g. Stokes et al., 2012) and what was documented from the LGM to present-day (Dyke, 2004). Furthermore, chronology constraints are largely based on conventional radiocarbon dates (e.g. Wyatt, 1989), or accelerator mass spectrometry (AMS) radiocarbon determinations made on peat or shell samples (e.g. McNeely, 2002), which can be subject to contamination and wide error ranges, depending on the context of samples selected for dating. As a result, evidence for an ice-free HBL during MIS 3 has been largely dismissed, with a lack of AMS dates on wood being cited as "a benchmark consideration against the possibility of Middle Wisconsinan deglaciation of the Hudson Bay Lowland" (McNeely, 2002).

2.2.2 Objectives

Here, we summarize all pre-LGM chronology data in the HBL and contribute new AMS radiocarbon, OSL and U-Th data to critically evaluate the age(s) of the Missinaibi Formation. Geochronological data originated from a range of government, academic and unpublished sources spanning several decades and covering a wide range of uncertainties and errors. To temper these uncertainties and ensure an objective research approach, we include a short discussion of all major issues inherent to dating Pleistocene deposits. This information is then used to rank the chronology data to distinguish between highly-reliable age determinations and those that have an increased chance of being erroneous. Particular attention is paid to radiocarbon age estimates, especially discussing the sample material and potential for modern-day contamination, since the MIS 3 period lies at the limit of this geochronometer. A similar approach was used by Wohlfarth (2010) to evaluate a pre-LGM chronology dataset from Sweden, by Hughes et al. (2016) for reconstructing the most recent 40,000 years of glaciation over Eurasia, and by Forman et al. (2014) for evaluating the chronology of Holocene-aged shells in Lake Turkana, Kenya.

2.3 Regional Setting

The HBL is a coastal plain encompassing 325,000 km^2 of land, located in central Canada, and constrained by the uplands of the Canadian Shield, James Bay and Hudson Bay (Riley, 2003) (Fig. 2-2). This remote region is dominated by ombrotrophic bogs, minerotrophic fens and permafrost along the northern coast (Riley, 2003), all of which are underlain by Paleozoic and Mesozoic sedimentary rocks. The HBL is situated a maximum of ~170 m above sea level, with a gradual decrease in elevation towards the James and Hudson bays. Several major rivers are deeply incised, but meander through this region, discharging into the James and Hudson bays. A marine incursion, the Tyrell Sea, inundated large parts of the HBL region following the post-LGM deglaciation owing to high sea levels and isostatically depressed land (Lee, 1960).

In the HBL, non-glacial deposits underlying till were first noted in a series of exploratory trips in the late 19th century (Bell, 1879, 1886), and are comprised of marine, fluvial, peat and forest-bed units (Skinner, 1973). The marine unit has rarely been noted in the HBL. These deposits are commonly overlain by two tills (Skinner, 1973; Nguyen, 2014), and subsequently overlain by Holocene-aged marine, lacustrine and peat deposits. This Pleistocene-aged stratigraphy is exposed along river banks and ranges in height from 10 to 30 m, with the non-glacial Missinaibi Formation commonly ranging from 1 to 5 m in thickness. The regional extent of these deposits is unknown because the occurrence is disparate, but it may be correlative with non-glacial deposits from central and southern Ontario (e.g. DiLabio et al., 1988; Bajc et al., 2015).

While the reason for the preservation of the Missinaibi Formation is not well understood, the relatively low topography of the HBL, in combination with the confining topographic high of the Canadian Shield, may have mitigated glacial erosion in this region, thus preserving these Pleistocene-aged sediments. Furthermore, the Missinaibi Formation commonly contains fluvial sediments, which would have presumably been deposited in river valleys similar to today, and these sheltered environments may have acted to protect these deposits from glacial erosion (Barnett and Finkelstein, 2013).

2.4 Critical evaluation of geochronological techniques

We assembled a database (n = 127) consisting of all previously published (n = 88) and new (n = 39) geochronological data for the Missinaibi Formation (Appendix A). These data consist of

AMS radiocarbon (n = 44), conventional radiocarbon (n= 36), amino acid (n = 13), U-Th (n = 14), TL (n = 15) and OSL (n = 5) methods. All chronology data were ranked on a scale of 1 to 3, with '1' representing most reliable dates; '2' representing ages with somewhat more uncertainty owing to sample material or depositional context, and '3' less reliable dates. Ranks and rationales are discussed below, and available in Appendix A.

2.4.1 Radiocarbon dating

Sample material, which can have a substantial bearing on the resulting data, varied widely in our database. So long as it is not reworked, wood is the ideal material for radiocarbon dating since cellulose does not exchange carbon with the atmosphere after formation (Bowman, 1990). As a result, we consider wood dates to be reliable (n = 27 ^{14}C AMS of which 25 are new contributions; n = 18 ^{14}C conventional).

Peat (n = 8 ^{14}C AMS; n = 15 ^{14}C conventional) and shell dates (n = 9 ^{14}C AMS; n = 12 ^{14}C conventional), which have unique contamination issues, are common in our database. To minimize the risk of modern-day contamination, peat samples were examined for root structures, and humic acids were removed prior to radiocarbon dating. Since no root structures were identified in the samples, and peat dates have been used commonly and accepted in Holocene HBL studies (Packalen et al., 2014), we assign high confidence to our newly contributed peat dates (n = 8). If similar details on the removal of humic acids and rootlets from the samples were noted for previously published peat dates, we consider those dates to be reliable as well.

Radiocarbon dating of marine shells from the HBL is problematic because most shells are located in till (e.g. McNeely, 2002), meaning that they are inherently transported and may not have originated in the HBL. These shell dates are assigned low confidence because they are not considered to have been deposited *in situ*. Furthermore, the calcium carbonate component of shells is commonly subject to post-death isotope fractionation, especially from modern carbon sources, which can cause artificially young dates (Pigati, 2002; Oviatt et al., 2014). Blake (1988) attempted to circumvent this issue by dating the inner and outer fraction of an *in situ* shell, but the inner fraction resulted in an infinite determination (sample GSC-1475 inner/outer), and is therefore of limited use in our analysis. The only other *in situ* marine shells in our dataset are from McNeely (2002) (samples AA-7563, TO-2503); however, there is limited information

about the pre-treatment and processing of those samples. As a result, we assign lower confidence to these shell dates in our database.

Radiocarbon ages up to 46,401 ^{14}C yr BP were calibrated using the CALIB Rev 7.0.4 and the INTCAL13 curve (Stuiver and Reimer, 1993; Reimer et al., 2013). Since finite ages greater than 46,401 (n = 5) exceed the calibration curve, they were left as radiocarbon years (yr ^{14}C). Following Stuiver and Polach (1977), all dates were rounded to the nearest 100, and error values were rounded up to the nearest 50-year increment. Some ages (n = 3) were not distinguishable from background (Stuiver and Polach, 1977), and were therefore considered to be the same age as background, which is ca. 49,600 ± 950 yr ^{14}C (Appendix B).

2.4.2 U-Th dating

Uranium-Thorium dating has provided a chronological constraint for the MIS 5 period in the HBL (Allard et al., 2012). This method measures the rate of decay of ^{238}U into daughter isotope species and can be used to date material up to ca. 350,000 yr BP (Geyh, 2008). The main requirements for this technique are that the material must contain uranium at deposition, and that it is not affected by uranium or thorium from the surrounding environment while buried (van Calsteren and Thomas, 2006). Wood is not commonly dated using this technique because it does not naturally contain uranium, therefore any uranium uptake must have originated from the surrounding sediment shortly after burial (Vogel and Kronfeld, 1980). Because U-Th dating of wood is dependent on initial uranium contamination of the sample, several corroborative age estimates from the same stratigraphic unit are needed to definitively assign an age (e.g. Mott and Grant, 1985; de Vernal et al., 1986; Causse and Vincent, 1989; Allard et al., 2012).

Wood pieces encased in clay result in limited permeability to surrounding groundwater, and are preferred for the U-Th method. Such conditions were met by Allard et al. (2012), who dated 9 wood logs from deposits underlying till along the Nottaway River. Although slightly different uranium concentrations were recorded on the outer edge of these logs, the inner, less permeable, portions yielded consistent age determinations (Allard et al., 2012), which we consider to be reliable. In the western HBL, two U-Th dates from Nielsen et al. (1986) are considered less reliable owing to the porosity of the surrounding environment (sand, silt), and evidence of thorium contamination, which are suspected to have caused dissimilar isotopic measurements on wood pieces from the same stratigraphic unit.

We made several new attempts to date wood from two sites in the HBL. Two wood pieces were submitted from 12-PJB-109 for analysis at Geotop, Université du Québec à Montréal, for which three dates were obtained (Appendix A). However, in all three cases, the system was believed to be open with respect to uranium, owing to significantly different results from the same stratigraphic unit. This exchange may have been caused by the composition of the sediment matrix, which, although clay-rich (~35%), contained ~50 % silt and ~15% sand. This texture may have promoted water infiltration. As a result, we consider these ages to be minimum estimates. A further attempt at 12-PJB-007 showed that there was no significant uranium uptake, therefore an age assignment was not possible at this site, and these results are excluded from our dataset.

2.4.3 OSL dating

Given that MIS 3, our period of interest, corresponds to the limit of radiocarbon dating, OSL techniques may hold potential to improve our understanding of the age of HBL deposits. However, OSL dating can be less successful on sediments derived from the Precambrian Shield, which yields quartz grains showing low light emissions with optical stimulation ("dim quartz") (e.g. Demuro et al., 2013). The reason for this low luminescence signal may be that newly-eroded quartz has a limited ability to store charge given a minimal number of cycles of dosing and solar resetting (Sawakuchi et al., 2011). Glacial environments associated with rapid burial and high energy settings may also result in partial resetting of electron traps (Lukas et al., 2007; Rhodes, 2011; King et al., 2014). As a result, there are no previously published studies which use OSL on quartz grains from the HBL.

In an attempt to resolve this issue, we used OSL dating on quartz at two separate sites, 12-PJB-109 as well as two samples from the Severn Marine site. An *a priori* assumption is that quartz grains in this fluvial system were not uniformly solar reset because of the short distance of transport in turbid water conditions and possible deposition during the fall and winter with sedimentation beneath ice cover. Single aliquot regeneration (SAR) protocols (Murray and Wintle, 2003; Wintle and Murray, 2006) were used to estimate the apparent equivalent dose for a different size fraction in each sample (Table 2-1). For 12-PJB-109, each aliquot contained approximately 10 to 30 quartz grains corresponding to a 2 mm circular diameter of grains adhered (with silicon) to a circular aluminum disc of 1-cm diameter. Such a small number of grains per aliquot was measured to isolate the youngest, full solar-reset grain population (cf.

Duller, 2008). It is suspected that < 20% of grains of each aliquot emitted light, i.e. 2 to 6 quartz grains.

An Automated Risø TL/OSL–DA–15 system was used for SAR analyses with light from blue diodes. Optical stimulation for all samples was completed at an elevated temperature (125°C) using a heating rate of 5°C/s. All SAR emissions were integrated over the first 0.8 s of stimulation out of 40 s of measurement, with background based on emissions for the last 30- to 40-second interval. In this study, we used the threshold "fast ratio" of > 15 (cf. Durcan and Duller, 2011) to quantitatively determine aliquots that are dominated by a fast component and thus, only those aliquots are included in equivalent dose calculations. The majority of aliquots (>75%) exhibited a clear so called "fast component" (Fig. 2-3) which is one of the requirements of the SAR protocols (Murray and Wintle, 2003).

Calculation of equivalent dose by the single aliquot protocols was accomplished for a majority of aliquots (Table 2-1). Aliquots were removed from analysis if (1) the fast ratio was <15 (Durcan and Duller, 2011), (2) the recycling ratio was not between 0.90 and 1.10, (3) the zero dose was >5 % of the natural emission or (4) the error in equivalent dose determination is >10%. Equivalent dose (D_e) distributions are log normal, highly negatively skewed and exhibited overdispersion values of 23% to 103% (Table 2-1; Fig. 2-3). An overdispersion percentage of a D_e distribution is an estimate of the relative standard deviation from a central D_e value in context of a statistical estimate of errors (Galbraith et al., 1999; Galbraith and Roberts, 2012). A zero overdispersion percentage indicates high internal consistency in D_e values with 95% of the D_e values within 2σ errors. Overdispersion values ≤ 20% are routinely assessed for small aliquots of quartz grains that are well solar reset, like far-traveled eolian and fluvial sands (e.g. Olley et al., 2004; Wright et al., 2011; Meier et al., 2013) and this value is considered a threshold metric for calculation of a D_e value using the central age model of Galbraith et al. (1999). Overdispersion values >20% may indicate mixing of grains of various ages or partial solar resetting of grains. The finite mixture model is an appropriate statistical treatment for such data (Galbraith and Green, 1990), and this model was used to calculate optical ages (Fig. 2-3; Table 2-1).

In addition to our new OSL data, Dubé-Loubert et al. (2013) dated sediments (n = 2) using feldspar grains, which can be used to date sediments back to 500,000 yr BP. However, feldspar is more commonly affected by anomalous fading, a process whereby electrons gradually vacate

their traps in the absence of light or heat exposure, which can lead to underestimation of results (Huntley et al., 1985). Dubé-Loubert et al. (2013) applied an equivalent dose correction developed by Lamothe et al. (2003) to mitigate anomalous fading, and we therefore consider these data points to be reliable.

2.4.4 Thermoluminescence dating

Similar to OSL dating, TL dating measures the last exposure of a sediment to sunlight. However, TL dating can be impacted by anomalous fading, which can lead to underestimation of results (Huntley et al., 1985). This issue can be mitigated by introducing sample preheats or adding days to weeks of wait time to allow the laboratory-induced luminescence to pre-fade. Forman et al. (1987) dated two marine sediments samples from the Severn River in the northern HBL using this approach to mitigate the effects of anomalous fading, and Berger and Nielsen (1990) used prolonged sample storage to remove pre-fade for five samples along the Nelson River (Appendix A). Since effort was made to mitigate the issue with anomalous fading, we retained the data in our dataset and increased the error to 2σ.

Eight TL samples from non-glacial intervals overlain by till from sites along the Nelson River were also analyzed by Roy (1998) to determine the extent of solar resetting and anomalous fading. Seven samples are considered to be unreliable owing to large grain sizes (150-250 μm) which are suspected to have caused improper solar resetting. This insufficient solar resetting was confirmed by a Holocene-aged sample which resulted in two age estimates of ca. 50,000 yr BP (Roy, 1998). However, one sample (MOON 2C (delayed)) is more likely a close estimate to the true depositional age because the grain size is much smaller (4-8μm), which would have allowed for prolonged sediment suspension prior to deposition, and therefore more effective solar resetting. Furthermore, this sample was corrected for anomalous fading by storing for one year prior to taking this measurement. However, Roy (1998) acknowledges that anomalous fading may have continued after the one-year delay.

2.4.5 Amino acid epimerization

Amino acid epimerization of allo-isoleucine to isoleucine from molluscs has provided some of the first evidence for a large-scale recession of the LIS during MIS 3 (Andrews et al., 1983). This technique measures the post-mortem changes in amino acid chirality (e.g. racemization) for molluscs, such as *Hiatella arctica* or *Mya truncata* (Rutter et al., 1979; Miller and Brigham-

Grette, 1989). Such changes to amino acid configuration can be detected for up to ca. 2,000,000 years, making this method suitable for materials of Pleistocene age (Miller and Brigham-Grette, 1989).

A disadvantage to amino acid dating is that it is a relative dating method. In the HBL, amino acid age inferences are based on the implicit assumption that the largest ratio corresponds to a marine incursion during MIS 5e. Younger dates are assigned an age according to this assumption. Consequently, the application of this technique in the HBL has been controversial (Andrews et al., 1983; Dyke, 1984), and we assign limited confidence to these age estimates. Nevertheless, we compiled age estimates from *in situ* shells in the database. Shells from till (e.g. Shilts, 1982; Andrews et al., 1983; Nielsen et al., 1986; Wyatt, 1989) are not included in this compilation because they were incorporated and resided within the glacier for an unknown amount of time where racemization may have ceased or slowed down (Barnett, 1992).

2.5 Results

Geochronological data for the Missinaibi Formation is largely confined to the most recent 130,000 yr BP, with one exception being an OSL date suggesting a fluvial deposit at ca. 211,000 ± 16,000 yr BP from the Harricana River, published by Dubé-Loubert et al. (2013) (sample 06HA30). This data point represents the oldest age estimate in the HBL region, and aligns with the interglaciation of MIS 7 (ca. 243,000 to ca. 190,000 yr BP) (Dubé-Loubert et al., 2013). Deposits dating to MIS 5 are situated along the Nottaway and Nelson Rivers, and have been described by Allard et al. (2012), Dubé-Loubert et al. (2013) and Roy (1998) (Fig. 2-4).

Much of our newly contributed data suggests the possibility of an ice-free MIS 3 in the HBL. Firstly, wood from 11-PJB-186, an organic-rich interval overlain by post-glacial marine sediments along the Black Duck River, suggests that organic accumulation began around 50,100 ± 3300 ^{14}C yr BP (sample ISGS A1995) and 49,600 ± 950 yr ^{14}C (sample UOC-0587), while the upper part of the unit dates to 46,300 ± 1750 cal. yr BP (sample ISGS A1656) (Fig. 2-5). Similarly, two sites located in close proximity (~ 1.3 km) along the Ridge River, 11-PJB-020 and 12-PJB-007 have yielded radiocarbon dates of 40,000 ± 400 cal. yr BP (sample UOC-0591), 49,600 ± 950 yr ^{14}C (sample UOC-0592; Appendix B), 46,300 ± 1750 cal. yr BP (sample UOC-0590) and ca. 46,500 ± 2100 ^{14}C yr BP (sample ISGS A2424) (Fig. 2-5). Both sites along the Ridge River are overlain and underlain by diamicton. At the Severn Marine site, our re-

evaluation of TL samples using OSL techniques have yielded ages of 52,480 ± 5055 (sample BG3807) and 42,190 ± 4010 (sample BG3808) (Fig. 2-3).

Data from the western region of the HBL also suggests an ice-free MIS 3, where Berger and Nielsen (1990) published a suite of TL data from fluviolacustrine sediments along a ~100 km stretch of the Nelson River. Another purported MIS 3 site is 24M, which is considered to be the type location for the Missinaibi Formation (Terasmae and Hughes, 1960; Skinner, 1973). Our AMS radiocarbon result of ca. 39,700 ± 800 cal. yr BP (sample TO-1753) corresponds well with other finite determinations in the range of 39,000 to 41,000 yr BP (Olson and Broecker, 1957, 1959); however, is in contrast with several infinite determinations, which suggest an older age (Preston et al., 1955; Olson and Broecker, 1959; MacDonald, 1971; Vogel and Waterbolk, 1972; Stuiver et al., 1978). We therefore consider the age of the 24M site to be unresolved.

In addition to the data listed above, there are several sites for which only one finite age estimate is available. Although not described in detail here, these samples are all included in Appendix A as well as plotted in Fig. 2-4.

2.6 Discussion

Our synthesis of available age estimates for non-glacial materials suggests that the HBL was ice-free during MIS 7 (Dubé-Loubert et al., 2013), MIS 5 (Roy, 1998; Allard et al., 2012) and possibly during MIS 3. Deposits dating to MIS 7 or MIS 5 are not surprising given that the LIS was thought to have retreated considerably at those times. However, if age estimations from the HBL are correct, deposits dating to MIS 3 imply significant reconfiguration of the LIS.

2.6.1 The validity of >40,000 yr BP radiocarbon dates

A major limitation of our results and subsequent interpretations is that radiocarbon dates are largely used to constrain the purported ice-free period during MIS 3. This is problematic because radiocarbon dates in the range of 40,000 to 50,000 yr BP have lost the majority of ^{14}C, and contamination by small amounts of modern carbon can cause otherwise infinite materials to appear finite (Beukens, 1990; Andrews and Dyke, 2007). For example, 0.2% modern-day carbon contamination will cause a 45,000 year old sample to yield an age of 40,000 years (Olsson and Eriksson, 1972). It is therefore possible that modern or re-worked carbon is influencing our radiocarbon dates, thus erroneously suggesting an ice-free MIS 3 in the HBL.

There is no way to determine whether a single sample has been contaminated by modern-day carbon. Only repeated measurements showing a high degree of precision can increase confidence that a true representation of the material's age has been obtained (Scott, 2007). For example, Bajc et al. (2015) investigated a purported MIS 3 site in Southern Ontario, re-dating wood pieces using three different cellulose extraction techniques, resulting in age estimate of ca. 42,000 to ca. 50,000 ^{14}C years BP, therefore strengthening a MIS 3 age assignment at that site. A similar approach was used at a Late Pleistocene site from Atlantic Canada by Rémillard et al. (2013), where both peat and wood consistently yielded ages of ca. 47,100 to ca. 50,100 yr BP, all of which overlap at 1σ, thus supporting the MIS 3 interpretation.

In addition to repeated dating of samples, the stratigraphy of age determinations can help determine whether modern contamination is responsible for finite age estimates. For example, at the Pilgrimstad site in Sweden, radiocarbon estimates from ca. 40,000 to ca. 50,000 cal. yr BP were older at the bottom of the stratigraphic sequence and gradually became younger towards the top (Wohlfarth, 2010 and references therein). If modern-day carbon contamination had influenced these age estimates, we would expect all determinations to be artificially finite, as well as possible age reversals in the stratigraphic sequence. Since age estimates largely follow stratigraphic order, it re-enforces the MIS 3 age assignment.

Following the techniques outlined above, to strengthen age estimates for the Missinaibi Formation, we made an effort to (1) sample several intervals at a given site to determine if the resulting age estimates follow stratigraphic order, and (2) date samples multiple times, and at different radiocarbon laboratories, to test the precision and reproducibility of each age assignment. These efforts were focussed on three purported MIS 3 sites, 11-PJB-186, 11-PJB-020 and 12-PJB-007 and the results can be seen in Fig. 2-5 and Appendix A. Although some re-dating attempts were limited because of low material availability, chronology data at these sites largely follows stratigraphic order, and samples which have been dated multiple times show significant reproducibility. Such an agreement would not be expected if these finite estimates were the result of modern carbon contamination. Therefore, on the basis of radiocarbon dating, we find no reason to discount the chronology at these three sites. Results from OSL dating further support the MIS 3 interpretation (Fig 2-3). However, fluvial and/or marine sediments were often missing from the sub-till sites, thus a direct comparison of OSL and radiocarbon dates from the same site has not yet been done. Nevertheless, both radiocarbon and OSL results

suggest an ice-free HBL during MIS 3. The discovery of new sub-till sites to perform OSL dating may hold potential to significantly improve our understanding of the age of the Missinaibi Formation.

The abundance of infinite radiocarbon dates (n = 47) is also worth considering, although the interpretation is challenging. Given that the MIS 3 period corresponds to ca. 29,000 to ca. 57,000 yr BP, radiocarbon dating should be able to capture any deposit up to ca. 50,000 yr BP, only missing those that lie at the lower boundary for MIS 3. It is possible that some of these infinite age estimates may be from that time. It is equally possible that these infinite dates represent multiple non-glacial intervals from earlier in the Pleistocene, perhaps correlative with the late MIS 5 ages from the Nottaway River (Allard et al., 2012). Based solely on chronological evidence, we do not consider the presence of infinite radiocarbon dates to be evidence in favor or against any particular age assignment for the Missinaibi Formation.

2.6.2 Ice sheet dynamics during MIS 5

Based on available age estimates, the warmest part of the penultimate interglacial, MIS 5e (peak: ca. 123,000 yr BP), which has been identified elsewhere in Canada (e.g. Karrow et al., 2001; Fréchette and de Vernal, 2013), is not preserved in the non-glacial sediments of the HBL at sites presented here. Instead, OSL data from the Nottaway River, and one TL age from the Nelson River correspond to the latter part of the MIS 5 interglaciation (Roy, 1998; Allard et al., 2012; Dubé-Loubert et al., 2013).

2.6.3 Laurentide Ice Sheet during MIS 3

Our data suggest that the HBL may have been deglaciated during ca. 50,000 to 40,000 yr BP, which, according to RSL and $\delta^{18}O$ from benthic foraminifera (Lisiecki and Raymo, 2005; Grant et al., 2014), corresponds to a time of partial deglaciation of the North American continent. If correct, data from the HBL constrain the ice-free eastern lobe of the LIS by 700 km westward and northward than what is suggested by most other Late Pleistocene sites. In Southern Ontario, these sites include conventional radiocarbon dates on sub-till material from a borehole and creek exposure (Karrow and Warner, 1984; Warner et al., 1988), three finite AMS dates on bone and peat samples from a sub-till site exposed along a railroad cut (Karrow et al., 2001) and six finite AMS dates on sub-till wood fragments from a quarry (Bajc et al., 2015). In Atlantic Canada, Rémillard et al. (2013) documented four finite AMS ages on sub-till peat, which suggests that

this region may have also been deglaciated during MIS 3. Fréchette and de Vernal (2013) also infer a deglaciation in Atlantic Canada during MIS 3, but no geochronological data were available at that site, and instead, age control was based on the stratigraphic position of the sub-till deposits.

Radiocarbon data from Repulse Bay, northwest of the HBL, may provide corroborative evidence for a very significant glacial recession during MIS 3. Recently-obtained radiocarbon data suggest that this region was ice-free for several thousand years during MIS 3 (McMartin et al., 2015). However, notably, these data were based on marine shells, which may have associated uncertainties (see Section 2.4.1). Nevertheless, duplicate samples analyzed by different laboratories produced the same interpretation at that site (McMartin et al., 2015), which strengthens the interpretation. Together with data from the HBL, there seems to be a growing amount of evidence suggesting that large parts of eastern and central North America may have been ice-free during MIS 3.

If evidence for a significant glacial recession during MIS 3 is correct, other parts of North America must have been fully glaciated to compensate for the relatively low sea level during that time (Grant et al., 2014). It may be possible that the mid- and western regions of North America were glaciated. For example, TL, and radiocarbon data from the Roxana Silt suggest the presence of the LIS in the mid-continent during MIS 3 (Forman, 1992; Forman and Pierson, 2002). Records from the Gulf of Mexico, most of which are dated using a series of AMS dates on foraminifera, also suggest that the LIS spanned into the continental United States for large parts of MIS 3 (Hill et al., 2006; Tripsanas et al., 2007; Sionneau et al., 2013).

Based on available age estimates of the Missinaibi Formation, it seems that the western sector of the LIS (Keewatin) was highly active, and the eastern sector (Labrador-Nouveau Québec) may have experienced restricted growth following MIS 5 and into MIS 3. Expansion of the eastern sector may have been preferentially eastward onto the expanding continental shelf as RSL fell. Its southern extension may have been affected by the isostatically depressed St Lawrence River valley, slowing expansion into the lower Great Lakes. This eastern sector of the LIS may have only reached the western end of Lake Ontario during MIS 3. In this scenario, it is possible for parts of the HBL to have remained unglaciated.

The lack of a marine unit at the base of most dated MIS 3 sites may provide supportive evidence for a MIS 3 age assignment. In the HBL, marine incursions can be expected immediately following deglaciation as a result of isostatic depression of the land and the close proximity to Hudson Bay (e.g. Tyrell Sea; Lee, 1960). To account for this missing marine unit, the Missinaibi Formation could have been deposited at a time when ice had recently receded beyond the boundaries of the HBL, but when significant parts of the continent remained glaciated to maintain low RSL, thus preventing a large-scale marine incursion. The early part of MIS 3 is the only time during the Late Pleistocene when what may have been an extensive deglaciation is not followed by a substantial rise in sea level to levels similar to present-day (Grant et al., 2014). We would expect such conditions to prevent a large-scale marine incursion in the HBL, allowing instead the growth of peat, forest bed and fluvial deposits directly overlying till, corresponding to the observed Missinaibi Formation. However, two newly-contributed OSL dates from the Severn River suggest that a marine incursion may have inundated the outer region of the HBL during this time (Fig. 2-3, 2-4).

Irrespective of the configuration of the LIS during ca. 50,000 to ca. 42,000 yr BP, there is a general consensus of substantial continental glaciation between ca. 42,000 to ca. 35,000 yr BP which would likely have covered the entire HBL region. Karig and Miller (2013) document a proglacial lake in upper New York state from ca. 37,000 to ca. 34,000 yr BP, and Berger and Eyles (1994) document till in Southern Ontario at ca. 41,000 yr BP, indicating the proximal presence of a glacial lobe during that time. Furthermore, sedimentological evidence from the Gulf of Mexico suggests that the eastern lobe of the LIS was extended beyond Lake Ontario at that time (Tripsanas et al., 2007; Sionneau et al., 2013), and radiocarbon and OSL dating of cave sediments indicates that the LIS may have grown to almost the LGM limit between ca. 40,000 to ca. 30,000 yr BP (Wood et al., 2010).

Taken together, evidence suggests that the LIS covered large parts of North America from ca. 42,000 to ca. 35,000 yr BP, which would have undoubtedly glaciated all of the HBL during that time. Our shortage of age estimates from this time period may be taken as indirect evidence for a fully glaciated HBL, since this time period is well within the acceptable range of most geochronological methods. After this purported glaciation, there may have been a brief retreat of the LIS at ca. 30,000 yr BP (Dyke et al., 2002), followed by a rapid build-up of the ice sheet towards the LGM (Dyke et al., 2002; Lambeck et al., 2014).

2.7 Conclusions

Our review of chronology data from the HBL, Canada, helps to constrain the boundaries of the LIS for periods prior to the LGM, which can help validate important models of ice sheet extent, build-up and growth (Ganopolski et al., 2010; Kleman et al., 2010; Ganopolski and Calov, 2011; Stokes et al., 2012). Chronology data suggest that the HBL was ice-free during parts of MIS 7, MIS 5 and possibly during parts of MIS 3. While glacial retreats at MIS 7 and MIS 5 are well-documented, evidence for an ice-free central region of the LIS during MIS 3 is noteworthy, since these data extend the ice-free eastern lobe of the LIS by at least 700 km westward and northward from what is suggested by existing Late Pleistocene sites in Southern Ontario and Atlantic Canada (Rémillard et al., 2013; Bajc et al., 2015).

Although largely based on radiocarbon determinations, evidence for an ice-free HBL during the MIS 3 period is reinforced by (1) our successful efforts to re-date purported MIS 3 sites and test the reliability of radiocarbon dating at the limit of this geochronometer, (2) paleorecords from Atlantic Canada and Southern Ontario suggesting largely ice-free conditions during MIS 3 (e.g. Bajc et al., 2009; Rémillard et al., 2013; Bajc et al., 2015), and for which the western extent is unknown, and (3) a strong agreement between low RSL during MIS 3 and the lack of marine deposits in the Missinaibi Formation. Future iterations of relevant Earth System Models should include land-based information of the layout and configuration of previous ice sheets, along with results from till correlations (Kaszycki et al., 2008; Dubé-Loubert et al., 2013; Nguyen, 2014), geomorphic evidence of ice flow regimes (Veillette et al., 1999; Kleman et al., 2010) and models of ice volume (Peltier et al., 2015).

2.8 Acknowledgements

Funding for this research was provided by the Ontario Geological Survey to PJB, Natural Sciences and Engineering Research Council (Canada) to SAF, Northern Scientific Training Program and University of Toronto Centre for Global Change Science to ASD. We also thank the Lalonde Radiocarbon Lab Training Program, as well as S. Williams, M. Nguyen and Missinaibi Headwaters Outfitters for assistance during fieldwork. Additional thanks to M. Roy and B. Ghaleb, Université du Québec à Montréal, for collaborations on U-Th dating as well as J. Bollmann for helpful discussions.

2.9 Tables

Table 2-1. Optically stimulated luminescence (OSL) ages on quartz grains from the sub-till Missinaibi Formation, Hudson Bay Lowlands, Canada

Sample/ Horizon	Laboratory number	Aliquots[a]	Particle Size (μm)	Equivalent dose (Gray)[b]	Over-dispersion (%)[c]	U (ppm)[d]	Th (ppm)[d]	K (%)[d]	Cosmic Dose rate (mGray/yr)[e]	Dose rate (mGray/yr)[f]	OSL age (yr)[g]
12-PJB-109	BG3800	98/67	250-150	72.27 ± 3.87	62 ± 5	1.22 ± 0.01	6.65 ± 0.01	1.31 ± 0.01	0.16 ± 0.01	1.69 ± 0.09	42,845 ± 3740
Severn Marine 84HBL022	BG3807	90/62	100-63	97.36 ± 6.23	30 ± 3	1.31 ± 0.01	5.78 ± 0.01	1.53 ± 0.01	0.10 ± 0.01	1.64 ± 0.09	52,480 ± 5055
Severn Marine 84HBL023	BG3808	50/30	64-44	85.14 ± 5.26	55 ± 7	1.38 ± 0.01	6.49 ± 0.01	1.64 ± 0.01	0.10 ± 0.01	2.02 ± 0.10	42,190 ± 4010

[a]Aliquots used in equivalent dose calculations versus original aliquots measured.

[b]Equivalent dose calculated on a pure quartz fraction analyzed under blue-light excitation (470 ± 20 nm) by single aliquot regeneration protocols (Murray and Wintle, 2003; Wintle and Murray, 2006). A finite mixture model was used with overdispersion values >20% to determine the youngest equivalent dose population, with at least 10 aliquots defining this equivalent dose population (Galbraith and Green, 1990).

[c]Values reflects precision beyond instrumental errors; values of ≤ 20% (at 1 sigma limit) indicate low dispersion in equivalent dose values and an unimodal distribution.

[d]U, Th and K content analyzed by inductively-coupled plasma-mass spectrometry analyzed by ALS Laboratories, Reno, NV; U content includes Rb equivalent.

[e]A cosmic dose rate calculated from parameters in Prescott and Hutton (1994)

[f]Assumes a moisture content (by weight) of 25 ± 5% for the burial period

[g]Systematic and random errors calculated in a quadrature at one standard deviation. Datum year is AD 2010

2.10 Figures

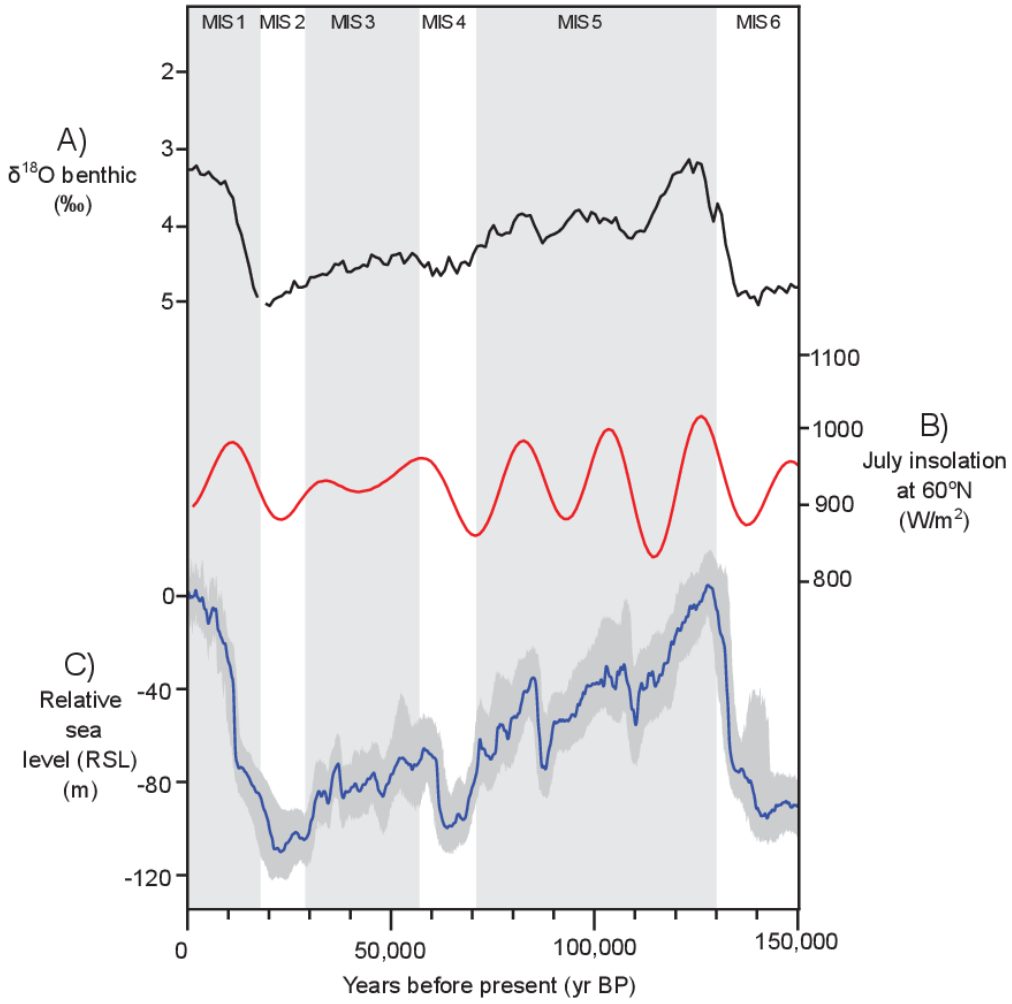

Fig. 2-1. Climate proxies for the most recent 150,000 years. (A) $\delta^{18}O$ record from benthic foraminifera (Lisiecki and Raymo, 2005); (B) July insolation at 60°N (Berger and Loutre, 1991); (C) Relative sea level from the Red Sea (Grant et al., 2014).

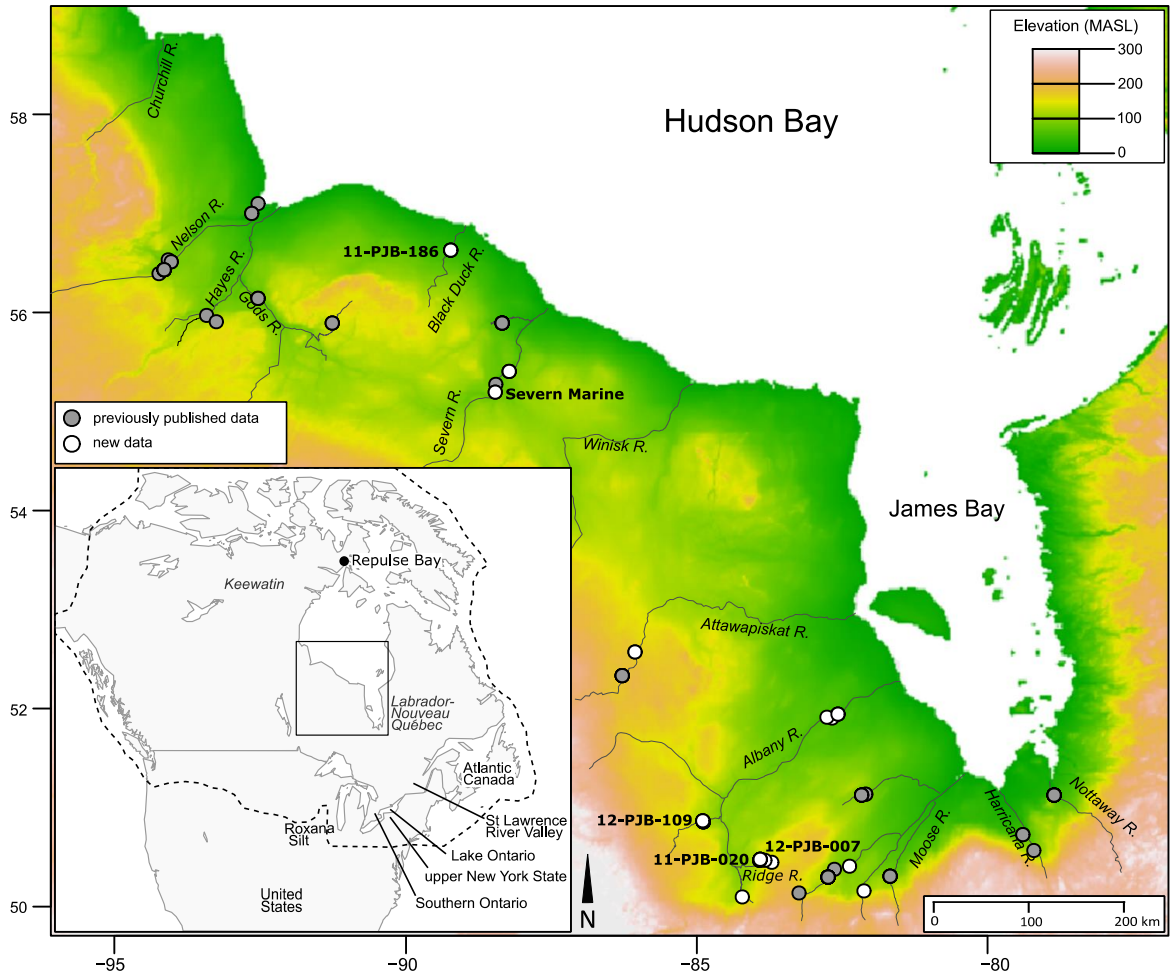

Fig. 2-2. Map of the Hudson Bay Lowlands (HBL) region, showing the locations of Late Pleistocene age estimates, which are compiled for this study. The location of key sites are noted on this map. Some sites contain several dates; details from each site are available in Appendix A. Topographic data were compiled by Amante and Eakins (2009). Inset map shows the HBL region (box), approximate maximum extent of the Wisconsinan Stage (hatched lined) (Dyke et al., 2002) and other sites/regions mentioned in the text. Names which are italicised represent sectors of the Laurentide Ice Sheet. Further details on the creation of this map are available in Appendix C.

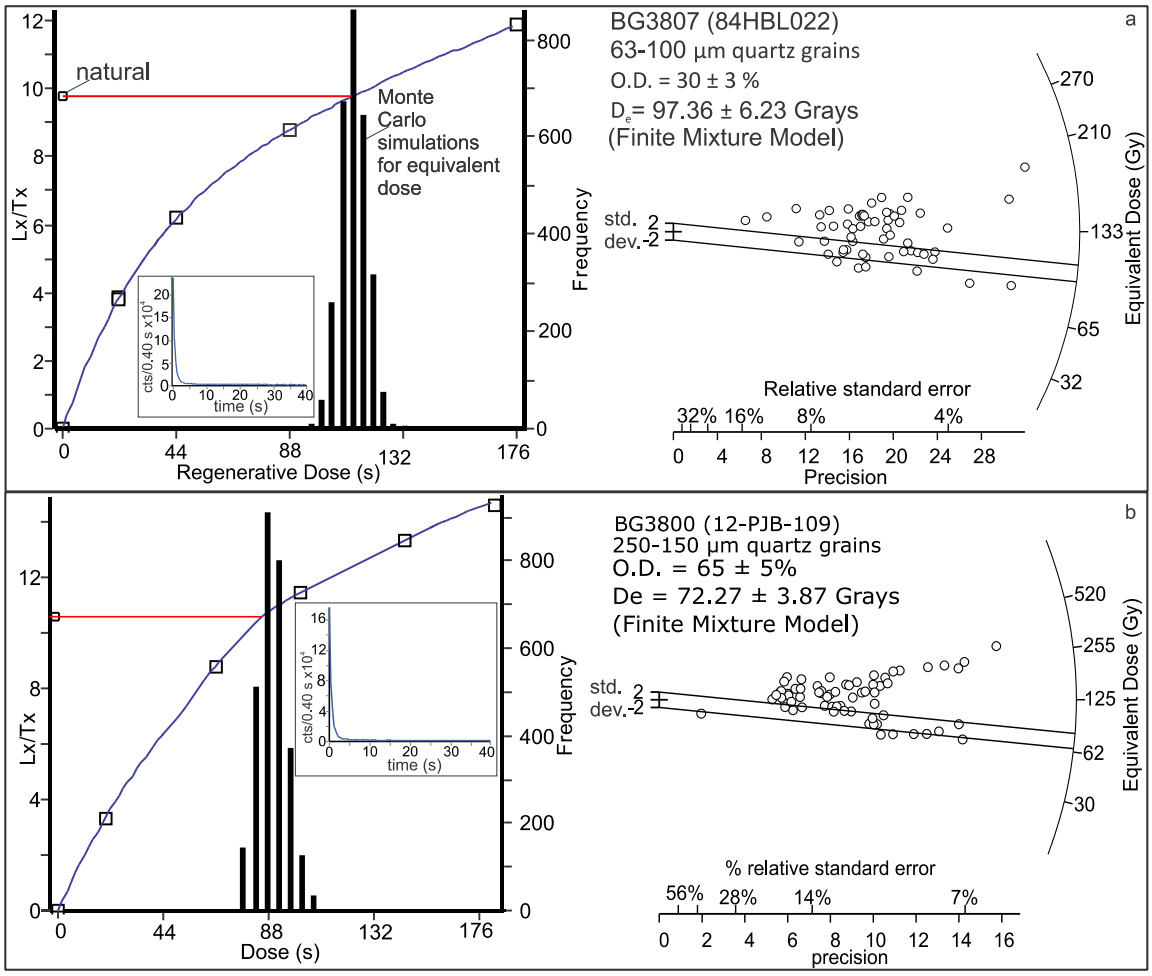

Fig 2-3. Optically stimulated luminescence data for quartz grains (BG3807 and BG3800) from waterlain deposits. Inset figure is a representative shine down curve of natural luminescence. Shown are regenerative growth curves, with errors by Monte Carlo simulations and radial plots defining statistical parameters for equivalent dose determinations. Mean equivalent dose was determined by the Finite Mixture Model (FMM) of Galbraith and Green (1990) because of high overdispersion values >25%; parallel lines denote the lowest significant equivalent dose population defined by at least 20 aliquots.

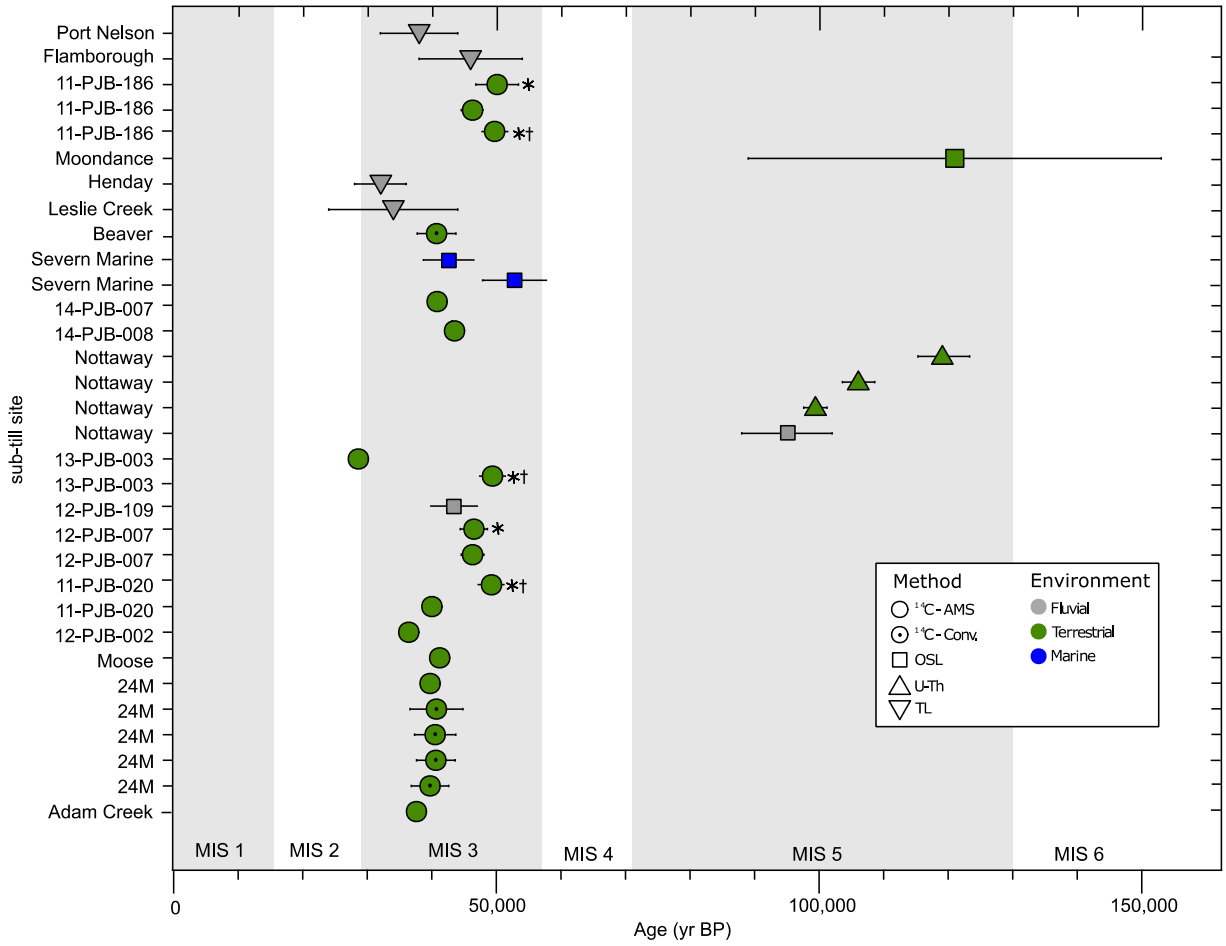

Fig. 2-4. Summary of chronology data for Pleistocene-aged sites in the Hudson Bay Lowlands (HBL), Canada. Sites are arranged from north to south. Asterix (*) symbol represents radiocarbon dates which could not be calibrated because of exceeding the calibration curve. Cross (†) symbol represents finite ages which are not statistically distinguishable from background, and are therefore considered to be the same age as background. Infinite determinations, ages exceeding 150,000 yr BP (n = 1) and those with a high chance of being erroneous (rank 3) were excluded from this figure. See Appendix A for more details.

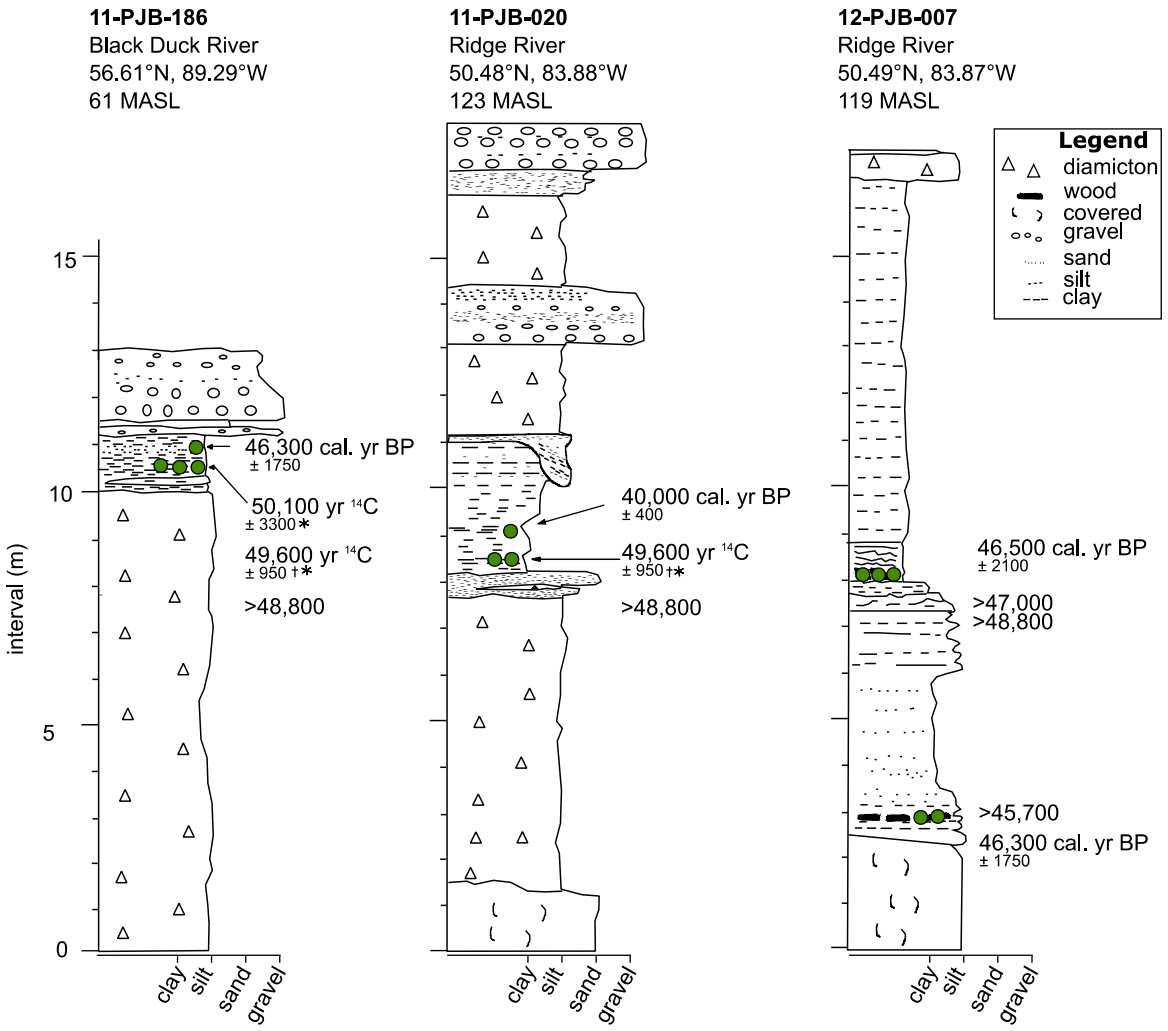

Fig. 2-5. Detailed stratigraphy of three pre-LGM sites from the Hudson Bay Lowlands, Canada, which have the best evidence of being MIS 3 deposits. All chronology data presented in this figure are new. Asterix (*) symbol represents radiocarbon dates which could not be calibrated because of exceeding the calibration curve. Cross (†) symbol represents finite ages which are not statistically distinguishable from background, and are therefore considered to be the same age as background.

Chapter 3
Pollen and macrofossil-inferred palaeoclimate at the Ridge Site, Hudson Bay Lowlands, Canada: Evidence for a dry climate and significant recession of the Laurentide Ice Sheet during Marine Isotope Stage 3

3.1 Abstract

We examine pollen, macrofossils and sedimentological proxies from the Ridge Site, an 18-m succession of glacial and non-glacial sediments exposed along the bank of the Ridge River in the southern Hudson Bay Lowlands (HBL), Canada. Since the HBL is located in the previously glaciated region of North America, palaeorecords from this region have important implications for understanding ice sheet palaeogeography and climate for the Late Pleistocene. Two diamicton units were interpreted as subglacial till deposited by a glacier actively flowing toward the south-southwest (lower diamicton) and west-southwest (upper diamicton), respectively. Confined between these tills is a 6-m non-glacial unit, constrained to Marine Isotope Stage 3 (MIS 3; *c*. 57 000 to *c*. 29 000 a BP) by 3 radiocarbon dates. Quantitative analyses of the pollen record (dominated by *Sphagnum*, Cyperaceae, *Pinus*, *Picea*, *Salix*, *Alnus* and *Betula*) suggest that average summer temperature (June, July, August) was 14.6±1.5°C, which is similar to present-day at the site. Total annual precipitation was 527±170 mm as compared to 705 mm present-day. The macrofossil record confirmed the local presence of *Betula*, *Salix* and conifers. Our results, in combination with other records from the periphery of the Laurentide Ice Sheet, suggest that vast boreal forest-type vegetation, along with a drier interstadial climate, existed in the region during MIS 3. We also compare pollen-derived palaeoclimate reconstructions from the Ridge Site with reconstructions from a previously published site along the Nottaway River, HBL, which was dated to MIS 5 a-d (*c*. 109 000 to *c*. 82 000 a BP). This comparison suggests that, with additional data, it may be possible to differentiate MIS 3 and MIS 5 deposits in the HBL on the basis of relative continentality, with MIS 3 characterized by lower total annual precipitation, and MIS 5 by values similar or greater than present-day.

3.2 Introduction

Quantitative palaeoenvironmental analyses of Pleistocene records allow for a better understanding of the role of carbon (Kleinen et al., 2015), abrupt climate variability (Helmens et al., 2015) and oceanic circulation (Böhm et al., 2015) in the climate system. Records from previously glaciated regions are particularly valuable since, when dated accurately, their age(s) can be used to infer the absence of regional ice, and therefore ice sheet palaeogeography. For example, basal radiocarbon dates have been used to reconstruct the maximum extent and subsequent recession of the Laurentide Ice Sheet over North America (Dyke et al., 2002; Dyke, 2004; Peteet et al., 2012). However, considerably less is known about the extent of glaciation during periods prior to the Last Glacial Maximum (LGM), since available records are often highly fragmented, poorly preserved and difficult to date. Therefore, when available, these rare palaeorecords are critically important for constraining numerical ice sheet models (Stokes et al., 2015).

The Missinaibi Formation is a suite of non-glacial sediments which underlie till in the Hudson Bay Lowlands (HBL), Canada (Fig. 3-1). Due to the position of the HBL at the centre of growth of many Pleistocene ice sheets, the age(s) of the Missinaibi Formation is important for understanding the palaeo-configuration of pre-LGM ice sheets. Chronology data suggest that some sites belonging to the Missinaibi Formation may date to Marine Isotope Stage 3 (MIS 3; *c*. 57 000 to *c*. 29 000 a BP; based on the chronology of Lisiecki and Raymo (2005)), indicating the possibility of a reduced or significantly different structure for the Laurentide Ice Sheet during the middle of the Wisconsinan Stage (Dalton et al., 2016; Chapter 2 of this dissertation). However, many sub-till sites in the HBL remain undated due to ages approaching or exceeding the limit of radiocarbon dating, and the scarcity of suitable materials for optically stimulated luminescence dating and uranium-thorium dating (Dalton et al., 2016; Chapter 2 of this dissertation). As a result, it is not known whether all sub-till sites in the HBL were deposited during MIS 3, or whether the Missinaibi Formation may represent both interstadial and interglacial periods during the Late Pleistocene (Terasmae and Hughes, 1960; Skinner, 1973).

Owing to the close relationship between vegetation and climate (Seppä and Birks, 2001; Väliranta et al., 2015), pollen and macrofossils may play a key role in resolving the age(s) of the Missinaibi Formation. For example, if edaphic and hydrological conditions were suitable, it may

be possible to recognize warmer MIS 5e (peak: *c*. 123 000 a BP) deposits by the presence of temperate tree pollen such as *Acer, Ulmus* and *Fraxinus*, all of which are found today in more temperate wetland regions (Bunting et al., 1998). However, none of the sub-till pollen records from the HBL report significant amounts of any such temperate taxa, and it is therefore unlikely that MIS 5e deposits are preserved as part of the Missinaibi Formation. Instead, most sub-till deposits contain boreal and wetland-type pollen dominated by *Picea* and *Pinus*, along with small amounts of *Salix, Alnus* and *Betula*. Some of these deposits appear to date to MIS 3 (Wyatt, 1989; Dalton et al., 2016; Chapter 2 of this dissertation), or MIS 5 a-d (*c*. 109 000 a BP to *c*. 82 000 a BP; henceforth referred to as "off-peak MIS 5") (Allard et al., 2012), but many are undated (e.g. Terasmae and Hughes, 1960; Netterville, 1974; Dredge et al., 1990). It is not known whether vegetation in the HBL is sufficiently sensitive to distinguish between interstadial (MIS 3) and off-peak interglacial (MIS 5 a-d) sites.

The main objective of this study is to reconstruct past vegetation and palaeoenvironment using pollen, macrofossils and sedimentological proxies at a purported MIS 3 site in the HBL. Fossil pollen data will be used to reconstruct a quantitative palaeoclimate signature for MIS 3 (total annual precipitation and average summer temperature). We use the North American Pollen Database (Whitmore et al., 2005), along with 49 newly compiled sites from the HBL region, as the basis for our modern-day calibration set. Results from our palaeoclimate reconstruction are discussed in context of other MIS 3 sites in the periphery of the Laurentide Ice Sheet, with the goal of developing an understanding of regional-scale climate during the interstadial period. We then reconstruct the palaeoclimate at a previously published off-peak MIS 5 site (Allard et al., 2012) to determine whether subtle vegetation and/or climate differences existed between MIS 3 and off-peak MIS 5. If quantitative statistical methods are able to discern subtle changes in vegetation assemblages and inferred palaeoclimate between MIS 3 and off-peak MIS 5 deposits, then it may be possible to use pollen records to assign ages to many of the undated sub-till sites in the HBL (e.g. Terasmae and Hughes, 1960; Netterville, 1974; Dredge et al., 1990).

3.3 Study site

The present-day HBL is a remote region that covers an area of >325 000 km^2 south and west of the Hudson and James Bays (Fig. 3-1). Bound to the south by the Canadian shield, this coastal plain is largely Paleozoic and Mesozoic carbonate and clastic rocks overlain by Pleistocene

glacial deposits and extensive Holocene-aged peatlands (Riley, 2003). Present-day isostatic rebound, paired with thick deposits of unconsolidated alluvial and glacial material, causes rivers in the HBL to meander northward at a very gradual gradient (Riley, 2003). The HBL is situated in the boreal forest zone, with tundra only occurring in the extreme northwest region and some coastal areas (MacDonald and Gajewski, 1992). The landscape is composed of ombrotrophic bogs (36%), minerotrophic fens (24%), permafrost wetlands (22%), swamps (13%) and marshland (5%), occurring in wooded or non-wooded environments (Riley, 2003).

The study site (referred to in the field as "11-PJB-020", but referred to here as the "Ridge Site") is an 18-m succession of Quaternary-aged sediments of both glacial and non-glacial origin, and is located along the Ridge River, a tributary of the Albany River, at 50.48° N, -83.88° W (Fig. 3-1). This site was first examined by Riley and Boissonneau (n.d.) who identified the presence of organic-bearing muds below till, but no subsequent studies were conducted. Elevation is approximately 115 metres above sea level (m.a.s.l) at the river level and 133 m.a.s.l. at the top of the section. Present-day total annual precipitation is estimated to be 705 mm and average summer temperature (June, July, August) is 15.5°C based on interpolated climate data between the closest weather stations (Natural Resources Canada, 2015).

3.4 Methods

3.4.1 Stratigraphic descriptions and diamicton analyses

The Ridge Site was visited by helicopter in June 2011 and again in July 2013. Three distinct units are noted: a lower diamicton, a non-glacial unit, and an upper diamicton (Fig. 3-2). Stratigraphic boundaries were determined by visual inspection of the section after overlying slump material was removed. Particle size for the diamicton was determined according to the Wentworth scale (Wentworth, 1922) using a combination of sieves for the coarse fraction, and a Microtrac Particle Size Analyzer for the finer (silt/clay) fraction of the matrix. Carbonate content and the calcite-to-dolomite ratio for the silt and clay fraction (<0.063 mm) of the diamictons was measured on 0.85 g samples using a Chittick apparatus (Dreimanis, 1962).

3.4.2 Multi-proxy analyses on the non-glacial unit

Three organic-bearing samples were collected from the non-glacial unit of the Ridge Site and submitted for radiocarbon dating (Fig. 3-2; Table 3-1). Organic matter was separated from the

clay-rich sediment matrix by ultrasound with the addition of distilled water and sieving with a 90-μm mesh, followed by a standard acid-alkali-acid radiocarbon treatment (Hatté and Jull, 2007). No rootlet structures were observed in the radiocarbon samples. One sample from the non-glacial unit was submitted for OSL dating (indicated on Fig. 3-2); however, only 4 of 40 total aliquots had a 'fast component' exceeding >15 (Durcan and Duller, 2011), as a result the ages were non-interpretable (data not shown). We did not pursue OSL dating at this site any further.

A set of 35 pollen samples was collected at 5- or 10-cm intervals from the non-glacial unit. The lower 20 samples were collected from the faintly bedded clay and silts, and the upper 15 samples were collected from the sandy and silty infill sediment facies (Fig. 3-2). Sub-samples of 1 cm^3 were processed for palynology using standard methods including acid digestion and sieving (Faegri and Iversen, 1975). Pollen was identified using the pollen reference collection at the Paleoecology Laboratory at the University of Toronto and at the Royal Ontario Museum (Toronto, Canada), in addition to Kapp et al. (2000) and McAndrews et al. (1973). Pollen concentrations were estimated by the addition of a known number of exotic *Lycopodium* spores (Stockmarr, 1971). An average of 156 arboreal, shrub and herb pollen grains was counted at each fossil interval. Only intervals where pollen concentration exceeded 5000 grains per cm^3 were considered for this study.

Sedimentological and macrofossil samples were taken along the lower 150 cm of the non-glacial unit during field sampling in 2013. Macrofossils were used to reconstruct local plant communities, as well as provide an independent qualitative proxy for temperature, since quantitative methods derived from pollen assemblages are subject to a variety of biases and errors (Birks and Birks, 2000; Salonen et al., 2013a; Salonen et al., 2013b). In total, 14 samples in 10-cm intervals were analysed for plant macrofossils. Macrofossil samples of 15 cm^3 were cleaned under running water using a 100-μm mesh sieve. The residuals remaining on the sieve were analysed under a stereomicroscope. Some of the samples were soaked in $Na_4P_2O_7$ x H_2O solution overnight to disaggregate mineral clusters.

Organic, carbonate and minerogenic contents of the non-glacial unit were estimated using standard loss-on-ignition (LOI) methods (Heiri et al., 2001). Particle size analysis (PSA) was used to obtain size class distributions for inorganic sediments. Samples were heated in HCl to

remove carbonates, then digested in H_2O_2 until all organic reaction ceased and finally soaked in 1% Na_2CO_3 for 2 hours to dissolve any diatoms. Samples were then disaggregated with sodium hexametaphosphate and particle size was determined by using a Malvern Mastersizer 3000 and Hydro MV wet dispersion unit.

3.4.3 Statistical analyses of pollen data

Palaeoclimate inferences are derived from the North American Modern Pollen Database (NAMPD; Whitmore et al., 2005), which has been shown to reliably estimate temperature and precipitation using the Modern Analogue Technique (MAT) over many vegetation biomes in North America (e.g. Fréchette and de Vernal, 2013; O'Reilly et al., 2014; Gajewski, 2015; Richerol et al., 2016). However, there are few data points in the NAMPD from the HBL. Thus, to ensure regional representation in the modern calibration set, and to improve the potential similarity of analogues, we first synthesized all available modern pollen data for the HBL and amalgamated this dataset with the NAMPD data. Sites not previously included in the NAMPD were obtained from several sources, including Potzger and Courtemanche (1956), Terasmae and Hughes (1960), Lichti-Federovich and Ritchie (1968), Terasmae and Anderson (1970), Skinner (1973), Farley-Gill (1980), Bazely (1981), Kettles et al. (2000), Dredge and Mott (2003), Glaser et al. (2004), Friel et al. (2014) and O'Reilly et al. (2014). We also contribute modern pollen assemblage data from 5 new sites, collected in the summer of 2010 and 2011, which were processed and counted using standard methods (Faegri and Iversen, 1975). The locations of modern pollen data from the HBL region are shown in Fig. 3-1 and all newly compiled data are provided in Appendix D.

Taxonomic harmonization was performed over the entire modern pollen dataset to enable statistical intercomparison of sites. This process involved grouping, for example, *Ambrosia*, *Artemisia,* Tubuliflorae, and Liguliflorae into “Asteraceae”. Similarly, *Picea glauca* and *P. mariana* were merged, since they were often not distinguished in the modern dataset. Family, genus and species names were then updated to reflect modern-day naming conventions as dictated by the Integrated Taxonomic Information System on-line database (http://www.itis.gov).

The original NAMPD contained 4833 sites, and we added 49 new sites from the HBL, resulting in a modern dataset of 4882 sites. However, to improve the accuracy of palaeoclimate estimates, only samples from the NAMPD that reached a sum of >150 grains of arboreal, shrub and herb

pollen types were retained for analysis. Further, only those samples in the conifer/hardwood, boreal and forest-tundra biomes, as defined by Fedorova et al. (1994) were included in the modern-day calibration set (1617 modern sites). Our decision to include only sites from the present-day biome of the HBL (boreal and forest-tundra) as well as the conifer/hardwood biome was based on examining the general assemblage contained in all sub-till records from the HBL, which, in addition to boreal-type pollen, contains infrequent hardwood-type taxa (e.g. *Acer*, *Quercus*).

Temperature and precipitation data for sites not already included in the NAMPD were based on a 30-year average (1971 to 2000), and obtained from Natural Resources Canada (2015), which interpolates climate variables based on the closest weather stations. Four different variables were explored for the potential for reconstruction: mean annual temperature, total annual precipitation, mean summer temperature (June, July, August), and total precipitation for the summer months. We used a stepwise variance inflation factor test to remove any variables that exhibited collinearity in the calibration dataset (R package "usdm": Naimi, 2015). This resulted in the removal of mean annual temperature. Next, the $\lambda 1/\lambda 2$ ratio was calculated (Ter Braak and Prentice, 1988). Only variables with a ratio of >1 were retained for reconstruction (Juggins et al., 2014).

Prior to reconstructing palaeoclimate at the Ridge Site, fossil pollen counts were converted to relative abundance using a sum of all arboreal, shrub and herb pollen. Thirty pollen types were present at >0.5% in any one fossil sample and were included in the paleoclimate reconstruction. These were composed largely of *Picea*, *Pinus*, *Betula*, *Salix*, Asteraceae, *Alnus*, Poaceae, Ericaceae and Amaranthaceae, all of which had a mean abundance of >1%. The remaining <1% of pollen grains were *Corylus*, *Tilia*, Ranunculaceae, *Selaginella*, *Shepherdia*, Aquifoliaceae, *Abies*, *Carpinus/Ostrya*, Cupressaceae, *Lycopodium*, Juglandaceae, Polygonaceae, *Ulmus*, *Fraxinus*, *Larix*, Rosaceae, Rubiaceae, *Quercus*, *Acer*, Onagraceae, and *Sarcobatus*. Wetland elements (Cyperaceae and *Sphagnum*), were excluded from the reconstruction on the basis of high and variable local over-production. While we acknowledge that some of the taxa retained in the analysis are locally present (e.g. *Salix*), the elimination of the most variable and abundant local wetland taxa results in fossil pollen assemblages that largely reflect a more regional signal. This approach has been used successfully in other pollen-based reconstructions and has resulted

in palaeoclimate reconstructions well-supported by independent proxies (e.g. Shuman et al., 2004; Viau and Gajewski, 2009).

A squared chord distance dissimilarity coefficient, implemented using the R package 'analogue' (Simpson, 2007; Simpson and Oksanen, 2014), was used to determine the similarity of modern and fossil pollen assemblages (Overpeck et al., 1985). Any samples exceeding a dissimilarity index of 0.15 were taken to be non-analogues. Predicted climate variables were based on k = 3 closest analogues (Williams and Shuman, 2008) and n = 500 bootstrap iterations. Errors for the quantitative estimates are based on the root mean squared error of prediction (RMSEP) at k = 3 analogues. Stratigraphic plots and constrained incremental sum-of-squares (CONISS) zoning by comparison to a broken stick model (Bennett, 1996) were implemented using the R package 'rioja' (Juggins, 2015).

3.5 Results

3.5.1 Stratigraphy of the Ridge Site

The lowermost exposed unit of the Ridge Site, the lower diamicton, consists of 6 m of massive to blocky very fine sandy silt, containing granules, pebbles, cobbles and boulders (Fig. 3-2). This diamicton contains isolated boulders with faceted and striated tops, with striations oriented between 180° and 220° Az. A boulder line observed one m above the exposed base of this unit had boulders with striated tops and a similar range of striation orientations. Low angle shear planes were observed within the diamicton and deformed lenses of sand and gravelly sand indicate movement toward the south-southwest. Particle size analysis of the matrix indicates that the lower diamicton consists of 36% sand, 50% silt and 14% clay. The carbonate content of the silt-clay fraction of the matrix is about 50% with a calcite-to-dolomite ratio of 1.6. At the time of sampling (June 2011 and August 2013), up to 1.5 m of slumped material covered the lower part of the exposure above river level. Thus, the full extent of the lower diamicton unit is not known, and it may extend below river level. The upper contact of the diamicton is irregular with low relief.

The middle unit at the Ridge Site, the non-glacial unit, is a 3.0-m interval of stratified sediments (Fig. 3-2). This is the location of the biostratigraphic (pollen, macrofossil) sampling. The lower 20 to 30 cm is composed of stratified sand and silty sand with rare thin diamicton lenses, resting

on an irregular lower contact (Fig. 3-3A). These sediments grade upward into approximately 280 cm of faintly laminated and colour-banded silty clay and clayey silt with finely disseminated organic matter and thin, discontinuous laminations of silt and rarely, very fine sand (Fig. 3-3B). The top of these fine-grained sediments is marked by an angular unconformity with at least 90 cm of negative relief, filled by sands and silts containing organic detritus (Fig. 3-3C,D). The entire Ridge Site can be seen in Fig. 3-3E. Organic content is 11 to 15% throughout the lower 150 cm of the non-glacial unit, and carbonates are generally less than 5%, but increase to 12% at the base of this section at the diamicton contact.

The upper unit at the Ridge Site, the upper diamicton, contains massive to blocky, very fine sandy silt with minor clay (Fig. 3-2). Granules, pebbles, cobbles and boulders are also present. This diamicton is about 6 m in thickness with a sharp lower contact with the underlying sediments. One large inclusion, up to 1.7 m, consisting of small pebble gravel and very fine sand and silt was observed within this diamicton layer. Rare, isolated boulders had striated tops with the orientations of 260° Az. Samples from the matrix of the diamicton average 26.5% sand, 57.5% silt and 16% clay. The average total carbonate content in the silt-clay fraction is 43% and the average carbonate ratio is 1.3. Overlying this massive, sandy silt diamicton is a 1.7-m to 3-m sediment interval that coarsens upward toward the top of the exposure. The interval consists of interbedded very fine sandy silt and very coarse sandy granule gravel, grading upward into pea-size pebble gravel with inter-beds of fine-grained sand.

3.5.2 Chronology

Two finite radiocarbon ages suggest that the non-glacial unit at the Ridge Site may date to MIS 3 (40 000±400 cal. a BP and 49 600±950 a ^{14}C), while one age was infinite (>48 800 a BP; Table 3-1).

3.5.3 Pollen and macrofossils

Overall, palynomorphs were moderately well-preserved at the Ridge Site, with 24 of 35 intervals containing sufficient concentrations (Fig. 3-4). Several intervals of poor pollen preservation correspond to the transition between clay-rich sediments toward more silt/sand rich sediments immediately above the unconformity, as well as the base and top of the non-glacial unit near the diamicton contact. Arboreal assemblages were dominated by *Picea* (mean 46%), and *Pinus*

(mean 30%), with *Salix*, *Alnus* and *Betula* all averaging less than 10%. The herbaceous component consisted of Asteraceae, Ericaceae, Amaranthaceae and Poaceae similarly averaging less than 10% throughout the non-glacial unit. Pollen of locally-abundant wetland indicators (*Sphagnum* and Cyperaceae) ranged from <10% to 110% of the herb, arboreal and shrub pollen sum. There are two significant zones in the pollen assemblages delineated using CONISS and the broken stick method: 0 to 230 cm, and 250 to 280 cm.

Macrofossils were present in all sampled intervals of the Ridge Site; however, preservation was at times poor and fragments were small. Woody plant remains, bryophytes and charcoal were the most commonly preserved macrofossils (Fig. 3-5). Bryophytes consisted of intact *Scorpidium* spp. and *Sarmentosum exannulatum*, as well as rare/fragmented *Polytrichum* spp., *Calliergon* spp., *Sarmentypnum sarmentosum*, *Sphagnum* spp. and *Tomenthypnum nitens*. Despite no obvious succession in the macrofossil record, some plant remains become more abundant within the 40-cm interval which corresponds to an increase in the clay fraction of the stratigraphy. In particular, conifer remains were continuously present in the samples above the 40-cm interval, indicating the persistent local presence of these taxa.

3.5.4 Pollen-derived palaeoclimate reconstruction

The pollen-climate model resulted in a predictive ability similar to what is reported in other studies (e.g. Williams and Shuman, 2008; Richerol et al., 2016). The coefficient of determination (R^2) between observed and predicted annual precipitation was 0.79, while that for mean summer temperature was 0.83. The RMSEP values were 170 and 1.5, respectively. Further details on the underlying statistical model are shown in Appendix E. Each fossil interval at the Ridge Site had >20 potential analogues, therefore satisfying the criteria for reconstruction using the modern analogue technique (Overpeck et al., 1985). Of the 72 possible analogues (e.g. k = 3 analogues for each of the 24 fossil intervals), only 32 unique sites were used for palaeoclimate reconstructions. Four of these sites were from our newly-compiled data used to supplement the NAMPD. Based on the 3 closest analogues, the total annual precipitation throughout the fossil interval was 527±170 mm per year, as compared to an estimated 705 mm per year at that site in present-day (Fig. 3-4). Estimates for summer temperature averaged 14.6±1.5 °C, which is indistinguishable from present-day temperature estimates for the Ridge Site (15.5 °C).

3.6 Discussion

3.6.1 Lower and upper diamicton

The lower diamicton is interpreted to be a subglacial till deposited by an actively flowing glacier moving toward the south-southwest (180° to 220° Az) over Middle Devonian formations dominated by limestone. This interpretation is supported by the boulder line with consistent orientation of striae in the lower part of the exposure, and the isolated boulders with striated tops that are similarly oriented. In addition, the low angle shear planes within the diamicton, and the direction of movement indicated by them, are consistent with the direction of movement indicated by the striae on the boulder tops, all of which would indicate the direction of ice flow that deposited the diamicton. In comparison to other till samples collected in the Ridge River area (Barnett and Yeung, 2012; Nguyen et al., 2012; Nguyen, 2014), the lowermost till contains the highest amount of total carbonates in the silt/clay fraction and the highest calcite-to-dolomite ratio.

The upper diamicton is also interpreted as till. Its massive nature and inclusion of clasts with striated tops indicate glacial movement to the west-southwest, which would traverse an even longer distance over the Middle Devonian limestone rocks. This is consistent with fluting that occurs on remotely sensed images and digital surface models in the area (Barnett et al., 2009). The large inclusion of gravelly sand may have been eroded from the underlying fluvial sediments in the non-glacial unit. The lower calcite and higher dolomite content in this till, however, might suggest that the underlying bedrock formations were covered during this advance, and that the more-distant dolomitic rocks of Upper Silurian and Lower Devonian formations sub-cropping in James Bay (Ontario Geological Survey, 1991) may have influenced the final carbonate content of this till. The uppermost unit exposed in the section, the stratified sands and gravels, is interpreted as beach and near shore deposits probably formed at the regressing margin of the post-glacial Tyrrell Sea (Lee, 1960).

3.6.2 Non-glacial unit

Age determinations from the non-glacial unit were previously discussed in a compilation of all available chronology data from the Missinaibi Formation, and contribute evidence towards an ice-free HBL during MIS 3 (Dalton et al., 2016; Chapter 2 of this dissertation). At the base of the

non-glacial unit, the irregular 20-cm lower contact is interpreted as erosional and likely marks the base of a former river channel. Here, the infilling sediments are gravelly and probably the result of the erosion of the till below. The diamicton lenses are interpreted as debris flows from the flanks of the channel; however, it is possible that they are flow tills and that the lower part of the non-glacial unit was deposited along the ice margin rather than in a fluvial setting.

Overlying these sediments, the predominantly silts (excluding the angular unconformity), are similar to the sediments described from Marion Lake, a now drained, but once perennial closed-basin oxbow lake in southern Manitoba (Brooks, 2003; Brooks and Medioli, 2003). Sediments deposited within oxbow lakes have been described as massive to faintly laminated, and dominated by silt-sized particles with little to no vertical textural grading throughout the fill sequence (Allen, 1965; Brooks, 2003; Brooks and Medioli, 2003), which is similar to the Ridge Site. However, aquatic indicators in the pollen and macrofossil data are in low abundance compared to other inferred lacustrine sites (Bos et al., 2009; Bajc et al., 2015), which suggests that standing water throughout the time of accumulation was unlikely. We therefore suggest that this interval may represent a drier surface, marginal to the river channel, possibly at the entrance to a cut-off meander, with local presence of shrubs including *Betula*, S*alix* and conifers, as confirmed by macrofossil analyses. A modern-day example of such an environment can be seen in Fig. 3-6. We interpret the upper part of the non-glacial unit, the unit contained within an angular unconformity, to be the base of a channel that cut into the material below by renewed river activity or localized drainage. These fluvial sediments suggest drainage-related changes to the river system, which are frequent processes in the modern landscape, as shown by the many oxbow lakes and ancient river scars that are present in the HBL today.

Typical boreal peatland taxa such as Cyperaceae, *Picea*, *Pinus* and *Sphagnum* suggest that vegetation communities similar to the present-day HBL are preserved at the Ridge Site (Figs 3-4, 3-5). Polypodiaceae spores suggest the local presence of ferns, and these, in combination with bryophyte remains, confirm the presence of riparian wetland conditions. Herbaceous taxa such as Asteraceae, Ericaceae, Amaranthaceae and Poaceae suggest an intermittently open canopy. The modest decline in *Sphagnum* spores paired with the small increase in pollen of Cyperaceae toward the top of the non-glacial unit may suggest increased nutrients over time in the local environment, reflecting stream dynamics. Occasional river flooding may have contributed to the sedimentological features of the preserved site, along with the occasional presence of aquatic

indicators (*Potamogeton*, *Pediastrum*; Fig. 3-4). These wet/dry cycles may help explain the intervals of poor pollen preservation, since corrosion of pollen grains can be indicative of exposure of the grains and the sedimentary matrix to aerobic environments or wet/dry cycles.

Although abundances are low, macrofossil data permit key inferences about palaeoenvironmental conditions at the Ridge Site. The presence of *Betula* and *Salix* bark, along with *Betula* seeds confirm that these taxa were locally present. These taxa are generally intolerant to shade and tend to grow along recently disturbed river banks, suggesting that local parts of the forest canopy were open. Such environments are common in the HBL today. Furthermore, the presence of conifer bark and needles (cf. *Pinus)* also confirms the local presence of these taxa. However, conifer remains are difficult to differentiate when fragments are small, rare and not well preserved. If these remains are indeed *Pinus*, this would be notable because this tree is not common in the area today; recent vegetation surveys indicate that *Pinus banksiana* is only occasionally noted in well-drained regions of the HBL (Riley, 2003). The presence of large (>1 mm) and small (<1 mm) charcoal fragments suggests local and regional forest fires. Although fire is a more significant process in the drier boreal regions of western Canada (e.g. Hickman and Schweger, 1996; Philibert et al., 2003), it is a component of ecosystem dynamics in the eastern Canadian boreal forest as well (e.g. Cyr et al., 2005). Fires may have been more frequent and/or more intense under drier climatic regimes. Although macrofossil remains were rare and low in diversity at the Ridge Site compared to other interstadial and interglacial sites from northern Europe (Bos et al., 2009; Väliranta et al., 2009; Helmens et al., 2012; Helmens et al., 2015; Houmark-Nielsen et al., 2016; Sarala et al., 2016), these data yield important supporting information for palaeoenvironmental inferences.

3.6.3 Palaeoclimate reconstruction

Our palaeoclimate reconstruction of the non-glacial unit of the Ridge Site suggests similar or perhaps somewhat cooler summer temperatures as compared to present-day, and lower total annual precipitation, as constrained by the errors on the reconstructions, and the limitations of the datasets available. Poaceae and *Salix* pollen in the fossil record are driving this result, and fossil pollen samples were, for the most part, most closely analogous to boreal/grassland transition sites in central and western Canada. This finding suggests that climate in the HBL may have been more continental in character during this period. These results are comparable to other

records from North America suggesting that annual precipitation patterns may have been different from present-day during MIS 3 (Van Meerbeeck et al., 2009; Brandefelt et al., 2011; Sionneau et al., 2013) owing to partial continental glaciation (Grant et al., 2014).

There are few available MIS 3 palaeoclimate datasets for comparison with the Ridge Site, because such records are rare owing to glacial erosion, difficulty in dating, poor preservation, and, when present, climate estimates are largely qualitative. For example, Bajc et al. (2015) inferred a boreal forest or perhaps treeline/tundra-type environment in southern Ontario during MIS 3 on the basis of pollen and plant macrofossils. Similarly, Karrow and Warner (1984), Karrow et al. (2001) and Warner et al. (1988) document a *Pinus* and *Picea*-dominated assemblage indicating that a boreal forest and/or tundra environment was present during that time at other sites near the southern periphery of the LIS. These studies are notable since they are all located 100-300 km south of the present-day boreal forest. Thus, results from the Ridge Site, as well as other purported MIS 3 sites from the periphery of the Laurentide Ice Sheet, suggest an expanded boreal forest zone as compared to present-day, with generally cooler and drier conditions throughout much of the previously glaciated region.

Along with characterizing the palaeoenvironment of a site that we tentatively assign to MIS 3 on the basis of radiocarbon dates, till stratigraphy and biological proxies, one of the main objectives of this study was to determine whether deposits belonging to MIS 3 could be differentiated from deposits dating to off-peak MIS 5 on the basis of pollen assemblages. Fig. 3-7 shows a palaeoclimate reconstruction from the Nottaway River in the James Bay Lowlands, adjacent to our study region, using the same methods and modern calibration set as the Ridge Site. The Nottaway River site was chronologically constrained broadly to off-peak MIS 5 based on U-Th dating (Allard et al., 2012). Similar to the Ridge Site, reconstructed summer temperature was comparable to present-day at the Nottaway River site (data not shown). However, notably, reconstructed annual precipitation was an average of 865±192 mm as compared to 652 mm present-day at the MIS 5 Nottaway River Site (Fig. 3-7), suggesting increased moisture during MIS 5 relative to today. However, this stands in contrast to the drier conditions documented for the Ridge Site, hypothesized to date to MIS 3 (Figs 3-4, 3-7). Thus, if chronology data and the resulting palaeoclimate interpretations from these sites are well supported, MIS 3 and off-peak MIS 5 sites from the HBL could be differentiated on the basis of relative continentality: MIS 3 is characterized by lower total annual precipitation and off-peak MIS 5 by similar or greater than

present-day. Additional MIS 3 and off-peak MIS 5 sites are needed to further test this hypothesis. Moreover, there is a need to better understand and quantify the climate variability during MIS 5a-d, which fluctuated between relative cool stadials (MIS 5d, 5b; peaks: *c*. 109 000 a BP and *c*. 87 000 a BP) and warmer interstadials (MIS 5c, 5a; peaks: *c*. 96 000 a BP and *c*. 82 000 a BP). Nevertheless, our results suggest that, with additional sites and additional data, pollen-based reconstructions may hold the potential to be developed into a valuable tool for assigning ages and characterizing palaeoenvironments in sediments of the Missinaibi Formation.

While the errors associated with the palaeoclimate estimates from the Ridge Site (±1.5 °C for average summer temperature; ±170 mm for total annual precipitation) are similar to Holocene palaeoclimate reconstructions from the HBL and the forest-tundra transition zone of Canada (Bunbury et al., 2012; Richerol et al., 2016), further reducing these errors is important if pollen-based inferences are to be used as a chronological tool for assigning age(s) to the Missinaibi Formation. However, a main obstacle in reducing this error is that typical boreal/peatland taxa are found extensively across large biogeographic ranges in North America (Whitmore et al., 2005) and therefore have widespread climatic tolerances. One way to reduce this error may be the removal of extra-regional (wind-transported) pollen grains, which can lead to a pollen assemblage which is inconsistent with the local vegetation (Birks and Birks, 2000). This technique permitted errors on palaeoclimate reconstructions from the Arctic to be reduced to ±0.6°C for July temperature and ±19 mm for total annual precipitation (Peros and Gajewski, 2008; Peros et al., 2010). However, this may not be appropriate in a treed landscape. Also, little is known about the distribution of local, regional or distant vegetation in the HBL during MIS 3 since macrofossil fragments were sparse and sometimes poorly preserved at the Ridge Site. In this case, the macrofossil record represents only a fraction of the local vegetation. The continued development of multi-proxy techniques and independent proxies for palaeoclimate such as chironomids, diatoms, insect remains, stable isotopes, leaf wax biomarkers and bacterial membrane lipids (Huang et al., 2006; Engels et al., 2008; Väliranta et al., 2009; Weijers et al., 2011; Helmens et al., 2012; Nichols et al., 2014; Helmens et al., 2015; Houmark-Nielsen et al., 2016) are critical for refining our understanding of the Missinaibi Formation and other Pleistocene palaeoenvironments.

Overall, there was less stratigraphic variation in pollen and macrofossil data at the Ridge Site as compared to sub-till interstadial and interglacial sites from northern Europe. This is probably the

result of depositional setting, since non-glacial records from Fennoscandia more frequently originate from lacustrine settings (Bos et al., 2009; Helmens et al., 2012; Helmens et al., 2015), which often record more detailed vegetation dynamics. For example, a biostratigraphic investigation of an inferred oxbow lake at Sokli, northern Finland, allowed for the recognition of succession from a birch- to pine- to spruce-dominated local environment during MIS 5c (Helmens et al., 2012). Similarly, Helmens et al. (2015) used pollen and macrofossil data to document a short-lived cooling event during MIS 5e, which was preserved in a gyttja deposit. Such detailed vegetation data allow the different time periods (e.g. MIS 3 and MIS 5) in Fennoscandia to be distinguished based not only on temperature and/or precipitation, but also from understanding succession of the vegetation community during the time period of question. An equally detailed pollen, diatom and macrofossil record dating to MIS 3 was also presented by Sarala et al. (2016). Since vegetation succession is not well preserved at the Ridge Site, there is less potential for detailed inferences of plant community changes during MIS 3 in the HBL. Nevertheless, oxbow lakes are common in the present-day HBL, so it is likely that lacustrine-type sediments are preserved as part of the Missinaibi Formation and will be the subject of future studies.

3.7 Conclusions

As the HBL is located near the centre of growth of many Pleistocene ice sheets, the occurrence of non-glacial intervals in this region corresponds to either largely retreated or highly dynamic ice sheets over North America. Radiocarbon dating suggests that the non-glacial interval at the Ridge Site may date to MIS 3, which would mean significant reduction of the central part of the Laurentide Ice Sheet prior to the build-up toward the last glacial maximum. Such MIS 3 ages had been previously reported in the region (Andrews et al., 1983; Berger and Nielsen, 1990), but remained tentative owing to errors and uncertainties in dating. Continued dating of similar Pleistocene-aged records is critical for developing an accurate understanding of past glaciation, and developing accurate climate models.

Pollen, macrofossils and sedimentological proxies at the Ridge Site provide one of the few quantitative accounts of palaeoenvironment from the previously glaciated region. Palaeoclimate reconstructions from the Ridge Site, along with other sites from the periphery of the Laurentide Ice Sheet, suggest that dry, expansive boreal vegetation colonized much of the previously

glaciated region. Our discovery of subtle vegetation (and thus, climate) differences between this purported MIS 3 site and an off-peak MIS 5 site in the adjacent James Bay Lowlands highlights the potential for vegetation assemblages to be used as an inferential dating technique. The continued development of such quantitative techniques may prove to be a valuable tool for assigning ages to sub-till records in the HBL region, since pollen is well preserved and thoroughly documented at many undated sub-till sites.

3.8 Acknowledgements

Funding for this study was provided by the Ontario Geological Survey and grants from the Natural Sciences and Engineering Research Council (Canada) to SAF, and from the Northern Scientific Training Program and University of Toronto Centre for Global Change Science to ASD. We thank Maurice Nguyen for valuable field assistance and for his work on the Ridge River till stratigraphies, along with Guillaume Allard and Martin Roy for providing pollen data from the Nottaway River site for comparative palaeoclimate analysis. A further thank you to D. Bazely for modern pollen records; J.-P. Iamonaco, M. Sobol, D. Valls, A. Megens and T. Hui for laboratory assistance; J. Desloges for the use of the Malvern Mastersizer 3000 and Hydro MV wet dispersion unit, and S. Forman for attempting an OSL date at the Ridge Site. Some data were obtained from the Neotoma Paleoecology Database (http://www.neotomadb.org), and the work of the data contributors and the Neotoma community is gratefully acknowledged. We also thank two anonymous reviewers whose insightful comments helped improve the paper.

3.9 Tables

Table 3-1. Radiocarbon dating results from the Ridge Site. 'F14C' indicates the percent of modern carbon measured in the sample. Where the F14C was not distinguishable from background, the age is marked with a dagger (†) and the background age was assigned to that sample (Stuiver and Polach, 1977). Dates that are finite were calibrated using CALIB Rev 7.0.4 and the 2013 calibration curve (Stuiver and Reimer, 1993; Reimer et al., 2013). Dates which exceed the calibration curve, denoted with an asterisk (*), could not be calibrated and are reported as radiocarbon years (a ^{14}C). All ages were rounded to the nearest 100 and errors were rounded to the nearest 50. All radiocarbon dates were analyzed at the A.E. Lalonde AMS Laboratory, Ottawa, Canada. Chronology data from the Ridge Site were previously reported in Dalton et al. (2016) (Chapter 2 of this dissertation).

Lab ID	Material dated	Sample interval (cm)	F14C	Assigned age
UOC-0591	peat	160 cm	0.0092 ± 0.0003	40 000±400
UOC-0592	peat	50 cm	0.002 ± 0.0002	49 600±950 †*
UOC-0842	peat	50 cm	0.0019 ± 0.0001	> 48 800

3.10 Figures

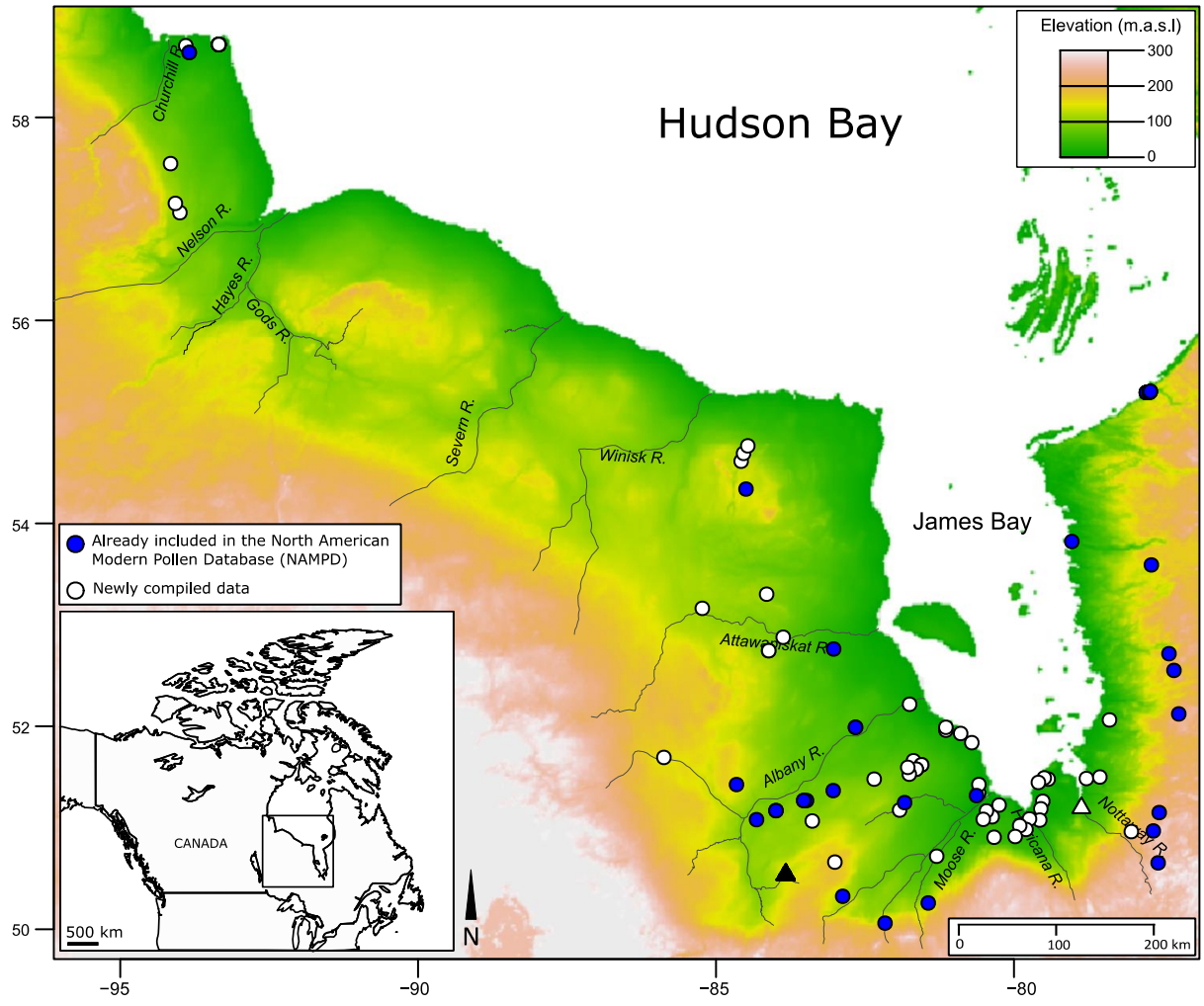

Fig. 3-1. Map of the Hudson Bay Lowlands showing the location of modern pollen samples from the North American Modern Pollen Database (NAMPD; blue circles) (Whitmore et al., 2005) along with modern data that were newly compiled for inclusion in this study (white circles; Appendix D). The Ridge Site is shown (black triangle), along with the Nottaway River Site (white triangle; Allard et al., 2012). Elevation data are from Amante and Eakins (2009). Inset map locates the study area (square) on the North American continent. Scale on inset map is approximated for 50° N.

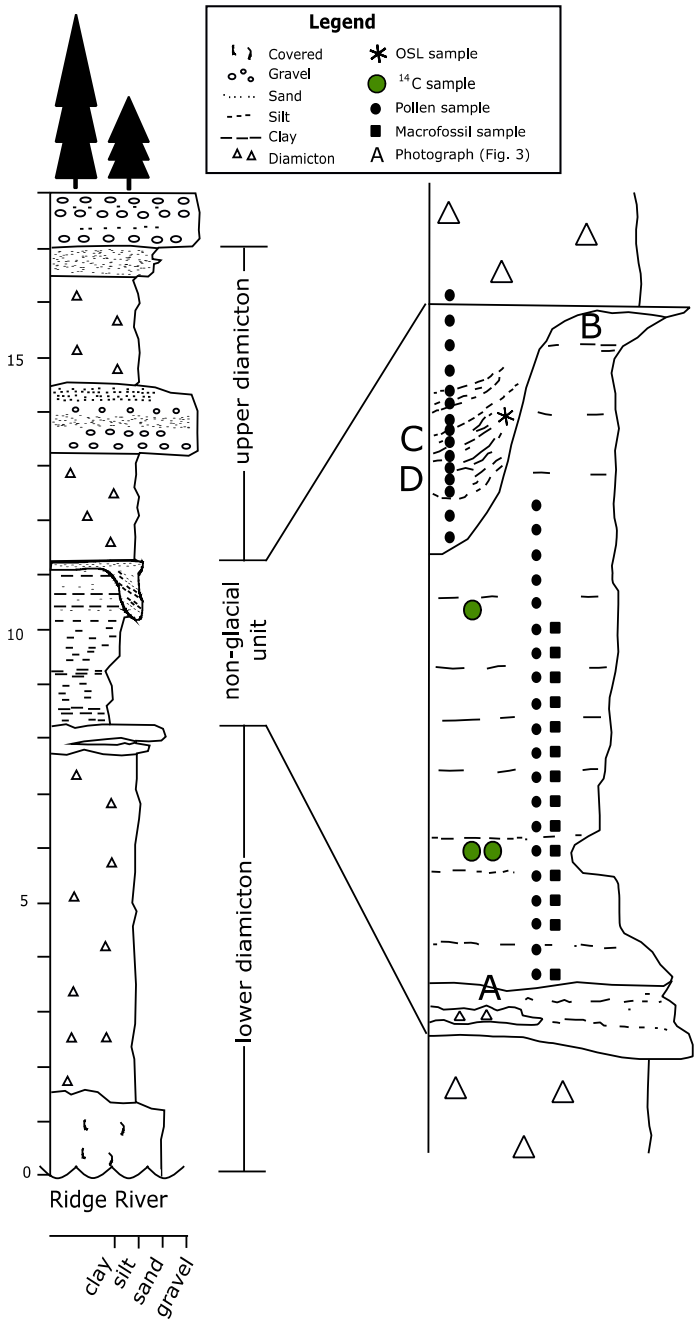

Fig. 3-2. Stratigraphy of the 18-m section studied at the Ridge Site, along with sampling details for pollen and macrofossils in the non-glacial unit. Tick marks on the left-most stratigraphic plot indicate elevation above river level (in m). Black circles indicate pollen sampling locations and black squares indicate macrofossil sampling locations. Green circles indicate location of samples for radiocarbon dating. See Fig. 3-3 for corresponding field photographs taken at points A, B, C and D.

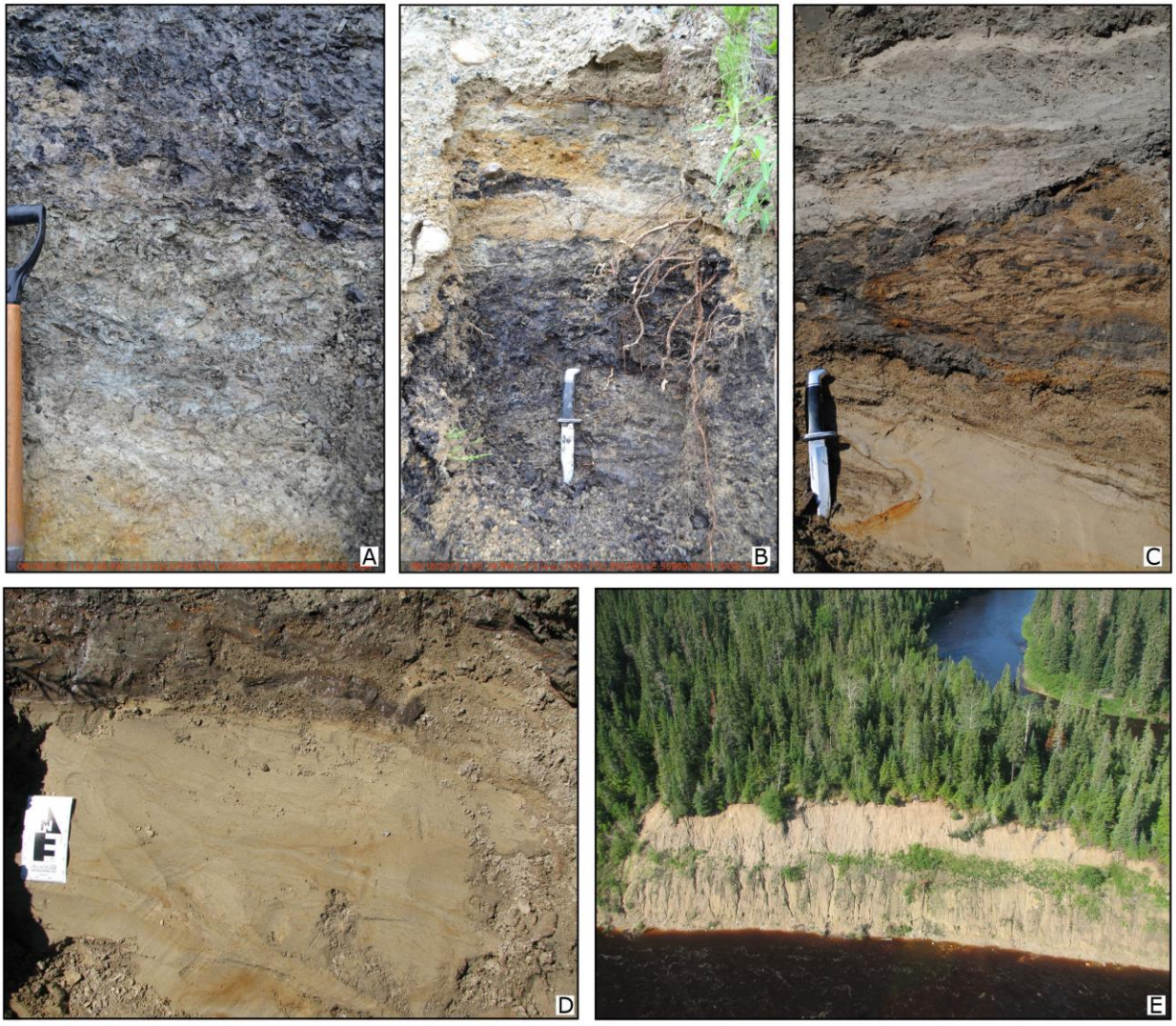

Fig. 3-3. Field photographs from the Ridge Site. The position of each photograph is indicated in the text as well as by letters A through D in Fig. 3-2. A. Lower 20 to 30 cm of the non-glacial unit where stratified sand and silty sand are separated with rare thin diamicton lenses. The irregular lower diamicton can be seen as the light-colored sediments at the bottom of the photograph. The dark interval at the top of the photograph is the location of pollen and macrofossil sampling. B. Upper part of the non-glacial unit at till contact. The dark interval at the bottom of the photograph is the location of pollen sampling. C and D. Close-up of interbedded sands and silts containing organic detritus. E. Aerial view of the Ridge Site in 2012. The vegetation line across the face of the river bank is where the organic-bearing muds occur.

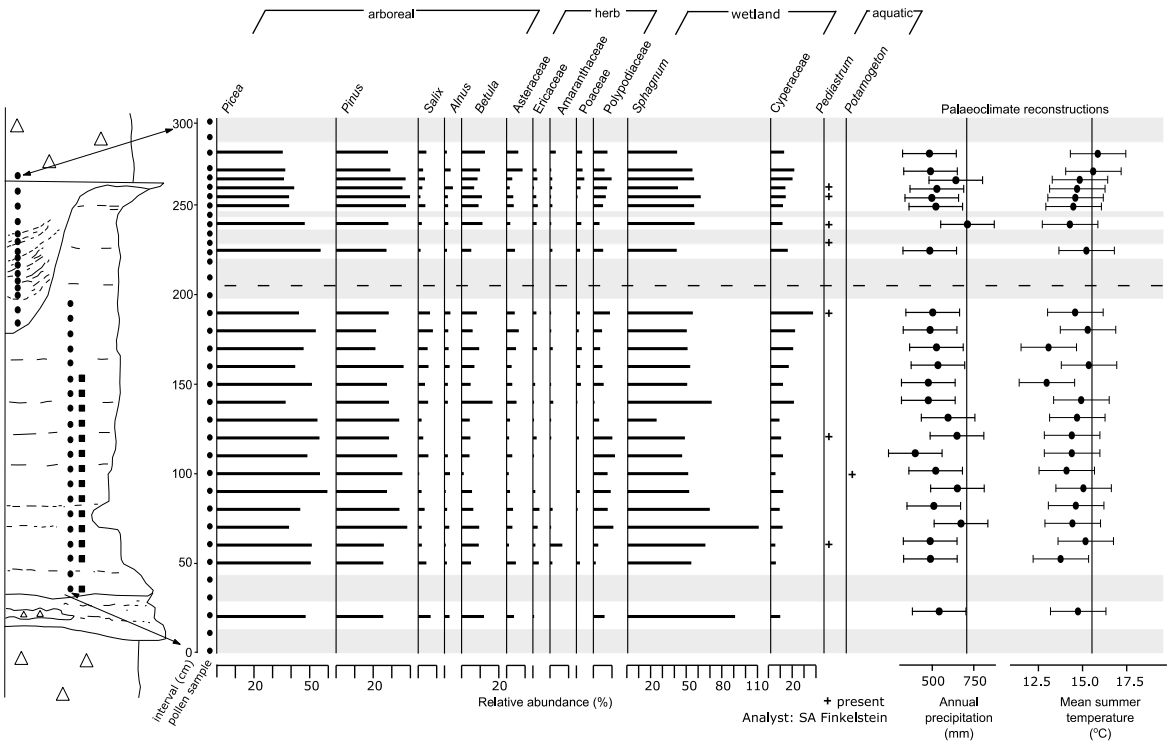

Fig. 3-4. Palynology and pollen-derived palaeoclimate reconstructions from the Ridge Site. The stratigraphic plot shows the location of each pollen interval at the site (circles) as well as the location of macrofossil samples (squares). See Fig. 3-2 for an explanation of symbols in the stratigraphy sketch. Shaded regions correspond to pollen samples that were excluded on the basis of poor preservation (e.g. <5000 pollen grains cm^{-3}). For intervals with good preservation, all pollen/spore taxa reaching 2.5% relative abundance in at least one sample are shown. See text for a complete list of pollen taxa used in the palaeoclimate reconstruction. Total annual precipitation and average summer temperature were reconstructed for the Ridge Site using the modern analogue technique (see text for details). Vertical lines indicate present-day summer temperature (15.5 °C) and total annual precipitation (705 mm) at the Ridge Site. NB: For the purposes of this figure, the samples in the overlying unconformity were placed above those from the clay/silt-rich unit. This transition is indicated by the dashed line.

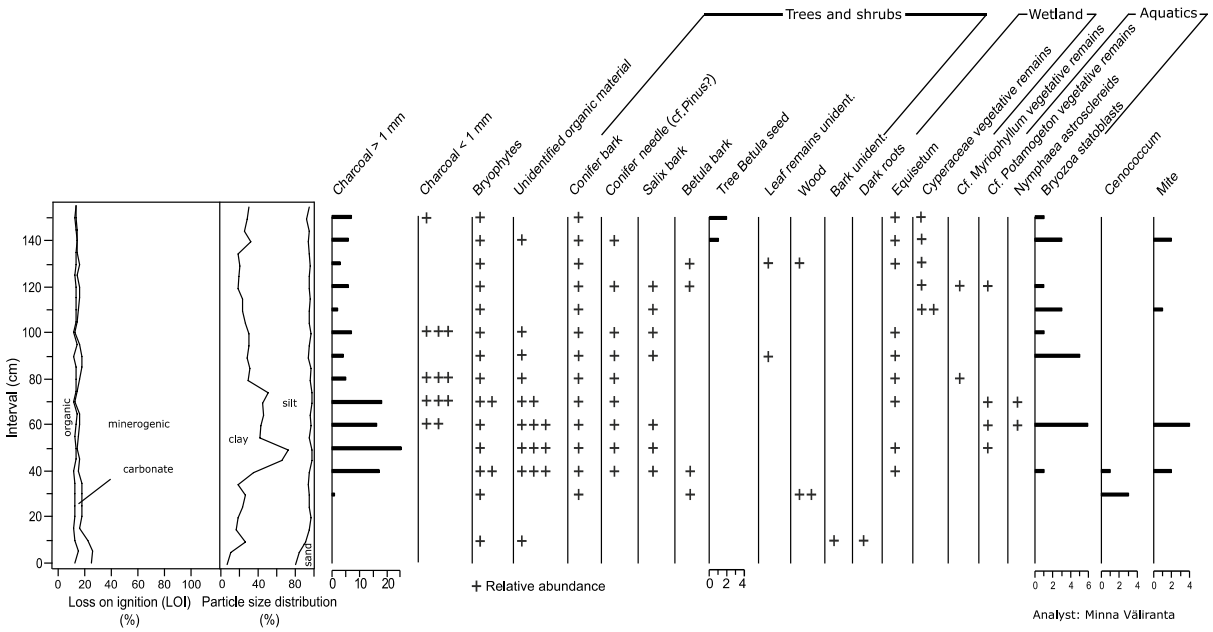

Fig. 3-5. Loss-on-ignition, particle size and macrofossil data from the lower 150-cm of the non-glacial unit at the Ridge Site. Macrofossil data are presented in raw counts, and crosses indicate present (+), frequent (++) and abundant (+++) representation in the sample. See Fig. 3-2 for the location of these samples relative to pollen samples.

Fig. 3-6. A modern-day example of the inferred palaeoenvironment preserved in the non-glacial unit at the Ridge Site: a shrub-covered area at entrance to cut-off meander (indicated by an arrow). The cutoff meander in this photograph is located ~50 m downstream from the Ridge Site.

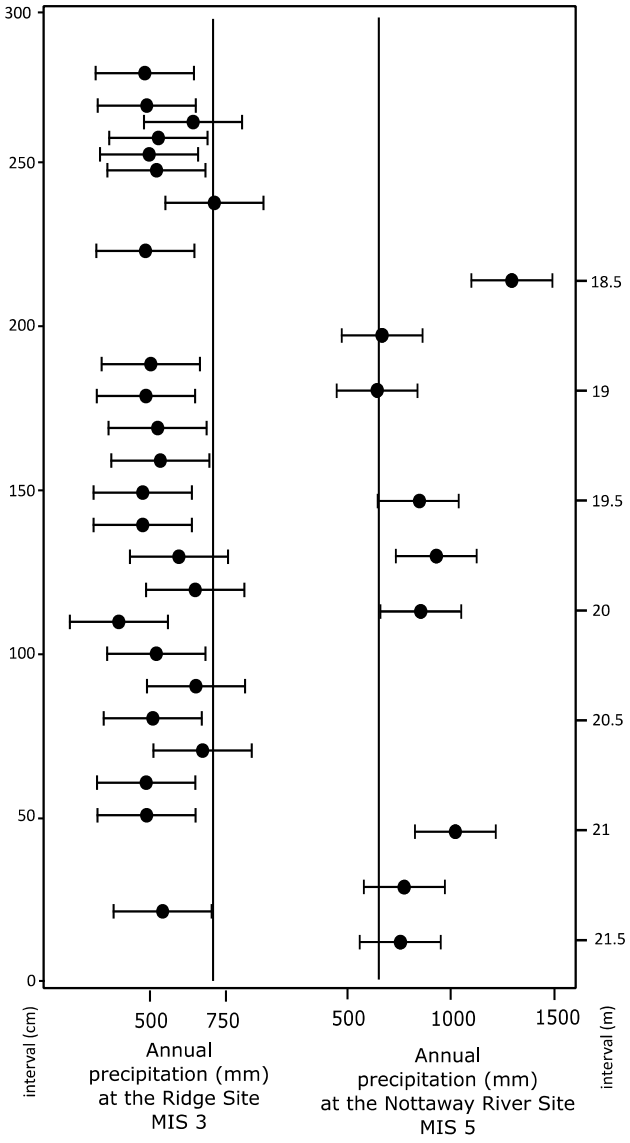

Fig. 3-7. A comparison of reconstructed total annual precipitation at the Ridge Site (MIS 3) and the Nottaway River Site (MIS 5; Allard et al., 2012).Vertical lines represent the present-day values at each site: 705 mm and 652 mm, respectively. Note: differing sample intervals at each site.

Chapter 4
Late Pleistocene chronology, paleoecology and stratigraphy at a suite of sites along the Albany River, Hudson Bay Lowlands, Canada

4.1 Abstract

Stratigraphic records from previously glaciated regions are critical for detailed study of the timing, onset and dynamics of past ice sheets and the paleoecology of previous ice free intervals. Here, we examine three stratigraphic sections from an 18-km stretch of the Albany River, Hudson Bay Lowlands, Canada, located at the center of many Late Pleistocene ice sheets. Results of till characterization and correlation suggest that at least three glacial advances from shifting ice centers within the Québec sector of the Laurentide Ice Sheet are preserved in these stratigraphic records. Intercalated between tills are fluvial deposits and organic-bearing units reflecting ice-free conditions that were constrained via optically stimulated luminescence to two possible non-glacial periods at ca. 73,000 to 68,000 yr BP and ca. 60,000 yr BP. Boreal and peatland taxa (*Picea*, *Pinus*, Poaceae, *Betula*, Cyperaceae, *Sphagnum*) dominated the pollen record at each site, suggesting a similar environment to present-day during these non-glacial intervals. Plant macrofossils analyzed at one site confirm the local presence of conifer trees (bark, needles, seed wings), bryophytes (largely *Scorpidium* spp), herbaceous plants (Caryophyllaceae, *Carex*, Poaceae), and an aquatic setting (e.g. *Potamogeton*, ephippia of *Daphnia* spp*)*. We interpret the non-glacial intervals at all three sites to be associated with a fluvial environment, perhaps oxbow lake sediments capable of supporting water-logged peatland biota. Quantitatively-derived average summer temperature (JJA) reconstructions suggested that local temperatures at these sites were between 12-15°C, which is marginally cooler to slightly warmer than present-day estimates for the region (14.2°C). Reconstructed annual precipitation estimates were 580 to 640 mm, which is similar to slightly higher than present-day estimates (564 mm). Results from this research contribute toward ongoing efforts to constrain ice sheet dynamicity during the last glacial cycle (e.g. 71-14 ka) and provide unique insight into the complex Late Pleistocene paleoclimate record at the innermost area of the previously glaciated region.

4.2 Introduction

The Quaternary is defined by repeated glaciations over the Northern Hemisphere that had large-scale influences on global sea level (Grant et al., 2014), atmospheric processes (Sionneau et al., 2013; Ullman et al., 2014), biotic migration and carbon cycling (Kleinen et al., 2015; Brovkin et al., 2016). These glaciations resulted in a highly fragmented stratigraphic record in the previously glaciated region, limiting our ability to study glacial timing, onset and dynamics, and the character of the ice-free periods. Little is known about Late Pleistocene paleoenvironments of the region thought to be covered by the Laurentide Ice Sheet during the Wisconsinan Stage (ca. 71,000 to ca. 24,000 yr BP), and during the Last Glacial Maximum (LGM), owing to the erosion of antecedent deposits. Most extant deposits of Late Pleistocene-age from formerly glaciated regions are found in the marginal areas of the former ice sheet(s) (e.g. Rémillard et al., 2013; Bajc et al., 2015; Rémillard et al., 2016) and thus offer limited constraint on the extent and dynamics of previous ice sheet(s), nor to the paleoecology of more immediate periglacial settings.

The Hudson Bay Lowlands (HBL) are a vast low-lying peatland in central Canada bordered by the James and Hudson bays (Fig. 4-1). This region is presently one of North America's largest wetlands, consisting of bogs and fens with flora dominated by boreal (*Alnus*, *Betula*, *Larix*, *Picea*, *Salix*) and peatland taxa (Cyperaceae, Ericaceae, *Sphagnum*) (Riley, 2011). Holocene peat deposits overlie a series of glacial and non-glacial deposits, including Pleistocene-aged sediments, which consist of multiple tills that are occasionally separated by *in situ* fluvial and organic-bearing deposits (e.g. Dredge et al., 1990; Allard et al., 2012). The HBL is located near the geographic centre of many Pleistocene ice sheets, and tills preserved in this region document the interaction between the northwest (Keewatin), and the northeast (Québec, sometimes referred to as the 'Labrador-Nouveau Québec') sectors of these former ice sheets (Fig. 4-1), whereas non-glacial materials document the paleoecology and character of ice-free intervals. The preservation of these deposits makes the HBL a critical region for studying the history of the Late Pleistocene (Dredge and Thorleifson, 1987; Kleman et al., 2010).

Here, we study the glacial and non-glacial records preserved at three riverbank exposures (informally named Sites 007, 008 and 009) along an 18-km stretch of the Albany River, HBL, Canada (51.9°N, 82.6°W; Fig. 4-1). Each site contains an organic-bearing non-glacial unit that is

contained between at least two glacial (diamicton) units. The Albany sites were first documented by exploratory trips in the 1960s (Al-62, Al-63 and Al-65, respectively; Ontario Water Resources Commission, 1969). We characterize the glacial units by examining lithology, geochemical composition, carbonate content and directional indicators to provide insight into the timing and direction of Late Pleistocene glacial dynamics over the region. We characterize the non-glacial intervals by attempting to constrain their ages by optically stimulated luminescence (OSL) and radiocarbon dating, and provide insight into the local biotic setting by examining biological proxies (pollen, macrofossils) along with sedimentological data. Pollen-inferred paleoclimate estimates are also presented. Similar studies have been completed in the peripheral areas of the previously glaciated region (Rémillard et al., 2013; Bélanger et al., 2014; Bajc et al., 2015; Rémillard et al., 2016); however, the Albany sites are located significantly closer to the centre of the former ice sheet, and thus provide a unique insight into the complex Late Pleistocene record of North America.

4.3 Methods

4.3.1 Fieldwork, sampling and geochronology

Fieldwork at the Albany sites was conducted by canoe during September 2014. Modern-day slump material was removed prior to making descriptions of each site, and a representative sample was taken from each diamicton unit for sedimentological and geochemical analyses. Samples were taken at 5-cm increments in the non-glacial interval for radiocarbon dating, loss on ignition (LOI), particle size analysis (PSA), pollen and macrofossil analysis (Figs. 4-2, 4-3, 4-4, 4-5). The only exception was at Site 009, where a steep slope restricted sampling to the bottom 2.7 m of the ~4-m non-glacial interval. When found, directional indicators (e.g. stone lines, striations) were measured in each glacial unit using a geological compass (typically one to five measurements per site). The composition of geological units in the study area was obtained by consulting with provincial geology maps (Ontario Geological Survey, 2015).

Previous radiocarbon attempts from the non-glacial intervals at the Albany sites are reported in Table 4-1. Here, we present five new single aliquot regeneration OSL dates on quartz grains that were taken in what are interpreted to be aeolian (Site 007) and fluvial (Site 008) sand-bearing units. Site 009 could not be dated via OSL because of a lack of suitable unit for sampling. Protocols are similar to those presented in Dalton et al. (2016) (Chapter 2 of this dissertation).

We limit the reporting of ages for those samples with at least 30 aliquots to determine an equivalent dose (Table 4-2). The majority of aliquots (79 to 94%) were used to calculate an equivalent dose, with aliquots removed if (1) the recycling ratio was not between 0.90 and 1.10, (2) recuperation was >5%, (3) error in equivalent dose values was >10%, reflecting low light emissions (Demuro et al., 2013), and (4) if the 'fast ratio' was <20 (Durcan and Duller, 2011). Ultra-small aliquots were used for equivalent dose determination with a plate area of 1 mm^2 corresponding to about 20 to 40 grains per aliquot. Overdispersion analyses of equivalent dose populations were relatively low at 16 to 24% which indicates a single log-normal distribution, and thus the central age model was used in the final calculation of equivalent dose (Galbraith and Roberts, 2012). Water content of 25 ± 5% was estimated based on initial inferred conditions and subsequent glacial compaction of the sediment. Where appropriate, dose rate was adjusted for organic content by dilution based on loss on ignition values. The U, Th, Rb and K content was determined by inductively coupled plasma-mass spectrometry / optical emission spectroscopy (ICP-MS/OES) and these values, in combination with a calculated cosmic dose, were used to resolve a dose rate (Table 4-2). Final OSL ages are presented in the Results section at 1-sigma error. However, errors are increased to 2-sigma ranges in the Discussion (Section 4.5.5) to cover any variability introduced by uncertainty in moisture content, burial history, organic content and other errors (Mallinson et al., 2008; Schaetzl and Forman, 2008; Wood et al., 2010).

4.3.2 Pollen, macrofossil and sedimentology methods

Pollen samples were processed using standard methods (Faegri and Iversen, 1975), plus density separation using sodium polytungstate to more effectively concentrate the pollen grains (Zabenskie, 2006). Identification of pollen grains follows Kapp et al. (2000), McAndrews et al. (1973) as well as reference collections held at the University of Toronto and the Royal Ontario Museum. Broken bisaccate pollen grains (*Pinus*, *Picea*) were rare, but when present, were counted if >50% of the grain was intact. A minimum of 150 pollen grains of herb, arboreal and shrub taxa were counted in each sample; taxa from these groups only were included in the pollen sum from which percentages were calculated. Samples that had < 5000 grains/cm^3 based on the addition of a *Lycopodium* spike, or contained >10% broken grains, were excluded from further analysis and are not reported here. A detrended correspondence analysis (DCA) plot of the fossil pollen assemblages was constructed using R package 'vegan' (Oksanen et al., 2015) and comprises all herb, arboreal and shrub pollen taxa. Stratigraphic plots were produced using R

package ‘rioja’ (Juggins, 2015) and include all taxa which reach 1% abundance in at least one fossil sample per site.

Pollen-derived paleoclimate reconstructions were developed using the modern analogue technique (Overpeck et al., 1985) and the North American Modern Pollen Database (n = 4833 sites; Whitmore et al., 2005) with additional sites from the HBL (n = 49; details on assembling this dataset are provided in Dalton et al., 2017; Chapter 3 of this dissertation). Only sites situated in the conifer/hardwood, boreal and forest-tundra biomes were included in the modern calibration set. Further, this calibration set was reduced to include only sites having pollen counts >150 grains, as well as those located in areas of <1200 mm of annual precipitation, resulting in a final calibration set of 1509 sites. The R package ‘analogue’ (Simpson, 2007; Simpson and Oksanen, 2014) using the k=3 closest analogues and cross-validation (n=500 bootstrap iterations) was used for pollen-based paleoclimate reconstructions. Three analogues were the optimal number to limit prediction error in the modern calibration set. Errors at each fossil site are based on the root mean squared error of prediction (RMSEP) of the modern calibration set using the k=3 closest analogues. Modern-day values for the Albany sites are taken from gridded climate data as there are no local weather stations in the study area: average summer temperature (June, July, August) is ~14.2°C, while annual precipitation is ~564 mm (Natural Resources Canada, 2015).

Plant macrofossils, examined exclusively at Site 009, were concentrated by rinsing 15 cm^3 of organic-bearing sediment under a 100-µm sieve using water (occasionally with $Na_4P_2O_7$ to disaggregate the sediment) and then identified under a stereomicroscope. Macrofossils provide direct evidence of local vegetation, and are thus important for validating and refining paleoclimate reconstructions based solely on pollen data (Birks and Birks, 2000; Väliranta et al., 2009). Loss-on-ignition involved heating ~2 g (dry weight) of sediment to 550°C for 4 hours and then to 950°C for 2 hours to remove the organic and carbonate fractions, respectively (Heiri et al., 2001). Sediment size distributions were determined using a Malvern Mastersizer 3000 and Hydro MV wet dispersion unit on samples that were first treated with H_2O_2 and HCl to remove organic and carbonate fractions.

4.3.3 Geochemical and sedimentology analyses on the diamictons

Geochemical data, particle size data, and the calcite-to-dolomite ratio (C:D) were used to characterize the diamictons, as well as assess the degree to which they could be correlated among the three Albany sites. The carbonate content and the C:D ratio of each diamicton was determined using a Chittick apparatus (Dreimanis, 1962) on the <63 µm fraction, while particle size distributions were determined according to the Wentworth scale (Wentworth, 1922) using sieves and a Microtrac Particle Size Analyzer. Elemental data were measured by inductively coupled plasma atomic emission spectroscopy (ICP-AES) and inductively coupled mass spectroscopy (ICP-MS) after digestion in aqua regia (Appendices F and G). When measured values exceeded or fell below the instrument detection limit, 'greater than' values were assigned to 1.7x the detection limit and all 'less than' values were assigned to 0.55 the detection limit (Sanford et al., 1993). Elements were eliminated if replacements had to be made to more than 20% of the samples, which resulted in the removal of Be, Ca, K, Mg, Au, Pt, Se and Ta. If an element was measured in both ICP-AES and ICP-MS, only the latter values were retained because of the improved detection limits. Prior to statistical analysis, the centered log-ratio was taken in order to correct for any compositional bias in the data and to down weight the influence of highly abundant elements (Aitchison, 1986; Grunsky, 2010). Geochemical data were visualized using Principal Component Analysis in R package 'vegan' (Oksanen et al., 2015), while cluster analysis was performed using the R base package using the 'average' agglomeration method (R Core Team, 2014). A similar multi-variate approach for characterising diamicton units was used by McMartin et al. (2016).

4.4 Results

4.4.1 Albany River Site 007

The lowermost exposed unit at Site 007 is a dark grey-brown diamicton (unit 1; Fig. 4-2A), which is massive to fissile, containing silt to sandy silt with pebbles, cobbles and boulders. This unit ranges from 2 to 11 m in thickness owing to a highly irregular contact with the overlying material. Rare stone lines along with isolated, faceted and striated boulders are contained in this diamicton; one stone line had striated top of clasts between 190 and 232 °N. Az (based on 5 readings). A nearly continuous 30-cm thick layer of sand sub-divides unit 1 about 7 m above river level. This layer is truncated by the irregular contact with the sediments above.

Overlying one part of the lowermost diamicton at Site 007 is a 1.8-m interval of brown to black, laminated, organic-bearing sediments (unit 2; Fig. 4-2A, also Fig. 4-2B, C) consisting of silty clay (~35%), very fine sand and silt (~40%). These sediments are interbedded and appeared to be deformed. This interval is generally less than 10% organic, with a 5-10% carbonate component (Fig. 4-2D). Radiocarbon dating of bulk peat from the 90-cm interval of this unit suggests that it was deposited at 40,800 ± 500 cal. yr BP (UOC-0597; Table 4-1). However, we interpret bulk radiocarbon dates with caution due to the risk of contamination in samples of mixed provenance (Dalton et al., 2016; Chapter 2 of this dissertation). A quartz-based OSL sample from the fine sand fraction (150-250 μm) at the same interval as the radiocarbon date suggests an age of 73,100 ± 6,365 yr BP (BG-4227; Table 4-2).

Overlying the organic-bearing interval is a light grey brown diamicton, containing massive sandy-silt to silty-sand, along with granules, pebbles, cobbles and boulders (unit 3; Fig. 4-2A). This diamicton ranges from 2 m (overlying the organic-bearing sediments) to 11 m in thickness where it is infilling a depression in the lower diamicton. One boulder contained striations oriented at 204 °N. Az. Lenses and discontinuous layers of 'u-shaped' stratified sediment bodies (predominantly sand, but also silt and clay laminate) occur throughout this diamicton, in particular within the depression in unit 1. The upper surface of these bodies are planar, sharp and near-horizontal.

The uppermost diamicton at Site 007 is also light grey brown in colour and is characterized by massive sandy-silt to silty-sand with granules, pebbles, cobbles and boulders (unit 4; Fig. 4-2A). Striations on the top of one faceted and striated boulder were oriented at 290 °N.az. This diamicton unit is slightly finer-textured than the diamicton beneath. Overlying this diamicton is a 2-m thick light brown, very fine sand and silt containing marine shells and shell fragments (unit 5). A thin, small pebble layer occurs at the base of the unit.

4.4.2 Albany River Site 008

The lowermost exposed unit at Site 008 is a dark grey-brown diamicton of 3 m thickness (unit 1; Fig. 4-3A), characterized as massive to fissile, containing sandy silt to silty sand with granules, pebbles, cobbles and boulders. A faceted boulder had striations oriented to 215 °N. Az. The upper surface of this diamicton gently slopes to the south (rightward on Fig. 4-3A). Two depressions in this diamicton contain non-glacial sediments; we identify the materials contained

at the northern end as Site 008a, while those at the southern end at a distance of ~50 m are Site 008b. The non-glacial sediments from Site 008a are present continuously along the exposure and outcrop directly overlying the non-glacial sediments of Site 008b, separated by a subtle, potentially oxidized contact.

At the base of the non-glacial unit at Site 008a (Fig. 4-2B; field photograph) is a 35-cm thick discontinuous band of stratified fine and medium-grained sand and small pebbly gravel. This sand-rich unit was dated via OSL to 59,120 ± 5,585 yr BP and 59,695 ± 5,500 yr BP (BG4228 and BG4262; Table 4-1). Overlying this sand deposit is approximately 2 m of greasy organic-bearing silt, silty clay with rare thin layers and lenses or small pebbly, medium to coarse sand, and layers of fine sand. The organic-bearing interval contains ~25% sand, ~45% silt and ~30% clay, which varied throughout the unit, while the organic component in this interval is 5-10%, with 5-8% carbonate (Fig. 4-3C). Radiocarbon dating of bulk organic-bearing sediment from the 70-cm interval at site 008a suggest that it was deposited at 43,500 ± 850 cal. yr BP (UOC-0594; Table 4-1).

At the southern end of the exposure, the non-glacial interval at Site 008b consists of brown to black organic matter, laminated and interbedded sediments with very fine sand and silt containing three peat beds. Overlying this dark organic-bearing unit is a 20-cm interval of gravelly and pebbly sand, followed by ~4 m of rhythmically or interbedded fine sand, silt and silty clay with organic laminae (unit 2; Fig. 4-3A). Sand beds obtain thicknesses up to 15 cm and rhythmically bedded finer sediment occurs in cycles of 1-2 cm. Optically stimulated luminescence analysis on quartz grains from this sand-rich unit yielded ages of 72,640 ± 5,990 yr BP and 67,605 ± 5,765 yr BP (BG4263 and BG 4264; Table 4-2). Radiocarbon attempts on wood pieces at this site yielded >47,800 and >49,200 yr BP (A. F. Bajc, personal communication, ISGS-A3320 and ISGS-A3321; Table 4-1).

A dark grey brown diamicton of ~7 m thickness (unit 3; Fig. 4-3A) overlies Site 008a and Site 008b. This diamicton is characterized by clayey silt with granules, pebbles, cobbles and some boulders. At the north end of Site 008a, this diamicton is massive, but numerous lenses and discontinuous layers of stratified sediment are present near the south of the exposure. At the south end of Site 008b, an additional diamicton is present (unit 4). This light grey, massive diamicton is 4 m in thickness and is characterized by sandy-silt to silty-sand with granules,

pebbles, cobbles and boulders. Numerous sand and gravel lenses and layers are also present. The uppermost unit at Site 008 is 3 m of light brown, stratified, very fine sand, containing silt, small pebble and gravel layers/lenses and a thin gravel layer at the base (unit 5). Marine shells are present in this unit.

4.4.3 Albany River Site 009

The lowermost exposed unit at Site 009 is a dark grey massive diamicton (unit 1; Fig. 4-4A), containing silty clay with granules and pebbles. Striations on the top of one boulder were oriented to 340 °N.Az. Overlying this diamicton is a 30-cm layer of brown, poorly-sorted pebbles to small cobble gravel (unit 2; also Fig. 4-4B, C), that is in turn overlain by 4 m of organic-bearing sediments (unit 3). The organic-bearing sediments are massive, laminated and consist of clay silt and silt, with peaty layers. This unit was composed of ~35% clay, ~40% silt and the remainder as sand. The organic content was ~10-20%, and carbonate component ~2.5% (Fig. 4-4D). Radiocarbon attempts to date this bulk organic-bearing sediment have all resulted in infinite determinations: >47,000, >48,800 and >54,000 yr BP (UOC-0595, UOC-0843, GSC-1185; Table 4-1).

Overlying the organic-bearing interval at Site 009 is a diamicton unit (unit 4; Fig. 4-4A). This diamicton is light grey-brown, loose, massive, and consists of silty sand with granules, pebbles, cobbles and boulders. Striations on one boulder were aligned to 170 °N. Az. The uppermost unit at this site was 3 m of light brown, stratified fine sand and silt with a thin small pebble gravel layer at the base (unit 5). This unit contains marine shells.

4.4.4 Correlation of till units among the Albany sites

The occurrence of striated and faceted clasts, boulder lines and the overall massive appearance of the diamicton layers led to the interpretation that the diamictons are subglacial till. Cluster analysis of the elemental data suggest that till from the Albany sites can be divided into four groups (Fig. 4-6) which are aligned along axis one of the PCA (accounts for 86% of the variance in the dataset). Till I, which is represented by only one sample (009-TM1), is characterized by the highest level of base metal elements of all the Albany sites, along with a relatively low carbonate content (14.3%), extremely low dolomite content (0.1%), and a grain composition largely consisting of clay (47%) and silt (40%) with a small sand component. Till II, comprised

of the lowermost till units at Site 007 and 008 (007-TM1; 008-TM1, respectively), are similar on the bases of geochemistry, particle size distribution and matrix carbonate content (Fig. 4-6B). Ice flow to the south-southwest is indicated for this group. Till III is comprised of two samples from the same diamicton unit at Site 008 (008-TM2; 008-TM3) and has a geochemical signature suggesting intermediate levels of base metal elements as compared to Till I and Till II (Fig. 4-6A). Particle size and the dolomite concentrations for Till III differed slightly among these two samples owing to extensive incorporation of the underlying sediments near the south end of Site 008b. The final group, Till IV, comprises the uppermost till units at each site (007-TM3, 007-TM2, 009-TM2, 008-TM4). Total carbonate ranges from 35.6 to 39%, and the C:D ratio ranges from 0.6 to 1.4. Texturally, Till IV is characterized by a low clay component (<20%), silt comprising ~40% and the remaining 40% being sand. Direction of ice movement indicated from 007-TM2 suggests that this till was deposited during glacial movement toward the south-southwest; however, indicators from 007-TM3, which is a slightly finer-textured till, suggest that it was deposited by a glacier flowing toward the west-northwest.

4.4.5 Biostratigraphy and paleoclimate at the Albany sites

The herb, arboreal and shrub component of the pollen assemblages at the Albany sites are very similar (Fig. 4-2D, 4-3C, 4-4D) and display little stratigraphic change through the organic-bearing intervals. Overall, *Picea* pollen dominated the assemblages with 53–55% of the average pollen count, followed by *Pinus* pollen at 19–23%, Poaceae at 8–9% and *Betula* at 6–9%. The remainder of the herbaceous, arboreal and shrub counts were dominated by *Salix* (2–3%), Asteraceae (1–2%), *Alnus* (~1%) and *Lycopodium* (~1%), along with <1% grains of *Abies*, Amaranthaceae, Caryophyllaceae, Cupressaceae, Ephedraceae, Ericaceae, Juglandaceae, Polygonaceae and Polypodiaceae. Wetland indicators (*Sphagnum* and Cyperaceae) were variable at each site, and generally ranged from 15–60% of the herb, arboreal and shrub pollen sum. Further, aquatic taxa *Equisetum* and *Pediastrum* were present at all three sites, with a few *Potamogeton* grains also present at Sites 007 and 008. Despite overall similarity among pollen at the fossil sites, subtle differences in the assemblages caused variability among sites in the ordination (Appendix H). For example, Site 007 had slightly more *Betula* (8.6%) and Site 009 overall had slightly higher *Pinus* (23.4%) than average values for the Albany sites. Temperate taxa were also present rarely in the record, notably *Tsuga* (three grains at Site 008; five grains at Site 009) and *Quercus* (one grain at Site 009).

The majority of fossil pollen intervals at the Albany sites (52 of 60 total examined samples) were suitable for quantitative paleoclimate inferences by modern analogue technique. Many of the same modern analogues were used in the reconstructions: of a possible 156 modern analogues (3 analogues used for each sample x 52 reconstructed intervals), 80 analogue sites (51%) were taken from the same three modern sites, one lying in the boreal forest of Central Canada, and two from the HBL. Pollen-based quantitative analysis from the organic-bearing interval at Site 007 yielded an average summer temperature of 13.3 ± 1.6°C (R^2 = 0.83), which is marginally cooler, but given the errors, is indistinguishable from present-day estimates from a gridded climate dataset (14.2°C). Reconstructed annual precipitation at Site 007 was 635 ± 127 mm (R^2 = 0.83), which may be slightly wetter, or the same as, estimated present-day values in this region (564 mm). Average summer temperature estimates for Site 008 and 009 were 14.1 ± 1.6°C (R^2 = 0.83) and 14.6 ± 1.5°C (R^2 = 0.84), respectively, while paleo-precipitation estimates at these two sites were 620 ± 127 mm (R^2 = 0.83) and 584 ± 122 mm (R^2 = 0.85). Errors associated with these paleoclimate reconstructions cause most estimates to overlap with present-day values at the Albany sites.

Macrofossils, examined only at Site 009, reveal more stratigraphic change than the pollen data (Fig. 4-5) and are indicative of a freshwater aquatic environment. Bryophytes are present throughout the examined record and are dominated by *Scorpidium* spp. Aquatic taxa are similarly present throughout the record, notably, ephippia of *Daphnia* along with statoblasts of *Fredericella, Plumatella* and *Cristatella*. Leaf remains of *Potamogeton* and potentially *Najas* are also noted, although identification of the latter is tenuous. Overall, aquatic taxa become increasingly abundant in the upper part of the stratigraphy, between 180 and 270 cm. Seeds of herbaceous Caryophyllaceae, *Carex*, Poaceae, *Luzula* and *Typha* are present occasionally in the record, while Cyperaceae and *Equisetum* remains are also common. Remnants of *Betula* (bark, seeds), along with conifer bark and needles are present throughout. Charcoal and mites are also present, and show a similar trend to the aquatic taxa, reaching highest abundances in the upper half of the sampling intervals.

4.5 Discussion

Stratigraphic records contained in the Albany sites are fragmented owing to glacial erosion. However, our use of till correlations allowed for the amalgamation of records from several sites,

permitting some reconstruction of Late Pleistocene history at the centre of the previously glaciated region. Glacial sediments provide insight into the timing and dynamicity of glacial movements over this region, whereas non-glacial sediments offer rare insight into the character, paleoecology and climate of interstadial/interglacial periods.

4.5.1 Deposit of subglacial till at the Albany sites

A simplified stratigraphic plot for each of the Albany sites showing sample locations, chronology and till groupings is presented in Fig. 4-7. We interpret the first event recorded at the Albany sites to be the deposition of the tills underlying the non-glacial intervals. The lowermost till layer at Site 009 (Till I) was deposited by ice flowing toward the north-northwest, as indicated by stone lines and striated boulders. This flow direction helps to explain the low dolomite content of this till because of the trajectory largely over the limestones of the Moose River basin and the granitic Canadian Shield. A similar flow direction has been noted in the Rocksand till in the HBL attributed to MIS 5 (Thorleifson et al., 1992; 1993) or MIS 4 (ca. 71,000 to 57,000 yr BP; Kleman et al., 2010). In the Matagami area of central Quebec, this northwest flow is the oldest one recorded (Veillette and Pomares, 1991). Contrastingly, the lower till units at Site 007 and 008 (Till II) were deposited by ice flowing toward the south-southwest, a trajectory over larger terrain underlain by Paleozoic limestone and dolomitic rocks, which is the cause of a high carbonate content in these units. A similar ice flow direction is present in till units underlying non-glacial sediments in the Moose River Basin, located 150 km southeast of the Albany sites (Skinner, 1973), which may suggest that the till and non-glacial units are synchronous at the Moose River and Albany River locations. However, we caution against using till flow indicators along with the relative position of the non-glacial units to correlate stratigraphic relations across the HBL given the highly fragmented stratigraphic record, along with the possibility that non-glacial units dating to several intervals are present in this region (Allard et al., 2012; Dalton et al., 2017; Chapter 3 of this dissertation). The 30-cm thick layer of sand in the subglacial till at Site 007 may represent a subglacial meltwater event that slightly lifted the sole of the glacier from its bed. Overall, the relative ages of Till I and Till II are not known; it is possible that they are the same age, representing different flow directions and shifting ice centres (Parent et al., 1995). Alternatively, they may have been deposited during different glacial advances.

4.5.2 Deposit of the non-glacial interval at the Albany sites

The next event recorded in the Albany River Sites is the non-glacial interval. At two of the Sites (008, 009), we interpret the non-glacial interval as a fluvial environment with the lowermost units representing basal sediments of an abandoned river channel, transitioning into fill sediments from river valley flooding. This may have been an oxbow lake capable of supporting water-logged peatland biota. At Site 008, gravels, followed by rhythmically and interbedded sediments are interpreted to be the remnants of a channel bar with overlying bar-top sediments. At Site 009, the poorly-sorted pebble and gravel unit is interpreted to be an active river channel lag deposit (gravel) overlain by finer sediments on a bar top, or an infilled meander cutoff. An oxbow lake setting is supported by comparison to the stratigraphy and sedimentology of present-day oxbow lakes, which contain organic material interbedded with silts (Brooks, 2003; Brooks and Medioli, 2003), along with the presence of aquatic indicators in the pollen and macrofossil record (see Section 4.5.4). Variations in the sedimentological component may be the result of flooding of the nearby river, or from precipitation events. Channel bars, overbank deposits and meander scars are common features along the present-day Albany River. Thus, river morphology along with conditions controlling river gradient, discharge and sediment supply during these non-glacial intervals was most likely similar to present-day conditions in the HBL.

Organic-bearing sediments at Site 007 overlie what we interpret to be an erosional contact representing the river valley wall, thus it is possible that the organic-bearing interval at this Site represents a tableland surface lying in the riparian region. This interpretation is supported by the higher relative elevation of this site compared to Site 008 and 009, along with increased *Betula* and *Sphagnum* pollen, which could be expected given the closer proximity to wetlands as opposed to fluvial environments. In this case, sediment input may be from a combination of runoff and aeolian sources. Our interpretation of a paleo-fluvial setting for the Albany sites aligns with the inferred setting of many other Pleistocene-aged sites in this region (Dredge et al., 1990; Allard et al., 2012). Thus, it is possible that shelter from riverbanks aided in preserving many of the non-glacial Pleistocene records in this region (Barnett and Finkelstein, 2013).

4.5.3 Last Glacial Maximum (LGM), deglaciation and Holocene

Following the non-glacial episode was the deposition of Till III, a dark grey-brown unit that was preserved solely at Site 008. Geochemical analysis suggests that it may have been derived from a

source area similar to Till I (009-TM1; ice flowing toward the northwest) owing to moderate base metal elements and a relatively high clay content (Fig. 4-5). However, no flow indicators were observed. Glacial shearing and incorporation of underlying sediment resulted in a different sedimentological character of this till near the south of Site 008. Till III is missing from Site 007 and 009, and may have been eroded, or in the case of Site 007, perhaps it did not extend that far west.

The uppermost till unit at all three Albany sites, Till IV, a light grey and light grey-brown unit, represents the most recent glacial event. Directional indicators suggest that this till was deposited by a south-southwestward flowing glacier, supported by high dolomite content, suggesting prolonged transport over the dolostone-dominated Paleozoic terrain of the HBL. This movement is in agreement with the most recent glacial advance over the Moose River Basin, documented in the Adam and Kipling tills (Skinner, 1973) and in the Matagami area (Veillette and Pomares, 1991). Different ice indicators from the uppermost till at Site 007 and its slightly finer texture suggest that ice flow toward the west-northwest may have resulted from a shift of the ice center, or may represent a distinct till unit. We interpret the truncated “u”-shaped lenses of stratified sediment at Site 007 as Nye channels cut into existing sediment beneath actively moving ice by subglacial meltwater, suggesting that meltwater was abundant at the time of deposition of this unit. The marine sediments overlying all three Albany sections are interpreted to be deposited by the Tyrell Sea in the Early Holocene (Lee, 1960).

4.5.4 Interpretation of paleoenvironments

The pollen assemblages at the Albany sites are similar to other Pleistocene records from the HBL that document boreal-peatland conditions (Terasmae and Hughes, 1960; Nielsen et al., 1986; Dredge et al., 1990; Allard et al., 2012). The boreal interpretation is supported by the abundance of *Picea* and *Pinus* pollen along with tree-type *Betula* seeds and bark, conifer seed wings, bark, needles and charcoal at Site 009. The presence of *Betula* seeds and conifer seed wings indicate that climate conditions were favorable for pollination and seed development. The wetland interpretation is supported by aquatic, fen and forest macrofossil remains at Site 009 (Fig. 4-5), which suggest a minerogenic, paludified surrounding terrain with trees locally present. The presence of *Pediastrum* and *Equisetum*, both aquatic indicators, corroborate sedimentological data which suggest that the organic-bearing intervals are shallow ponds or depressions on a flood

plain. At all three Albany sites, the presence of Poaceae, along with occasional Asteraceae and other herb groups suggest that the canopy of the forested riparian region was occasionally open, and the paleo-riverbanks may have supported *Salix*, *Alnus* and *Abies*. At Site 009, increased abundances of bryophytes, charcoal, sedge and aquatic remains between 180 and 270 cm correspond to a transition towards layering and laminated sediments near the top of the section (Fig. 4-4). Therefore we do not interpret this to reflect a climate signal, but more likely a transition in the local lacustrine conditions or perhaps increased erosion into the catchment.

All pollen-inferred paleotemperatures overlap with present-day estimates for the region, but vary from slightly cooler (Site 007) to similar (Site 008) to slightly warmer (Site 009). The inclusion of rare temperate taxa (e.g. *Tsuga*, *Quercus*) in the pollen records at Site 008 and 009, along with the higher percentage of *Pinus* at Site 009, cause the slight temperature increase over what is inferred at Site 007. Temperate pollen grains are present in similar abundances in Holocene peat and lake cores from the HBL (McAndrews et al., 1982; O'Reilly et al., 2014), therefore it is possible that the organic-bearing sediments at the Albany sites were deposited when the temperate/boreal transition was in a similar position to today. The macrofossil record at Site 009 yielded few specific temperature indicators; while *Typha* is an indicator species in Finland following the 15.7°C July isotherm (Väliranta et al., 2015), this taxon is present throughout modern and Holocene records in the HBL (Farley-Gill, 1980; Glaser et al., 2004; O'Reilly et al., 2014). Precipitation at the Albany sites is similar or slightly higher compared to present-day, which may suggest that it was deposited during an interglacial (e.g. MIS 5) as opposed to an interstadial (e.g. MIS 3), since paleorecords dating to MIS 3 are thought to be characterized by less annual precipitation (see comparison of MIS 5 and MIS 3 paleoenvironments presented in Dalton et al., 2017; Chapter 3 of this dissertation).

Most paleoclimate studies using the North American Modern Pollen Database report R^2 values for temperature of ~0.9, and values of ~0.8 for precipitation (Fréchette and de Vernal, 2013; O'Reilly et al., 2014; Richerol et al., 2016). However both fall between 0.82 to 0.85 for the Albany sites, suggesting that annual precipitation may be better predicted at the Albany sites than other studies using the same calibration set. Errors reported for the paleo-temperature and paleo-precipitation reconstructions for the Albany sites are similar or less to what has previously been reported in Holocene and Pleistocene sites in the boreal region (Bunbury et al., 2012; O'Reilly et al., 2014; Dalton et al., 2017; Chapter 3 of this dissertation). However, errors for most samples

overlap with present-day values at the Albany sites, which places a limit on the inferences that can be made based on pollen data. Ordination of fossil pollen data (Appendix H) showed that the impact of rare temperate indicator taxa (e.g. *Tsuga*) was significantly minimized by the ubiquitous boreal taxa, thus adjusting the pollen sum (e.g. Gajewski, 2015) to down-weight the influence of boreal species may be critical for improving reconstructions in boreal environments. However this was not possible at the Albany sites given the rarity of temperate taxa (few grains per interval) and the overwhelming abundance of boreal taxa in the pollen assemblage (>90%). An additional source of error is the accuracy of modern-day climate estimates for the HBL, which are interpolated from gridded datasets owing to a scarcity of weather stations.

4.5.5 Age of the non-glacial intervals preserved at the Albany sites

Age assignments for the non-glacial intervals at the Albany sites are complex. Firstly, we consider finite radiocarbon ages (UOC-0597, UOC-0594; Site 007, 008a) as 'minimum ages' because they are bulk peat dates where the carbon may have mixed provenance, and because of the lack of confirmatory attempts at the same site (Dalton et al., 2016; Chapter 2 of this dissertation). We consider the OSL ages to be robust owing to the significant fast component (majority of aliquots retained for analysis), low overdispersion values (all < 25%; Table 4-2), reproducibility of ages at Site 008a and 008b, and the fluvial setting that suggests sediments were well-bleached prior to deposition. Thus, the OSL data suggest that the HBL, located at the innermost area of the glaciated region, was ice-free and characterized by river systems and boreal peatlands at some point between ~86,000 and ~48,000 yr BP (taking into account 2-sigma errors). However, the fall in global sea level during MIS 4 suggests that the Laurentide Ice Sheet may have grown to near LGM extent during that time (sea level -100 m below present-day; Grant et al., 2014), which would have covered the HBL region. Thus the non-glacial interval(s) at the Albany sites very likely either pre- or post-date the MIS 4 glacial event, and we present the following hypotheses: either all sites are late MIS 5 (e.g. MIS 5a) or both MIS 5a and MIS 3 time intervals are present at the Albany sites. Discussion on Site 009 is limited here since it has no finite age estimates.

Taking into account the 2-sigma errors on the OSL dates, we suggest that the non-glacial intervals at Site 007 and Site 008 both date to MIS 5a, a time when sea levels may have been similar to present-day (Dorale et al., 2010; Creveling et al., 2017; Wainer et al., 2017), which

would most likely have left the HBL ice-free. This hypothesis is supported by pollen data at both sites which reflect vegetation similar in character to present-day (Figs. 4-2, 4-3), consistent with an interglacial interpretation (Dalton et al., 2017; Chapter 3 of this dissertation). This interpretation is corroborated by a record from eastern Canada constrained to MIS 5a via U-Th dating, and suggests that climate was similar to present-day at that time (de Vernal et al., 1986).

However, it is possible that two different non-glacial intervals are present at Site 008. Large errors on the OSL ages, particularly when considered at 2-sigma range, allow the non-glacial interval at Site 008a to be placed into early MIS 3 (e.g. 57,000 to 48,000 yr BP), an ice-free interval which is supported by other sites in the HBL (Dalton et al., 2016; 2017; Chapter 2, 3 of this dissertation) as well as emerging sea level and geophysical estimates (Pico et al., 2016; 2017) that support significantly reduced ice cover in the eastern sector of the Laurentide Ice Sheet during that time. Sediments from Site 008a stratigraphically overlie Site 008b, and are separated by a subtle contact, thus it is possible that both MIS 5a (008b) and MIS 3 (008a) sediments are present at the same site. No intervening (e.g. MIS 4) glacial activity is noted; however, it could have been removed by erosional processes. If correct, a MIS 3 age assignment for Site 008a may be supported by a finite radiocarbon age at that site (UOC-0594; 43,500 ± 850 yr BP), and Site 008 may be one of the first documented sites in the HBL which contains organic bearing sediments from more than one non-glacial interval. However, a drier pollen signal, which is hypothesized to represent MIS 3 deposits (Dalton et al., 2017; Chapter 3 of this dissertation), is not noted at Site 008a. Thus, there is a need to perform additional attempts (both geochronological and vegetation-based) to confirm the age assignments at all Albany sites.

4.6 Conclusion

Glacial sediments at the Albany sites document the growth and dynamics of ice sheets at the innermost part of the previously glaciated region, while non-glacial sediments document the paleoecology of Late Pleistocene periglacial environments. Elemental, sedimentological and geomorphological analyses of the till units, along with comparison of geochronological age attempts and paleoecological analyses of the non-glacial intervals, permit the development of a stratigraphic framework for all three sites. Examination of the tills preserved at these sites suggest that at least three glacial advances are preserved that document ice advance from shifting ice centers of the Quebec sector of the Laurentide Ice Sheet. Efforts to constrain the timing of the

non-glacial interval are ongoing; OSL attempts suggest that non-glacial intervals date to some point between ~86,000 and ~48,000; however these estimates are of low precision. We hypothesize that these sites date to either MIS 5a (ca. 82,000 yr BP) and perhaps some to MIS 3 (ca. 57,000 – 29,000 yr BP), the former being favored by pollen data. Biostratigraphic work (pollen, macrofossils) suggest that the HBL was a boreal peatland with precipitation and temperature similar to present-day during these Late Pleistocene glacial recessions. Results from this research are important for reconstructing the movement, timing and dynamics of Late Pleistocene ice sheets over North America, as well as understanding the character and distribution of boreal peatlands during previous non-glacial periods.

4.7 Acknowledgements

This research was supported by funding from the Natural Sciences and Engineering Research Council of Canada (NSERC) to S.A.F; Northern Scientific Training Program to A.S.D; and the Ontario Geological Survey. We are grateful to S. Williams and Missinaibi Headwaters Outfitters for fieldwork assistance; J. Davison, A. Soleski and T. Hui for laboratory assistance; J. Desloges for the use of the Malvern Mastersizer 3000 and Hydro MV wet dispersion unit. Some of the modern pollen data used in the calibration set were obtained from the Neotoma Paleoecology Database (http://www.neotomadb.org), and the work of the data contributors and the Neotoma community is gratefully acknowledged. We also thank Andy Bajc for helpful discussions.

4.8 Tables

Table 4-1. Radiocarbon age determinations from Sites 007, 008 and 009. All data have been previously published except for the two data points from 008b, which are new contributions from A. F. Bajc. Infinite ages are in radiocarbon years; finite ages were calibrated using CALIB Rev 7.0.4 and the 2013 radiocarbon calibration curve (Stuiver and Reimer, 1993; Reimer et al., 2013).

Site	Lat	Long	Interval	Lab Code	Dated material	F14C	Age (cal. yr BP)	Publication
007	51.93	-82.72	90-cm	UOC-0597	peat	0.008 ± 0.0003	40,800 ± 500	Dalton et al. (2016)
008a	51.92	-82.63	70-cm	UOC-0594	peat	0.0053 ± 0.0003	43,500 ± 850	Dalton et al. (2016)
2014-AFB-167 (008b)	51.92	-82.63	organic-bearing interval	ISGS-A3320	wood	0.0004 ± 0.0011	> 47,800	A.F. Bajc, personal communication, May 2017
2014-AFB-167 (008b)	51.92	-82.63	organic-bearing interval	ISGS-A3321	wood	-0.0003 ± -0.0011	> 49,200	A.F. Bajc, personal communication, May 2017
009	51.96	-82.53	55-cm	UOC-0595	peat	0.0007 ± 0.0005	> 47,000	Dalton et al. (2016)
009	51.96	-82.53	55-cm	UOC-0843	peat	0.0014 ± 0.0001	> 48,800	Dalton et al. (2016)
009 “Albany Island”	51.96	-82.53	unknown	GSC-1185	peat in clay	unknown	> 54,000	MacDonald (1969, 1971)

Table 4-2. Optically stimulated luminescence (OSL) ages on quartz grains from the Albany sites, the Hudson Bay Lowlands, Canada.

Field #	Lab number	Aliquots[a]	Grain Size (µm)	Equivalent dose (Gray)[b]	Over-dispersion (%)[c]	U (ppm)[d]	Th (ppm)[d]	K (%)[d]	H_20 (%)	Cosmic Dose rate (mGray/yr)	Dose rate (mGray/yr)	OSL age (yr)[h]
Site 007	BG4227	31/35	150-250	131.83 ± 6.17	16 ± 2	1.07 ± 0.01	4.40 ± 0.01	1.78 ± 0.01	25 ± 5	0.12 ± 0.01	1.80 ± 0.09[g]	73,100 ± 6365
Site 008a	BG4228	38/48	150-250	81.57 ± 4.43	24 ± 3	0.80 ± 0.01	2.77 ± 0.01	1.41 ± 0.01	25 ± 5	0.06 ± 0.006	1.38 ± 0.07	59,120 ± 5585
Site 008a	BG4262	30/32	150-250	87.97 ± 4.87	21 ± 3	1.03 ± 0.01	4.33 ± 0.01	1.36 ± 0.01	25 ± 5	0.05 ± 0.005	1.47 ± 0.08	59,695 ± 5500
Site 008b	BG4263	40/48	150-250	125.25 ± 5.60	19 ± 2	1.68 ± 0.01	4.34 ± 0.01	1.55 ± 0.01	25 ± 5	0.05 ± 0.005	1.72 ± 0.09	72,640 ± 5990
Site 008b	BG4264	42/52	150-250	134.72 ± 6.45	20 ± 2	2.18 ± 0.01	6.22 ± 0.01	1.64 ± 0.01	25 ± 5	0.05 ± 0.005	1.99 ± 0.10	67,605 ± 5765

[a]Aliquots used in equivalent dose calculations versus original aliquots measured.
[b]Equivalent dose calculated on a pure quartz fraction with about 20-40 grains/aliquot and analyzed under blue-light excitation (470 ± 20 nm) by single aliquot regeneration protocols (Murray and Wintle, 2003). The central age model of Galbraith et al. (1999) was used to calculated equivalent dose when overdispersion values are <25% (at one sigma errors; a finite mixture or minimum age model was used with overdispersion values >20% to determine the youngest equivalent dose population.
[c]Values reflects precision beyond instrumental errors; values of ≤ 25% (at 1 sigma limit) indicate low dispersion in equivalent dose values and an unimodal distribution.
[d]U, Th and K content analyzed by inductively-coupled plasma-mass spectrometry analyzed by ALS Laboratories, Reno, NV; U content includes Rb equivalent.
includes also a cosmic dose rate calculated from parameters in Prescott and Hutton (1994).
[f]Assumes an organic content of 25 ± 5% derived from lost on ignition values.
[g]Assumes an organic content of 2 ± 1%
[h]Systematic and random errors calculated in a quadrature at one standard deviation. Datum year is AD 2010

4.9 Figures

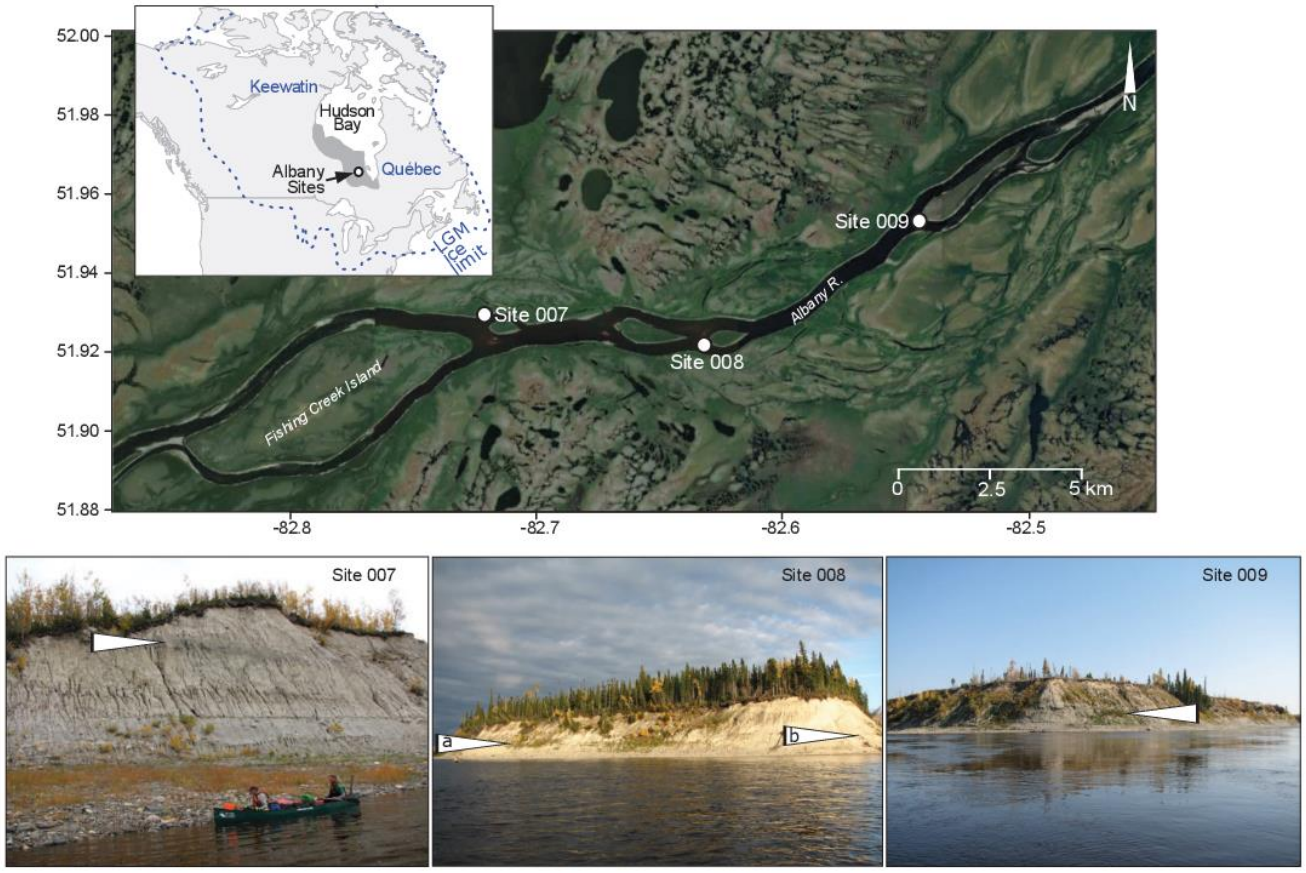

Fig. 4-1. Map of Albany River sites and photographs. Satellite imagery is taken from Google Earth. Inset map situates the study area within North America; shaded area is the Hudson Bay Lowlands. Arrows on each field photograph show the location of the organic-bearing interval.

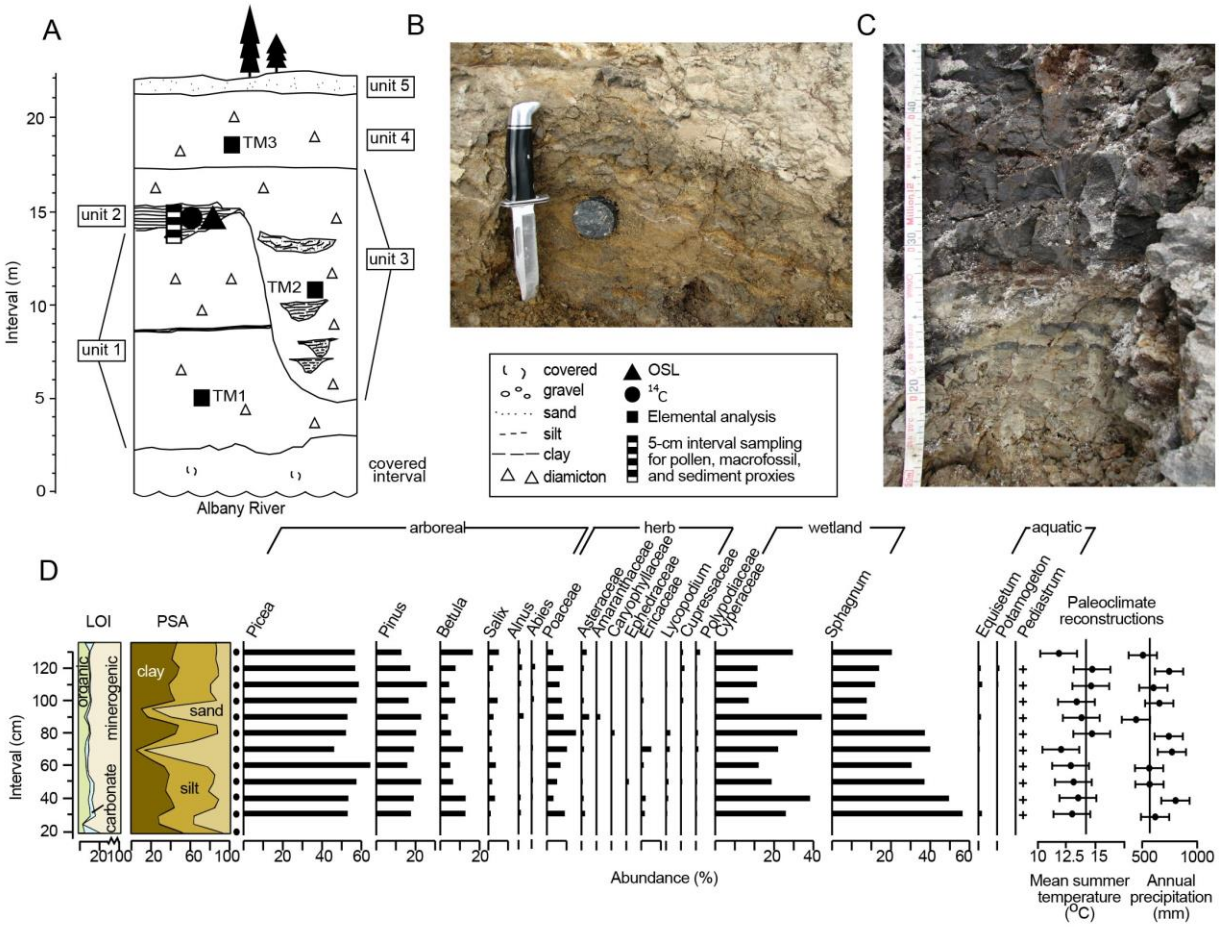

Fig. 4-2. Stratigraphy and pollen data for Site 007. A: sketch of section and locations of samples; B: photograph showing OSL sample location and surrounding sediment; C: base of the non-glacial interval showing the transition from sand-rich (light colours) sediments to silt- and clay-rich organic sediments (darker colours). Note the intervals of interbedded/deformed silty clay, very fine sand and silt; D: biostratigraphic data from the non-glacial interval at Site 007, including LOI and PSA. Pollen samples were examined every 10 cm (indicated by the filled circles adjacent to the PSA data); missing pollen data indicate an interval of poor preservation. All arboreal, herb and shrub taxa reaching 1% in at least one sample are show here, in addition to all wetland and aquatic indicators. Vertical lines in the paleoclimate reconstructions represent present-day values.

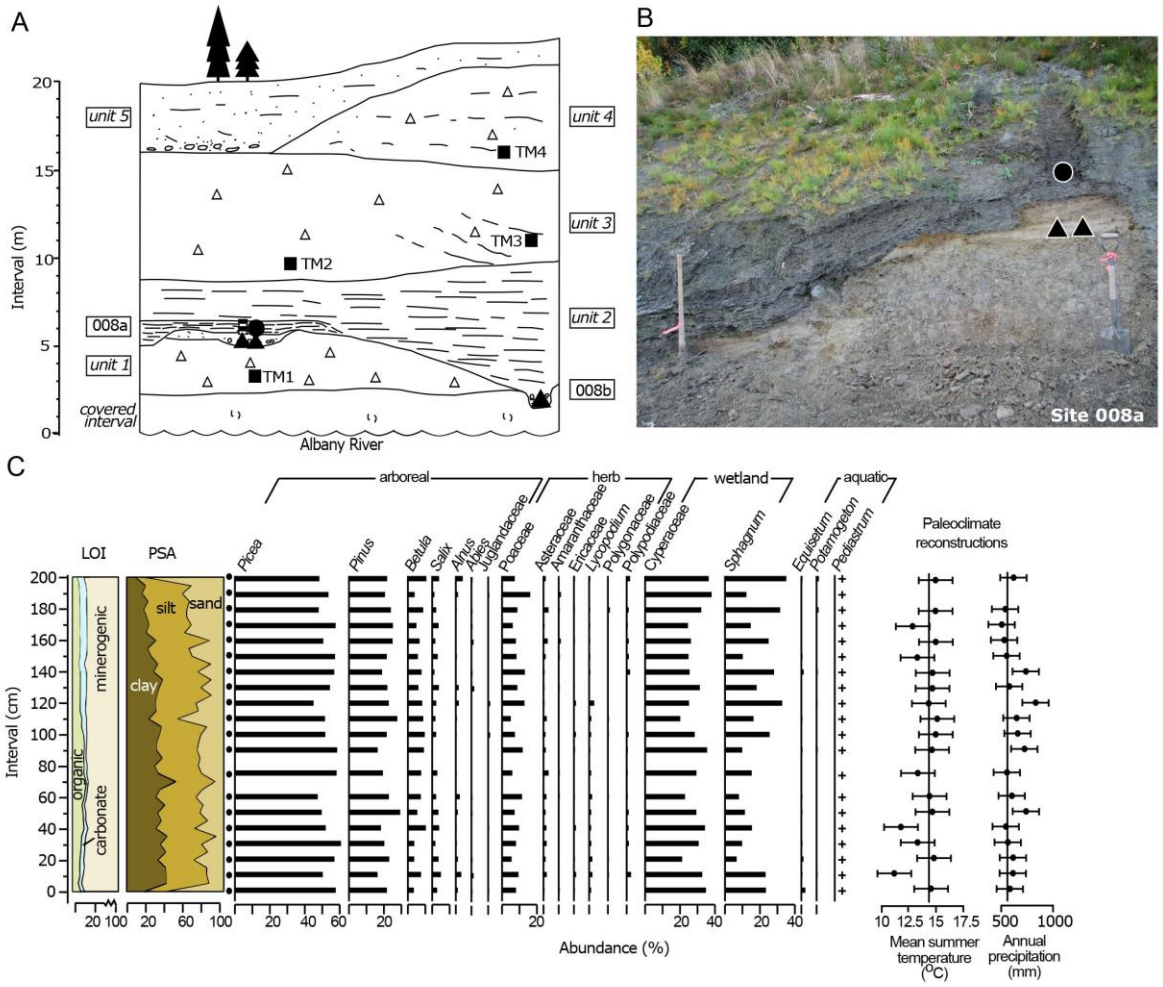

Fig. 4-3. Stratigraphy and pollen data for Site 008. A: sketch of section and locations of samples. Panel B: photograph showing Site 008a, along with the location of 5-cm sampling intervals, OSL and radiocarbon sample locations; C: biostratigraphic data from the non-glacial interval at Site 008, including LOI and PSA. See caption in Fig. 4-2 for further details on the stratigraphic legend and biostratigraphy plot.

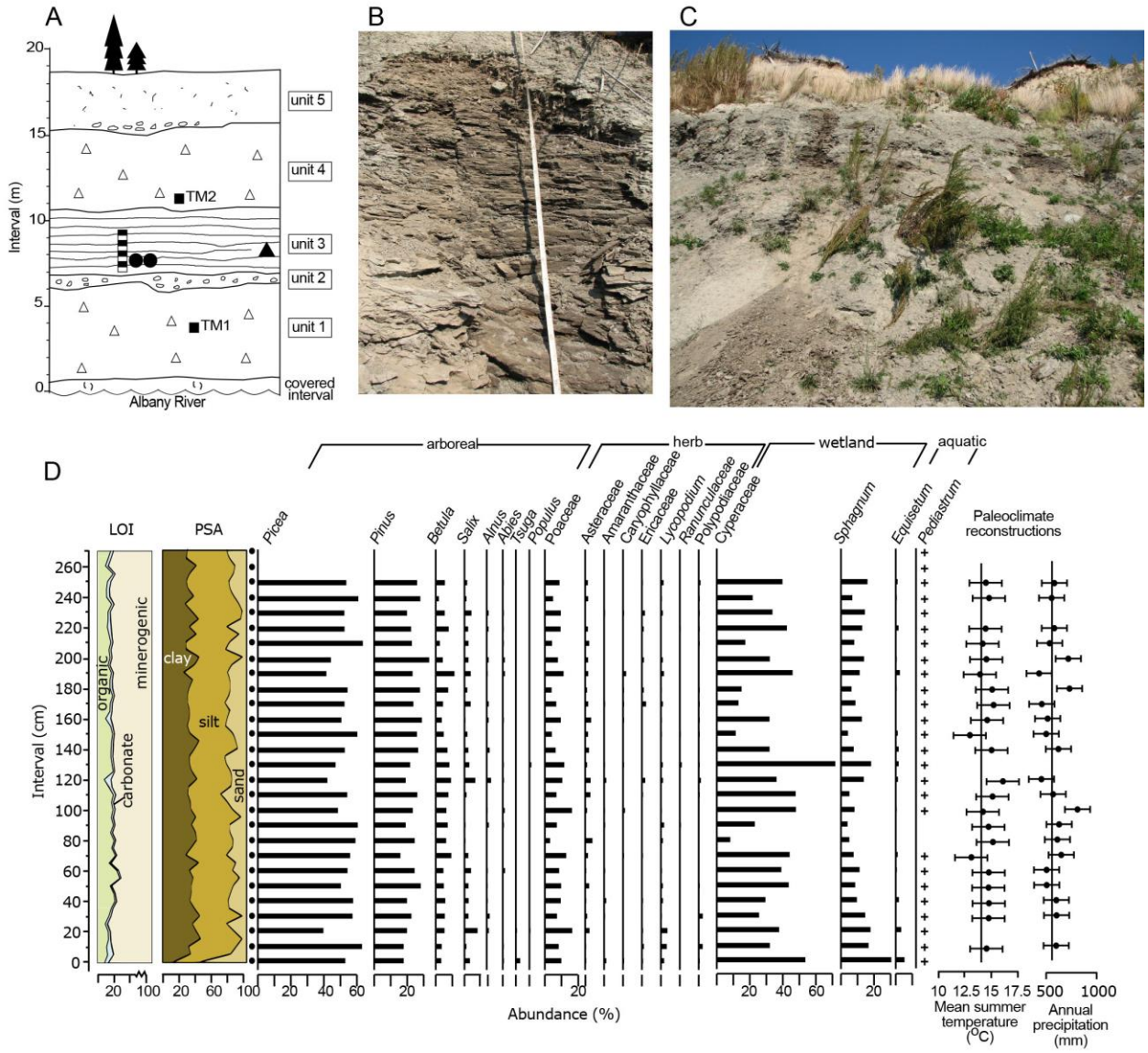

Fig. 4-4. Stratigraphy and pollen data for Site 009. A: sketch of section and locations of samples; B: photograph showing sediments from the non-glacial interval; C: photograph taken from the base of Site 009 showing the location of 5-cm sampling intervals, OSL and radiocarbon sample locations; D: biostratigraphic data from the non-glacial interval at Site 009, including LOI and PSA.

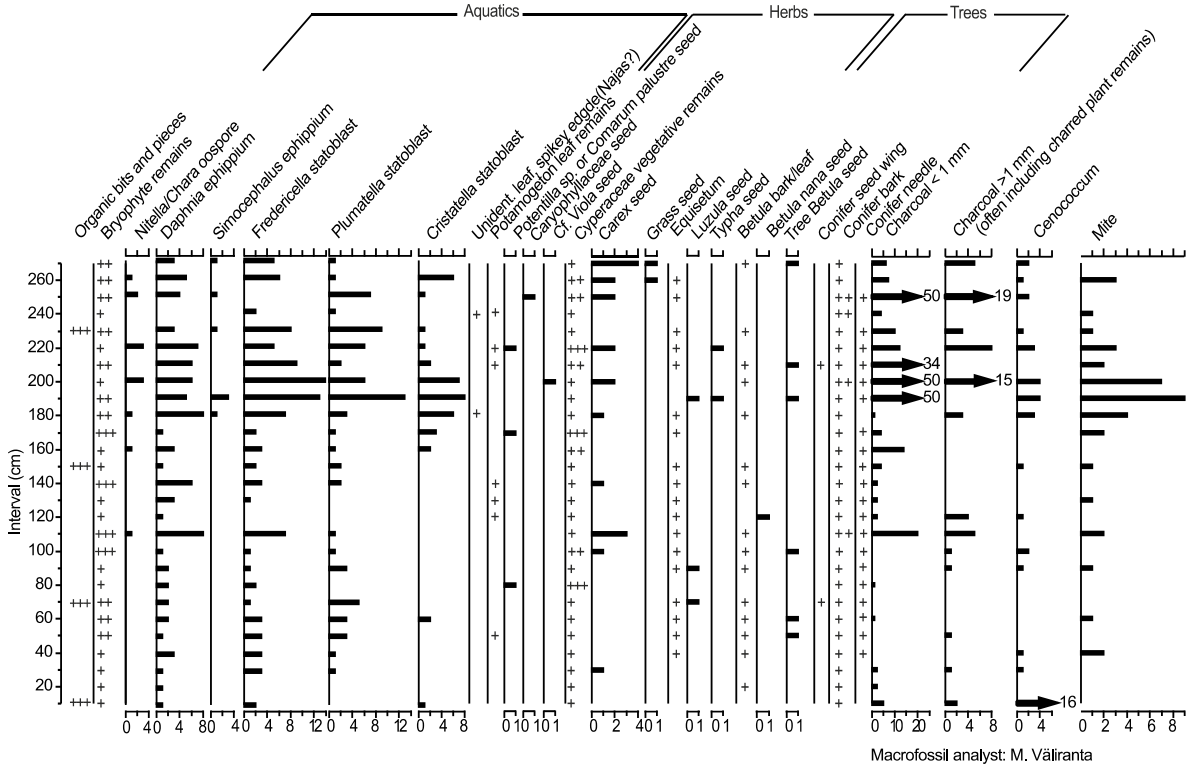

Fig. 4-5. Macrofossil data for Site 009. Most data are presented in raw counts; however, some taxa are qualitatively described as present (+), frequent (++) and abundant (+++). Bryophytes consist mainly of *Scorpidium* spp, but fen species are nearly continuously present, including *Aulacomnium palustre*, *Cinclidium stygium/Rhizomnium* sp., *Meesia triquetra,* and *Tomentypnum nitens.*

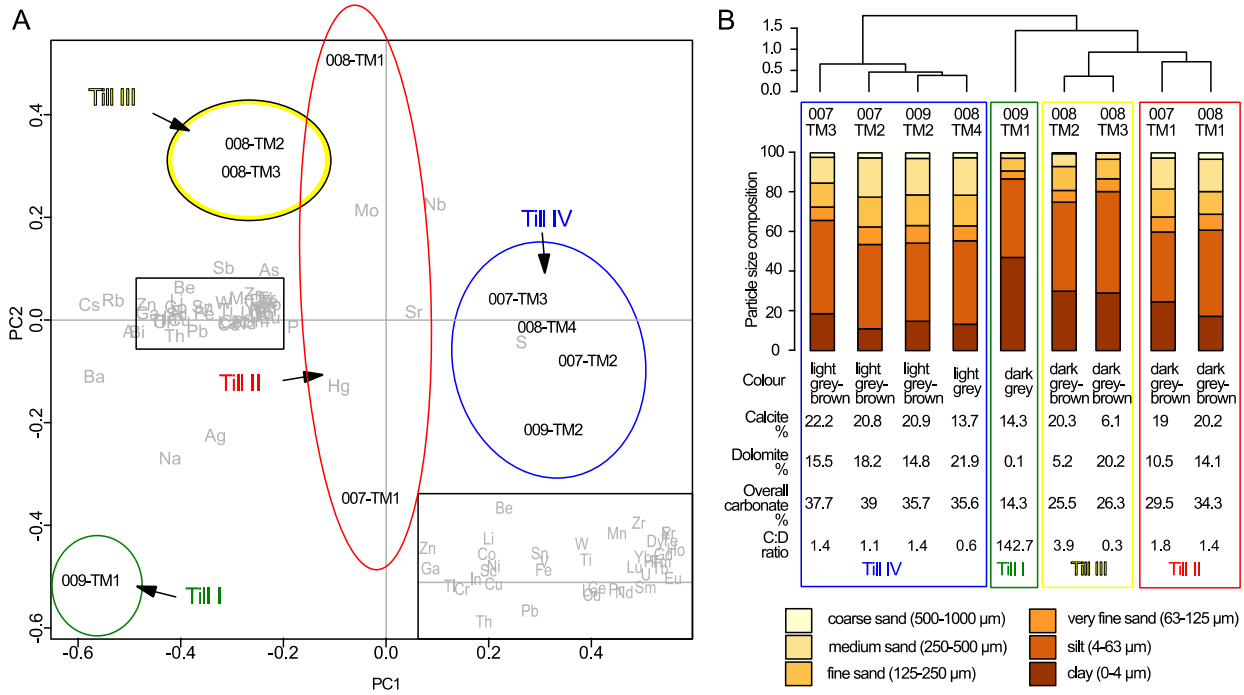

Fig. 4-6. Results of till elemental analysis and sedimentology of the diamicton units at the Albany sites. A: Ordination by PCA of samples by elemental data. All till samples (black text) and elements (grey text) are plotted in the ordination space. B: Sediment size distribution, colour descriptions and carbonate determinations for each sample, showing cluster analysis groups that were derived from the elemental data.

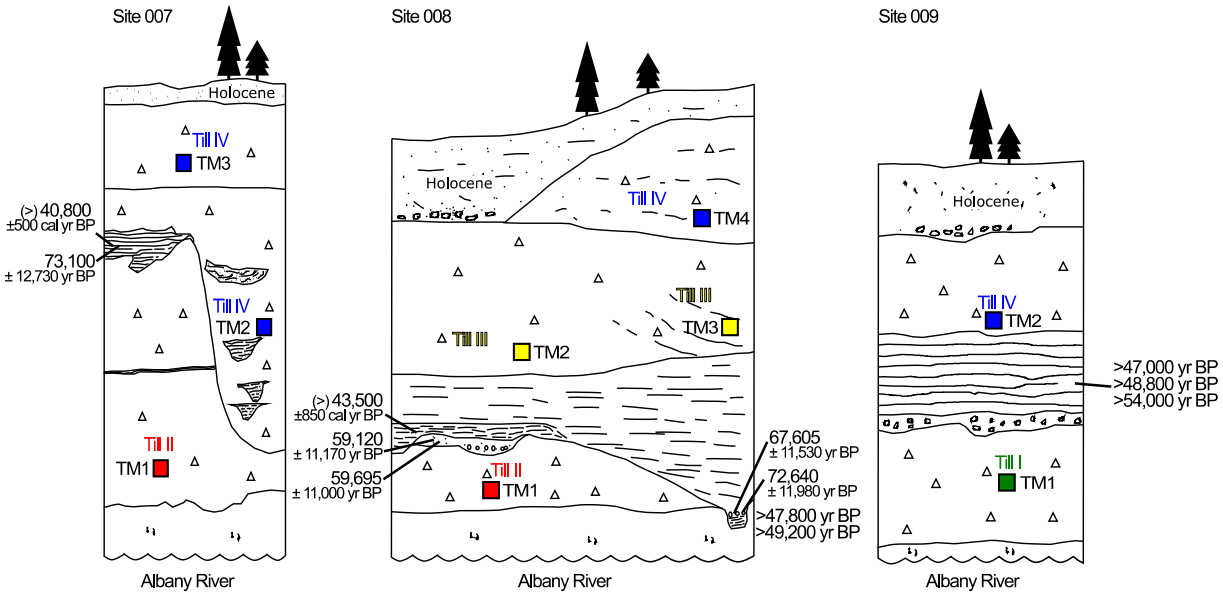

Fig. 4-7. Simplified stratigraphic plot for each of the Albany sites showing sample locations, chronology and till groupings. Finite radiocarbon ages at Site 007 and 008 are shown here as minimum ages and OSL data are presented with 2-sigma errors (see text for details). Sites are located along an 18-km stretch of the Albany River.

Chapter 5
Land-based evidence suggests a significantly reduced Laurentide Ice Sheet during Marine Isotope Stage 3

5.1 Abstract

The paleogeography of the Laurentide Ice Sheet prior to the Last Glacial Maximum (LGM) is largely unknown; however, it is critical for developing accurate glacial models and refining sea level history. Here, we present a hypothesis for the ice extent during Marine Isotope Stage 3 (MIS 3; 57–29 ka) by synthesizing and mapping 671 age determinations from the previously glaciated region. Results from this synthesis suggest a significant glacial recession during that time; much of the previously glaciated region may have been ice-free and the remnant ice sheet may have been restricted to small peripheral domes flanking Hudson Bay. Key evidence in support of this hypothesis comes from the Hudson Bay Lowlands, lying at the center of the previously glaciated region, where geochronological attempts on subaerial deposits range from 40 to 50 ka, are reproducible and show stratigraphic agreement at several sites. The ice configuration implied by these data is a challenge to the long-held assumption that North America was moderately glaciated for the duration of the Wisconsinan Stage (71–24 ka), and necessitates a global mean sea level for MIS 3 at the very highest end of published estimates. Results from this research provide critical empirical data to test emerging hypotheses of global sea level and ice sheet dynamics, and provide an impetus for the development of models of the Laurentide Ice Sheet which integrate terrestrial, sea level and geophysical constraints.

5.2 Introduction

The Laurentide Ice Sheet influenced many global systems, including Earth rheology, ocean circulation, climate variability and biotic migration across continents (Ullman et al., 2014; Peltier et al., 2015; Bacon et al., 2016; Wassenburg et al., 2016). Whereas much is known about the ultimate retreat of this ice sheet (Dyke, 2004), little is known about the growth and dynamics prior to the Last Glacial Maximum (LGM), partly because glacial erosion removed most land-based evidence. The Laurentide Ice Sheet was the largest inferred contributor to global sea level variations during the most recent glacial event (Wisconsinan Stage; ca. 71 to 14 ka; Lambeck et

al., 2014), therefore the paleo-volume of continental ice is tightly linked to records of global mean sea level (GMSL). However, estimates of GMSL vary widely for Marine Isotope Stage 3 (MIS 3; 57–29 ka), the time period preceding the LGM; proxy work on oxygen isotopes of benthic foraminifera suggest that sea levels were between -80 and -30 m (Siddall et al., 2008); a speleothem record constrained sea level to ~-80 m (Grant et al., 2014), and a series of sediment cores from the Bohai Sea suggests that GMSL during MIS 3 may have been closer to -40 m (Pico et al., 2016). Improved constraints on the configuration of the Laurentide Ice Sheet will refine estimates for GMSL during MIS 3.

Well-dated terrestrial records can be used to infer the configuration of past ice sheets and are therefore important for validating ice sheet models and constraining estimates of GMSL (Stokes et al., 2015). One of the most recent attempts to synthesize land-based evidence for the pre-LGM ice position was by Dyke et al. (2002). In that study, ~200 radiocarbon dates from key sites in the Prairies of Central Canada, Eastern Canada and the Great Lakes region were used to hypothesize an ice sheet boundary for the late part of MIS 3 (30–27 ka). The Laurentide Ice Sheet was inferred to have covered the Keewatin district, central Canada, Hudson Bay, Québec, and extended northward to Baffin Island (Fig. 5-1) (Dyke et al., 2002). This ice configuration is often taken to represent the entire MIS 3 interval because few geochronological data exist for earlier parts of MIS 3. This implied moderate glaciation aligns with most models for MIS 3, which suggest only peripheral recession of the ice sheet prior to the build-up toward the LGM (Lambeck and Chappell, 2001; Siddall et al., 2008; Grant et al., 2014). Since 2002, however, additional sites situated within the ice margin suggested by Dyke et al. (2002) have been described, including many with ages older than 30 ka (Rémillard et al., 2013; Bélanger et al., 2014; Bajc et al., 2015; Dalton et al., 2016; Rémillard et al., 2016). These new data provide incentive to update and examine the dataset of land-based evidence to infer ice sheet extent for the period prior to 30 ka.

Here, we present a synthesis of 601 radiocarbon ages, 52 cosmogenic exposure ages, 9 thermoluminescence (TL) ages and 9 optically stimulated luminescence (OSL) ages from sites located in the previously glaciated region (the area contained within the envelope of the Laurentide Ice Sheet during the LGM) of North America which date to MIS 3 (Appendix I). Preservation was largely in contexts where sediments escape glacial scour such as river valleys (Dalton et al., 2016; Chapter 2 of this dissertation), coastal cliffs (Rémillard et al., 2013; 2016),

underground cave sediments (Munroe et al., 2016) and deep lake sediments (Guyard et al., 2011; Stroup et al., 2013). Results presented here delineate the spatial and temporal extent of Late Pleistocene glacial recession over the entire MIS 3 interval, therefore these data are not necessarily in conflict with what was proposed by Dyke et al. (2002) since the temporal focus of that paper was late MIS 3 (30–27 ka). All data are plotted onto a map, and the position of the MIS 3 ice sheet is inferred by comparison to previously published hypotheses for ice extents: the LGM ice extent (Dyke, 2004), the 30–27 ka extent presented by Dyke et al. (2002), and a multi-domed hypothesis presented by Dredge and Thorleifson (1987). Results are discussed in context of the relationship between ice sheet configuration, volume, and GMSL for MIS 3.

5.3 Land-based evidence from the previously glaciated region

The Hudson Bay Lowlands (HBL), Canada, situated in the innermost area of the previously glaciated region, contains an extensive stratigraphic record for the Late Pleistocene. Earlier chronological work in this region suggested that some of these non-glacial intervals may date to the Wisconsinan Stage (Andrews et al., 1983; Forman et al., 1987; Berger and Nielsen, 1990; McNeely, 2002), an age assignment that was met with criticism owing to potential inaccuracies in the chronology data as well as the long-held assumption that the HBL was glaciated throughout the Late Pleistocene. However, recent radiocarbon work by Dalton et al. (2016) (Chapter 2 of this dissertation) supports the Wisconsinan Stage age assignment for many non-glacial intervals in the HBL. In that study, radiocarbon dates were vetted to minimize the potential for contamination and there was stratigraphic agreement at sites where multiple dating attempts were completed.

If chronological evidence from the HBL is correctly interpreted, then this region underwent deglaciation, marine incursion, isostatic adjustment and development of terrestrial landscapes during MIS 3. The Severn Marine site (see Section 2.5), was dated via OSL to 52 ka and 42 ka, which suggests that the ice margin had retreated beyond this location and a marine incursion from the Hudson Bay had inundated this region. Additionally, eight shell dates from a till unit near Repulse Bay, located in the northern portion of Hudson Bay, and the coast of Labrador, have yielded MIS 3 ages which support an ice-free interval during that time (Ives, 1977; McMartin et al., 2015). There is also evidence for the development of subaerial landscapes in the HBL: Three sites from the Hudson Bay Lowlands have been dated to MIS 3 by means of

corroborative radiocarbon dates on bulk peat, wood and organic-bearing sediments (Twelve ^{14}C ages from sites 11-PJB-186, 11-PJB-020, 12-PJB-007; see Section 2.5). The dated portions of these stratigraphic sections consist of organic-bearing, fluvial and lacustrine sediments that underlie till. In addition, paleo-fluviolacustrine sediments from exposures along the Nelson River, western HBL, have been dated to 46–32 ka via TL dating (Berger and Nielsen, 1990). These subaerial landscapes are only possible if the ice sheet had retreated beyond Hudson Bay and isostatic uplift was sufficient for these sites to emerge from below local sea level. This landscape progression suggests a significant and prolonged recession of the ice sheet during MIS 3, which is supported by the timing of chronological determinations from the region.

Most other land-based data published since 2002 lie along the periphery of the 30–27 ka ice extent suggested by Dyke et al. (2002), and therefore extend the timing of glacial recession in these regions to earlier parts of MIS 3. In Eastern Canada, the Anse à la Cabane East section has been dated to 50–40 ka (^{14}C and OSL; Rémillard et al., 2013; 2016), while farther inland, plant fragments from sub-till organic-bearing units have been dated to 33–31 ka (^{14}C; Parent et al., 2015). In the Great Lakes region, several new sites have been constrained to the mid-Wisconsinan Stage, including Zorra Quarry at 50–42 ka (^{14}C; Bajc et al., 2015); the Sixmile Creek Site at 43–27 ka (^{14}C; Karig and Miller, 2013); Genesee Valley at 48–27 ka (^{14}C; Young and Burr, 2006) and Weybridge Cave at 68–36 ka (OSL; Munroe et al., 2016). In the Prairies (Central Canada) sub-till organic-bearing intervals at Jean Lake have been dated to 33 ka (^{14}C; Paulen et al., 2005), and re-worked correlative wood and peat samples have been noted nearby (^{14}C; Fisher et al., 2009). Multiple corroborative charcoal dates from a paleosol located proximal to the Canadian Shield suggests ice-free interval(s) dating to 50–28 ka (^{14}C; Bélanger et al., 2014).

The ice configuration implied by our land-based dataset suggest that MIS 3 ice extent may have been similar to that proposed by Dredge and Thorleifson (1987) (Fig. 5-1). Much of this interpretation is based on radiocarbon data, which can be problematic in the range of >40 ka. However, data from key sites discussed here show significant reproducibility and stratigraphic coherence, lending confidence to the MIS 3 age assignment. It is difficult to assess whether the area was continuously ice-free or whether there may have been periods of ice advance and retreat because of low precision of some data, as well as the fact that most data are associated with fragmented and/or glacially altered stratigraphic records. Further, there is an overall scarcity of

chronology data from the Canadian Shield - a Precambrian crystalline geological unit of exposed bedrock, thin soils and deranged drainage systems that covers a large swath of Canada and that hinders preservation of stratigraphic records (shaded region; Fig. 5-1). Nevertheless, the existing dataset suggests that much of the innermost area of the glaciated region was ice-free during MIS 3, and ice domes may have been restricted to Keewatin, Québec and Baffin Island (Fig. 5-1).

5.4 Support for reduced ice during MIS 3

The ice configuration implied by our results (cf. Dredge and Thorleifson, 1987) is most similar to the ice extent at ~7.5 ka, when ice domes straddled Hudson Bay and the HBL was simultaneously ice-free (Dyke, 2004). This time period corresponds to a GMSL of ~-20 m below present day levels (Fleming et al., 1998). Thus, assuming the Laurentide Ice Sheet is the main contributor to ocean water volume, land-based evidence aligns best with the highest estimated GMSL for MIS 3 (-40 m; Pico et al., 2016). The 20 m discrepancy (Fig. 5-2D) between our qualitatively inferred GMSL based on Holocene comparisons and the model predicted by Pico et al. (2016) could be accounted for by growth of the eastern or western sectors of the ice sheet during MIS 3, which is suggested by aeolian deposits to the southwest (see Section 5.5). This potential glacial growth is not noted in our data synthesis because age determinations presented here reflect only ice-free conditions, and not glacial expansion.

The possibility of ice collapse at the heart of the Laurentide Ice Sheet during MIS 3 is supported by several global proxy records. Summer insolation at 60°N was at its most stable point for the whole of the last glacial cycle during MIS 3, and was also slightly higher than present-day (Fig. 5-2B), which could have contributed towards a sustained glacial recession at that time. Further, ice-core derived atmospheric methane concentrations increased to between ~500 and ~600 ppbV during MIS 3 (Fig. 5-2C) suggesting global peatland expansion. While this expansion could have taken place at lower latitudes, paleoecological analyses of pollen and plant macrofossils in the HBL indicate that extensive peatlands may have been present (Dalton et al., 2017; Chapter 3 of this dissertation), which today are significant contributors to global atmospheric methane (Yu et al., 2013; Packalen et al., 2014). In addition, land-based efforts to place the ice sheet during MIS 3 suggest that the Québec and Keewatin domes of the Laurentide Ice Sheet remained independent throughout much of the Wisconsinan Stage (Kleman et al., 2010) which aligns with an ice-free HBL. Lastly, recent modelling work has shown that the removal of glacial ice from

Hudson Bay and the eastern sector of the Laurentide Ice Sheet during MIS 3, paired with a GMSL of -40 m, helps to reconcile higher-than-expected sea level markers along the US coastline for that time (Pico et al., 2017). In sum, the ice configuration implied by our synthesis of land-based data aligns well with existing and emerging lines of evidence in support of reduced continental ice over North America during MIS 3.

5.5 Addressing evidence for glacial growth during MIS 3

An outstanding issue is reconciling the reduced MIS 3 ice configuration inferred from land-based data (Fig. 5-1) with counterevidence supporting glacial growth during that time. Sionneau et al. (2013) examined clay minerals in a sediment core from the Gulf of Mexico to determine drainage patterns and sediment provenance from the Mississippi River watershed over the Late Pleistocene. In that paper, increases in clay minerals illite and chlorite were noted in the MIS 3 interval of the sediment core. This mineral assemblage is unique to the geology of the Northeastern Great Lakes region, therefore the authors hypothesized that the eastern sector of the ice sheet advanced into the Great Lakes region during that time, contributing clay minerals into the watershed that were eventually transported into the Gulf of Mexico. However, we interpret the data presented by Sionneau et al. (2013) differently, chiefly because the present-day drainage divide separating the Great Lakes and Mississippi Basin is located ~500 km south of the position used in that paper. Assuming our alternative placement of the drainage divide, any clay resulting from glacial advance into the Great Lakes area would have remained in that basin and not be carried over the drainage divide into the Gulf of Mexico. For these reasons, we refute the MIS 3 ice advance proposed by Sionneau et al. (2013) and, instead, suggest that observed changes to clay minerology were related to erosion, precipitation, or shifting of distributary channels in the region south of the drainage divide.

Additional evidence suggests occasional growth of the western sector of the ice sheet to almost LGM extent during MIS 3. The Mississippi River catchment in the mid-continental United States contains several loess deposits that may occur as the result of large sediment and water inputs into the watershed owing to the presence of glacial ice (Johnson and Follmer, 1989). One such loess deposit, the Roxana Silt, has been constrained via radiocarbon and luminescence techniques to MIS 3 (Forman, 1992; Forman and Pierson, 2002), which suggests ice growth to almost LGM extent in the western sector the Laurentide Ice Sheet during that time. However, it

is possible that these loess deposits originated from spillway sediments associated with a pro-glacial lake (Winters et al., 1988). Under this scenario, the ice sheet may not have grown as far south as implied by the Johnson and Follmer (1989) hypothesis. Additional sedimentological evidence from the Gulf of Mexico supports ice advance into the Mississippi River watershed (Tripsanas et al., 2007). The glacial growth implied by these records may help to explain the 20 m discrepancy (Fig. 5-2D) between our inferred GMSL and the model predicted by Pico et al. (2016), and may suggest a highly dynamic ice margin during MIS 3 which is not noted in our synthesis of land-based data.

5.6 Conclusion and future work

Further work is needed to corroborate the hypothesis of a reduced Laurentide Ice Sheet and higher sea level during MIS 3 as well as to provide insight into potential dynamicity of the ice sheet during that time. The application of chronological techniques which extend beyond the theoretical limit of radiocarbon dating (~50 ka) may also improve our understanding of ice sheet configuration and refinement of GMSL into earlier intervals of the Pleistocene. For example, provisional age determinations suggest that ice recession in the HBL and more peripheral areas may extend into MIS 4 and potentially also the late stages of MIS 5a (Shapiro et al., 2004; Briner et al., 2005; Chapter 4 of this dissertation; Fréchette et al., 2006). Thus, it is possible that much of the previously glaciated region was ice-free for a long duration of the Wisconsinan Stage, and ice growth toward the LGM may only have commenced between ~42 ka and ~34 ka as evidenced by proglacial lake sediments and till records in the peripheral regions of the ice sheet (Berger and Eyles, 1994; Wood et al., 2010; Karig and Miller, 2013). The results presented here provide an impetus for continued geochronological and stratigraphic work in the previously glaciated region as a means to further understand GMSL and ice-sheet climate relations over the Late Pleistocene.

5.7 Acknowledgements

This research was funded by the Ontario Geological Survey, Natural Sciences and Engineering Research Council (Canada) (RGPIN 327197-11), Northern Scientific Training Program and University of Toronto Centre for Global Change Science. We thank Art Dyke for insightful comments as well as providing some of the chronology data; Tamara Pico and Jerry Mitrovica

for helpful discussion; as well as S. Williams, M. Nguyen and Missinaibi Headwaters Outfitters for fieldwork and sampling.

5.8 Figures

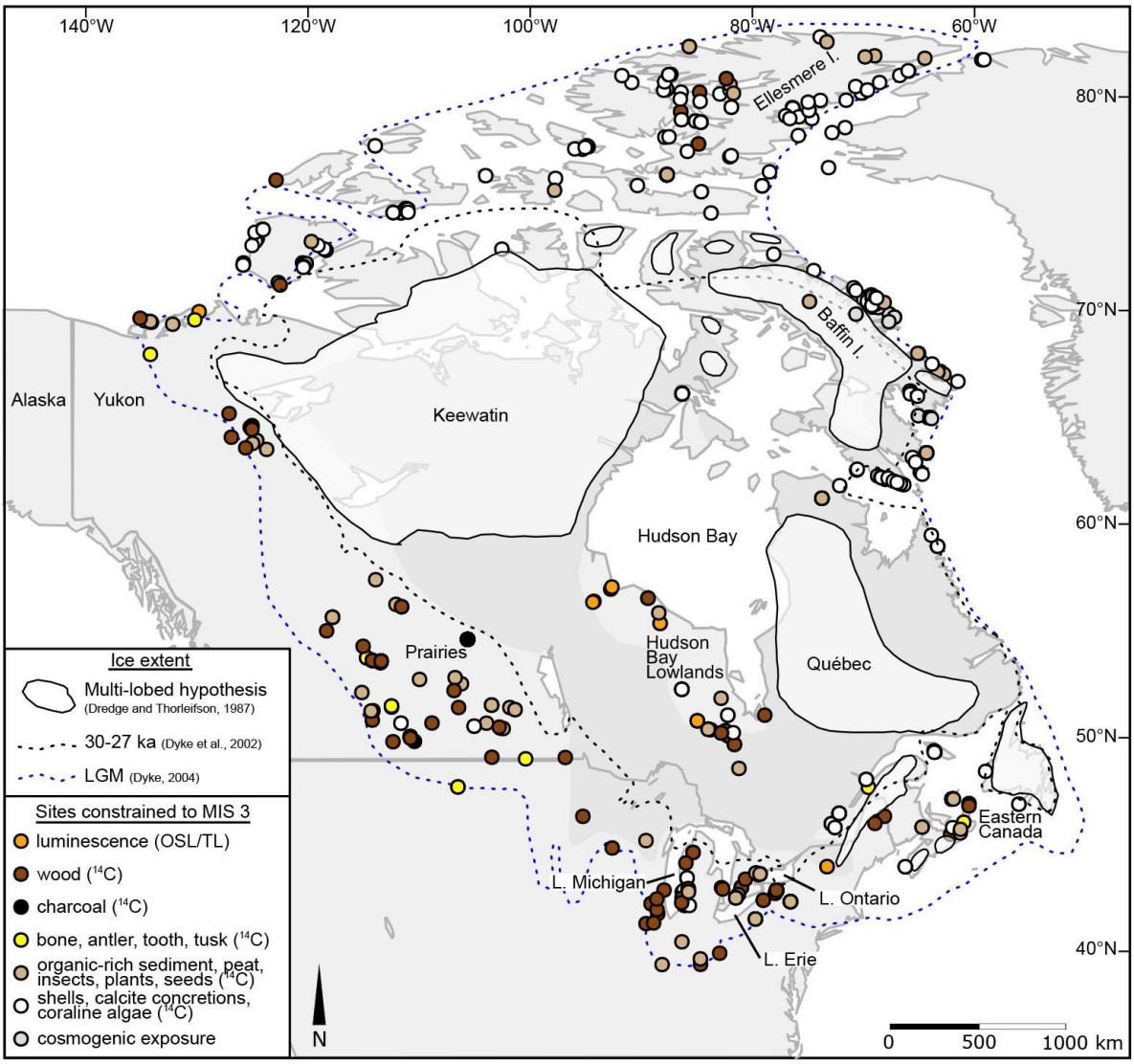

Fig. 5-1. Geochronological data points (n=671 total) lying in the previously glaciated region that are chronologically constrained to MIS 3 (57–29 ka). Data points are colored by type and/or sample material. Some sites contain overlapping data. Contour lines delineate three ice extents: the multi-dome MIS 3 ice configuration after Dredge and Thorleifson (1987), the 30–27 ka ice extent after Dyke et al. (2002), and the LGM ice extent at ~22 ka after Dyke (2004). The shaded region represents the extent of the Canadian Shield. Map was created in R with package 'maps' (Brownrigg et al., 2014).

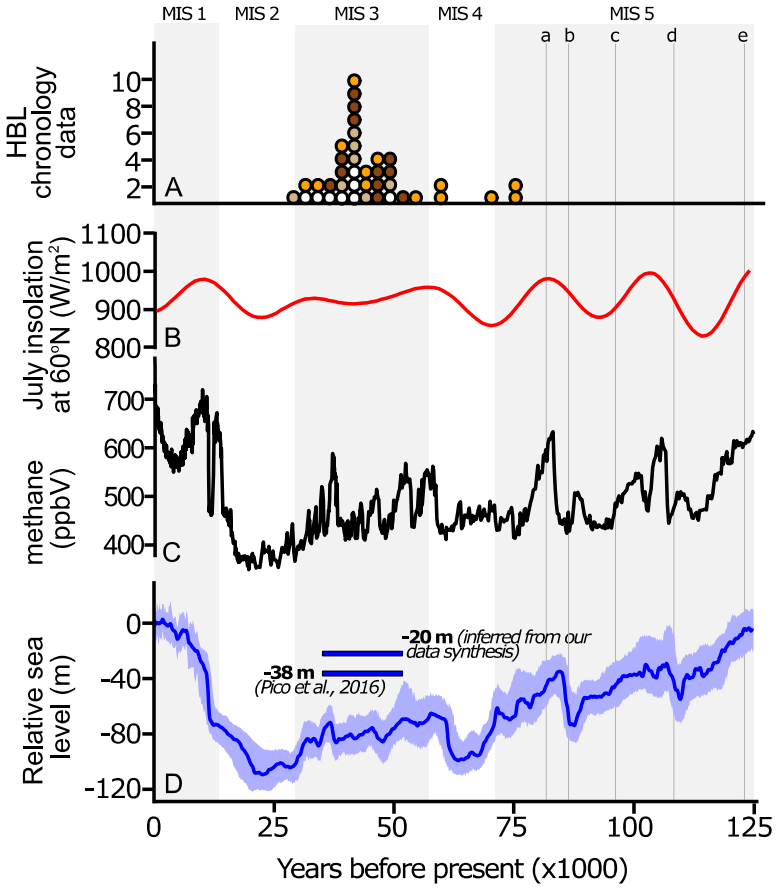

Fig. 5-2. Paleoclimate and orbital parameters over the last glacial cycle (130,000 yr BP to present-day). A: chronology data points from the Hudson Bay Lowlands grouped into 2500-year median age intervals. OSL data from MIS 4 and MIS 5 (Chapter 4, this dissertation) are also shown; 2-sigma errors in these data are in the range of 10 ka. Radiocarbon dates have been calibrated as described in Dalton et al. (2016) (Chapter 2 of this dissertation). Data points are colored according to scheme on Fig. 5-1. B: July insolation at 60°N after Berger and Loutre (1991). C: Atmospheric methane estimates after Loulergue et al. (2008) for the EPICA Dome C ice core. D. Relative sea level estimates after Grant et al. (2014), along with the MIS 3 estimate inferred from our data synthesis (see text for rationale), as well as from Pico et al. (2016) overlaid. Marine Isotope Stages after Lisiecki and Raymo (2005).

Chapter 6
Summary and future work

Stratigraphic records preserved in the Hudson Bay Lowlands (HBL), Canada, have escaped glacial erosion and represent an invaluable archive of paleo-history for the Late Pleistocene. Research presented in this dissertation has provided important insight into the chronology and paleoecology of non-glacial sediments in this periglacial region, documented glacial dynamicity, and provided a land-based dataset to test hypothesized ice volume and global mean sea level (GMSL) during the Late Pleistocene.

6.1 Summary of chronological findings

Results from our critical analysis of chronological data (Chapter 2) suggest that the HBL may have been ice-free during parts of Marine Isotope Stage 7 (MIS 7; ca. 243,000 to ca. 190,000 yr BP), MIS 5 (ca. 130,000 to ca. 71,000 yr BP) and MIS 3 (ca. 57,000 to ca. 29,000 yr BP). Glacial recession during MIS 7 and MIS 5 is expected since most global records suggest minimal continental ice during those times (e.g. sea level curve, $\delta^{18}O$ record, methane). However, recession during MIS 3 is in conflict with generally-accepted models of ice volume (Peltier et al., 2015) and records of sea level (Grant et al., 2014), both of which imply moderate continental glaciation. The age and location of these MIS 3 deposits suggest a highly dynamic ice sheet during the Wisconsinan Stage which is an important land-based constraint for refining and validating ice sheet models. This reduced ice hypothesis is supported by recent sea level and glacial isostatic adjustment models that suggest a significantly reduced ice sheet over the Hudson Bay area during MIS 3 (Pico et al., 2016; 2017). Additional optically stimulated luminescence (OSL) data from the Albany sites (Chapter 4) are of low precision; however, we hypothesize that non-glacial intervals at the Albany sites either date to MIS 5a (ca. 82,000 yr BP), MIS 3, or both time intervals.

6.1.1 Future chronology work

While this dissertation presents a case for ice-free intervals during MIS 3 and MIS 5a, further work is required to refine age estimates. Improving age control on the Missinaibi Formation

should come from techniques which extend beyond the limitation of radiocarbon dating. Results from this dissertation have shown that OSL dating of sub-till fluvial sediments in this region is possible if the sample location is carefully selected to maximize optical exposure and data are filtered to remove low-light emitting quartz grains. Therefore, additional OSL age attempts and increased number of aliquots, perhaps in the form of a regional dataset, will provide a higher precision and better age control on these sediments. An additional avenue is single-grain dating of OSL samples, where individual grains which have low light-emitting characteristics could be eliminated from the age calculation. Measuring only the most reactive sediment grains allows for the equivalent dose to be obtained with high accuracy, thus increasing the precision of the resulting age (Duller, 2008). The drawback is that single-grain OSL dating is extremely time consuming both in the laboratory methods as well as equipment time for measuring the dose rate.

Other chronological methods have also been used to understand the age of Quaternary deposits, some of which have never been tested in the HBL. Magnetostratigraphy, used to measure the orientation of magnetic minerals in sediment, may aid in determining whether sediments were deposited pre- or post- the Brunhes–Matuyama reversal (ca. 780,000 yr BP). This technique is commonly used to date sediment successions in western Canada (Barendregt, 2011; Duk-Rodkin and Barendregt, 2011). Another potential avenue is tephrochronology, whereby tephra shards in the non-glacial intervals are characterized and then compared to known volcanic events. Distal tephra can undergo 5000+ km of transportation in the atmosphere prior to deposition (Lowe et al., 2013; Jensen et al., 2014; Mackay et al., 2016), opening the possibility that cryptotephra layers are preserved in non-glacial samples in the HBL. In addition, if wood samples can be found that are encased in clay, thus ensuring a closed system with respect to uranium, this would be suitable material for U-Th dating (Allard et al., 2012). However, wood samples encased in clay were not found in the sites examined for this dissertation. A final consideration would be amino acid dating. Despite the fact that it is a relative dating method, it is notable that it was the first method to influentially suggest that the region was ice-free during MIS 3. Although it cannot be used to assign absolute ages, it may be a useful tool for correlating non-glacial intervals between sites which are in relative close proximity and which have undergone a similar burial history.

6.2 Summary of paleoecological findings

Quantitative climate reconstructions from the HBL provide insight into Late Pleistocene climate variability from the glaciated region, provide important insight into vegetation adaptation under conditions of climate change, and facilitate comparison to other local, regional and global Pleistocene-aged records. At both the Ridge and Albany sites (Chapter 3, 4), the non-glacial intervals were characterized by boreal-peatland assemblages dominated by *Sphagnum*, Cyperaceae, *Pinus*, *Picea*, *Salix*, *Alnus* and *Betula* along with herbaceous taxa such as Asteraceae, Ericaceae, Amaranthaceae and Poaceae. Macrofossils provided additional insight into the local vegetation by identifying the presence of local boreal species, evidence of forest fires and proximity to aquatic environments. This interpretation aligns with other pollen data from the HBL (Terasmae and Hughes, 1960; Nielsen et al., 1986; Dredge et al., 1990; Allard et al., 2012) that suggest the region was a wetland during all non-glacial intervals of the Quaternary.

Pollen-based paleoclimate reconstruction was undertaken at the Ridge Site (dated to MIS 3; Chapter 3) and the Albany sites (hypothesized to be MIS 5a and possibly also MIS 3; Chapter 4) using the modern analogue technique and a modern-day calibration set comprised of the North American Modern Pollen Database (Whitmore et al., 2005) along with 49 new sites from the HBL. Both the Ridge and Albany sites yielded temperatures similar to present-day, although paleo-precipitation estimates were notably lower at the Ridge Site, suggesting that it may be possible to differentiate the MIS 3 deposits on the basis of less inferred annual precipitation than present-day. Comparison of additional sub-till pollen records is needed; however, these results suggest that pollen-based reconstructions may be developed into an inferential dating tool for Late Pleistocene deposits in the HBL. Macrofossils, which are useful for refining pollen-based paleoclimate estimates, were examined at the Ridge Site and one of the Albany sites, but these records contained few temperature-indicative taxa, and were thus of limited use for refining the pollen-based temperature estimates.

6.2.1 Future paleoecological work

Paleoecological work presented here was largely based on pollen owing to good preservation at many sub-till sites in the HBL, thus priority should be placed on developing methods that optimize the potential for this proxy. The root of many uncertainties in the reconstructions lies in

the fact that taxa typical of the HBL span large geographic ranges. The addition of n = 49 additional sites from the HBL to the modern pollen dataset (Whitmore et al., 2005) improved the accuracy of reconstruction; however, further improving the spatial resolution of northern peatlands is important. There is also a need to better quantify the errors inherent to the modern analogue technique. The error metric presented in this dissertation was the root mean squared error of prediction (RMSEP), which is a statistical measure that reflects the predictive accuracy of the modern calibration set. The RMSEP does not account for any variability or errors that may be present in the modern calibration set or fossil data. For example, the effect of using precipitation and temperature values from a gridded climate dataset are not taken into account. There are very few weather stations in the HBL, therefore the accuracy of these climate data on a local scale (such as along the Albany River) is not known. Additional uncertainties are introduced when enumerating fossil pollen data; for example, there is no measurement of variability in sampling, processing or enumerating pollen slides. Developing methods to properly incorporate errors from all data inputted into the modern analogue technique is key for improving the accuracy of paleoclimate estimates.

Other areas for improvement are the continued testing of quantitative pollen methods other than the modern analogue technique, notably ordinations to examine the structure of pollen data, examination of species response curves (Huisman et al., 1993) and developing methods to better understand the role of rare temperate taxa that are present in the samples (Gajewski, 2015). It may also be valuable to explore other forms of quantitative pollen reconstructions. For example, several numerical techniques have been developed that work well on pollen data (Felde et al., 2014), but are not widely applied to palynology. Much of these techniques are focused on classification, whereby the modern dataset is examined in terms of categories which are then reconstructed in the fossil data; for example, eocregions, ecozones, or wetland classes (e.g. fen, bog, swamp). Examples include discriminant analysis (Zhang et al., 2013), various forms of classification trees (Goring et al., 2010) as well as the application of plant functional types (Williams et al., 1998; Thompson and Anderson, 2000). In the future, these techniques may permit paleo-wetland mapping, which would be highly complementary for understanding how the climate system worked in the past, in particular with respect to wetland carbon storage.

Other paleoecological proxies are underutilized in the HBL, and hold potential to compliment pollen-based reconstructions. For example, insects, in particular Coleoptera and Chironomidae,

can be highly diagnostic with respect to climate (e.g. Engels et al., 2008; Khorasani et al., 2015), and have been used to support paleo-interpretations at other sub-till sites in the HBL (Netterville, 1974; Nielsen et al., 1986; Dredge et al., 1990). However, in some cases it can take a substantial amount of sediment to yield any insects (e.g. 18 kg of sediment yielded only 350 moderate or poorly preserved insect fragments; Nielsen et al., 1986). When preserved, microfossils such as dinoflagellate cysts, foraminifera, diatoms and/or chironomids, are useful paleo-indicators of past environmental conditions. A preliminary investigation showed the preservation of diatoms at one sub-till site. Further, non-biological proxies such as stable isotopes and biomarkers can provide insight into vegetation transition and paleoclimate variables, which can be highly complementary to the pollen and macrofossil record (Kuhl and Moschen, 2012; Margalef et al., 2013; Sachs et al., 2013).

6.3 Summary of stratigraphic findings

At the Albany sites (Chapter 4), elemental, sedimentological and geomorphological analyses of the till units, along with comparison of geochronological age attempts and paleoecological analyses of the non-glacial intervals permitted the recognition of at least three glacial advances, separated by a non-glacial interval. Till units observed along the Albany River have similar flow directions as tills previously assigned to MIS 5 (Thorleifson et al., 1992; 1993) or MIS 4 (Kleman et al., 2010) and the most recent glacial advance over the area (Skinner, 1973; Veillette and Pomares, 1991). Therefore, this research contributes toward the spatial reconstruction of at least three glacial advances from shifting ice centers within the Québec sector of the Laurentide Ice Sheet, along with the occurrence of at least one non-glacial interval. Stratigraphic analyses were also used as a tool to place the Ridge Site (Chapter 3) in context to nearby stratigraphic work. In addition, stratigraphic analyses were key for interpreting the paleo-setting of the non-glacial units examined at the Ridge and Albany sites. At all sites, loss-on-ignition, particle size and carbon content analysis were used to infer a fluvial environment, and most sites showed evidence for the development of an abandoned river channel that transitioned into overbank or possibly oxbow lake sediments capable of supporting water-logged peatland biota.

6.3.1 Future stratigraphic work

Stratigraphic work presented here was focused on a few select sites; however, future efforts should focus on improving the spatial resolution of stratigraphic studies so that the regional

stratigraphy can be constructed. Future stratigraphic work in the HBL should focus on better characterization of the glacial (till) and non-glacial units. In particular, finding and studying sites which contain multiple non-glacial intervals (sites along the Nelson River; Nielsen et al., 1986), is highly valuable because these sites would help to definitively show the difference(s), if any, between the non-glacial intervals in this region. This may help to resolve issues pertaining to stratigraphic correlations in the immediate area, as well as provide insight into the validity of pollen as an inferential dating tool (presented in Chapter 3). Another stratigraphic consideration is the elevation of non-glacial units relative to present-day; it is possible that non-glacial intervals that are exposed near present-day river levels were deposited at a time when rivers were similarly incised as they are today (e.g. interglacial), and that interstadial deposits might be situated at a higher elevation. The study of additional sites may allow for the testing of this hypothesis. A final stratigraphic research direction is the study of glacially-incorporated biota from the antecedent non-glacial sediments (e.g. shells, foraminifera, *Sphagnum*) via amino acid analysis, paleoecological analysis and biomarkers that may be an important stratigraphic marker for correlating fragmented records (Andrews et al., 1983; Dredge et al., 1990; Battram et al., 2015).

The Moose River Basin (south of James Bay) is relatively easy to access and contains a rich and understudied glacial and non-glacial record. Site 24M, the type section for the Missinaibi Formation, contains two till units overlain by an extensive non-glacial unit, which is topped by glacial sediments (Terasmae and Hughes, 1960). Little work has gone into understanding the stratigraphy of this site in recent years, despite significant advances in stratigraphic, chronological and paleoecological techniques. There is also evidence for a large proglacial lake in this region which is thought to have formed after an interglacial when the ice sheet was advancing (Skinner, 1973). To our knowledge, this is the only area in the HBL which contains evidence of a pre-LGM proglacial lake. There is also evidence suggesting that at least two non-contemporaneous marine deposits are present in the Moose River area (Bell Sea, Prest Sea; Skinner, 1973; Andrews et al., 1983; Laymon, 1991). These marine sites are highly valuable because they provide a direct marker of sea level and are therefore important for understanding the regional stratigraphic record.

6.4 Summary of using land-based data to infer past ice extents

The age and location of 671 data points synthesized in Chapter 5 suggest a significant reduction of the Laurentide Ice Sheet during MIS 3; it is possible that the HBL was ice-free and that ice was restricted to domes over the Keewatin and Québec sector during that time. These data support the presence of multiple ice growth centers (domes) during the Wisconsinan Stage as opposed to a single ice dome that was first proposed by Flint (1943). This interpretation is a challenge to the long-held assumption that North America was moderately glaciated prior to the LGM, and implies a global mean sea level at the very highest end of published estimates for MIS 3 (-40 m; Pico et al., 2016). Results from this research highlight the importance of terrestrial data for refining glacial models and sea level history.

6.4.1 Future work on past ice sheet extent

Work presented here suggests that North America may have been ice-free during MIS 3; however, there is a need to integrate marine and terrestrial datasets, along with geophysical models, to accurately reconstruct past ice sheets (Stokes et al., 2015). Future research directions may involve testing the implied ice sheet configuration (Chapter 5) with geophysical models which incorporate ice histories, isostatic uplift and sea level records (Lambeck and Chappell, 2001; Creveling et al., 2017), or the reconciliation of our chronology dataset with other land-based evidence (e.g. landform data; Kleman et al., 2010) to better understand the terrestrial record for this time period. Another research avenue may be determining whether the HBL was continuously ice-free during MIS 3 or whether there were intervals of glacial advance and retreat. This may be possible in the future with continued dating of deposits in the HBL as well as the development of techniques to improve the precision of age estimates. It may also be valuable to examine the Heinrich and Dansgaard-Oeschger records (Dansgaard et al., 1993; Hemming, 2004) to evaluate whether instabilities in the ice sheet or abrupt warming events can be aligned with glacial processes or ecosystem development in the paleorecord of the HBL. In addition, continued study of loess deposits, proglacial lake sediments and other paleo-records from the regions proximal to the ice sheet will help to infer the position of the ice margin as well as any dynamicity (Forman, 1992; Wood et al., 2010).

References

Aitchison, J., 1986. The Statistical Analysis of Compositional Data. Chapman & Hall, New York.

Allard, G., Roy, M., Ghaleb, B., Richard, P.J.H., Larouche, A.C., Veillette, J.J., Parent, M., 2012. Constraining the age of the last interglacial–glacial transition in the Hudson Bay lowlands (Canada) using U–Th dating of buried wood. Quaternary Geochronology 7, 37-47.

Allen, J.R.L., 1965. A review of the origin and characteristics of recent alluvial sediments. Sedimentology 5, 89-191.

Amante, C., Eakins, B.W., 2009. ETOPO1 1 Arc-Minute Global Relief Model: Procedures, Data and Analysis, NOAA Technical Memorandum NESDIS NGDC-24, National Geophysical Data Center, NOAA. doi: 10.7289/V5C8276M.

Anderson, R.S., David, R.B., Stuckenrath, R., Borns, H.W., Jr., 1988. Interstadial conifer wood from northern Maine. Quaternary Research 30, 98-101.

Andrews, J.T., 1987. The Late Wisconsin Glaciation and deglaciation of the Laurentide Ice Sheet, North America and adjacent oceans during the last deglaciation. The Geological Society of America, pp. 13-37.

Andrews, J.T., Dyke, A.S., 2007. Glaciations: Late Quaternary in North America, in: Elias, S.A. (Ed.), Encyclopedia of Quaternary Science. Elsevier, Amsterdam, pp. 1095-1101.

Andrews, J.T., Laymon, C.A., Briggs, W.M., 1989. Radiocarbon date list III: Labrador and Northern Quebec, Canada and Radiocarbon List VI: Baffin Island, N.W.T., Canada. Institute of Arctic and Alpine Research Occasional Paper No. 46.

Andrews, J.T., Shilts, W.W., Miller, G.H., 1983. Multiple deglaciations of the Hudson Bay Lowlands, since deposition of the Missinaibi (Last-Interglacial?) Formation. Quaternary Research 19, 18-37.

Auguie, B., 2012. gridExtra: functions in Grid graphics. R package version 0.9.1, http://CRAN.R-project.org/package=gridExtra.

Bacon, C.D., Molnar, P., Antonelli, A., Crawford, A.J., Montes, C., Vallejo-Pareja, M.C., 2016. Quaternary glaciation and the Great American Biotic Interchange. Geology 44, 375-378.

Bajc, A.F., Karrow, P.F., Jasinski, P., Warner, B.G., 2009. New occurrences of sub-till organic deposits in southwestern Ontario: Are they really all that rare? [abstract], 2009 Joint Assembly [CGU, GAC, IAH-CNC, MAC, SEG, MSA, GS, AGU], Toronto, ON.

Bajc, A.F., Karrow, P.F., Yansa, C.H., Curry, B.B., Nekola, J.C., Seymour, K.L., Mackie, G.L., 2015. Geology and paleoecology of a Middle Wisconsin fossil occurrence in Zorra Township, southwestern Ontario, Canada. Canadian Journal of Earth Sciences 52, 386-404.

Balco, G., Rovey, C.W.I., 2010. Absolute chronology for major Pleistocene advances of the Laurentide Ice Sheet. Geology 38, 795-798.

Barendregt, R.W., 2011. Magnetostratigraphy of Quaternary Sections in Eastern Alberta, Saskatchewan and Manitoba. Developments in Quaternary Sciences 15, 591-600.

Barnett, P.J., 1992. Chapter 21: Quaternary Geology of Ontario, The Geology of Ontario. Ontario Geological Survey, Special Volume 4; pt. 2, pp. 1011-1088.

Barnett, P.J., Finkelstein, S.A., 2013. Sub-till organic-bearing sediments of the Hudson Bay Lowland: stratigraphy and geochronology, CANQUA-CGRG Conference 2013, Edmonton, Alberta, p. 53.

Barnett, P.J., Webb, J.L., Hill, J.L., 2009. Flow indicator map of the Far North of Ontario; Ontario Geological Survey, Preliminary Map P.3610, scale 1:1,000,000.

Barnett, P.J., Yeung, K.H., 2012. Field investigations for remote predictive terrain mapping in the far north of Ontario. Summary of Field Work and Other Activities 2012: Ontario Geological Survey, Open File Report 6280, 24-21 to 24-25.

Barr, W., 1971. Postglacial Isostatic Movement in Northeastern Devon Island: A Reappraisal. Arctic 24, 249-268.

Barrette, L., La Salle, P., Samson, C., 1981. Quebec radiocarbon measurements III. Radiocarbon 23, 241-251.

Bateman, M.D., Murton, J.B., 2006. The chronostratigraphy of Late Pleistocene glacial and periglacial aeolian activity in the Tuktoyaktuk Coastlands, NWT, Canada. Quaternary Science Reviews 25, 2552-2568.

Battram, N.M., Eyles, N., Lau, P.S., Simpson, M.J., 2015. Organic matter biomarker analysis as a potential chemostratigraphic tool for Late Pleistocene tills from the Hudson Bay Lowlands, Canada. Palaeogeography, Palaeoclimatology, Palaeoecology 418, 377-385.

Bazely, D., 1981. The surface pollen spectra of La Pérouse Bay, Manitoba, Canada, B.Sc thesis, Biogeography and Environmental Studies. University of Toronto.

Bednarski, J.M., 1995. Glacial advances and stratigraphy in Otto Fiord and adjacent areas, Ellesmere Island, Northwest Territories. Canadian Journal of Earth Sciences 32, 52-64.

Bednarski, J.M., 1998. Quaternary history of Axel Heiberg Island bordering Nansen Sound, Northwest Territories, emphasizing the last glacial maximum. Canadian Journal of Earth Sciences 35, 520-533.

Bélanger, N., Carcaillet, C., Padbury, G.A., Harvey-Schafer, A.N., Van Rees, K.J., 2014. Periglacial fires and trees in a continental setting of Central Canada, Upper Pleistocene. Geobiology 12, 109-118.

Bell, R., 1879. Report on the country between Lake Winnipeg and Hudson's Bay, 1978. Geological Survey of Canada, 31 p.

Bell, R., 1886. An exploration of portions of the At-ta-wa-pish-kat & Albany Rivers, Lonely Lake to James Bay. Geological and Natural History Survey of Canada, 38 p.

Bell, T., 1992. Glacial and sea level history of western Fosheim Peninsula, Ellesmere Island, Arctic Canada, Department of Geography. University of Alberta.

Bell, T., 1996. The last glaciation and sea level history of Fosheim Peninsula, Ellesmere Island, Canadian High Arctic. Canadian Journal of Earth Sciences 33, 1075-1086.

Bell, T., Batterson, M., Blundon, P., 2008. A re-evaluation of the coastal stratigraphy along the southwestern Burin Peninsula. Current Research (2008) Newfoundland and Labrador Department of Natural Resources Geological Survey Report 08-1, 35.

Bennett, K.D., 1996. Determination of the number of zones in a biostratigraphical sequence. New Phytologist 132, 155-170.

Berger, A., Loutre, M.F., 1991. Insolation values for the climate of the last 10 million years. Quaternary Science Reviews 10, 297-317.

Berger, G.W., 1984. Thermoluminescence dating studies of glacial silts from Ontario. Canadian Journal of Earth Sciences 21, 1393-1399.

Berger, G.W., Eyles, N., 1994. Thermoluminescence chronology of Toronto-area Quaternary sediments and implications for the extent of the midcontinent ice sheet(s). Geology 22, 31-34.

Berger, G.W., Nielsen, E., 1990. Evidence from thermoluminescence dating for Middle Wisconsinan deglaciation in the Hudson Bay Lowland of Manitoba. Canadian Journal of Earth Sciences 28, 240-249.

Berti, A.A., 1975. Paleobotany of Wisonsinan Insterstadials, Eastern Great Lakes Region, North America. Quaternary Research 5, 591-619.

Beukens, R.P., 1990. High-precision intercomparion at ISOTRACE. Radiocarbon 32, 335-339.

Birks, H.H., Birks, H.J.B., 2000. Future uses of pollen analysis must include plant macrofossils. Journal of Biogeography 27, 31-35.

Blake, W.J., 1983. Geological Survey of Canada Radiocarbon Dates XXII. Geological Survey of Canada Paper 83-7.

Blake, W.J., 1984. Geological Survey of Canada Radiocarbon Dates XXIV. Geological Survey of Canada Paper 84-7.

Blake, W.J., 1986. Geological Suvey of Canada Radiocarbon Dates XXV. Geological Survey of Canada Paper 85-7.

Blake, W.J., 1987. Geological Survey of Canada Radiocarbon Dates XXVI. Geological Survey of Canada Paper 86-7.

Blake, W.J., 1988. Geological Survey of Canada Radiocarbon Dates XXVII. Geological Survey of Canada Paper 87-7.

Blake, W.J., 1993. Holocene emergence along the Ellesmere Island coasts of northernmost Baffin Bay. Norsk Geologisk Tidsskrift 73, 147-160.

Böhm, E., Lippold, J., Gutjahr, M., Frank, M., Blaser, P., Antz, B., Fohlmeister, J., Frank, N., Andersen, M.B., Deininger, M., 2015. Strong and deep Atlantic meridional overturning circulation during the last glacial cycle. Nature 517, 73-76.

Bos, J.A.A., Helmens, K., Bohncke, S.J.P., Seppä, H., Birks, H., J, B, 2009. Flora, vegetation and climate at Sokli, northern Fennoscandia, during the Weichselian Middle Pleniglacial. Boreas 38, 335-348.

Boulton, G.S., Clark, C.D., 1990. A highly mobile Laurentide ice sheet revealed by satellite images of glacial lineations. Nature 346, 813-817.

Bowman, S., 1990. Radiocarbon Dating. University of California Press.

Brandefelt, J., Kjellström, E., Näslund, J.O., Strandberg, G., Voelker, A.H.L., Wohlfarth, B., 2011. A coupled climate model simulation of Marine Isotope Stage 3 stadial climate. Climate of the Past 7, 649-670.

Briner, J.P., 2003. The last glaciation of the Clyde Region, Northeastern Baffin Island, Arctic Canada: Cosmogenic isotpe constrains on Laurentide Ice Sheet dynamics and chronology, Department of Geological Sciences. University of Colorado.

Briner, J.P., Miller, G.H., Davis, P.T., Finkel, R.C., 2005. Cosmogenic exposure dating in arctic glacial landscapes: implications for the glacial history of northeastern Baffin Island, Arctic Canada. Canadian Journal of Earth Sciences 42, 67-84.

Briner, J.P., Miller, G.H., Davis, P.T., Finkel, R.C., 2006. Cosmogenic radionuclides from fiord landscapes support differential erosion by overriding ice sheets. Geological Society of America Bulletin 118, 406-420.

Brooks, G.R., 2003. Alluvial deposits of a mud-dominated stream: the Red River, Manitoba, Canada. Sedimentology 50, 441-458.

Brooks, G.R., Medioli, B.E., 2003. Deposits and Cutoff Ages of Horseshoe and Marion Oxbow Lakes, Red River, Manitoba. Géographie physique et Quaternaire 57, 151-158.

Brovkin, V., Brücher, T., Kleinen, T., Zaehle, S., Joos, F., Roth, R., Spahni, R., Schmitt, J., Fischer, H., Leuenberger, M., Stone, E.J., Ridgwell, A., Chappellaz, J., Kehrwald, N., Barbante, C., Blunier, T., Dahl Jensen, D., 2016. Comparative carbon cycle dynamics of the present and last interglacial. Quaternary Science Reviews 137, 15-32.

Brownrigg, R., Minka, T.P., Becker, R.A., Wilks, A.R., 2014. maps: Draw Geographical Maps. R package version 2.3-, http://CRAN.R-project.org/package=maps.

Buckley, J., Willis, E.H., 1972. Isotopes' radiocarbon measurements IX. Radiocarbon 14, 114-139.

Bunbury, J., Finkelstein, S.A., Bollmann, J., 2012. Holocene hydro-climatic change and effects on carbon accumulation inferred from a peat bog in the Attawapiskat River watershed, Hudson Bay Lowlands, Canada. Quaternary Research 78, 275-284.

Bunting, M.J., Warner, B.G., Morgan, C.R., 1998. Interpreting pollen diagrams from wetlands: pollen representation in surface samples from Oil Well Bog, southern Ontario. Canadian Journal of Botany 76, 1780-1797.

Calkin, P.E., Muller, E.H., Barnes, J.H., 1982. The Gowanda hospital interstadial site, New York. American Journal of Science 282, 1110-1142.

Causse, C., Vincent, J.S., 1989. Th-U disequilibium dating of Middle and Late Pleistocene wood and shells from Banks and Victoria islands, Arctic Canada. Canadian Journal of Earth Sciences 26, 2718-2723.

Christiansen, E.A., Gendzwill, D.J., Meneley, W.A., 1982. Howe lake: a hydrodynamic blowout structure. Canadian Journal of Earth Sciences 19, 1122-1139.

Colgan, P.M., Vanderlip, C.A., Braunschneider, K.N., 2015. Athens Subepisode (Wisconsin Episode) non-glacial, and older glacial sediments in the subsurface of southwestern Michigan, USA. Quaternary Research 84, 382-397.

Cong, S., Ashworth, A.C., Schwert, D.P., 1996. Fossil Beetle Evidence for a Short Warm Interval near 40,000 yr B.P. at Titusville, Pennsylvania. Quaternary Research 45, 216-225.

Creveling, J.R., Mitrovica, J.X., Clark, P.U., Waelbroeck, C., Pico, T., 2017. Predicted bounds on peak global mean sea level during marine isotope stages 5a and 5c. Quaternary Science Reviews 163, 193-208.

Cyr, D., Bergeron, Y., Gauthier, S., Larouche, A.C., 2005. Are the old-growth forests of the Clay Belt part of a fire-regulated mosaic? Canadian Journal of Forest Research 35, 65-73.

Dallimore, S.R., Wolfe, S.A., Matthews, J.V.J., Vincent, J.S., 1997. Mid-Wisconsinan eolian deposits of the Kittigazuit Formation, Tuktoyaktuk Coastlands, Northwest Territories, Canada. Canadian Journal of Earth Sciences 34, 1421-1441.

Dalton, A.S., Finkelstein, S.A., Barnett, P.J., Forman, S.L., 2016. Constraining the Late Pleistocene history of the Laurentide Ice Sheet by dating the Missinaibi Formation, Hudson Bay Lowlands, Canada. Quaternary Science Reviews 146, 288-299.

Dalton, A.S., Väliranta, M., Barnett, P.J., Finkelstein, S.A., 2017. Pollen and macrofossil-inferred paleoclimate at the Ridge Site, Hudson Bay Lowlands, Canada: Evidence for a dry climate and significant recession of the Laurentide Ice Sheet during Marine Isotope Stage 3. Boreas 46, 388-401.

Dansgaard, W., Johnsen, S.J., Clausen, H.B., Dahl-Jensen, D., Gundestrup, N.S., Hammer, C.U., Hvidberg, C.S., Steffensen, J.P., Sveinbjörnsdottir, A.E., Jouzel, J., Bond, G., 1993. Evidence for general instability of past climate from a 250-kyr ice-core record. Nature 364, 218-220.

de Vernal, A., Causse, C., Hillaire-Marcel, C., Mott, R., Occhietti, S., 1986. Palynostratigraphy and Th/U ages of upper Pleistocene interglacial and interstadial deposits on Cape Breton Island, eastern Canada. Geology 14, 554-557.

Demuro, M., Arnold, L.J., Froese, D.G., Roberts, R.G., 2013. OSL dating of loess deposits bracketing Sheep Creek tephra beds, northwest Canada: Dim and problematic single-grain OSL characteristics and their effect on multi-grain age estimates. Quaternary Geochronology 15, 67-87.

DiLabio, R.N.W., Miller, R.F., Mott, R.J., Coker, W.B., 1988. The Quaternary stratigraphy of the Timmins area, Ontario, as an aid to mineral exploration by drift prospecting. Geological Survey of Canada paper 88-1C, 61-66.

Dionne, J.-C., Occhietti, S., 1996. Aperçu du Quaternaire à l'embouchure du Saguenay, Québec. Géographie physique et Quaternaire 50, 5-34.

Dorale, J.A., Edwards, R.L., Ito, E., González, L.A., 1998. Climate and Vegetation History of the Midcontinent from 75 to 25 ka: A Speleothem Record from Crevice Cave, Missouri, USA. Science 282, 1871-1874.

Dorale, J.A., Onac, B.P., Fornós, J.J., Ginés, J., Ginés, A., Tuccimei, P., Peate, D.W., 2010. Sea-Level Highstand 81,000 Years Ago in Mallorca. Science 327, 860-863.

Dorion, C.C., 1997. An updated high resolution chronology of deglaciation and accompanying marine transgression in Maine, Geological Sciences. University of Maine, p. 147 p.

Dredge, L.A., Morgan, A.V., Nielsen, E., 1990. Sangamon and Pre-Sangamon Interglaciations in the Hudson Bay Lowlands of Manitoba. Géographie physique et Quaternaire 44, 319-336.

Dredge, L.A., Mott, R.J., 2003. Holocene Pollen Records and Peatland Development, Northeastern Manitoba. Géographie physique et Quaternaire 57, 7-19.

Dredge, L.A., Thorleifson, L.H., 1987. The Middle Wisconsinan History of the Laurentide Ice Sheet. Géographie physique et Quaternaire 41, 215-235.

Dreimanis, A., 1962. Quantitative gasometric determination of calcite and dolomite by using Chittick apparatus. Journal of Sedimentary Research 32, 520-529.

Dubé-Loubert, H., Roy, M., Allard, G., Lamothe, M., Veillette, J.J., 2013. Glacial and nonglacial events in the eastern James Bay lowlands, Canada. Canadian Journal of Earth Sciences 50, 379-396.

Duk-Rodkin, A., Barendregt, R.W., 2011. Chapter 49: Stratigraphical Record of Glacials/Interglacials in Northwest Canada, in: Ehlers, J., Gibbard, P.L., Hughes, P.D. (Eds.), Developments in Quaternary Science Vol. 15. Elsevier, pp. 661-698.

Duller, G.A.T., 2008. Single-grain optical dating of Quaternary sediments: why aliquot size matters in luminescence dating. Boreas 37, 589-612.

Dunhill, G., Andrews, J.T., Kristjánsdóttir, G.B., 2004. Radiocarbon Date List X: Baffin Bay, Baffin Island, Iceland, Labrador Sea, and the Northern North Atlantic. Institute of Arctic and Alpine Research Occasional Paper No. 56.

Durcan, J.A., Duller, G.A.T., 2011. The fast ratio: A rapid measure for testing the dominance of the fast component in the initial OSL signal from quartz. Radiation Measurements 46, 1065-1072.

Dyck, W., Fyles, J.G., 1962. Geological Survey of Canada Radiocarbon Dates I. Radiocarbon 4, 13-26.

Dyck, W., Fyles, J.G., 1963. Geological Survey of Canada Radiocarbon Dates II. Radiocarbon 5, 39-55.

Dyck, W., Fyles, J.G., 1964. Geological Survey of Canada Radiocarbon Dates III. Radiocarbon 6, 167-181.

Dyke, A.S., 1984. Multiple Deglaciations Deposition of the Hudson Bay Lowlands , Canada, of the Missinaibi (Last-Interglacial ?) Formation: Discussion. Quaternary Research 22, 247-252.

Dyke, A.S., 1999. Last Glacial Maxiumm and deglaciation of Devon Island, Arctic Canada: support for an Innuitian ice sheet. Quaternary Science Reviews 18, 393-420.

Dyke, A.S., 2004. An outline of North American deglaciation with emphasis on central and northern Canada, in: Ehlers, J., Gibbard, P.L. (Eds.), Quaternary Glaciations - Extent and Chronology, Part II. Elsevier, pp. 373-424.

Dyke, A.S., Andrews, J.T., Clark, P.U., England, J.H., Miller, G.H., Shaw, J., Veillette, J.J., 2002. The Laurentide and Innuitian ice sheets during the Last Glacial Maximum. Quaternary Science Reviews 21, 9-31.

Engels, S., Bohncke, S.J.P., Bos, J.A.A., Brooks, S.J., Heiri, O., Helmens, K.F., 2008. Chironomid-based palaeotemperature estimates for northeast Finland during Oxygen Isotope Stage 3. Journal of Paleolimnology 40, 49-61.

England, J., 1977. The glacial geology of northeastern Ellesmere Island, N.W.T., Canada. Canadian Journal of Earth Sciences 15, 603-617.

England, J., 1990. The late Quaternary history of Greely Fiord and its tributaries, west-central Ellesmere Island. Canadian Journal of Earth Sciences 27, 255-270.

England, J., 1996. Glacier dynamics and paleoclimatic change during the last glaciation of eastern Ellesmere Island, Canada. Canadian Journal of Earth Sciences 33, 779-799.

England, J., 1999. Coalescent Greenland and Innuitian ice during the Last Glacial Maximum: revising the Quaternary of the Canadian High Arctic. Quaternary Science Reviews 18, 421-456.

England, J., Smith, I.R., Evans, D.J.A., 2000. The last glaciation of east-central Ellesmere Island, Nunavut: ice dynamics, deglacial chronology, and sea level change. Canadian Journal of Earth Sciences 37, 1355-1371.

England, J.H., Furze, M.F.A., Doupé, J.P., 2009. Revision of the NW Laurentide Ice Sheet: implications for paleoclimate, the northeast extremity of Beringia, and Arctic Ocean sedimentation. Quaternary Science Reviews 28, 1573-1596.

Eschman, D.F., 1980. Some evidence of Mid-Wisconsinan Events in Michigan. Michigan Academian 12, 423-436.

Evans, D.J.A., Campbell, I.A., 1992. Glacial and postglacial stratigraphy of Dinosaur Park and surrounding plains, southern Alberta, Canada. Quaternary Science Reviews 11, 535-555.

Evans, D.J.A., Campbell, I.A., 1995. Quaternary Stratigraphy of the buried valleys of the lower Red Deer River, Alberta, Canada. Journal of Quaternary Science 10, 123-148.

Evans, D.J.A., Mott, R.J., 1993. Stratigraphy and palaeoecology of a possible interglacial site, northernmost Ellesmere Island, Canada. Journal of Quaternary Science 8, 251-262.

Faegri, K., Iversen, J., 1975. Text Book of Pollen Analysis, 3rd Edition ed. Munksgaard, Copenhagen and Denmark.

Farley-Gill, L.D., 1980. Contemporary pollen spectra in the James Bay Lowland, Canada, and comparison with other forest-tundra assemblages. Géographie physique et Quaternaire 34, 321-334.

Farley-Wilson, L.D., 1975. Contemporary pollen spectra from the eastern James Bay area, Quebec, Geological Survey of Canada Paper 75-1B : Report of Activities, pp. 129-134.

Fedorova, I.T., Volkova, Y.A., Varlyguin, D.L., 1994. World vegetation cover. Digital raster data on a 30-minute cartesian orthonormal geodetic (lat/long) 1080x2160 grid, in: USDOC/NOAA National Geophysical Data Center (Ed.), Global Ecosystems Database Version 2.0, Boulder, CO.

Felde, V.A., Bjune, A.E., Grytnes, J.A., Birks, H.J.B., 2014. A comparison of novel and traditional numerical methods for the analysis of modern pollen assemblages from major vegetation–landform types. Review of Palaeobotany and Palynology 210, 22-36.

Fisher, T.G., Waterson, N., Lowell, T.V., Hajdas, I., 2009. Deglaciation ages and meltwater routing in the Fort McMurray region, northeastern Alberta and northwestern Saskatchewan, Canada. Quaternary Science Reviews 28, 1608-1624.

Fleming, K., Johnston, P., Zwartz, D., Yokoyama, Y., Lambeck, K., Chappell, J., 1998. Refining the eustatic sea-level curve since the Last Glacial Maximum using far-and intermediate-field sites. Earth and Planetary Science Letters 163, 327-342.

Flint, R.F., 1943. Growth of North American Ice Sheet During the Wisconsin Age. GSA Bulletin 54.

Forman, S.L., 1992. Chronologic evidence for multiple periods of loess deposition during the Late Pleistocene in the Missouri and Mississippi River Valley, United States: Implications for the activity of the Laurentide ice sheet. Palaeogeography, Palaeoclimatology, Palaeoecology 93, 71-83.

Forman, S.L., Pierson, J., 2002. Late Pleistocene luminescence chronology of loess deposition in the Missouri and Mississippi river valleys, United States. Palaeogeography, Palaeoclimatology, Palaeoecology 186, 25-46.

Forman, S.L., Wintle, A.G., Thorleifson, L.H., Wyatt, P.H., 1987. Thermoluminescence properties and age estimates for Quaternary raised marine sediments, Hudson Bay Lowland, Canada. Canadian Journal of Earth Sciences 24, 2405-2411.

Forman, S.L., Wright, D.K., Bloszies, C., 2014. Variations in water level for Lake Turkana in the past 8500 years near Mt. Porr, Kenya and the transition from the African Humid Period to Holocene aridity. Quaternary Science Reviews 97, 84-101.

Fréchette, B., de Vernal, A., 2013. Evidence for large-amplitude biome and climate changes in Atlantic Canada during the last interglacial and mid-Wisconsinan periods. Quaternary Research 79, 242-255.

Fréchette, B., Wolfe, A.P., Miller, G.H., Richard, P.J.H., de Vernal, A., 2006. Vegetation and climate of the last interglacial on Baffin Island, Arctic Canada. Palaeogeography, Palaeoclimatology, Palaeoecology 236, 91-106.

Friel, C.E., Finkelstein, S.A., Davis, A.M., 2014. Relative importance of hydrological and climatic controls on Holocene paleoenvironments inferred using diatom and pollen records from a lake in the central Hudson Bay Lowlands, Canada. The Holocene 24, 295-306.

Fulton, R.J., 1995. Proboscidean tusk of Middle Wisconsinan age from sub-till gravel, near Turtle Mountain, southwestern Manitoba, Current Research 1995-E; Geological Survey of Canada, pp. 91-96.

Gajewski, K., 2015. Quantitative reconstruction of Holocene temperatures across the Canadian Arctic and Greenland. Global and Planetary Change 128, 14-23.

Galbraith, R.F., Green, P.F., 1990. Estimating the component ages in a finite mixture. International Journal of Radiation Applications and Instrumentation. Part D. Nuclear Tracks and Radiation Measurements 17, 197-206.

Galbraith, R.F., Roberts, R.G., 2012. Statistical aspects of equivalent dose and error calculation and display in OSL dating: An overview and some recommendations. Quaternary Geochronology 11, 1-27.

Galbraith, R.F., Roberts, R.G., Laslett, G.M., Yoshida, H., Olley, J.M., 1999. Optical dating of single and multiple grains of quartz from Jinmium rock shelter, northern Australia: Part I, Experimental design and statistical models. Archaeometry 41, 339-364.

Ganopolski, A., Calov, R., 2011. The role of orbital forcing, carbon dioxide and regolith in 100 kyr glacial cycles. Climate of the Past 7, 1415-1425.

Ganopolski, A., Calov, R., Claussen, M., 2010. Simulation of the last glacial cycle with a coupled climate ice-sheet model of intermediate complexity. Climate of the Past 6, 229-244.

Gao, C., McAndrews, J.H., Wang, X., Menzies, J., Turton, C.L., Wood, B.D., Pei, J., Kodors, C., 2012. Glaciation of North America in the James Bay Lowland, Canada, 3.5 Ma. Geology 40, 975-978.

Gephart, G.D., 1983. Stratigraphic evidence for a significant readvance of the Michigan ice lobe to the Kalamazoo Moraine - Southwestern Michigan [abstract no. 14780]. Geological Society of America abstracts with programs 15, 161.

Gephart, G.D., Monaghan, G.W., Larson, G.J., 1982. A mid-Wisconsinan event in the Lake Michigan Basin [abstract]. Geological Society of America abstracts with programs 14, 260.

Geyh, M.A., 2008. 230Th/U dating of interglacial and interstadial fen peat and lignite: Potential and limits. Eiszeitalter und Gegenwart Quaternary Science Journal 57, 77-94.

Glaser, P.H., Hansen, B.C.S., Siegel, D.I., Reeve, A.S., Morin, P.J., 2004. Rates, pathways and drivers for peatland development in the Hudson Bay Lowlands, northern Ontario, Canada. Journal of Ecology 92, 1036-1053.

Goring, S., Lacourse, T., Pellatt, M.G., Walker, I.R., Mathewes, R.W., 2010. Are pollen-based climate models improved by combining surface samples from soil and lacustrine substrates? Review of Palaeobotany and Palynology 162, 203-212.

Government of Canada, 2017. Historical Hydrometric Data, https://wateroffice.ec.gc.ca/mainmenu/historical_data_index_e.html.

Grant, K.M., Rohling, E.J., Ramsey, C.B., Cheng, H., Edwards, R.L., Florindo, F., Heslop, D., Marra, F., Roberts, A.P., Tamisiea, M.E., Williams, F., 2014. Sea-level variability over five glacial cycles. Nature communications 5, 5076.

Gratton, D., Gwyn, Q.H.J., M. Dubois, J.M., 1984. Les paléoenvironnements sédimentaires au Wisconsinien moyen et supérieur, île d'Anticosti, golfe du Saint-Laurent, Québec. Géographie physique et Quaternaire 38, 229.

Grimm, E.C., Watts, W.A., Jacobson Jr, G.L., Hansen, B.C.S., Almquist, H.R., Dieffenbacher-Krall, A.C., 2006. Evidence for warm wet Heinrich events in Florida. Quaternary Science Reviews 25, 2197-2211.

Grunsky, E.C., 2010. The interpretation of geochemical survey data. Geochemistry: Exploration, Environment, Analysis 10, 27-74.

Guyard, H., St-Onge, G., Pienitz, R., Francus, P., Zolitschka, B., Clarke, G.K.C., Hausmann, S., Salonen, V.-P., Lajeunesse, P., Ledoux, G., Lamothe, M., 2011. New insights into Late Pleistocene glacial and postglacial history of northernmost Ungava (Canada) from Pingualuit Crater Lake sediments. Quaternary Science Reviews 30, 3892-3907.

Harington, C.R., 2003. Annotated Bibliography of Quaternary Vertebrates of Northern North America. University of Toronto Press, Toronto.

Hatté, C., Jull, A.J.T., 2007. Radiocarbon Dating: Plant Macrofossils, in: Elias, S.A. (Ed.), Encyclopedia of Quaternary Science. Elsevier, Amsterdam, pp. 2958-2965.

Head, M., Aubry, M.-P., Walker, M., Miller, K., Pratt, B., 2017. A case for formalizing subseries (subepochs) of the Cenozoic Era. Episodes 40, 22-27.

Head, M.J., Gibbard, P.L., 2015. Formal subdivision of the Quaternary System/Period: Past, present, and future. Quaternary International 383, 4-35.

Heiri, O., Lotter, A.F., Lemcke, G., 2001. Loss on ignition as a method for estimating organic and carbonate content in sediments: reproducibility and comparability of results. Journal of Paleolimnology 25, 101-110.

Helmens, K.F., Bos, J.A.A., Engels, S., Van Meerbeeck, C.J., Bohncke, S.J.P., Renssen, H., Heiri, O., Brooks, S.J., Seppä, H., Birks, H.J.B., Wohlfarth, B., 2007. Present-day temperatures in northern Scandinavia during the last glaciation. Geology 35, 987-990.

Helmens, K.F., Engels, S., 2010. Ice-free conditions in eastern Fennoscandia during early Marine Isotope Stage 3: lacustrine records. Boreas 39, 399-409.

Helmens, K.F., Salonen, J.S., Plikk, A., Engels, S., Väliranta, M., Kylander, M., Brendryen, J., Renssen, H., 2015. Major cooling intersecting peak Eemian Interglacial warmth in northern Europe. Quaternary Science Reviews 122, 293-299.

Helmens, K.F., Väliranta, M., Engels, S., Shala, S., 2012. Large shifts in vegetation and climate during the Early Weichselian (MIS 5d-c) inferred from multi-proxy evidence at Sokli (northern Finland). Quaternary Science Reviews 41, 22-38.

Hemming, S.R., 2004. Heinrich events: Massive late Pleistocene detritus layers of the North Atlantic and their global climate imprint. Reviews of Geophysics 42, RG1005, 1001-1043.

Herring, E.M., Gavin, D.G., 2015. Climate and vegetation since the Last Interglacial (MIS 5e) in a putative glacial refugium, northern Idaho, USA. Quaternary Science Reviews 117, 82-95.

Hickman, M., Schweger, C.E., 1996. The Late Quaternary palaeoenvironmental history of a presently deep freshwater lake in east-central Alberta, Canada and paleoclimate implications. Palaeogeography, Palaeoclimatology, Palaeoecology 123, 161-178.

Hill, C.L., 2006. Stratigraphic and geochronologic contexts of mammoth (Mammuthus) and other Pleistocene fauna, Upper Missouri Basin (northern Great Plains and Rocky Mountains), U.S.A. Quaternary International 142-143, 87-106.

Hill, H.W., Flower, B.P., Quinn, T.M., Hollander, D.J., Guilderson, T.P., 2006. Laurentide Ice Sheet meltwater and abrupt climate change during the last glaciation. Paleoceanography 21, PA1006.

Hillaire-Marcel, C., 1979. Les mers post-glaciaires du Quebec: quelques aspects. University Pierre et Marie Curie Paris VI, p. 293 p.

Hillaire-Marcel, C., Page, P., 1980. Paléotempératures Isotopiques du Lac Glaciaire de Deschaillons, in: Mahaney, W.C. (Ed.), Quaternary Paleoclimate. Geo Abstracts Ltd., Norwich, pp. 273-298.

Hodgson, D.A., 1985. The last glaciation of west-central Ellesmere Island, Arctic Archipelago, Canada. Canadian Journal of Earth Sciences 22, 347-368.

Houmark-Nielsen, M., Bennike, O., Lemdahl, G., Lüthgens, C., 2016. Evidence of ameliorated Middle Weichselian climate and sub-arctic environment in the western Baltic region: coring lake sediments at Klintholm, Møn, Denmark. Boreas 45, 347-359.

Huang, Y., Shuman, B., Wang, Y., Webb, T., Grimm, E.C., Jacobson, G.L., 2006. Climatic and environmental controls on the variation of C3 and C4 plant abundances in central Florida for the past 62,000 years. Palaeogeography, Palaeoclimatology, Palaeoecology 237, 428-435.

Hughes, A.L.C., Gyllencreutz, R., Lohne, O.S., Mangerud, J., Svendsen, J.I., 2016. The last Eurasian ice sheets – a chronological database and time-slice reconstruction, DATED-1. Boreas 45, 1-45.

Hughes, O.L., Tarnocai, C., Schweger, C.E., 1993. Pleistocene stratigraphy, paleopedology, and paleoecology of a multiple till sequence exposed on the Little Bear River, Western District of Mackenzie, N.W.T., Canada. Canadian Journal of Earth Sciences 30, 851-866.

Huisman, J., Olff, H., Fresco, L.F.M., 1993. A hierarchical set of models for species response analysis. Journal of Vegetation Science 4, 37-46.

Huntley, D., Mills, A., Paulen, R., 2008. Surficial deposits, landforms, glacial history, and reconnaissance drift sampling in the Trout Lake map area, Northwest Territories. Geological Survey of Canada Current Research 2008-14.

Huntley, D.J., Godfrey-Smith, D.I., Thewalt, M.L.W., 1985. Optical dating of sediments. Nature 313, 105-107.

Ives, J.D., 1977. Were parts of the north coast of Labrador ice-free at the Wisconsin glacial maximum? Géographie physique et Quaternaire 31, 401-403.

Ives, J.D., Buckley, J.T., 1969. Glacial Geomorphology of Remote Peninsula, Baffin Island, N.W.T., Canada. Arctic and Alpine Research 1, 83-95.

Jackson, L.E., Andriashek, L.D., Phillips, F.M., 2011. Chapter 45: Limits of Successive Middle and Late Pleistocene Continental Ice Sheets, Interior Plains of Southern and Central Alberta and Adjacent Areas, in: Ehlers, J., Gibbard, P.L., Hughes, P.D. (Eds.), Developments in Quaternary Science Vol.15. Elsevier, pp. 575-589.

Jackson, L.E., Pawson, M., 1984. Alberta Radiocarbon Dates: Listings of radiocarbon dates with regional significance to the late Quaternary geochronology and geomorphology of Alberta. Geological Survey of Canada Paper 83-25.

Jass, C.N., Beaudoin, A.B., 2014. Radiocarbon Dates of Late Quaternary Megafauna and Botanical Remains from Central Alberta, Canada. Radiocarbon 56, 1215-1222.

Jensen, B.J.L., Pyne-O'Donnell, S., Plunkett, G., Froese, D.G., Hughes, P.D.M., Sigl, M., McConnell, J.R., Amesbury, M.J., Blackwell, P.G., van den Bogaard, C., Buck, C.E., Charman, D.J., Clague, J.J., Hall, V.A., Koch, J., Mackay, H., Mallon, G., McColl, L., Pilcher, J.R., 2014. Transatlantic distribution of the Alaskan White River Ash. Geology 42, 875-878.

Jiménez-Moreno, G., Anderson, R.S., Desprat, S., Grigg, L.D., Grimm, E.C., Heusser, L.E., Jacobs, B.F., López-Martínez, C., Whitlock, C.L., Willard, D.A., 2010. Millennial-scale variability during the last glacial in vegetation records from North America. Quaternary Science Reviews 29, 2865-2881.

Johnson, W.H., Follmer, L.R., 1989. Source and Origin of Roxana Silt and Middle Wisconsinan Miscontinent Glacial Activity. Quaternary Research 31, 319-331.

Juggins, S., 2015. rioja: Analysis of Quaternary Science Data. R package version (0.9-5), http://cran.r-project.org/package=rioja.

Juggins, S., Simpson, G.L., Telford, R.J., 2014. Taxon selection using statistical learning techniques to improve transfer function prediction. The Holocene 25, 130-136.

Kaplan, M.R., 1999. The last glaciation of the Cumberland Sound region, Baffin Island, Canada, based on glacial geology, cosmogenic dating, and numerical modeling, Department of Geological Sciences. Univesity of Colorado.

Kapp, R.O., Davis, O.K., King, J.E., 2000. Ronald O. Kapp's Pollen and Spores, 2nd edition ed, College Station, Texas, USA.

Karig, D.E., Miller, N.G., 2013. Middle Wisconsin glacial advance into the Appalachian Plateau, Sixmile Creek, Tompkins Co., NY. Quaternary Research 80, 522-533.

Karrow, P.F., McAndrews, J.H., Miller, B.B., Morgan, A.V., Seymour, K.L., White, O.L., 2001. Illinoian to Late Wisconsinan stratigraphy at Woodbridge, Ontario. Canadian Journal of Earth Sciences 38, 921-942.

Karrow, P.F., Seymour, K.L., Miller, B.B., E., M.J., 1997. Pre-Late Wisconsinian Pleistocene biota from southeastern Michigan, U. S. A. Palaeogeography, Palaeoclimatology, Palaeoecology 133, 81-101.

Karrow, P.F., Warner, B.G., 1984. A subsurface Middle Wisconsinian interstadial site at Waterloo, Ontario, Canada. Boreas 13, 67-85.

Kaszycki, C.A., Dredge, L.A., Groom, H., 2008. Surficial geology and glacial history, Lynn Lake - Leaf Rapids area, Manitoba. Geological Survey of Canada Open file 5873, 1-105.

Kaufman, D.S., Williams, K.M., 1992. Radiocarbon Date List VII: Baffin Island, N.W.T., Canada. Institute of Arctic and Alpine Research Occasional Paper No. 48.

Kehew, A.E., Beukema, S.P., Bird, B.C., Kozlowski, A.L., 2005. Fast flow of the Lake Michigan Lobe: evidence from sediment-landform assemblages in southwestern Michigan, USA. Quaternary Science Reviews 24, 2335-2353.

Kettles, I.M., Garneau, M., Jette, H., 2000. Macrofossil, pollen, and geochemical records of peatlands in the Kinosheo Lake and Detour Lake areas, Northern Ontario. Geological Survey of Canada Bulletin 545, 1-24.

Khorasani, S., Panagiotakopulu, E., Engelmark, R., Ralston, I., 2015. Late Holocene beetle assemblages and environmental change in Gammelhemmet, northern Sweden. Boreas 44, 368-382.

King, G.E., Robinson, R.A.J., Finch, A.A., 2014. Towards successful OSL sampling strategies in glacial environments: deciphering the influence of depositional processes on bleaching of modern glacial sediments from Jostedalen, Southern Norway. Quaternary Science Reviews 89, 94-107.

King, W.A., Martini, I.P., 1983. Morphology and recent sediments of the lower anastomosing reaches of the Attawapiskat River, James Bay, Ontario, Canada. Sedimentary Geology 37, 295-320.

Klassen, R.W., 1986. Surficial geology of north-central Manitoba, Geological Survey of Canada Memoir 419, p. 57.

Kleinen, T., Brovkin, V., Munhoven, G., 2015. Carbon cycle dynamics during recent interglacials. Climate of the Past Discussions 11, 1945-1983.

Kleman, J., Jansson, K., De Angelis, H., Stroeven, A.P., Hättestrand, C., Alm, G., Glasser, N., 2010. North American Ice Sheet build-up during the last glacial cycle, 115–21kyr. Quaternary Science Reviews 29, 2036-2051.

Kuhl, N., Moschen, R., 2012. A combined pollen and $\delta^{18}O$ *Sphagnum* record of mid-Holocene climate variability from Durres Maar (Eifel, Germany). The Holocene 22, 1075-1085.

Lakeman, T.R., 2012. Quaternary glaciation of central Banks Island, NT, Canada, Department of Earth and Atmospheric Sciences. University of Alberta, Edmonton, Alberta.

Lambeck, K., Chappell, J., 2001. Sea Level Change Through the Last Glacial Cycle. Science 292, 679-686.

Lambeck, K., Rouby, H., Purcell, A., Sun, Y., Sambridge, M., 2014. Sea level and global ice volumes from the Last Glacial Maximum to the Holocene. Proceedings of the National Academy of Sciences 111, 15296-15303.

Lamothe, M., 1985. Lithostratigraphy And Geochronology Of The Quaternary Deposits Of The Pierreville And St-pierre Les Becquets Areas, Quebec, Department of Geology. University of Western Ontario, London, Ontario, Canada.

Lamothe, M., Auclair, M., Hamzaoui, C., Huot, S., 2003. Towards a prediction of long-term anomalous fading of feldspar IRSL. Radiation Measurements 37, 493-498.

Lamothe, M., Hillaire-Marcel, C., Page, P., 1983. Découverte de concrétions calcaires striées dans le till de Gentilly, basses-terres du Saint-Laurent, Québec. Canadian Journal of Earth Sciences 20, 500-505.

Lamoureux, S.F., England, J.H., 2000. Late Wisconsinan Glaciation of the Central Sector of the Canadian High Arctic. Quaternary Research 54, 182-188.

Laymon, C.A., 1991. Marine episodes in Hudson Strait and Hudson Bay, Canada, during the Wisconsin Glaciation. Quaternary Research 35, 53-62.

Lee, H.A., 1960. Late Glacial and Postglacial Hudson Bay Sea Episode. Science 131, 1609-1611.

Lemmen, D.S., 1989. The last glaciation of Marvin Peninsula, northern Ellesmere Island, High Arctic, Canada. Canadian Journal of Earth Sciences 26, 2578-2590.

Lichti-Federovich, S., Ritchie, J.C., 1968. Recent pollen assemblages from the Western Interior of Canada. Review of Palaeobotany and Palynology 7, 297-344.

Lisiecki, L.E., Raymo, M.E., 2005. A Pliocene-Pleistocene stack of 57 globally distributed benthic $\delta^{18}O$ records. Paleoceanography 20, PA1003.

Liu, C.-L., Riley, K.M., Coleman, D.D., 1986. Illinois State Geological Survey radiocarbon dates IX. Radiocarbon 28, 110-133.

Liverman, D.G.E., Catto, N.R., Rutter, N.W., 1989. Laurentide glaciation in west-central Alberta: a single (Late Wisconsin) event. Canadian Journal of Earth Sciences 26, 266-274.

Loulergue, L., Schilt, A., Spahni, R., Masson-Delmotte, V., Blunier, T., Lemieux, B., Barnola, J.-M., Raynaud, D., Stocker, T.F., Chappellaz, J., 2008. Orbital and millennial-scale features of atmospheric CH4 over the past 800,000 years. Nature 453, 383-386.

Loutre, M.F., Berger, A., 2003. Marine Isotope Stage 11 as an analogue for the present interglacial. Global and Planetary Change 36, 209-217.

Lowdon, J.A., Blake, W.J., 1968. Geological Survey of Canada Radiocarbon Dates VII. Radiocarbon 10, 207-245.

Lowdon, J.A., Blake, W.J., 1970. Geological Survey of Canada Radiocarbon Dates IX. Radiocarbon 12, 46-86.

Lowdon, J.A., Blake, W.J., 1980. Geological Survey of Canada radiocabron dates XX. Geological Survey of Canada Paper 80-7, 1-28.

Lowdon, J.A., Robertson, I.M., Blake, W.J., 1971. Geological Survey of Canada Radiocarbon Dates XI. Radiocarbon 13, 255-324.

Lowe, D.J., Blaauw, M., Hogg, A.G., Newnham, R.M., 2013. Ages of 24 widespread tephras erupted since 30,000 years ago in New Zealand, with re-evaluation of the timing and palaeoclimatic implications of the Lateglacial cool episode recorded at Kaipo bog. Quaternary Science Reviews 74, 170-194.

Lowell, T.V., 1995. The application of radiocarbon age estimates to the dating of glacial sequences: an example from the Miami sublobe, Ohio, U.S.A. Quaternary Science Reviews 14, 85-99.

Lukas, S., Spencer, J.Q.G., Robinson, R.A.J., Benn, D.I., 2007. Problems associated with luminescence dating of Late Quaternary glacial sediments in the NW Scottish Highlands. Quaternary Geochronology 2, 243-248.

Lüthi, D., Le Floch, M., Bereiter, B., Blunier, T., Barnola, J.-M., Siegenthaler, U., Raynaud, D., Jouzel, J., Fischer, H., Kawamura, K., Stocker, T.F., 2008. High-resolution carbon dioxide concentration record 650,000-800,000 years before present. Nature 453, 379-382.

MacDonald, B.G., 1969. Glacial and interglacial stratigraphy, Hudson Bay Lowlands, Geological Survey of Canada Paper 65-23, pp. 78-99.

MacDonald, B.G., 1971. Late Quaternary stratigraphy and deglaciation in eastern Canada, The late Cenozoic Glacial Ages. Yale Univeristy Press, pp. 331-353.

MacDonald, B.G., Gajewski, K., 1992. The northern treeline of Canada, in: Janelle, D.G. (Ed.), Geographical Snapshots of North America. The Guilford Press, New York, pp. 34-37.

Mackay, H., Hughes, P.D.M., Jensen, B.J.L., Langdon, P.G., Pyne-O'Donnell, S.D.F., Plunkett, G., Froese, D.G., Coulter, S., Gardner, J.E., 2016. A mid to late Holocene cryptotephra framework from eastern North America. Quaternary Science Reviews 132, 101-113.

MacKay, J.R., Matthews, J.V.J., 1983. Pleistocene ice and sand wedges, Hooper Island, Northwest Territories. Canadian Journal of Earth Sciences 20, 1087-1097.

Mallinson, D., Burdette, K., Mahan, S., Brook, G., 2008. Optically stimulated luminescence age controls on late Pleistocene and Holocene coastal lithosomes, North Carolina, USA. Quaternary Research 69, 97-109.

Manley, W.F., Jennings, A.E., 1996. Radiocarbon Date List VIII: Eastern Canadian Arctic, Labrador, Northern Quebec, East Greenland Shelf, Iceland Shelf, and Antarctica, Occasional Paper No. 50. University of Colorado, Institute of Arctic and Alpine Research.

Margalef, O., Cañellas-Boltà, N., Pla-Rabes, S., Giralt, S., Pueyo, J.J., Joosten, H., Rull, V., Buchaca, T., Hernández, A., Valero-Garcés, B.L., Moreno, A., Sáez, A., 2013. A 70,000 year multiproxy record of climatic and environmental change from Rano Aroi peatland (Easter Island). Global and Planetary Change 108, 72-84.

Mason, O.K., 2010. Beach Ridge Geomorphology at Cape Grinnell, northern Greenland: A Less Icy Arctic in the Mid-Holocene. Geografisk Tidsskrift-Danish Journal of Geography 110, 337-355.

McAndrews, J.H., Berti, A.A., Norris, G., 1973. Key to the Quaternary Pollen and Spores of the Great Lakes Region. Royal Ontario Museum, Toronto, Canada.

McAndrews, J.H., Riley, J.L., Davis, A.M., 1982. Vegetation history of the Hudson Bay Lowland: A postglacial pollen diagram from the Sutton Ridge. Naturaliste Canadien 109, 597-608.

McLearn, F.H., 1927. Mesozoic and Pleistocene deposits of lower Missinaibi Opastika and Mattagami Rivers, Ontario, Summary Report C. Geological Survey of Canada, pp. 16-47.

McMartin, I., Campbell, J.E., Dredge, L.A., LeCheminant, A.N., McCurdy, M.W., Scromeda, N., 2015. Quaternary geology and till composition north of Wager Bay, Nunavut: results from the GEM Wager Bay Surficial Geology Project. Geological Survey of Canada Open File 7748.

McMartin, I., Dredge, L.A., Grunsky, E., Pehrsson, S., 2016. Till Geochemistry in West-Central Manitoba: Interpretation of Provenance and Mineralization Based on Glacial History and Multivariate Data Analysis. Economic Geology 111, 1001-1020.

McNeely, R., 2002. Geological Survey of Canada Radiocarbon Dates XXXIII. Geological Survey of Canada Current Research 2001, 1-51.

McNeely, R., 2005. Geological Survey of Canada Radiocarbon Dates XXXIV. Geological Survey of Canada Paper 2005-G1, 1-117.

McNeely, R., 2006. Geological Survey of Canada Radiocarbon Dates XXXV. Geological Survey of Canada Paper 2006-G, 1-156.

McNeely, R., Atkinson, D.E., 1995. Geological Survey of Canada Radiocarbon Dates XXXII. Geological Survey of Canada Paper 1995-G, 1-92.

McNeely, R., Brennan, J., 2005. Geological Survey of Canada revised shell dates. Geological Survey of Canada, p. 530.

McNeely, R., Jorgensen, P.K., 1992. Geological Survey of Canada Radiocarbon Dates XXX. Geological Survey of Canada Paper 90-7, 1-84.

McNeely, R., McCuaig, S., 1991. Geological Survey of Canada Radiocarbon Dates XXIX. Geological Survey of Canada Paper 89-7, 1-134.

Meier, H.A., Nordt, L.C., Forman, S.L., Driese, S.G., 2013. Late Quaternary alluvial history of the middle Owl Creek drainage basin in central Texas: A record of geomorphic response to environmental change. Quaternary International 306, 24-41.

Meyer, G.N., 1985. The Wadena till revisited - some new ideas about an old till [abstract no.61638]. Geological Society of America abstracts with programs 17, 318.

Miller, G.H., 1979. Radiocarbon Date List IV: Baffin Island, N.W.T., Canada. Institute of Arctic and Alpine Research Occasional Paper No. 29.

Miller, G.H., Andrews, J.T., Short, S.K., 1977. The last interglacial-glacial cycle, Clyde foreland, Baffin Island, N.W.T.: stratigraphy, biostratigraphy, and chronology. Canadian Journal of Earth Sciences 14, 2824-2857.

Miller, G.H., Brigham-Grette, J., 1989. Amino acid geochronology: Resolution and precision in carbonate fossils. Quaternary International 1, 111-128.

Miller, G.H., Mode, W.N., Wolfe, A.P., Sauer, P.E., Bennike, O., Forman, S.L., Short, S.K., Stafford, T.W.J., 1999. Stratified interglacial lacustrine sediments from Baffin Island, Arctic Canada: chronology and paleoenvironmental implications. Quaternary Science Reviews 18, 789-810.

Monaghan, G.W., Larson, G.J., Gephart, G.D., 1986. Late Wisconsin drift stratigraphy of the Lake Michigan Lobe in southwestern Michigan. Geological Society of America Bulletin 97, 329-334.

Morlan, R.E., McNeely, R., Wolfe, S.A., Schreiner, B.T., 2001. Quaternary Date and Vertebrate Faunas in Saskatchewan. Geological Survey of Canada Open File 3888, 139.

Mott, R.J., DiLabio, R.N.W., 1990. Paleoecology of Organic Deposits of Probable Last Interglacial Age in Northern Ontario. Géographie physique et Quaternaire 44, 309.

Mott, R.J., Grant, D.R., 1985. Pre-Late Wisconsinan Paleoenvironments in Atlantic Canada. Géographie physique et Quaternaire 39, 239-254.

Munroe, J.S., Perzan, Z.M., Amidon, W.H., 2016. Cave sediments constrain the latest Pleistocene advance of the Laurentide Ice Sheet in the Champlain Valley, Vermont, USA. Journal of Quaternary Science 31, e2913.

Murray, A.S., Wintle, A.G., 2003. The single aliquot regenerative dose protocol: potential for improvements in reliability. Radiation Measurements 37, 377-381.

Naimi, B., 2015. usdm: Uncertainty Analysis for Species Distribution Model. R package version 1.1-15, http://CRAN.R-project.org/package=usdm.

Natural Resources Canada, 2014. Climate estimates for 1971-2000, 30 year long term averages. Government of Canada, http://gmaps.nrcan.gc.ca/cl_p/climatepoints.php.

Natural Resources Canada, 2015. Obtain climate estimates at your locations. Government of Canada.

NEEM community members, 2013. Eemian interglacial reconstructed from a Greenland folded ice core. Nature 493, 489-494.

Netterville, J.A., 1974. Quaternary Stratigraphy of the Lower Gods River Region, Hudson Bay Lowlands, Manitoba, M.Sc thesis, Department of Geology. University of Calgary, Calgary, Alberta, p. 79 pp.

Nguyen, M., 2014. Glacial Stratigraphy of the Ridge River Area, Northern Ontario: Refining Wisconsinian Glacial History and Evidence for Laurentide Ice Streaming, M.Sc thesis, Geology Department. Western Univeristy, London, Ontario, p. 68.

Nguyen, M., Hicock, S.R., Barnett, P.J., 2012. Quaternary Stratigraphy of the Ridge River Area in Support of Far-North Terrain Mapping. Summary of Field Work and Other Activities 2012, Ontario Geological Survey, Open File Report 6280, 25-21 to 25-23.

Nichols, J.E., Peteet, D.M., Moy, C.M., Castañeda, I.S., McGeachy, A., Perez, M., 2014. Impacts of climate and vegetation change on carbon accumulation in a south-central Alaskan peatland assessed with novel organic geochemical techniques. The Holocene 24, 1146-1155.

Nielsen, E., Churcher, C.S., Lammers, G.E., 1988. A woolly mammoth (Proboscidea, Mammuthus primigenius) molar from the Hudson Bay Lowland of Manitoba. Canadian Journal of Earth Sciences 25, 933-938.

Nielsen, E., Morgan, A.V., Morgan, A., Mott, R.J., Rutter, N.W., Causse, C., 1986. Stratigraphy, paleoeology, and glacial history of the Gillam area, Manitoba. Canadian Journal of Earth Sciences 23, 1641-1661.

North Greenland Ice Core Project members, 2004. High-resolution record of Northern Hemisphere climate extending into the last interglacial period. Nature 431, 147-151.

Ó'Cofaigh, C., England, J., Zreda, M., 2000. Late Wisconsinan glaciation of southern Eureka Sound: evidence for extensive Innuitian ice in the Canadian High Arctic during the Last Glacial Maximum. Quaternary Science Reviews 19, 1319-1341.

O'Reilly, B.C., Finkelstein, S.A., Bunbury, J., 2014. Pollen-Derived Paleovegetation Reconstruction and Long-Term Carbon Accumulation at a Fen Site in the Attawapiskat River Watershed, Hudson Bay Lowlands, Canada. Arctic, Antarctic, and Alpine Research 46, 6-18.

Oerter, E.J., Sharp, W.D., Oster, J.L., Ebeling, A., Valley, J.W., Kozdon, R., Orland, I.J., Hellstrom, J., Woodhead, J.D., Hergt, J.M., Chadwick, O.A., Amundson, R., 2016. Pedothem carbonates reveal anomalous North American atmospheric circulation 70,000-55,000 years ago. Proceedings of the National Academy of Sciences of the United States of America 113, 919-924.

Oksanen, J., Blanchet, F.G., Kindt, R., Legendre, P., Minchin, P.R., O'Hara, R.B., Simpson, G.L., Solymos, P., Stevens, M.H.H., Wagner, H., 2015. vegan: Community Ecology Package. R package version 2.2-1, http://CRAN.R-project.org/package=vegan.

Olley, J.M., Pietsch, T., Roberts, R.G., 2004. Optical dating of Holocene sediments from a variety of geomorphic settings using single grains of quartz. Geomorphology 60, 337-358.

Olson, E.A., Broecker, W.S., 1957. Validity of radiocarbon dates in organic samples with ages greater than 25,000 years [abs.]. Geological Society of America Bulletin 68, 1775-1776.

Olson, E.A., Broecker, W.S., 1959. Lamont natural radiocarbon measurements V. American Journal of Science Radiocarbon Supplement 1, 1-28.

Olsson, I.U., Eriksson, K.G., 1972. Fractionation studies of the shells of Foraminifera, Etudes sur le Quaternaire dans le Monde. INQUA Congress, Paris, pp. 921-923.

Ontario Geological Survey, 1991. Bedrock geology of Ontario, explanatory notes and legend, Map 2545.

Ontario Geological Survey, 2015. Geology and selected mineral deposits of Ontario. Queen's Printer for Ontario, Ontario, Canada.

Ontario Water Resources Commission, 1969. Data for Northern Ontario water resource studies 1966 to 1968 Water Resources Bulletin 1-1, Toronto, Ontario.

Orlova, J., Branfireun, B.A., 2014. Surface Water and Groundwater Contributions to Streamflow in the James Bay Lowland, Canada. Arctic, Antarctic, and Alpine Research 46, 236-250.

Overpeck, J.T., Webb, T., III, Prentice, I.C., 1985. Quantitative Interpretation of Fossil Pollen Spectra: Dissimilarity Coefficients and the Method of Modern Analogs. Quaternary Research 23, 87-108.

Oviatt, C.G., Chan, M.A., Jewell, P.W., Bills, B.G., Madsen, D.B., Miller, D.M., 2014. Interpretations of evidence for large Pleistocene paleolakes in the Bonneville basin, western North America COMMENT on: Bonneville basin shoreline records of large lake intervals duringmarine isotope stage 3 and the last glacialmaximum, by Nishizawa et al. (2013). Palaeogeography, Palaeoclimatology, Palaeoecology 401, 173-176.

Packalen, M.S., Finkelstein, S.A., McLaughlin, J.W., 2014. Carbon storage and potential methane production in the Hudson Bay Lowlands since mid-Holocene peat initiation. Nature communications 5, 4078.

Parent, M., Lefebvre, R., Rivard, C., Lavoie, M., Guilbault, J.-P., 2015. Midwisconsinan fluvial and marine sediments in the Central St Lawrence Lowlands- implications for glacial and deglacial events in the Appalachian Uplands, Geological Society of America Northeastern Section - 50th Annual Meeting, Bretton Woods, New Hampshire, USA.

Parent, M., Paradis, S.J., Bolsvert, E., 1995. Ice-flow patterns and glacial transport in the eastern Hudson Bay region: implications for the late Quaternary dynamics of the Laurentide Ice Sheet. Canadian Journal of Earth Sciences 32, 2057-2070.

Paulen, R.C., Beaudoin, A.B., Pawlowicz, J.G., 2005. An interstadial Site in the Birch Mountains, North-Central Alberta, CANQUA Program and abstracts p. A66, Winnipeg, Canada.

Peltier, W.R., Argus, D.F., Drummond, R., 2015. Space geodesy constrains ice age terminal deglaciation: The global ICE-6G_C (VM5a) model. Journal of Geophysical Research: Solid Earth 120, 450-487.

Peros, M., Gajewski, K., Paull, T., Ravindra, R., Podritske, B., 2010. Multi-proxy record of postglacial environmental change, south-central Melville Island, Northwest Territories, Canada. Quaternary Research 73, 247-258.

Peros, M.C., Gajewski, K., 2008. Holocene climate and vegetation change on Victoria Island, western Canadian Arctic. Quaternary Science Reviews 27, 235-249.

Peteet, D.M., Beh, M., Orr, C., Kurdyla, D., Nichols, J., Guilderson, T., 2012. Delayed deglaciation or extreme Arctic conditions 21-16 cal. kyr at southeastern Laurentide Ice Sheet margin? Geophysical Research Letters 39, L11706.

Philibert, A., Prairie, Y.T., Campbell, I., Laird, L., 2003. Effects of late Holocene wildfires on diatom assemblages in Christina Lake, Alberta, Canada. Canadian Journal of Forest Research 33, 2405-2415.

Pico, T., Creveling, J.R., Mitrovica, J.X., 2017. Sea-Level Records from the U.S. Mid-Atlantic Constrain Laurentide Ice Sheet Extent During Marine Isotope Stage 3. Nature communications 8, 15612 / DOI 15610.11038/ncomms15612.

Pico, T., Mitrovica, J.X., Ferrier, K.L., Braun, J., 2016. Global ice volume during MIS 3 inferred from a sea-level analysis of sedimentary core records in the Yellow River Delta. Quaternary Science Reviews 152, 72-79.

Pigati, J.S., 2002. On correcting 14C ages of gastropod shell carbonate for fractionation. Radiocarbon 44, 755-760.

Potzger, J.E., Courtemanche, A., 1956. A series of bogs across Quebec from the St. Lawrence Valley to James Bay. Canadian Journal of Botany 34, 473-500.

Prescott, J.R., Hutton, J.T., 1994. Cosmic ray contributions to dose rates for luminescence and ESR dating: Large depths and long-term time variations. Radiation Measurements 23, 497-500.

Preston, R.S., Person, E., Deevey, E.S., 1955. Yale Natural Radiocarbon Measurements II. Science 122, 954-960.

R Core Team, 2014. R: A language and environment for statistical computing. R Foundation for Statistical Computing, Vienna, Austria.

Railsback, L.B., Gibbard, P.L., Head, M.J., Voarintsoa, N.R.G., Toucanne, S., 2015. An optimized scheme of lettered marine isotope substages for the last 1.0 million years, and the climatostratigraphic nature of isotope stages and substages. Quaternary Science Reviews 111, 94-106.

Reimchen, T.H.F., 1968. Pleistocene mammals from the Saskatchewan gravels in Alberta, Canada, M.Sc thesis. University of Alberta, Edmonton, Canada, p. 92 p.

Reimer, P.J., Bard, E., Bayliss, A., Beck, J.W., Blackwell, P.G., Bronk Ramsey, C., Buck, C.E., Cheng, H., Edwards, R.L., Friedrich, M., Grootes, P.M., Guilderson, T.P., Haflidason, H., Hajdas, I., Hatté, C., Heaton, T.J., Hoffmann, D.L., Hogg, A.G., Hughen, K.A., Kaiser, K.F., Kromer, B., Manning, S.W., Niu, M., Reimer, R.W., Richards, D.A., Scott, E.M., Southon, J.R., Staff, R.A., Turney, R.S.M., van der Plicht, J., 2013. IntCal13 and Marine13 Radiocarbon Age Calibration Curves 0–50,000 Years cal BP. Radiocarbon 55, 1869-1887.

Rémillard, A.M., Hétu, B., Bernatchez, P., Bertran, P., Fisher, T.G., 2013. The Drift des Demoiselles on the Magdalen Islands (Québec, Canada): sedimentological and micromorphological evidence of a Late Wisconsinan glacial diamict. Canadian Journal of Earth Sciences 50, 545-563.

Rémillard, A.M., St-Onge, G., Bernatchez, P., Hétu, B., Buylaert, J.-P., Murray, A.S., Vigneault, B., 2016. Chronology and stratigraphy of the Magdalen Islands archipelago from the last glaciation to the early Holocene: new insights into the glacial and sea-level history of eastern Canada. Boreas DOI: 10.1111/bor.12179.

Rhodes, E.J., 2011. Optically Stimulated Luminescence Dating of Sediments over the Past 200,000 Years. Annual Review of Earth and Planetary Sciences 39, 461-488.

Richerol, T., Fréchette, B., Rochon, A., Pienitz, R., 2016. Holocene climate history of the Nunatsiavut (northern Labrador, Canada) established from pollen and dinoflagellate cyst assemblages covering the past 7000 years. The Holocene 26, 44-60.

Rieck, R.L., Klasner, J.S., Winters, H.A., Marlette, P.A., 1991. Glaciotectonic effects on a Middle-Wisconsin boreal fenland peat in Michigan, USA. Boreas 20, 155-167.

Rieck, R.L., Winters, H.A., 1980. Distribution and Significance of Glacially Buried Organic Matter in Michigan's Southern Peninsula. Physical Geography 1, 74-89.

Riley, J., Boissonneau, A., n.d. Unpublished field notes and photographs. Ontario Ministry of Natural Resources, Peterborough, Ontario.

Riley, J.L., 2003. Flora of the Hudson Bay Lowlands and its Postglacial Origins. NRC Press, Ottawa.

Riley, J.L., 2011. Wetlands of the Hudson Bay Lowland: an Ontario overview Nature Conservancy of Canada, Toronto, ON.

Roy, M., 1998. Pleistocene stratigraphy of the lower Nelson River area—implications for the evolution of the Hudson Bay lowland of Manitoba, Canada, M.Sc thesis, University of Quebec, Montreal, p. 220 p.

Roy, M., Dell'Oste, F., Veillette, J.J., de Vernal, A., Hélie, J.F., Parent, M., 2011. Insights on the events surrounding the final drainage of Lake Ojibway based on James Bay stratigraphic sequences. Quaternary Science Reviews 30, 682-692.

Rozanski, K., Stichler, W., Gonfiantini, R., Scott, E.M., Beukens, R.P., Kromer, B., Van der Plicht, J., 1992. The IAEA ^{14}C intercomparison exercise 1990. Radiocarbon 34, 506-519.

Rubin, M., Alexander, C., 1960. U.S. Geological Survey Radiocarbon Dates V. American Journal of Science Radiocarbon Supplement 2, 129-185.

Rutter, N.W., Crawford, R.J., Hamilton, R.D., 1979. Dating Methods of Pleistocene Deposits and Their Problems: IV Amino Acid Racemization Dating. Geoscience Canada 6, 122-128.

Sachs, J.P., Pahnke, K., Smittenberg, R., Zhang, Z., 2013. Biomarker Indicators of Past Climate, in: Elias, S.A. (Ed.), The Encyclopedia of Quaternary Science. Elsevier, Amsterdam.

Salonen, J.S., Helmens, K.F., Seppä, H., Birks, H.J.B., 2013a. Pollen-based palaeoclimate reconstructions over long glacial-interglacial timescales: methodological tests based on the Holocene and MIS 5d-c deposits at Sokli, northern Finland. Journal of Quaternary Science 28, 271-282.

Salonen, J.S., Seppä, H., Birks, H.J.B., 2013b. The effect of calibration data set selection on quantitative palaeoclimatic reconstructions. The Holocene 23, 1650-1654.

Salvador, A., 1994. International Stratigraphic Guide: a Guide to Stratigraphic Classification, Terminology, and Procedure, second ed., Boulder, Colorado.

Sanford, R.F., Pierson, C.T., Crovelli, R.A., 1993. An objective replacement method for censored geochemical data. Mathematical Geology 25, 59-80.

Sarala, P., Väliranta, M., Eskola, T., Vaikutiene, G., 2016. First physical evidence for forested environment in the Arctic during MIS 3. Scientific Reports 6, 29054.

Sawakuchi, A.O., Blair, M.W., DeWitt, R., Faleiros, F.M., Hyppolito, T., Guedes, C.C.F., 2011. Thermal history versus sedimentary history: OSL sensitivity of quartz grains extracted from rocks and sediments. Quaternary Geochronology 6, 261-272.

Schaetzl, R.J., Forman, S.L., 2008. OSL ages on glaciofluvial sediment in northern Lower Michigan constrain expansion of the Laurentide ice sheet. Quaternary Research 70, 81-90.

Scott, E.M., 2007. Radiocarbon Dating: Sources of Error, in: Elias, S.A. (Ed.), Encyclopedia of Quaternary Science. Elsevier, Amsterdam, pp. 2918-2923.

Sella, G.F., Stein, S., Dixon, T.H., Craymer, M., James, T.S., Mazzotti, S., Dokka, R.K., 2007. Observation of glacial isostatic adjustment in "stable" North America with GPS. Geophysical Research Letters 34, L02306.

Seppä, H., Birks, H.J.B., 2001. July mean temperature and annual precipitation trends during the Holocene in the Fennoscandian tree-line area: pollen-based climate reconstructions. The Holocene 11, 527-539.

Shapiro, B., Drummond, A.J., Rambaut, A., Wilson, M.C., Matheus, P.E., Sher, A.V., Pybus, O.G., Gilbert, M.T.P., Barnes, I., Binladen, J., Willerslev, E., Hansen, A.J., Baryshnikov, G.F., Burns, J.A., Davydov, S., Driver, J.C., Froese, D.G., Harington, C.R., Keddie, G., Kosintsev, P., Kunz, M.L., Martin, L.D., Stephenson, R.O., Storer, J., Tedford, R., Zimov, S., Cooper, A., 2004. Rise and Fall of the Beringian Steppe Bison. Science 306, 1561-1564.

Shilts, W.W., 1980. Flow patterns in the central North American ice sheet. Nature 286, 213-218.

Shilts, W.W., 1982. Quaternary evolution of the Hudson/James Bay Region. Naturaliste Canadien 109, 309-332.

Shuman, B., Newby, P., Huang, Y., Webb, T., III, 2004. Evidence for the close climatic control of New England vegetation history. Ecology 85, 1297-1310.

Siddall, M., Rohling, E.J., Thompson, W.G., Waelbroeck, C., 2008. Marine Isotope Stage 3 sea level fluctuations: Data synthesis and new outlook. Reviews of Geophysics 46, RG4003.

Simpson, G.L., 2007. Analogue Methods in Palaeoecology: Using the analogue Package. Journal of Statistical Software 22, 1-29.

Simpson, G.L., Oksanen, J., 2014. analogue: Analogue matching and Modern Analogue Technique transfer function models. R package version 0.14-0, http://cran.r-project.org/package=analogue.

Sionneau, T., Bout-Roumazeilles, V., Meunier, G., Kissel, C., Flower, B.P., Bory, A., Tribovillard, N., 2013. Atmospheric re-organization during Marine Isotope Stage 3 over

the North American continent: sedimentological and mineralogical evidence from the Gulf of Mexico. Quaternary Science Reviews 81, 62-73.

Skinner, R.G., 1973. Quaternary stratigraphy of the Moose River Basin, Ontario. Geological Survey of Canada Bulletin 225, 1-77.

Sloan, V.F., 1990. The glacial history of central Canon Fiord, west-central Ellesmere Island, arctic Canada, Department of Geography. University of Alberta, Edmonton, Alberta.

Smith, D.G., 1992. Glacial Lake Mackenzie, Mackenzie Valley, Northwest Territoties, Canada. Canadian Journal of Earth Sciences 29, 1756-1766.

Smith, I.R., 1999. Late Quaternary glacial history of Lake Hazen Basin and eastern Hazen Plateau, northern Ellesmere Island, Nunavut, Canada. Canadian Journal of Earth Sciences 36, 1547-1565.

Soetaert, K., 2014. shape: Functions for plotting graphical shapes, colors. R package version 1.4.2, http://CRAN.R-project.org/package=shape.

Stalker, A.M., 1976. Quaternary Stratigraphy of the Southwestern Canadian Prairies, in: Mahaney, W.C. (Ed.), Quaternary Stratigraphy of North America. Dowden, Hutchinson & Ross, New York, pp. 381-407.

Steig, E.J., Wolfe, A.P., Miller, G.H., 1998. Wisconsinan refugia and the glacial history of eastern Baffin Island, Arctic Canada: Coupled evidence from cosmogenic isotopes and lake sediments. Geology 26, 835-838.

Stewart, M.T., Mickelson, D.M., 1976. Clay mineralogy and relative age of tills in north-central Wisconsin. Journal of Sedimentary Petrology 46, 200-205.

Stockmarr, J., 1971. Tablets with spores used in absolute pollen analysis. Pollen et Spores 13, 615-621.

Stokes, C.R., Tarasov, L., Blomdin, R., Cronin, T.M., Fisher, T.G., Gyllencreutz, R., Hättestrand, C., Heyman, J., Hindmarsh, R.C.A., Hughes, A.L.C., Jakobsson, M., Kirchner, N., Livingstone, S.J., Margold, M., Murton, J.B., Noormets, R., Peltier, W.R., Peteet, D.M., Piper, D.J.W., Preusser, F., Renssen, H., Roberts, D.H., Roche, D.M., Saint-Ange, F., Stroeven, A.P., Teller, J.T., 2015. On the reconstruction of palaeo-ice sheets: Recent advances and future challenges. Quaternary Science Reviews 125, 15-49.

Stokes, C.R., Tarasov, L., Dyke, A.S., 2012. Dynamics of the North American Ice Sheet Complex during its inception and build-up to the Last Glacial Maximum. Quaternary Science Reviews 50, 86-104.

Stroup, J.S., Lowell, T.V., Breckenridge, A., 2013. A model for the demise of large, glacial Lake Ojibway, Ontario and Quebec. Journal of Paleolimnology 50, 105-121.

Stuiver, M., Deevey, E.S., Rouse, I., 1963. Yale Natural Radiocarbon Measurements VIII. Radiocarbon 5, 312-341.

Stuiver, M., Heusser, C.J., Yang, I.C., 1978. North American Glacial History Extended to 75,000 Years Ago. Science 200, 16-21.

Stuiver, M., Polach, H.A., 1977. Discussion: reporting of ^{14}C data. Radiocarbon 19, 355-363.

Stuiver, M., Reimer, P.J., 1993. Extended ^{14}C data base and revised Calib 3.0 ^{14}C age calibration program. Radiocarbon 35, 215-230.

Ter Braak, C.J.F., Prentice, I.C., 1988. A Theory of Gradient Analysis. Advances in Ecological Research 34, 271-217.

Terasmae, J., Anderson, T.W., 1970. Hypsithermal range extension of white pine (*Pinus stobus L.*) in Quebec, Canada. Canadian Journal of Earth Sciences 7, 406-413.

Terasmae, J., Hughes, O.L., 1960. A palynological and geological study of Pleistocene deposits in the James Bay Lowlands, Ontario (45 N1/2). Geological Survey of Canada Bulletin 62, 1-15.

Thompson, R.S., Anderson, K.H., 2000. Biomes of western North America at 18,000, 6000 and 0 ^{14}C yr BP reconstructed from pollen and packrat midden data. Journal of Biogeography 27, 555-584.

Thorleifson, L.H., Wyatt, P.H., Shilts, W.W., 1992. Hudson Bay lowlands Quaternary stratigraphy: Evidence for early Wisconsinan glaciation centred in Quebec, Special Paper 270. Geological Society of America, pp. 207-221.

Thorleifson, L.H., Wyatt, P.H., Warman, T.A., 1993. Quaternary stratigraphy of the Severn and Winisk drainage basins, Northern Ontario. Geological Survey of Canada.

Tripsanas, E.K., Bryant, W.R., Slowey, N.C., Bouma, A.H., Karageorgis, A.P., Berti, D., 2007. Sedimentological history of Bryant Canyon area, northwest Gulf of Mexico, during the last 135 kyr (Marine Isotope Stages 1–6): A proxy record of Mississippi River discharge. Palaeogeography, Palaeoclimatology, Palaeoecology 246, 137-161.

Ullman, D.J., LeGrande, A.N., Carlson, A.E., Anslow, F.S., Licciardi, J.M., 2014. Assessing the impact of Laurentide Ice Sheet topography on glacial climate. Climate of the Past 10, 487-507.

Väliranta, M., Birks, H.H., Helmens, K., Engels, S., Piirainen, M., 2009. Early Weichselian interstadial (MIS 5c) summer temperatures were higher than today in northern Fennoscandia. Quaternary Science Reviews 28, 777-782.

Väliranta, M., Salonen, J.S., Heikkila, M., Amon, L., Helmens, K., Klimaschewski, A., Kuhry, P., Kultti, S., Poska, A., Shala, S., Veski, S., Birks, H.H., 2015. Plant macrofossil evidence for an early onset of the Holocene summer thermal maximum in northernmost Europe. Nature communications 6, 6809.

van Calsteren, P., Thomas, L., 2006. Uranium-series dating applications in natural environmental science. Earth-Science Reviews 75, 155-175.

Van Meerbeeck, C.J., Renssen, H., Roche, D.M., 2009. How did Marine Isotope Stage 3 and Last Glacial Maximum climates differ? – Perspectives from equilibrium simulations. Climate of the Past 5, 33-51.

Veillette, J.J., Dyke, A.S., Roy, M., 1999. Ice-flow evolution of the Labrador Sector of the Laurentide Ice Sheet: a review, with new evidence from northern Quebec. Quaternary Science Reviews 18, 993-1019.

Veillette, J.J., Pomares, J.-S., 1991. Older ice flows in the Matagami-Chapais area Quebec. Geological Survey of Canada, Paper 91-1C Current Research, part C, 143-148.

Viau, A.E., Gajewski, K., 2009. Reconstructing Millennial-Scale, Regional Paleoclimates of Boreal Canada during the Holocene. Journal of Climate 22, 316-330.

Vogel, J.C., Kronfeld, J., 1980. A new method for dating peat. South African Journal of Science 76, 557-558.

Vogel, J.C., Waterbolk, H.T., 1972. Groningen Radiocarbon Dates X. Radiocarbon 14, 6-110.

Wainer, K.A.I., Rowe, M.P., Thomas, A.L., Mason, A.J., Williams, B., Tamisiea, M.E., Williams, F.H., Düsterhus, A., Henderson, G.M., 2017. Speleothem evidence for MIS 5c and 5a sea level above modern level at Bermuda. Earth and Planetary Science Letters 457, 325-334.

Warner, B., Morgan, A.V., Karrow, P.F., 1988. A Wisconsinan interstadial arctic flora and insect fauna from Clarksburg, southwestern Ontario, Canada. Palaeogeography, Palaeoclimatology, Palaeoecology 68, 27-47.

Wassenburg, J.A., Dietrich, S., Fietzke, J., Fohlmeister, J., Jochum, K.P., Scholz, D., Richter, D.K., Sabaoui, A., Spötl, C., Lohmann, G., Andreae, Meinrat O., Immenhauser, A., 2016. Reorganization of the North Atlantic Oscillation during early Holocene deglaciation. Nature Geoscience 9, 602-605.

Weijers, J.W.H., Bernhardt, B., Peterse, F., Werne, J.P., Dungait, J.A.J., Schouten, S., Sinninghe Damsté, J.S., 2011. Absence of seasonal patterns in MBT–CBT indices in mid-latitude soils. Geochimica et Cosmochimica Acta 75, 3179-3190.

Wentworth, C.K., 1922. A Scale of Grade and Class Terms for Clastic Sediments. The Journal of Geology 30, 377-392.

Whitmore, J., Gajewski, K., Sawada, M., Williams, J.W., Shuman, B., Bartlein, P.J., Minckley, T., Viau, A.E., Webb, T., III, , Anderson, P.M., Brubaker, L.B., 2005. North American and Greenland modern pollen data for multi-scale paleoecological and paleoclimatic applications. Quaternary Science Reviews 24, 1828-1848.

Wickham, H., 2009. ggplot2: elegant graphics for data analysis. Springer, New York.

Williams, J.W., Shuman, B., 2008. Obtaining accurate and precise environmental reconstructions from the modern analog technique and North American surface pollen dataset. Quaternary Science Reviews 27, 669-687.

Williams, J.W., Summers, R.L., Webb, T., III, 1998. Applying plant functional types to construct biome maps from eastern North American pollen data: comparisons with model results. Quaternary Science Reviews 17, 607-627.

Winters, H.A., Alford, J.J., Rieck, R.L., 1988. The anomalous Roxana Silt and mid-Wisconsinian events in and Near Southern Michigan. Quaternary Research 29, 25-35.

Winters, H.A., Rieck, R.L., 1991. Late Glacial Terrain Transformation in Michigan. Michigan Academian 23, 137-148.

Winters, H.A., Rieck, R.L., Kapp, R.O., 1986. Significance and ages of mid Wisconsinan organic deposits in southern Michigan. Physical Geography 7, 292-305.

Wintle, A.G., Murray, A.S., 2006. A review of quartz optically stimulated luminescence characteristics and their relevance in single-aliquot regeneration dating protocols. Radiation Measurements 41, 369-391.

Wohlfarth, B., 2010. Ice-free conditions in Sweden during Marine Oxygen Isotope Stage 3? Boreas 39, 377-398.

Wolfe, A.P., Fréchette, B., Richard, P.J.H., Miller, G.H., Forman, S.L., 2000. Paleoecology of a >90,000-year lacustrine sequence from Fog Lake, Baffin Island, Arctic Canada. Quaternary Science Reviews 19, 1677-1699.

Wolfe, A.P., Härting, J.W., 1996. The late Quaternary development of three ancient tarns on southwestern Cumberland Peninsula, Baffin Island, Arctic Canada: paleolimnological evidence from diatoms and sediment chemistry. Journal of Paleolimnology 15, 1-18.

Wood, J.R., Forman, S.L., Everton, D., Pierson, J., Gomez, J., 2010. Lacustrine sediments in Porter Cave, Central Indiana, USA and possible relation to Laurentide ice sheet marginal positions in the middle and late Wisconsinan. Palaeogeography, Palaeoclimatology, Palaeoecology 298, 421-431.

Wright, D.K., Forman, S.L., Waters, M.R., Ravesloot, J.C., 2011. Holocene eolian activation as a proxy for broad-scale landscape change on the Gila River Indian Community, Arizona. Quaternary Research 76, 10-21.

Wyatt, P.H., 1989. The stratigraphy and amino acid chronology of Quaternary sediments in central Hudson Bay Lowland, M.Sc thesis, Department of Geological Sciences. University of Colorado, Boulder, Colorado, p. 119.

Wyatt, P.H., 1990. Amino Acid Evidence Indicating Two or More Ages of Pre-Holocene Nonglacial Deposits In Hudson Bay Lowland, Northern Ontario. Géographie physique et Quaternaire 44, 389-393.

Young, R.A., Burr, G.S., 2006. Middle Wisconsin glaciation in the Genesee Valley, NY: A stratigraphic record contemporaneous with Heinrich Event, H4. Geomorphology 75, 226-247.

Young, R.R., Burns, J.A., Rains, R.B., Schowalter, D.B., 1999. Late Pleistocene glacial geomorphology and environment of the Hand Hills region and southern Alberta, related to Middle Wisconsin fossil prairie dog sites. Canadian Journal of Earth Sciences 36, 1567-1581.

Young, R.R., Burns, J.A., Smith, D.G., Arnold, L.D., Rains, R.B., 1994. A single, late Wisconsin, Laurentide glaciation, Edmonton area and southwestern Alberta. Geology 22, 683-686.

Yu, Z., Loisel, J., Turetsky, M.R., Cai, S., Zhao, Y., Frolking, S., MacDonald, G.M., Bubier, J.L., 2013. Evidence for elevated emissions from high-latitude wetlands contributing to high atmospheric CH_4 concentration in the early Holocene. Global Biogeochemical Cycles 27, 131-140.

Zabenskie, S., 2006. Postglacial Climatic Change on Boothia Peninsula, Nunavut, Canada, M.Sc. thesis, Department of Geography. University of Ottawa.

Zhang, Y., Kong, Z., Zhang, H., 2013. Multivariate analysis of modern and fossil pollen data from the central Tianshan Mountains, Xinjiang, NW China. Climatic Change 120, 945-957.

Appendices

Appendix A: Synthesis of all chronology determinations on sub-till deposits from the Hudson Bay Lowlands

Description:

The following table is a synthesis of all chronology determinations on sub-till deposits from the Hudson Bay Lowlands (HBL). Column 'F14C' and 'F14C error' lists the percent modern carbon along with measurement error for each new radiocarbon contribution, where available. In the case of optically stimulated luminescence (OSL), uranium-thorium (U-Th) and amino acid estimates, the 'Assigned Age' column represents the age described in the associated publication. For thermoluminescence (TL) ages, the error was increased to 2σ. For ^{14}C AMS and ^{14}C conventional, finite dates are calibrated using the CALIB Rev 7.0.4 and the 2013 calibration curve (Stuiver and Reimer, 1993; Reimer et al., 2013) and reported as calibrated yr BP (where present day = 1950 AD) in the column labelled "Assigned Age". Since finite ages exceeding 46,401 (n = 5) exceed the calibration curve, they were left as radiocarbon years (yr ^{14}C), which is indicated with an asterix (*). Following Stuiver and Polach (1977), all dates were rounded to the nearest 100, and error values were rounded up to the nearest 50-year increment. Some ages (n=3) were not distinguishable from a background sample with a finite age (Stuiver and Polach, 1977), and were therefore considered to be the same age as background, which is ca. 49,600 ± 950 yr ^{14}C, which is indicated by a cross (†). All chronology data was ranked on a scale of 1 to 3, with '1' representing most reliable dates; '2' representing ages with somewhat more uncertainty owing to sample material or depositional context, and '3' less reliable dates. Rationales are noted in the 'notes' column, as well as in Chapter 2 of this dissertation. Elevation data were compiled using an online database (Natural Resources Canada, 2014).

Site	River	Lat. (DD)	Long. (DD)	Elev (MASL)	Method	Lab no.	F14C	F14C error	Radiocarbon age (^{14}C yrs)	Assigned age (calibrated yr BP, in case of radiocarbon)	Dated material	Surround-ing material	Rank	Associated publication	Notes
11-PJB-020	Ridge	50.48	-83.88	123	^{14}C-AMS	UOC-0591	0.0092	0.0003	37600 ± 250	42000 ± 350	peat	organic-rich silt and clay	1	this publication	
11-PJB-020	Ridge	50.48	-83.88	123	^{14}C-AMS	UOC-0592	0.002	0.0002	49600 ± 950	49600 ± 950 †*	peat	organic-rich silt and clay	1	this publication	
11-PJB-020	Ridge	50.48	-83.88	123	^{14}C-AMS	UOC-0842	0.0019	0.0001	> 48800	> 48800	peat	organic-rich silt and clay	1	this publication	
11-PJB-186	Black Duck	56.61	-89.29	61	^{14}C-AMS	ISGS A1656	0.0034	0.0005	45700 ± 1300	48300 ± 1750	wood	organic-rich silt	1	this publication	
11-PJB-186	Black Duck	56.61	-89.29	61	^{14}C-AMS	ISGS A1995	0.002	0.0008	50100 ± 3300	50100 ± 3300*	wood	organic-rich silt	1	this publication	
11-PJB-186	Black Duck	56.61	-89.29	61	^{14}C-AMS	UOC-0587	0.0021	0.0002	49600 ± 950	49600 ± 950 †*	wood	organic-rich silt and clay	1	this publication	
11-PJB-186	Black Duck	56.61	-89.29	61	^{14}C-AMS	UOC-0839	0.001	0.0001	> 48800	> 48800	wood	organic-rich silt and clay	1	this publication	
11-PJB-187	Severn	55.22	-88.44	49	^{14}C-AMS	ISGS A1996	0.0002	0.0008	> 50800	> 50800	wood	sand	1	this publication	
11-PJB-187	Severn	55.22	-88.44	49	^{14}C-AMS	ISGS A2459	0.0002	0.0009	> 50400	> 50400	wood	very fine and fine-grained sand	1	this publication	
12-PJB-002	Ridge	50.46	-83.67	142	^{14}C-AMS	ISGS A2460	0.0144	0.0009	34100 ± 500	38300 ± 1350	wood	sand	2	this publication	Detrital wood located in subaqueous fan sediments
12-PJB-005	Ridge	50.48	-83.79	137	^{14}C-AMS	ISGS A2461	0	-0.0009	> 51400	> 51400	wood	sand	1	this publication	
12-PJB-007	Ridge	50.49	-83.87	119	^{14}C-AMS	UOC-0588	0.0012	0.0003	> 47000	> 47000	wood	organic-rich silt and clay	1	this publication	
12-PJB-007	Ridge	50.49	-83.87	119	^{14}C-AMS	UOC-0590	0.0034	0.0005	45600 ± 1250	48300 ± 1750	wood	sand	1	this publication	
12-PJB-007	Ridge	50.49	-83.87	119	^{14}C-AMS	UOC-0840	0.001	0.0001	> 48800	> 48800	wood	organic-rich silt and clay	1	this publication	
12-PJB-007	Ridge	50.49	-83.87	119	^{14}C-AMS	ISGS A2271	0.001	0.0012	> 45700	> 45700	wood	silt and sand	1	this publication	
12-PJB-007	Ridge	50.49	-83.87	119	^{14}C-AMS	ISGS A2424	0.0031	0.0008	46500 ± 2100	46500 ± 2100*	wood	organic-rich silt and clay	1	this publication	
12-PJB-021	Kabinaka-gami	50.11	-84.18	129	^{14}C-AMS	ISGS A2462	0.0001	0.0009	> 50900	> 50900	wood	sand	1	this publication	
12-PJB-109	Drowning	50.87	-84.85	130	U-Th	12-PJB-109 'LogB' (1)			n/a	> 13300	wood	sand and silt	3	this publication	Suspected open system with respect to uranium.
12-PJB-109	Drowning	50.87	-84.85	130	U-Th	12-PJB-109 'LogB' (2)			n/a	> 14300	wood	sand and silt	3	this publication	Suspected open system with respect to uranium.
12-PJB-109	Drowning	50.87	-84.85	130	^{14}C-AMS	Beta - 380664	0.0022	0.0003	> 43500	> 43500	wood	peat	1	this publication	
12-PJB-109	Drowning	50.87	-84.85	130	OSL	BG3800			n/a	42800 ± 3750	sand	silt and clay	2	this publication	

Site	River	Lat. (DD)	Long. (DD)	Elev (MASL)	Method	Lab no.	F14C	F14C error	Radiocarbon age (^{14}C yrs)	Assigned age (calibrated yr BP, in case of radiocarbon)	Dated material	Surround-ing material	Rank	Associated publication	Notes
12-PJB-109	Drowning	50.87	-84.85	130	^{14}C-AMS	ISGS A2425	-0.0003	-0.0008	> 51700	> 51700	wood	organic-rich forest litter	1	this publication	
12-PJB-109	Drowning	50.87	-84.85	130	^{14}C-AMS	ISGS A2463	0.0007	0.0009	> 48400	> 48400	wood	organic-rich forest litter	1	this publication	
12-PJB-109	Drowning	50.87	-84.85	130	^{14}C-AMS	ISGS A2464	0.0015	0.0009	> 46100	> 46100	wood	sand and gravel	1	this publication	
12-PJB-109	Drowning	50.87	-84.85	130	U-Th	Wood			n/a	> 44965	wood	organic-rich silt and clay	3	this publication	Suspected open system with respect to uranium.
13-PJB-003	Drowning	50.88	-84.86	102	^{14}C-AMS	UOC-0589	0.0018	0.0002	49600 ± 950	49600 ± 950 †*	wood	organic-rich silt and clay	1	this publication	
13-PJB-003	Drowning	50.88	-84.86	102	^{14}C-AMS	UOC-0593	0.038	0.0006	26300 ± 150	30600 ± 350	peat	organic-rich silt and clay	1	this publication	
13-PJB-003	Drowning	50.88	-84.86	102	^{14}C-AMS	UOC-0841	0.0018	0.0002	> 48800	> 48800	wood	organic-rich silt and clay	1	this publication	
14-PJB-007	Albany	51.93	-82.72	36	^{14}C-AMS	UOC-0597	0.008	0.0003	38800 ± 350	42700 ± 500	peat	organic-rich silt and clay	1	this publication	
14-PJB-008	Albany	51.92	-82.63	40	^{14}C-AMS	UOC-0594	0.0053	0.0003	42100 ± 450	45500 ± 850	peat	organic-rich silt and clay	1	this publication	
24M	Missinaibi	50.31	-82.7	85	Amino Acid	24M			n/a	Missinaibi Formation	*Picea spp.*		3	Nielsen et al. (1986)	No numerical date given.
24M	Missinaibi	50.31	-82.7	85	^{14}C-conv.	GrN-1435			> 50000	> 50000	peat	silt and clay	2	MacDonald (1971)	
24M	Missinaibi	50.31	-82.7	85	^{14}C-conv.	Gro-1435			> 53000	> 53000	wood	silt and clay	2	MacDonald (1971); Vogel and Waterbolk (1972)	
24M	Missinaibi	50.31	-82.7	85	^{14}C-conv.	L-369B			> 42600	> 42600	wood	colluvium	2	Olson and Broecker (1959); MacDonald (1971)	
24M	Missinaibi	50.31	-82.7	85	^{14}C-conv.	L-369B (untreated)			> 40500	> 40500	wood	colluvium	2	Olson and Broecker (1959)	
24M	Missinaibi	50.31	-82.7	85	^{14}C-conv.	L-369B peat cellulose			39700 ± 2900	43800 ± 5400	peat cellulose	peat	2	Olson and Broecker (1957, 1959)	
24M	Missinaibi	50.31	-82.7	85	^{14}C-conv.	L-369B peat lignin			40600 ± 3000	44700 ± 5200	peat lignin	peat	2	Olson and Broecker (1957, 1959)	
24M	Missinaibi	50.31	-82.7	85	^{14}C-conv.	L-369B wood cellulose			40500 ± 3200	44500 ± 5450	wood cellulose	colluvium	2	Olson and Broecker (1957, 1959)	

Site	River	Lat. (DD)	Long. (DD)	Elev (MASL)	Method	Lab no.	F14C	F14C error	Radiocarbon age (^{14}C yrs)	Assigned age (calibrated yr BP, in case of radiocarbon)	Dated material	Surround-ing material	Rank	Associated publication	Notes
24M	Missinaibi	50.31	-82.7	85	^{14}C-conv.	L-369B wood lignin			40700 ± 4100	43700 ± 6300	wood lignin	colluvium	2	Olson and Broecker (1957, 1959)	
24M	Missinaibi	50.31	-82.7	85	^{14}C-conv.	QL-197			> 72500	> 72500	wood	unknown	2	Stuiver et al. (1978)	
24M	Missinaibi	50.31	-82.7	85	^{14}C-AMS	TO-1753	data not available	data not available	37250 ± 490	41600 ± 800	wood	compressed peat	1	this publication	
24M	Missinaibi	50.31	-82.7	85	^{14}C-conv.	W-241			> 37000	> 37000	peat	peat	2	MacDonald (1971)	
24M	Missinaibi	50.31	-82.7	85	^{14}C-conv.	W-242			> 38000	> 38000	wood	till/pebble contact	2	MacDonald (1971)	
24M	Missinaibi	50.31	-82.7	85	^{14}C-conv.	Y269			> 29600	> 29600	peat	peat	2	Preston et al. (1955)	
24M	Missinaibi	50.31	-82.7	85	^{14}C-conv.	Y270			> 30800	> 30800	wood	peat	2	Preston et al. (1955)	
26M	Missinaibi	50.31	-82.7	101	^{14}C-conv.	GSC-5071HP			> 50000	> 50000	wood (*Picea spp.*)	peat	2	Thorleifson et al. (1992); McNeely and Atkinson (1995)	
Adam Creek	Adam Creek	50.17	-82.08	100	^{14}C-AMS	TO-1751	data not available	data not available	35000 ± 350	39500 ± 800	wood	organic rich sediments	1	this publication	
Albany Island	Albany	51.96	-82.53	38	^{14}C-conv.	GSC-1185			> 54000	> 54000	peat	clay	2	MacDonald (1969, 1971)	
Albany Island	Albany	51.96	-82.53	38	^{14}C-AMS	UOC-0595	0.0007	0.0005	> 47000	> 47000	peat	organic-rich silt and clay	1	this publication	
Albany Island	Albany	51.96	-82.53	38	^{14}C-AMS	UOC-0843	0.0014	0.0001	> 48800	> 48800	peat	organic-rich silt and clay	1	this publication	
Attawapiskat Marine	Attawapis-kat	52.35	-86.25	178	^{14}C-AMS	AA-7564			> 39300	> 39300	shell (*Hiatella arctica*)	clay-rich till	3	McNeely (2002)	Radiocarbon date on marine shell suspected to be problematic - most likely a minumim age estimate.
Attawapiskat Marine	Attawapis-kat	52.35	-86.25	178	^{14}C-AMS	TO-1892			30380 ± 230	34400 ± 400	shell (*Hiatella arctica*)	clay-rich till	3	McNeely (2002)	Radiocarbon date on marine shell suspected to be problematic - most likely a minumim age estimate.
Attawapiskat Marine	Attawapis-kat	52.35	-86.25	178	^{14}C-AMS	TO-1893			33070 ± 310	37300 ± 900	shell (*Hiatella arctica*)	clay-rich till	3	McNeely (2002)	Radiocarbon date on marine shell suspected to be problematic - most likely a minimum age estimate.
Attawapiskat Marine	Attawapis-kat	52.35	-86.25	178	^{14}C-AMS	TO-1894			28800 ± 220	32900 ± 700	shell (*Hiatella arctica*)	clay-rich till	3	McNeely (2002)	Radiocarbon date on marine shell suspected to be problematic - most likely a minimum age estimate.

Site	River	Lat. (DD)	Long. (DD)	Elev (MASL)	Method	Lab no.	F14C	F14C error	Radiocarbon age (^{14}C yrs)	Assigned age (calibrated yr BP, in case of radiocarbon)	Dated material	Surround-ing material	Rank	Associated publication	Notes
Attawapiskat Marine	Attawapis-kat	52.35	-86.25	178	^{14}C-AMS	TO-2501			38120 ± 460	42300 ± 600	shell (*Hiatella arctica*)	clay-rich till	3	McNeely (2002)	Radiocarbon date on marine shell suspected to be problematic - most likely a minimum age estimate.
Attawapiskat Marine	Attawapis-kat	52.35	-86.25	178	^{14}C-AMS	TO-2502			35520 ± 460	40100 ± 1050	shell (*Hiatella arctica*)	clay-rich till	3	McNeely (2002)	Radiocarbon date on marine shell suspected to be problematic - most likely a minimum age estimate.
Beaver	Beaver	55.92	-88.32	40	Amino Acid	Beaver			n/a	76000	shell (*Hiatella arctica*)		3	Wyatt (1989, 1990)	This is a relative age assignment based on the assumption that the Bell Sea is 130,000 yr BP.
Beaver	Beaver	55.92	-88.32	40	^{14}C-conv.	GSC-4146			> 38000	> 38000	peat	peat	2	Wyatt (1990); McNeely and McCuaig (1991)	
Beaver	Beaver	55.92	-88.32	40	^{14}C-conv.	GSC-4154			> 43000	> 43000	peat	peat	2	McNeely and McCuaig (1991)	
Beaver	Beaver	55.92	-88.32	40	^{14}C-conv.	GSC-4423HP			> 51000	> 51000	peat	peat	2	Wyatt (1989, 1990); McNeely and McCuaig (1991)	
Beaver	Beaver	55.92	-88.32	40	^{14}C-conv.	GSC-4453			> 51000	> 51000	peat	peat	2	Mott and DiLabio (1990)	
Beaver	Beaver	55.92	-88.32	40	^{14}C-AMS	ISGS A1658	0.0008	0.0005	> 50800	> 50800	wood	peat	1	this publication	
Beaver	Beaver	55.92	-88.32	40	^{14}C-conv.	WAT-1378			37400 ± 1600	41400 ± 2900	peat	peat	2	Wyatt (1989)	
Bull's Bay	Missinaibi	50.15	-83.2	149	^{14}C-conv.	GrN-1921			> 42000	> 42000	plant detritus	peat	3	MacDonald (1971); Vogel and Waterbolk (1972)	
Echoing	Echoing	55.92	-91.25	141	^{14}C-conv.	GSC-4444HP			> 51000	> 51000	wood (*Picea spp.*)	peat	2	Dredge et al. (1990)	
Echoing	Echoing	55.92	-91.25	141	^{14}C-conv.	GSC-892			> 37000	> 37000	wood	laminated silt	2	MacDonald (1969); Dredge et al. (1990)	
Flamborough	Nelson	57.03	-92.64	19	TL	EKN-8			n/a	46000 ± 4000	silty clay	silty clay	2	Berger and Nielsen (1990)	Anomalous fading potentially an issue (increased error to 2 sigma)

Site	River	Lat. (DD)	Long. (DD)	Elev (MASL)	Method	Lab no.	F14C	F14C error	Radiocarbon age (^{14}C yrs)	Assigned age (calibrated yr BP, in case of radiocarbon)	Dated material	Surround-ing material	Rank	Associated publication	Notes
Gods	Gods	56.17	-92.53	76	^{14}C-conv.	GSC-1736			> 41000	> 41000	wood (*Picea spp.*)	silty peat	2	Lowdon and Blake (1980); Klassen (1986)	
Gods	Gods	56.17	-92.53	76	^{14}C-conv.	GSC-4471HP			> 49000	> 49000	wood (*Picea spp.*)	sand	2	Dredge et al. (1990)	
Harricana	Harricana	50.74	-79.34	36	OSL	06HA30			n/a	211000 ± 16000	sand	sand	1	Dubé-Loubert et al. (2013)	
Harricana	Harricana	50.74	-79.34	36	^{14}C-AMS	CAMS-130897			> 54800	> 54800	wood fragments	sand	1	Dubé-Loubert et al. (2013)	
Hayes	Hayes	55.93	-93.25	117	Amino Acid	Hayes			n/a	76000	shell (*Hiatella arctica*)		3	Shilts (1982)	This is a relative age assignment based on the assumption that the Bell Sea is 130,000 yr BP.
Henday	Nelson	56.46	-94.15	64	TL	EKN-5			n/a	32000 ± 2000	silty clay	silty clay	2	Berger and Nielsen (1990)	Anomalous fading potentially an issue (increased error to 2 sigma)
Henday	Nelson	56.46	-94.15	64	^{14}C-conv..	GSC-4420HP			> 49000	> 49000	wood (*Picea spp.*)	sand	2	Nielsen et al. (1988); McNeely and McCuaig (1991)	
Henday	Nelson	56.46	-94.15	64	Amino Acid	Henday			n/a	Missinaibi Formation	wood (*Picea spp.*)		3	Nielsen et al. (1986)	No numerical date given.
Henday	Nelson	56.46	-94.15	64	Amino Acid	Henday 2			n/a	Missinaibi Formation	wood (*Picea spp.*)		3	Nielsen et al. (1986)	No numerical date given.
Henday	Nelson	56.46	-94.15	64	Amino Acid	Henday 3			n/a	Missinaibi Formation	wood (*Picea spp.*)		3	Nielsen et al. (1986)	No numerical date given.
Henday	Nelson	56.46	-94.15	64	Amino Acid	Henday 4			n/a	Missinaibi Formation	wood (*Picea spp.*)		3	Nielsen et al. (1986)	No numerical date given.
Henday	Nelson	56.46	-94.15	64	U-Th	UA-1708			n/a	49000 ± 2500	wood	sand	3	Nielsen et al. (1986)	Ssystem believed to be open with respect to uranium.
Henday	Nelson	56.46	-94.15	64	U-Th	UA-1709			n/a	> 200000	wood	sand	3	Nielsen et al. (1986)	Suspected open system with respect to uranium.
Kwataboa-hegan II	Kwataboa-hegan	51.15	-82.05	79	Amino Acid	Kwataboa-hegan II			n/a	135000	shell (*Hiatella arctica*)		3	Shilts (1982)	This is a relative age assignment based on the assumption that the Bell Sea is 130,000 yr BP.

Site	River	Lat. (DD)	Long. (DD)	Elev (MASL)	Method	Lab no.	F14C	F14C error	Radiocarbon age (^{14}C yrs)	Assigned age (calibrated yr BP, in case of radiocarbon)	Dated material	Surround-ing material	Rank	Associated publication	Notes
Kwataboa-hegan Marine	Kwataboa-hegan	51.14	-82.12	90	Amino Acid	Kwataboa-hegan Marine			n/a	135000	shell (*Hiatella arctica*)		3	Shilts (1982)	This is a relative age assignment based on the assumption that the Bell Sea is 130,000 yr BP.
Kwataboa-hegan Marine	Kwataboa-hegan	51.14	-82.12	90	Amino Acid	Kwataboa-hegan Marine1			n/a	130000	shell (*Hiatella arctica*)		3	Andrews et al. (1983)	This is a relative age assignment based on the assumption that the Bell Sea is 130,000 yr BP.
Kwataboa-hegan Marine	Kwataboa-hegan	51.14	-82.12	90	Amino Acid	Kwataboa-hegan Marine2			n/a	130000	shell (*Hiatella arctica*)		3	Wyatt (1989, 1990)	This is a relative age assignment based on the assumption that the Bell Sea is 130,000 yr BP.
Kwataboa-hegan Marine	Kwataboa-hegan	51.14	-82.12	90	^{14}C-conv.	GSC-1475 inner			> 37000	> 37000	shell (*Hiatella arctica*)	sand	3	Skinner (1973); Blake (1988)	Radiocarbon date on marine shell suspected to be problematic - most likely a minumim age estimate.
Kwataboa-hegan Marine	Kwataboa-hegan	51.14	-82.12	90	^{14}C-conv.	GSC-1475 outer			38200 ± 2000	42100 ± 3650	shell (*Hiatella arctica*)	sand	3	Skinner (1973); McNeely and Brennan (2005)	Radiocarbon date on marine shell suspected to be problematic - most likely a minumim age estimate.
Kwataboa-hegan Marine	Kwataboa-hegan	51.14	-82.12	90	^{14}C-AMS	TO-2503			47850 ± 1090	47850 ± 1090*	shell	silt and clay	3	McNeely (2002)	Radiocarbon date on marine shell suspected to be problematic - most likely a minumim age estimate.
Kwataboa-hegan Peat	Kwataboa-hegan	51.15	-82.05	82	^{14}C-conv.	GSC-4614 HP			> 51000	> 51000	peat	silty clay	2	McNeely and Jorgensen (1992)	
Leslie Creek	Nelson	56.42	-94.24	69	TL	EKN-3			n/a	34000 ± 5000	silty clay	silty clay	2	Berger and Nielsen (1990)	Anomalous fading potentially an issue (increased error to 2 sigma)
Limestone Dam	Nelson	56.54	-94.03	50	TL	EKN-2			n/a	119000 ± 18000	silty clay	silty clay	3	Berger and Nielsen (1990)	Suspected overestimate based on inefficient solar resetting.
Limestone Dam	Nelson	56.54	-94.03	50	^{14}C-conv.	GSC-6011			> 37000	> 37000	wood	peat	2	McNeely (2005)	
Limestone Dam	Nelson	56.54	-94.03	50	TL	LMS 2D (delayed)			n/a	46000 ± 3000	sand	sand	3	Roy (1998)	Suspected anomalous fading and improper solar resetting.
Limestone Dam	Nelson	56.54	-94.03	50	TL	LMS 2D (prompt)			n/a	46000 ± 3000	sand	sand	3	Roy (1998)	Suspected anomalous fading and improper solar resetting.
Moondance	Nelson	56.52	-94.08	59	TL	MOON 1E (delayed)			n/a	46000 ± 3000	sand	sand	3	Roy (1998)	Suspected anomalous fading and improper solar resetting.
Moondance	Nelson	56.52	-94.08	59	TL	MOON 1E (prompt)			n/a	46000 ± 3000	sand	sand	3	Roy (1998)	Suspected anomalous fading and improper solar resetting.

Site	River	Lat. (DD)	Long. (DD)	Elev (MASL)	Method	Lab no.	F14C	F14C error	Radiocarbon age (^{14}C yrs)	Assigned age (calibrated yr BP, in case of radiocarbon)	Dated material	Surround-ing material	Rank	Associated publication	Notes
Moondance	Nelson	56.52	-94.08	59	TL	MOON 2C (delayed)			n/a	121000 ± 16000	silt	silt	2	Roy (1998)	Likely the closest to the real age because the grain size is 4-8 µm instead of larger 150-250 µm for the rest of the samples. Also, this is the 'delayed' sample, meaning that anomalous fading is taken into account.
Moondance	Nelson	56.52	-94.08	59	TL	MOON 2C (prompt)			n/a	46000 ± 3000	silty clay	silty clay	3	Roy (1998)	Suspected anomalous fading and improper solar resetting.
Moose	Moose	50.42	-82.33	89	^{14}C-AMS	TO-1752	data not available	data not available	39200 ± 500	43100 ± 800	wood	compressed peat	1	this publication	
Nottaway	Nottaway	51.14	-78.8	24	OSL	06NO21			n/a	95000 ± 7000	sand	sand	1	Dubé-Loubert et al. (2013)	
Nottaway	Nottaway	51.14	-78.8	24	U-Th	6N01A-center			n/a	99400 ± 1800	wood (*Picea mariana*)	clay	2	Allard et al. (2012)	There is a "reasonable agreement" between edge and centre values. Keep center.
Nottaway	Nottaway	51.14	-78.8	24	U-Th	6N01A-edge			n/a	100800 ± 2800	wood (*Picea mariana*)	clay	3	Allard et al. (2012)	Uranium contamination suspected in this sample because it is along the outer rim of the log.
Nottaway	Nottaway	51.14	-78.8	24	U-Th	6N01B-center			n/a	106100 ± 2500	wood (*Picea mariana*)	clay	2	Allard et al. (2012)	There is a "reasonable agreement" between edge and centre values. Keep center.
Nottaway	Nottaway	51.14	-78.8	24	U-Th	6N01B-edge			n/a	99400 ± 6100	wood (*Picea mariana*)	clay	3	Allard et al. (2012)	Uranium contamination suspected in this sample because it is along the outer rim of the log.
Nottaway	Nottaway	51.14	-78.8	24	U-Th	6N01B2-center			n/a	119300 ± 4000	wood (*Picea mariana*)	clay	2	Allard et al. (2012)	There is a "reasonable agreement" between edge and centre values. Keep center.
Nottaway	Nottaway	51.14	-78.8	24	U-Th	6N01C-center			n/a	105400 ± 5700	wood (*Picea mariana*)	clay	3	Allard et al. (2012)	Uranium contamination suspected in this sample because it is along the outer rim of the log.
Nottaway	Nottaway	51.14	-78.8	24	U-Th	6N01C-edge			n/a	118700 ± 4400	wood (*Picea mariana*)	clay	3	Allard et al. (2012)	Uranium contamination suspected in this sample because it is along the outer rim of the log.

Site	River	Lat. (DD)	Long. (DD)	Elev (MASL)	Method	Lab no.	F14C	F14C error	Radiocarbon age (^{14}C yrs)	Assigned age (calibrated yr BP, in case of radiocarbon)	Dated material	Surround-ing material	Rank	Associated publication	Notes
Nottaway	Nottaway	51.14	-78.8	24	U-Th	6N01E			n/a	59600 ± 15100	wood (*Picea mariana*)	clay	3	Allard et al. (2012)	System was probably open with respect to uranium because of large grain size of sediment matrix. Called "unreliable" by original authors.
Nottaway	Nottaway	51.14	-78.8	24	U-Th	6N021			n/a	28800 ± 8400	wood (*Thuja occidentalis*)	sand	3	Allard et al. (2012)	System was probably open with respect to uranium because of large grain size of sediment matrix. Called "unreliable" by original authors.
Nottaway	Nottaway	51.14	-78.8	24	^{14}C-AMS	CAMS-130896			> 55200	> 55200	wood (*Picea mariana*)	clay	1	Dubé-Loubert et al. (2013)	
Nottaway	Nottaway	51.14	-78.8	24	^{14}C-conv.	GSC-5070 HP			> 48000	> 48000	wood (*Picea spp.*)	clay	2	McNeely and Atkinson (1995)	
Port Nelson	Nelson / Hudson Bay	57.13	-92.53	0	TL	EKN-7			n/a	38000 ± 3000	silty clay	silty clay	2	Berger and Nielsen (1990)	Anomalous fading potentially an issue (increased error to 2 sigma)
Prest Sea Type	Abitibi	50.32	-81.63	89	Amino Acid	Prest Sea Type			n/a	75000	shell (*Hiatella arctica*)		3	Wyatt (1989, 1990)	This is a relative age assignment based on the assumption that the Bell Sea is 130,000 yr BP.
Prest Sea Type	Abitibi	50.32	-81.63	89	^{14}C-AMS	AA-7563			> 42900	> 42900	shell	silt and clay	3	McNeely (2002)	Radiocarbon date on marine shell suspected to be problematic - most likely a minumim age estimate.
Prest Sea Type	Abitibi	50.32	-81.63	89	^{14}C-conv.	GSC-1535			> 19000	> 19000	shells (*Hiatella sp.*, *Macoma sp.*, and *Portlandia arctica*)	silty clay	3	Skinner (1973); Blake (1988)	Radiocarbon date on marine shell suspected to be problematic - most likely a minumim age estimate.
Prest Sea Type	Abitibi	50.32	-81.63	89	^{14}C-AMS	TO-125			40040 ± 400	43700 ± 750	shell (*Hiatella arctica*)		3	Andrews (1987)	Radiocarbon date on marine shell suspected to be problematic - most likely a minumim age estimate.
Seven Mile	Harricana	50.58	-79.15	90	^{14}C-conv.	Y-1165			> 42000	> 42000	peat	silt and sand	2	Stuiver et al. (1963)	
Severn	Severn	55.3	-88.43	61	^{14}C-conv.	GSC-1011			> 41000	> 41000	peat	clayey sand	2	MacDonald (1969)	

Site	River	Lat. (DD)	Long. (DD)	Elev (MASL)	Method	Lab no.	F14C	F14C error	Radiocarbon age (^{14}C yrs)	Assigned age (calibrated yr BP, in case of radiocarbon)	Dated material	Surround-ing material	Rank	Associated publication	Notes
Severn Marine	Severn	55.43	-88.2	55	OSL	BG3807			n/a	52500 ± 5050	sandy-silt and clay	sandy-silt and clay	2	this publication	One of two dates from Forman et al. (1987) which were originally suspected to be overestimates due to anomalous fading.
Severn Marine	Severn	55.43	-88.2	55	OSL	BG3808			n/a	42200 ± 4000	sandy-silt and clay	sandy-silt and clay	2	this publication	One of two dates from Forman et al. (1987) which were originally suspected to be overestimates due to anomalous fading.
Severn Marine	Severn	55.43	-88.2	55	TL	CTLH2			n/a	77000 ± 11000	sandy-silt and clay	sandy-silt and clay	3	Forman et al. (1987)	Anomalous fading potentially an issue.
Severn Marine	Severn	55.43	-88.2	55	TL	CTLH3			n/a	69000 ± 10000	sandy-silt and clay	sandy-silt and clay	3	Forman et al. (1987)	Anomalous fading potentially an issue.
Severn Marine	Severn	55.43	-88.2	55	Amino Acid	Severn Marine			n/a		shell (*Hiatella arctica*)		3	Wyatt (1989, 1990)	This is a relative age assignment based on the assumption that the Bell Sea is 130,000 yr BP.
Stupart	Stupart	56.00	-93.42	84	^{14}C-conv.	GSC-2481			> 37000	> 37000	wood (*Picea spp.*)	till unit overlying silt unit	2	Dredge et al. (1990)	
Sundance	Nelson	56.53	-94.08	52	TL	SUN (delayed)			n/a	46000 ± 3000	sand	till	3	Roy (1998)	Suspected anomalous fading and improper solar resetting.
Sundance	Nelson	56.53	-94.08	52	TL	SUN (prompt)			n/a	46000 ± 3000	sand	till	3	Roy (1998)	Suspected anomalous fading and improper solar resetting.
VK Prest Site	Attawapis-kat	52.59	-86.03	160	^{14}C-conv.	GSC-83			> 35800	> 35800	wood fragments (unidentified)	clay	2	Dyck and Fyles (1963)	
VK Prest Site	Attawapis-kat	52.59	-86.03	160	^{14}C-AMS	NZA 30792	0.0002	0.0008	> 47000	> 47000	wood	gravel to silt rhythmites	1	this publication	

Appendix B: Treatment of radiocarbon dates which are close to background

Description:

Stuiver and Polach (1977) state that radiocarbon ages lying close to the background measurements should be deemed "not statistically distinguishable from background" when F14C (fraction of modern carbon) of the sample is within 1σ of the background standard. The IAEA-C4 Kauri Wood standard is an internationally recognized finite standard (0.002 to 0.0044 F14C; Rozanski et al., 1992) which lies close to the limit of radiocarbon dating. As a result, samples which lie within 1σ of the F14C reported by this standard are temporally equivalent to the standard. As seen in the accompanying table, one batch of samples yielded an average 14C reading for this Kauri Wood standard of 0.0021 ± 0.000247, which results in an age assignment of 49,586 ± 949 using the formula -8033*ln(F14C). Since the F14C of samples UOC-0587, UOC-0589 and UOC-0592 overlap at 1σ with that of the Kauri wood, they have been assigned the same age as the IAEA-4 standard for that batch, and these data are reported in the accompanying table.

Table Appendix B. Fraction of modern carbon (F14C) for the radiocarbon batch where n = 3 samples, UOC-0587, UOC-0589 and UOC-0592, are considered to be "not statistically distinguishable from background" (Stuiver and Polach, 1977), and we therefore consider them to be the same age as background.

Lab ID	Description	material	F14C	Measurement error
UOC-0587	11 PJB 186 Bulk 2-Wood	wood	0.0021	0.0002
UOC-0589	13 PJB 003 Wood	wood	0.0018	0.0002
UOC-0592	11 PJB 020 50cm	peat	0.0020	0.0002
UOC-0598	IAEA-C4 (Kauri wood)	wood	0.0019	0.0002
UOC-0599	IAEA-C4 (Kauri wood)	wood	0.0023	0.0003
UOC-0600	IAEA-C4 (Kauri wood)	wood	0.0021	0.0002

Appendix C: Mapping considerations

Where site coordinates were not provided, they were estimated from maps in the relevant publication. Because samples were taken over the span of several decades using varying degrees of accuracy for mapping, we considered any series of dates within 500 m of each other to be the same site. Plots and maps were compiled using R (R Core Team, 2014). Figures and maps were made using R packages 'ggplot2' (Wickham, 2009), 'gridExtra'(Auguie, 2012) and 'maps' (Brownrigg et al., 2014). Gridded elevation data in Fig. 2-2 is from Amante and Eakins (2009) and was plotted using the 'shape' package by Soetaert (2014).

Several minor mapping adjustments had to be made. Firstly, GSC-4146, GSC-4423HP and GSC4154 originally plotted 700 m to the northwest of WAT1378, ISGSA 1658 and GSC-4453, but according to Mott and DiLabio (1990) these dates are all from the same site. As a result, coordinates for GSC-4146, GSC-4423HP and GSC4154 were adjusted to match those of WAT1378, ISGSA 1658, and GSC-4453 along the Beaver River. Total adjustment was 0.8 km southeastward. Secondly, GSC-83 was adjusted to the same coordinates as NZA30792 because literature indicates that it was located on the Attawapiskat River and matched the site of NZA 30792. Total adjustment was 1.4 km southward. Thirdly, TO-2503 was moved 0.6 km northward to match GSC-1475 taken from the banks of the Kwataboahegan River. Lastly, GRN1435, GRo1435, Y269 and Y270 and L-369B were are plotted on their described site 10 km upstream on the Missinaibi River from the confluence with the Soweska River. Plotting given coordinates would have them in a peat bog. GSC_1737 was quoted in Dredge et al. (1990), but it is believed to be a typo of GSC-1736, so it was omitted. As such, this date was not included in our analysis.

Appendix D: Raw data counts for previously published and newly counted modern pollen sites in the Hudson Bay Lowlands, Canada

Description:

Raw data counts for previously published and newly counted modern pollen sites in the Hudson Bay Lowlands, Canada. When raw pollen counts were not provided in the original publication, relative abundance data was approximated from the pollen figure(s) of the original publication and converted to raw data using the pollen sum. The column "ID" refers to a unique code assigned to that site, while "original ID" refers to the name/number of that site from the original publication. Elevation and climate data were collected from Natural Resources Canada (2015). Climate data are based on a 30-year average (1971 to 2000). Mean summer temperature is for the months of June, July and August. An artificial pollen sum was used for Skinner (1973) and Terasmae and Hughes (1960), since no sum was indicated in the original publication. Despite being located in wetland settings, some of the modern sites were missing Cyperaceae and *Sphagnum* counts, or they were indicated in qualitative terms (e.g. "abundant" or "present"). Since wetland taxa are not incorporated into the palaeoclimate reconstruction in this paper, we retained these sites, compiling only the arboreal, herb and shrub counts. In the case of Bazely (1981), there were originally 21 sites (with different pollen counts) associated with the same geographic coordinate. To resolve this issue, we chose a representative sample by creating a DCA of the 21 sites and picking the central site to incorporate into our dataset. Most data in this table are from surface samples; however, a few were extracted from the top (or modern) sample of a peat and/or lake core. Sites are ordered from east to west.

ID	original ID	Lat. (DD)	Long. (DD)	Elevation (MASL)	Total annual precipitation (mm)	Summer temperature (°C)	Source
LH	Lake Horden	50.91	-78.02	214	719	14.2	Potzger and Courtemanche (1956); Terasmae and Anderson (1970)
JR	Jack River	52.02	-78.39	12	625	13.7	Potzger and Courtemanche (1956); Terasmae and Anderson (1970)
SHF	Smoky Hills Falls	51.45	-78.56	19	644	14.3	Potzger and Courtemanche (1956); Terasmae and Anderson (1970)
RH	Rupert House	51.44	-78.78	4	637	14.3	Potzger and Courtemanche (1956); Terasmae and Anderson (1970)
FG01	1	51.43	-79.43	1	632	14.2	Farley-Gill (1980)
FG02	2	51.45	-79.50	1	632	14.1	Farley-Gill (1980)
FG04	4	51.21	-79.53	10	644	14.4	Farley-Gill (1980)
FG05	5	51.14	-79.56	11	647	14.4	Farley-Gill (1980)
FG06	6	51.03	-79.58	14	651	14.6	Farley-Gill (1980)
FG03	3	51.40	-79.60	1	634	14.2	Farley-Gill (1980)
FG07	7	51.04	-79.75	7	652	14.5	Farley-Gill (1980)
FG08	8	50.93	-79.81	19	659	14.6	Farley-Gill (1980)
FG09	9	50.97	-79.92	24	661	14.5	Farley-Gill (1980)
FG10	10	50.86	-79.99	30	667	14.7	Farley-Gill (1980)
FG11	11	51.18	-80.27	14	660	14.3	Farley-Gill (1980)
FG12	12	50.85	-80.35	57	683	14.6	Farley-Gill (1980)
FG13	13	51.06	-80.38	30	671	14.4	Farley-Gill (1980)
FG14	14	51.12	-80.48	23	670	14.3	Farley-Gill (1980)
FG15	15	51.03	-80.53	25	674	14.4	Farley-Gill (1980)
FG18	18	51.38	-80.61	10	648	14.1	Farley-Gill (1980)
FG17	17	51.30	-80.61	7	659	14.1	Farley-Gill (1980)
FG16	16	51.29	-80.63	8	660	14.1	Farley-Gill (1980)
FG19	19	51.80	-80.73	2	591	13.9	Farley-Gill (1980)
FG20	20	51.89	-80.92	3	574	13.8	Farley-Gill (1980)
FG21	21	51.92	-81.17	12	562	13.9	Farley-Gill (1980)
FG22	22	51.95	-81.17	12	559	13.9	Farley-Gill (1980)
S2	SK2	50.67	-81.32	45	704	15.2	Skinner (1973)
FG24a	24a	51.58	-81.58	65	606	14.1	Farley-Gill (1980)
FG24b	24b	51.58	-81.58	65	606	14.1	Farley-Gill (1980)
FG25a	25a	51.53	-81.67	68	611	14.1	Farley-Gill (1980)
FG25b	25b	51.53	-81.67	68	611	14.1	Farley-Gill (1980)
FG23	23	52.18	-81.78	17	515	13.9	Farley-Gill (1980)
FG26	26	51.48	-81.79	70	616	14.2	Farley-Gill (1980)
KLB	Kinosheo Lake bog	51.55	-81.81	68	606	14.2	Kettles et al. (2000)
S4	SK4	51.13	-81.95	88	661	14.6	Skinner (1973)
ARB	Albany River Bog	51.43	-82.38	92	622	14.4	Glaser et al. (2004)
S3	SK3	50.61	-83.05	180	723	15.1	Skinner (1973)
MVRT03	n/a	52.85	-83.93	82	560	13.2	current publication
OR1	Victor Fen	52.71	-84.17	102	572	13.4	O'Reilly et al. (2014)
HVMS-03	n/a	52.71	-84.18	103	572	13.4	current publication
AT01	n/a	53.28	-84.21	113	561	12.6	Friel et al. (2014)
HLM17	n/a	54.75	-84.53	89	533	10.4	current publication
HLM11	n/a	54.68	-84.60	95	536	10.5	current publication
HLM03	n/a	54.60	-84.64	127	543	10.5	current publication
TH1	Attawapiskat River	53.13	-85.30	109	580	13.2	Terasmae and Hughes (1960)
BZ12	Level 12	58.75	-93.50	3	409	10.2	Bazely (1981)
LF24	Site 24	58.74	-94.06	1	417	10.4	Lichti-Federovich and Ritchie (1968)
DM1	Thibaudeau site 127B	57.08	-94.16	126	450	12.4	Dredge and Mott (2003)
SC52	Silox Core 52	57.17	-94.24	142	452	12.2	Dredge and Mott (2003)

ID	Cyperaceae	*Sphagnum*	*Drosera*	*Equisetum*	*Isoetes*	Juncaginaceae	*Lycopus*	*Menyanthes*	*Myriophyllum*	*Nuphar*
LH	5	0	0	0	0	0	0	0	0	0
JR	5	0	0	0	0	0	0	0	0	0
SHF	15	0	0	0	0	0	0	0	0	0
RH	6	0	0	0	0	0	0	0	0	0
FG01	84	1294	0	0	0	0	1	0	0	0
FG02	55	8	0	1	12	0	0	0	0	0
FG04	158	108	0	0	0	0	0	0	0	0
FG05	76	137	2	0	0	0	0	0	0	0
FG06	817	46	0	19	2	0	0	0	0	0
FG03	72	2587	0	2	0	0	0	0	0	0
FG07	71	57	0	1	0	0	1	0	0	0
FG08	8	1777	0	1	0	0	0	0	0	0
FG09	0	2245	0	1	0	0	0	0	0	0
FG10	0	132	0	3	0	0	0	0	0	0
FG11	53	56	0	1	0	0	0	0	0	0
FG12	39	56	0	1	0	0	0	0	0	0
FG13	41	429	0	1	0	0	0	0	0	0
FG14	75	2066	0	0	0	0	0	0	0	0
FG15	42	592	0	0	0	0	0	0	0	0
FG18	99	369	0	1	0	0	0	0	0	0
FG17	30	175	0	20	0	0	0	0	2	0
FG16	1	12	0	0	1	0	0	0	0	0
FG19	6	720	0	0	0	0	0	0	0	0
FG20	69	160	0	2	0	0	0	0	0	0
FG21	49	2047	0	2	0	0	0	1	0	0
FG22	36	306	1	2	0	0	0	0	0	0
S2	0	0	0	0	0	0	0	0	0	0
FG24a	36	56	0	1	0	0	1	0	0	0
FG24b	59	750	0	0	0	0	0	0	0	0
FG25a	37	97	0	1	0	0	0	0	0	0
FG25b	6	1744	0	0	0	0	0	0	0	0
FG23	86	1220	1	2	0	0	0	0	1	0
FG26	19	8880	0	1	0	0	0	0	0	0
KLB	39	129	0	0	0	0	0	0	0	0
S4	0	0	0	0	0	0	0	0	0	0
ARB	3	59	0	0	0	0	0	0	0	0
S3	0	0	0	0	0	0	0	0	0	0
MVRT03	78	28	0	10	0	0	0	0	0	0
OR1	131	64	0	0	0	0	0	0	0	0
HVMS-03	7	97	0	53	0	0	0	0	0	0
AT01	4	8	0	0	0	0	0	0	0	0
HLM17	12	496	0	0	0	0	0	0	0	0
HLM11	98	204	0	0	0	0	0	0	0	0
HLM03	118	62	0	0	0	0	0	0	0	0
TH1	3	120	0	0	0	0	0	0	0	0
BZ12	88	12	0	0	0	0	0	0	1	0
LF24	210	0	0	0	0	0	0	0	0	0
DM1	4	151	0	0	0	0	0	0	0	0
SC52	4	214	0	0	0	0	0	0	0	0

ID	*Nymphaea*	*Potamogeton*	*Sagittaria*	*Sparaganium*	*Typha*	*Picea*	*Abies*	*Pinus*	*Betula*	*Fraxinus*
LH	0	0	0	0	0	133	2	30	15	0
JR	0	0	0	0	0	111	5	60	6	0
SHF	0	0	0	0	0	139	10	33	10	0
RH	0	0	0	0	1	124	40	26	8	0
FG01	0	0	0	1	1	173	1	52	42	1
FG02	0	0	0	1	4	131	1	55	72	0
FG04	0	3	0	1	1	84	0	82	34	1
FG05	0	2	0	0	1	96	1	78	37	1
FG06	0	0	0	0	1	60	1	85	42	1
FG03	0	2	0	0	0	70	0	31	71	0
FG07	0	0	0	0	1	94	1	116	52	0
FG08	0	0	0	0	0	165	0	39	51	1
FG09	0	0	0	0	0	98	1	57	39	0
FG10	0	0	0	0	1	104	1	80	52	3
FG11	0	1	0	0	0	48	1	99	102	1
FG12	0	0	0	0	1	93	1	78	41	1
FG13	0	0	0	0	0	114	0	65	37	0
FG14	0	0	0	0	0	107	1	94	67	1
FG15	0	0	0	0	0	127	1	39	39	0
FG18	0	4	0	2	0	94	0	61	56	1
FG17	0	1	1	0	0	106	0	40	60	1
FG16	0	0	1	0	2	145	1	32	14	0
FG19	0	0	0	0	2	251	0	21	14	0
FG20	0	0	0	0	0	142	0	23	51	0
FG21	0	0	0	0	0	94	0	45	50	0
FG22	0	0	0	0	0	124	0	54	46	0
S2	0	0	0	0	0	88	2	32	10	1
FG24a	0	0	0	0	0	86	1	37	42	0
FG24b	0	0	0	0	0	155	0	47	50	1
FG25a	0	0	0	0	0	55	0	25	52	1
FG25b	0	0	0	0	1	89	1	36	44	0
FG23	0	1	0	0	0	105	0	56	42	4
FG26	0	0	0	0	1	78	0	20	45	2
KLB	0	0	0	0	0	105	0	63	18	0
S4	0	0	0	0	0	40	1	38	28	0
ARB	0	0	0	0	0	80	23	86	29	0
S3	0	0	0	0	0	70	1	24	18	0
MVRT03	0	0	0	1	0	69	0	53	24	0
OR1	0	0	0	0	0	87	0	29	90	0
HVMS-03	0	0	0	0	0	93	0	54	16	0
AT01	0	0	0	0	0	180	0	132	9	0
HLM17	0	0	0	1	0	97	0	37	27	0
HLM11	0	0	0	0	0	77	0	46	14	0
HLM03	0	0	0	0	0	82	0	41	14	1
TH1	0	0	0	0	0	92	0	19	18	0
BZ12	0	0	0	0	0	35	0	63	10	0
LF24	0	37	0	0	0	106	0	112	22	0
DM1	0	0	0	0	0	65	0	30	13	0
SC52	0	0	0	0	0	192	0	51	38	0

ID	*Quercus*	*Ulmus*	*Carpinus/Ostrya*	*Acer*	*Tilia*	Juglandaceae	*Tsuga*	*Alnus*	*Salix*	*Larix*
LH	2	0	0	0	0	0	0	7	0	0
JR	0	0	0	0	0	0	0	19	0	0
SHF	0	0	0	0	0	0	0	2	0	0
RH	0	0	0	0	0	0	0	0	0	0
FG01	1	0	0	0	0	0	1	30	1	0
FG02	3	0	0	0	0	0	0	26	4	0
FG04	1	0	1	4	0	0	0	43	8	1
FG05	1	0	0	0	0	0	0	38	1	1
FG06	1	0	1	0	0	0	0	27	1	4
FG03	4	1	0	0	0	0	0	29	3	0
FG07	6	0	0	0	0	0	0	25	6	3
FG08	3	0	0	1	0	0	0	35	0	0
FG09	4	0	0	4	0	0	0	39	0	1
FG10	8	5	0	1	0	1	0	42	0	3
FG11	3	3	0	0	0	1	0	43	1	1
FG12	5	1	0	0	0	0	0	29	5	1
FG13	1	0	0	0	0	0	0	36	15	1
FG14	3	0	1	1	0	0	0	38	6	1
FG15	4	0	0	1	0	0	0	34	1	1
FG18	5	0	1	1	0	0	0	27	1	0
FG17	3	0	1	1	0	0	0	21	8	20
FG16	1	0	0	1	0	0	0	32	33	0
FG19	1	1	0	0	0	0	0	10	1	0
FG20	2	0	0	0	0	0	0	8	4	0
FG21	6	1	1	1	0	0	0	32	0	1
FG22	2	0	1	1	0	0	0	12	5	1
S2	1	0	1	0	0	0	0	14	2	1
FG24a	4	0	0	0	0	1	0	25	1	0
FG24b	3	0	0	1	0	0	0	28	1	1
FG25a	1	1	1	1	0	1	1	25	3	1
FG25b	2	1	2	0	0	3	1	17	0	2
FG23	1	0	0	0	0	0	0	21	1	0
FG26	2	0	2	0	0	1	1	35	4	1
KLB	0	0	0	0	0	0	0	24	0	3
S4	1	0	1	0	0	0	0	38	3	1
ARB	0	0	0	0	0	0	0	17	3	3
S3	1	0	1	0	0	0	0	24	2	1
MVRT03	0	0	2	0	0	0	0	12	1	0
OR1	0	0	0	0	0	2	0	40	10	0
HVMS-03	0	0	0	0	0	0	0	15	2	0
AT01	1	0	0	0	0	0	0	3	0	1
HLM17	0	0	0	0	0	1	0	15	1	0
HLM11	0	0	0	0	0	0	0	15	1	0
HLM03	0	0	0	0	0	0	0	30	1	1
TH1	1	0	0	0	0	0	0	25	0	3
BZ12	0	0	0	0	0	0	0	6	14	0
LF24	0	0	0	0	1	0	0	14	0	1
DM1	0	0	0	0	0	0	0	22	0	0
SC52	0	0	0	0	0	0	0	17	21	0

ID	Platanaceae	*Populus*	Poaceae	Asteraceae	Amaranthaceae	*Androsace*	*Apiaceae*	Cannabaceae	Caryophyllaceae	Ericaceae
LH	0	0	11	9	0	0	0	0	0	2
JR	0	0	16	3	0	0	0	0	0	2
SHF	0	0	17	4	0	0	0	0	0	15
RH	0	0	0	0	0	0	0	0	0	9
FG01	0	6	1	13	3	0	0	0	0	10
FG02	0	3	1	14	3	0	0	0	0	4
FG04	0	1	2	6	2	0	0	0	0	0
FG05	0	0	5	8	1	0	0	0	0	1
FG06	0	1	1	5	1	0	0	0	0	1
FG03	0	4	2	3	1	0	0	0	0	36
FG07	0	1	11	4	3	0	0	0	0	1
FG08	0	1	1	4	1	0	0	0	0	28
FG09	0	1	1	8	2	0	0	0	0	33
FG10	0	1	3	9	1	0	0	0	0	67
FG11	0	1	8	7	3	0	0	0	0	6
FG12	0	1	2	8	2	1	0	0	0	20
FG13	0	1	1	8	5	0	0	0	0	1
FG14	1	0	0	7	3	0	0	0	0	12
FG15	0	2	0	7	2	0	0	0	0	43
FG18	0	2	7	8	1	0	0	0	0	10
FG17	0	3	5	5	1	0	0	0	0	1
FG16	0	1	14	12	0	3	2	0	1	0
FG19	0	0	0	12	1	0	0	0	0	5
FG20	0	2	4	7	0	0	0	0	0	24
FG21	0	0	1	10	4	0	0	0	0	19
FG22	0	1	2	6	5	0	0	0	0	19
S2	0	1	0	0	0	0	0	0	0	0
FG24a	0	2	4	10	0	0	0	0	0	107
FG24b	0	1	3	11	3	0	0	0	0	21
FG25a	0	1	1	4	1	0	0	0	0	157
FG25b	0	1	2	6	0	0	0	0	0	69
FG23	0	1	1	6	4	0	0	0	0	19
FG26	0	2	2	8	2	0	0	0	0	94
KLB	0	0	0	9	0	0	0	0	0	30
S4	0	1	0	0	0	0	0	0	0	0
ARB	0	0	3	17	3	0	0	0	0	11
S3	0	6	0	0	0	0	0	0	0	0
MVRT03	0	0	0	4	1	0	0	0	0	2
OR1	0	0	0	16	2	0	0	0	0	1
HVMS-03	0	0	0	20	0	0	0	0	0	15
AT01	0	0	2	0	1	0	0	0	0	0
HLM17	0	0	2	3	1	0	0	0	0	2
HLM11	0	0	3	11	1	0	0	0	0	8
HLM03	0	0	2	2	0	0	0	0	0	3
TH1	0	0	0	3	0	0	0	0	0	25
BZ12	0	0	23	7	3	0	0	0	2	0
LF24	0	0	6	8	2	0	0	1	0	4
DM1	0	0	43	4	0	0	0	0	0	22
SC52	0	0	4	0	0	0	0	0	0	124

ID	Liliaceae	*Lycopodium*	Plantaginaceae	Polygonaceae	Ranunculaceae	Rosaceae	*Selaginella*	Urticaceae	Aquifoliaceae	*Corylus*
LH	0	6	0	0	0	0	0	0	0	1
JR	0	1	0	0	0	0	0	0	0	0
SHF	0	25	0	0	0	0	0	0	0	1
RH	0	0	0	0	0	0	0	0	0	0
FG01	0	0	0	0	0	1	1	0	0	0
FG02	0	2	0	0	0	3	0	0	0	0
FG04	0	0	0	0	9	9	0	0	0	1
FG05	0	0	0	0	0	5	0	0	0	4
FG06	0	0	0	0	0	0	0	1	0	1
FG03	0	0	0	0	0	0	0	0	0	0
FG07	29	0	0	0	0	1	0	0	0	0
FG08	0	1	0	0	1	0	0	0	0	0
FG09	1	0	0	0	1	1	0	0	0	0
FG10	1	0	0	0	1	0	0	0	0	0
FG11	0	0	0	0	0	1	0	0	0	0
FG12	0	0	1	0	0	0	0	0	0	0
FG13	0	0	0	0	0	0	0	0	0	0
FG14	0	0	0	0	0	0	0	1	0	0
FG15	16	0	0	0	2	0	0	0	0	0
FG18	0	0	0	0	2	1	0	1	0	0
FG17	0	1	0	0	0	0	0	0	0	0
FG16	0	0	0	0	1	6	0	0	0	0
FG19	0	0	0	0	0	1	0	0	0	0
FG20	12	1	0	0	0	1	2	0	0	0
FG21	0	0	0	0	1	0	0	2	7	0
FG22	0	0	0	0	0	1	0	0	0	1
S2	0	0	0	0	0	0	0	0	0	1
FG24a	0	0	0	1	0	0	0	0	0	0
FG24b	0	3	0	0	0	0	0	0	0	1
FG25a	0	4	0	0	0	1	0	0	1	0
FG25b	0	1	0	1	1	0	0	0	5	2
FG23	2	3	1	0	0	1	0	1	13	0
FG26	0	2	0	0	0	0	0	0	0	0
KLB	0	0	0	0	0	0	0	0	0	0
S4	0	0	0	0	0	0	0	0	0	1
ARB	0	0	0	0	0	0	0	0	0	0
S3	0	0	0	0	0	0	0	0	0	1
MVRT03	0	0	0	0	0	1	0	0	0	0
OR1	0	0	0	0	0	0	0	0	0	0
HVMS-03	0	0	0	0	0	1	0	0	0	0
AT01	0	0	0	0	0	0	0	0	0	0
HLM17	0	0	0	0	0	0	0	0	0	0
HLM11	0	0	0	0	0	0	0	0	0	0
HLM03	1	0	0	0	0	0	1	0	0	2
TH1	0	0	0	0	0	0	0	0	0	0
BZ12	0	3	0	1	0	3	0	0	0	0
LF24	0	0	0	13	0	0	0	0	0	0
DM1	0	0	0	0	0	4	0	0	0	0
SC52	0	0	0	0	0	0	0	0	0	0

ID	Cupressaceae	*Myrica*	Rhamuceae	*Sarcobatus*	*Taxus*	*Botrychium*	*Osmunda*	Polypodiaceae	*Pteridophytina*	*Bryophytina*	unidentified
LH	0	0	0	0	0	0	0	0	0	0	9
JR	0	0	0	0	0	0	0	0	0	0	1
SHF	0	0	0	0	0	0	0	0	0	0	10
RH	0	0	0	0	0	0	0	0	0	0	0
FG01	1	9	0	0	0	0	0	1	0	0	1
FG02	1	16	0	0	0	0	0	0	2	0	4
FG04	0	14	0	0	0	0	0	0	0	0	2
FG05	0	0	0	0	0	0	0	1	0	0	2
FG06	0	1	0	0	0	0	0	1	1	0	3
FG03	0	43	0	0	1	0	0	0	1	0	2
FG07	0	0	0	0	0	0	0	0	0	0	2
FG08	0	6	0	0	1	0	0	2	0	0	0
FG09	0	1	0	1	0	0	0	0	0	0	1
FG10	0	1	0	0	0	0	0	0	0	0	1
FG11	0	1	0	1	0	0	0	0	0	0	0
FG12	0	1	0	0	0	0	0	1	0	0	0
FG13	0	1	0	0	0	0	0	3	0	0	1
FG14	1	1	0	0	0	0	0	1	0	0	0
FG15	1	1	1	2	0	0	0	0	0	0	0
FG18	0	1	1	0	0	0	0	1	0	0	0
FG17	0	1	0	0	0	0	0	1	0	0	0
FG16	0	1	0	0	0	0	0	0	0	0	8
FG19	0	1	0	0	0	0	0	0	0	0	0
FG20	0	14	1	0	0	0	0	1	0	0	0
FG21	0	10	0	0	0	0	0	0	0	0	2
FG22	0	27	0	0	0	0	0	0	0	0	0
S2	1	0	0	0	0	0	0	0	0	0	0
FG24a	1	7	0	0	1	0	0	0	2	0	1
FG24b	0	6	0	0	0	0	0	0	0	0	1
FG25a	0	4	0	0	0	1	0	0	0	0	4
FG25b	0	10	0	0	0	0	0	0	1	0	2
FG23	0	10	0	0	0	0	0	0	0	0	0
FG26	0	7	0	0	0	0	0	1	6	0	3
KLB	0	3	0	0	0	0	0	0	0	0	0
S4	1	0	0	0	0	0	0	0	0	0	0
ARB	0	9	0	0	0	0	29	0	0	0	0
S3	1	0	0	0	0	0	0	0	0	0	0
MVRT03	0	0	0	0	0	0	0	0	1	0	5
OR1	0	0	0	0	0	0	0	0	0	0	0
HVMS-03	0	0	0	0	0	0	0	0	2	0	3
AT01	0	0	0	0	0	0	0	0	0	0	0
HLM17	0	0	0	0	0	0	0	1	0	0	11
HLM11	0	0	0	0	0	0	0	0	0	0	10
HLM03	0	0	0	0	0	0	0	0	0	0	14
TH1	0	3	0	0	0	0	0	1	0	0	0
BZ12	0	5	0	0	0	0	0	0	0	0	12
LF24	0	0	0	0	0	0	0	0	0	9	0
DM1	4	0	0	0	0	0	0	0	0	0	0
SC52	0	0	0	0	0	0	0	0	0	0	4

Appendix E: Model performance for the modern pollen calibration set

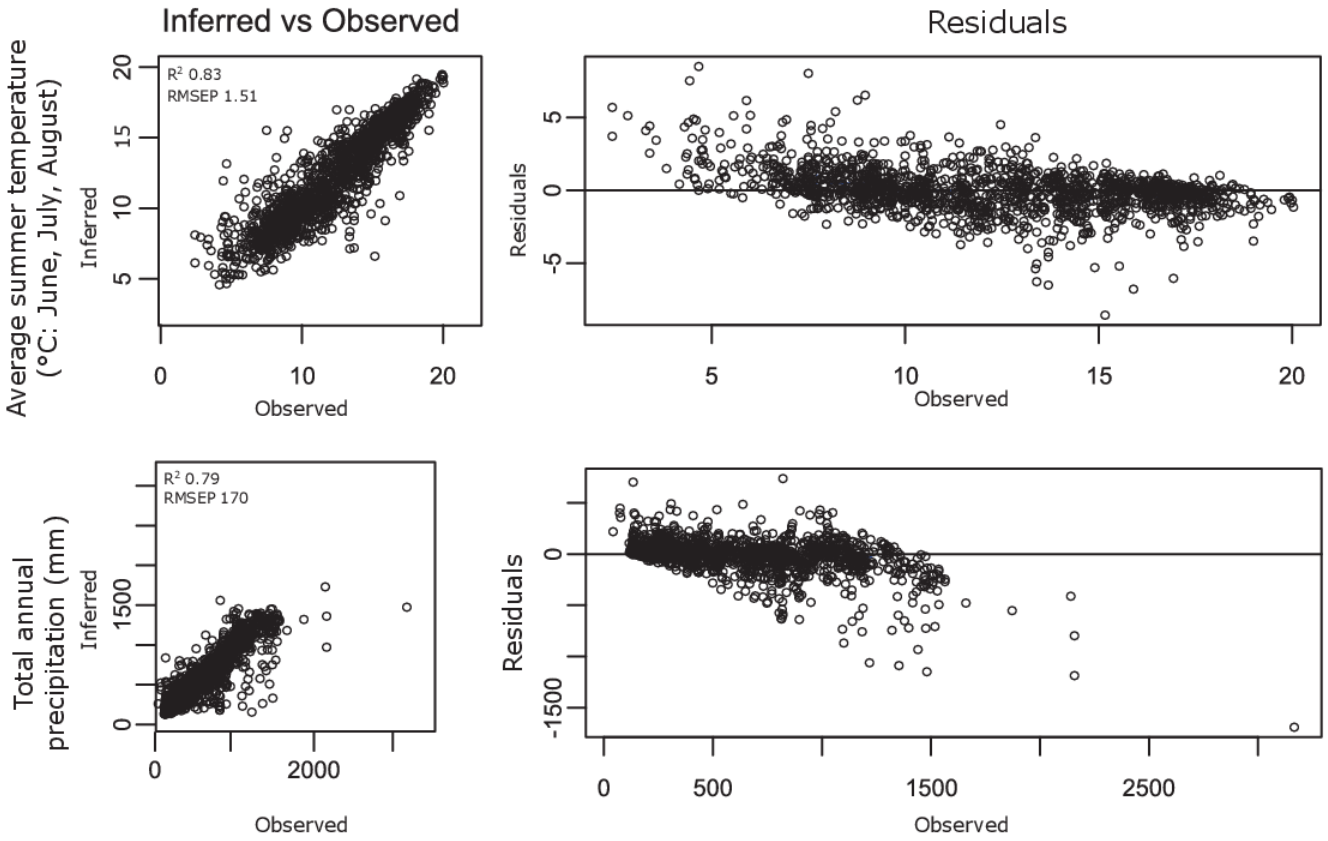

Description:

Model performance for the modern pollen calibration set that was used to reconstruct paleoclimate variables at the Ridge and Albany sites (Chapter 3 and 4 of this dissertation). Modern pollen data were taken from the North American Modern Pollen Database (Whitmore et al., 2005) as well as newly-compiled data from the Hudson Bay Lowlands (Appendix D). See main text for details on which species were included in this analysis.

Appendix F: Elemental results from ICP-AES with aqua regia digestion.

Description:

Elemental results from ICP-AES with aqua regia digestion. All measurements are in parts per million (PPM). Some data were removed and/or censored prior to analysis: see text for details.

	detection limit (PPM)	Site 007 TM1	Site 007 TM2	Site 007 TM3	Site 008a TM1	Site 008a TM2	Site 008b TM3	Site 008b TM4	Site 009 TM1	Site 009 TM2
Al	10	12410	6355	7681	12490	14990	15966	7129	24980	7264
Ba	1	67	29	39	50	75	79	35	152	37
Be	1	<1	<1	<1	<1	<1	<1	<1	1	<1
Ca	8	>65000	>65000	>65000	>65000	>65000	>65000	>65000	39611	>65000
Co	1.2	5	3	4	6	7	7	3	11	4
Cr	1	34	18	23	29	42	42	20	61	22
Cu	1.2	17	12	15	16	21	22	13	31	12
Fe	3	19659	12723	14377	20946	24744	25159	13854	32435	13926
K	35	2623	1258	1484	2827	>2850	>2850	1415	>2850	1510
Li	1	25	19	21	27	28	30	19	>30	21
Mg	1.6	>14000	>14000	>14000	>14000	>14000	>14000	>14000	>14000	>14000
Mn	1	295	211	251	313	394	394	235	428	225
Na	14	493	262	315	239	468	485	314	>670	308
Ni	3	15	8	11	15	21	20	9	31	10
P	40	437	361	391	426	525	503	387	603	384
S	70	697	708	634	527	611	682	906	418	1490
Sc	1	4	2	3	4	5	5	3	7	3
Sr	0.14	91	84	82	82	77	73	79	74	81
Ti	1	1148	834	898	1056	1551	1570	939	>1700	864
V	3	40	26	30	40	51	53	29	>60	28
Y	1	8	7	7	9	10	10	7	12	6
Zn	1	31	17	22	32	42	42	19	63	20

Appendix G: Elemental results from ICP-MS with aqua regia digestion.

Description:

Elemental results from ICP-MS with aqua regia digestion. All measurements are in parts per million (PPM). Some data were removed and/or censored prior to analysis: see text for details.

	detection limit (PPM)	**Site 007 TM1**	**Site 007 TM2**	**Site 007 TM3**	**Site 008a TM1**	**Site 008a TM2**	**Site 008b TM3**	**Site 008b TM4**	**Site 009 TM1**	**Site 009 TM2**
Ag	0.01	0.04	0.02	0.01	0.02	0.03	0.03	0.02	0.05	0.03
As	0.8	2.3	1.9	1.8	3.1	3.2	2.6	1.8	2.9	1.8
Au	0.002	0.004	0.002	<0.002	<0.002	0.002	<0.002	<0.002	0.002	0.002
Ba	0.1	65.4	26.8	34.6	48.4	67.5	75.8	31.1	140.8	32.1
Be	0.04	0.48	0.29	0.32	0.56	0.51	0.59	0.25	0.68	0.25
Bi	0.01	0.07	0.04	0.05	0.07	0.1	0.11	0.05	0.16	0.05
Cd	0.02	0.07	0.05	0.07	0.07	0.1	0.09	0.07	0.13	0.05
Ce	1.9	42.3	29.6	31.5	41.3	48.7	50.4	29.9	62.8	28.6
Co	0.03	6.37	3.95	4.7	7.18	8.6	8.48	4.27	11.56	4.25
Cr	1	32	18	22	31	42	43	20	58	21
Cs	0.023	1.03	0.47	0.61	1.1	1.43	1.55	0.51	2.11	0.59
Cu	0.7	13.5	9.2	10.8	14.8	18.8	18.9	10.2	27.4	9.4
Dy	0.06	1.43	1.18	1.25	1.76	1.81	1.82	1.25	2.22	1.17
Er	0.011	0.7	0.57	0.63	0.85	0.9	0.96	0.65	1.06	0.61
Eu	0.03	0.55	0.43	0.45	0.58	0.65	0.63	0.46	0.78	0.43
Ga	0.004	4.1	2.31	2.78	4.37	5.43	5.53	2.51	7.82	2.49
Gd	0.15	2.28	1.85	2.04	2.6	2.87	2.85	1.95	3.41	1.86
Hf	0.05	0.43	0.34	0.37	0.57	0.57	0.59	0.48	0.77	0.42
Hg	0.01	0.01	0.01	0.02	0.01	0.01	0.01	0.01	0.02	0.01
Ho	0.013	0.264	0.222	0.237	0.318	0.337	0.335	0.244	0.404	0.222
In	0.002	0.015	0.008	0.01	0.015	0.019	0.017	0.009	0.025	0.009
La	0.8	20.44	14.41	15.6	20.18	23.86	24.89	14.5	31.53	14
Li	0.03	19.23	11.37	13.48	22.06	22.84	24.06	10.68	31.01	11.74
Lu	0.003	0.091	0.069	0.082	0.103	0.115	0.113	0.076	0.145	0.073
Mo	0.03	0.21	0.19	0.2	0.32	0.32	0.29	0.23	0.17	0.24
Nb	0.02	0.65	0.92	0.89	0.73	1.23	1.35	1	0.47	0.89
Nd	0.6	17.22	12.73	13.53	17.22	20.68	20.61	13.3	26.09	12.92
Ni	0.7	22.2	13.9	16.9	23.8	30.5	31.7	15.9	41.2	15.8
Pb	0.2	4.9	3.2	3.8	4.6	6.2	6.6	3.4	8.7	3.5
Pr	0.2	4.84	3.47	3.7	4.79	5.7	5.72	3.56	7.2	3.47
Pt	0.003	<0.003	<0.003	<0.003	<0.003	<0.003	<0.003	<0.003	<0.003	<0.003
Rb	0.15	18.75	8.86	11.1	20.37	24.94	25.34	9.27	34.3	10.57
Sb	0.06	0.1	0.06	0.09	0.15	0.12	0.13	0.08	0.15	0.07

	detection limit (PPM)	Site 007 TM1	Site 007 TM2	Site 007 TM3	Site 008a TM1	Site 008a TM2	Site 008b TM3	Site 008b TM4	Site 009 TM1	Site 009 TM2
Sc	0.5	3.86	2.41	2.82	4.26	5.09	5.16	2.71	7.22	2.57
Se	0.4	<0.4	<0.4	<0.4	<0.4	<0.4	<0.4	<0.4	<0.4	<0.4
Sm	0.06	2.94	2.24	2.35	2.98	3.51	3.53	2.36	4.33	2.28
Sn	0.04	0.45	0.31	0.35	0.51	0.61	0.65	0.36	0.8	0.34
Sr	1.6	83.3	80.21	77.46	82.61	72.3	67.76	72.22	65.05	74.54
Ta	0.004	<0.004	<0.004	<0.004	<0.004	<0.004	<0.004	<0.004	<0.004	<0.004
Tb	0.02	0.3	0.244	0.256	0.334	0.369	0.371	0.255	0.453	0.244
Te	0.01	<0.01	0.01	0.01	0.01	0.02	0.01	0.01	0.02	0.01
Th	0.07	5.44	3.29	3.87	5.13	6.97	7.24	3.45	10.2	3.92
Ti	7.4	1058.9	780	854.6	1048.7	1489	1452.6	855.2	1679.6	790.8
Tl	0.003	0.116	0.069	0.084	0.113	0.157	0.169	0.076	0.223	0.075
Tm	0.004	0.098	0.084	0.091	0.112	0.123	0.127	0.086	0.154	0.079
U	0.01	0.79	0.63	0.69	0.75	1.09	1.03	0.62	1.16	0.66
V	4	33	22	25	35	44	44	24	55	24
W	0.02	0.1	0.1	0.1	0.1	0.2	0.2	0.1	0.2	0.1
Y	0.3	7.09	6.07	6.48	8.63	9.05	9.23	6.27	10.73	5.75
Yb	0.02	0.65	0.48	0.56	0.74	0.8	0.8	0.55	0.98	0.52
Zn	3	30.58	18.26	22.26	35.4	44.13	44.85	20.11	62.12	20.17
Zr	0.2	16.08	12.88	13.25	24.56	20.56	23	18.67	28.82	14.84

Appendix H: DCA showing Albany sites 007,008 and 009

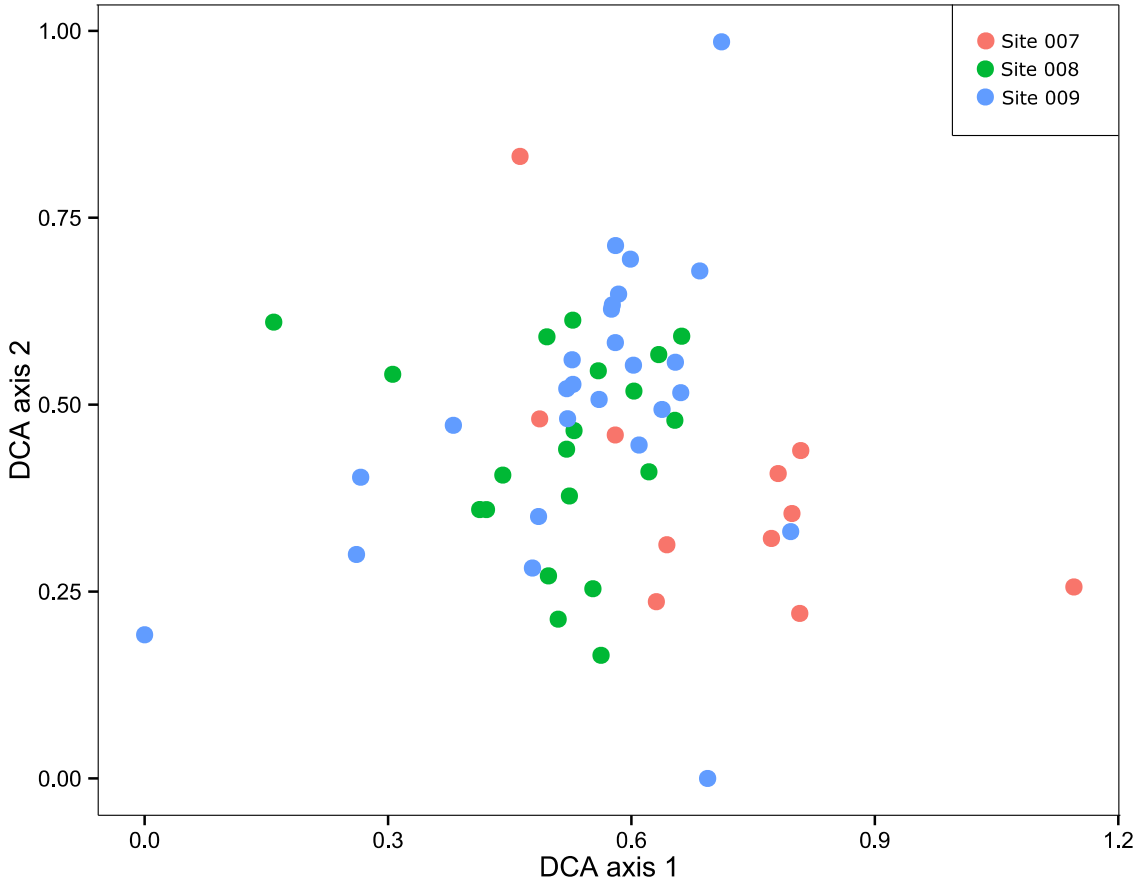

Description:

Detrended correspondence analysis (DCA) showing the similarity of pollen assemblages between Albany Sites 007, 008 and 009.

Appendix I: Synthesis of chronology data from sites located in the previously glaciated region that date to the Wisconsinan Stage (~73-27 ka).

Description:

Synthesis of chronology data from sites located in the previously glaciated region that date to the Wisconsinan Stage (~73-27 ka). Radiocarbon data are reported in ^{14}C yr BP (uncalibrated). Information in this table was compiled from the original publication for each site. Latitude (Lat) and longitude (Long) values were rounded to the nearest two decimal points. The column "Sample type" refers to the way we classified each sample; see the original publication for more details on the specific sample material. Luminescence samples are either thermoluminescence (TL) or optically stimulated luminescence (OSL). Radiocarbon samples were either accelerator mass spectrometry (AMS), conventional (Conv.), or left blank when data were not available in the original publication. Entries in this table are grouped by year of publication and then by sample type.

Lab code	Site name	Lat	Long	Sample type	Reported age	Reference
ISGS A1656	11-PJB-186	56.61	-89.29	^{14}C AMS (wood)	45700 ± 1300	Dalton et al. (2016)
ISGS A1995	11-PJB-186	56.61	-89.29	^{14}C AMS (wood)	50100 ± 3300	Dalton et al. (2016)
UOC-0587	11-PJB-186	56.61	-89.29	^{14}C AMS (wood)	49600 ± 950	Dalton et al. (2016)
UOC-0589	13-PJB-003	50.88	-84.86	^{14}C AMS (wood)	49600 ± 950	Dalton et al. (2016)
ISGS A2424	12-PJB-007	50.49	-83.87	^{14}C AMS (wood)	46500 ± 2100	Dalton et al. (2016)
UOC-0590	12-PJB-007	50.49	-83.87	^{14}C AMS (wood)	45600 ± 1250	Dalton et al. (2016)
ISGS A2460	12-PJB-002	50.46	-83.67	^{14}C AMS (wood)	34100 ± 500	Dalton et al. (2016)
TO-1753	24M	50.31	-82.70	^{14}C AMS (wood)	37300 ± 500	Dalton et al. (2016)
TO-1752	Moose	50.42	-82.33	^{14}C AMS (wood)	39200 ± 500	Dalton et al. (2016)
TO-1751	Adam Creek	50.17	-82.08	^{14}C AMS (wood)	35000 ± 350	Dalton et al. (2016)
UOC-0593	13-PJB-003	50.88	-84.86	^{14}C AMS (peat)	28300 ± 150	Dalton et al. (2016)
UOC-0591	11-PJB-020	50.48	-83.88	^{14}C AMS (peat)	37600 ± 200	Dalton et al. (2016); Dalton et al. (2017)
UOC-0592	11-PJB-020	50.48	-83.88	^{14}C AMS (peat)	49600 ± 950	Dalton et al. (2016); Dalton et al. (2017)
UOC-0597	14-PJB-007	51.93	-82.72	^{14}C AMS (peat)	38800 ± 350	Dalton et al. (2016)
UOC-0594	14-PJB-008	51.92	-82.63	^{14}C AMS (peat)	42100 ± 450	Dalton et al. (2016)
BG3807	Severn Marine	55.43	-88.20	luminescence (OSL)	52500 ± 5050	Dalton et al. (2016)
BG3808	Severn Marine	55.43	-88.20	luminescence (OSL)	42200 ± 4000	Dalton et al. (2016)
BG3800	12-PJB-109	50.87	-84.85	luminescence (OSL)	42800 ± 3750	Dalton et al. (2016)
M011	Weybridge Cave Sediments	44.06	-73.21	luminescence (OSL)	36100 ± 6600	Munroe et al. (2016)
M016	Weybridge Cave Sediments	44.06	-73.21	luminescence (OSL)	51800 ± 14700	Munroe et al. (2016)

Lab code	Site name	Lat	Long	Sample type	Reported age	Reference
OSL03	Anse à la Cabane	47.22	-61.99	luminescence (OSL)	41000 ± 4000	Rémillard et al. (2016)
OSL04	Anse à la Cabane	47.22	-61.99	luminescence (OSL)	44000 ± 4000	Rémillard et al. (2016)
Beta-329000	Hemlock Crossing	42.87	-86.20	^{14}C AMS (wood)	37840 ± 400	Colgan et al. (2015)
Beta-353120	Hemlock Crossing	42.87	-86.20	^{14}C AMS (wood)	40790 ± 400	Colgan et al. (2015)
A3030	Zorra Quarry	43.10	-80.90	^{14}C AMS (wood)	44900 ± 1500	Bajc et al. (2015)
TO-13125	Zorra Quarry	43.10	-80.90	^{14}C AMS (wood)	45160 ± 1260	Bajc et al. (2015)
TO-13125R	Zorra Quarry	43.10	-80.90	^{14}C AMS (wood)	47220 ± 1050	Bajc et al. (2015)
TO-13126	Zorra Quarry	43.10	-80.90	^{14}C AMS (wood)	42900 ± 1050	Bajc et al. (2015)
TO-13126R	Zorra Quarry	43.10	-80.90	^{14}C AMS (wood)	50520 ± 1570	Bajc et al. (2015)
TO-13126RR	Zorra Quarry	43.10	-80.90	^{14}C AMS (wood)	47640 ± 680	Bajc et al. (2015)
Beta-339716	Repulse Bay	66.17	-86.26	^{14}C AMS (carbonate)	33950 ± 270	McMartin et al. (2015)
Beta-339715	Repulse Bay	66.14	-86.24	^{14}C AMS (carbonate)	38240 ± 410	McMartin et al. (2015)
Beta-339713	Repulse Bay	66.19	-86.22	^{14}C AMS (carbonate)	38000 ± 400	McMartin et al. (2015)
Beta-315076	Repulse Bay	66.16	-86.21	^{14}C AMS (carbonate)	39820 ± 460	McMartin et al. (2015)
Beta-339717	Repulse Bay	66.16	-86.21	^{14}C AMS (carbonate)	36590 ± 350	McMartin et al. (2015)
Keck-122480	Repulse Bay	66.16	-86.21	^{14}C AMS (carbonate)	36950 ± 590	McMartin et al. (2015)
Beta-339718	Repulse Bay	66.17	-86.21	^{14}C AMS (carbonate)	39450 ± 460	McMartin et al. (2015)
Keck-122338	Repulse Bay	66.17	-86.21	^{14}C AMS (carbonate)	32290 ± 210	McMartin et al. (2015)
SacA16558	North of Montreal Lake	54.68	-105.50	^{14}C AMS (charcoal)	41200 ± 1200	Bélanger et al. (2014)
SacA16559	North of Montreal Lake	54.68	-105.50	^{14}C AMS (charcoal)	39430 ± 940	Bélanger et al. (2014)
SacA16560	North of Montreal Lake	54.68	-105.50	^{14}C AMS (charcoal)	43800 ± 1600	Bélanger et al. (2014)
SacA16561	North of Montreal Lake	54.68	-105.50	^{14}C AMS (charcoal)	39030 ± 890	Bélanger et al. (2014)
SacA16562	North of Montreal Lake	54.68	-105.50	^{14}C AMS (charcoal)	44200 ± 1700	Bélanger et al. (2014)
SacA16563	North of Montreal Lake	54.68	-105.50	^{14}C AMS (charcoal)	41000 ± 1100	Bélanger et al. (2014)
SacA16564	North of Montreal Lake	54.68	-105.50	^{14}C AMS (charcoal)	31470 ± 360	Bélanger et al. (2014)
SacA16566	North of Montreal Lake	54.68	-105.50	^{14}C AMS (charcoal)	43800 ± 1600	Bélanger et al. (2014)
SacA16567	North of Montreal Lake	54.68	-105.50	^{14}C AMS (charcoal)	50000 ± 3500	Bélanger et al. (2014)
SacA27173	North of Montreal Lake	54.68	-105.50	^{14}C AMS (charcoal)	28290 ± 260	Bélanger et al. (2014)
SacA27175	North of Montreal Lake	54.68	-105.50	^{14}C AMS (charcoal)	38250 ± 790	Bélanger et al. (2014)

Lab code	Site name	Lat	Long	Sample type	Reported age	Reference
SacA27176	North of Montreal Lake	54.68	-105.50	^{14}C AMS (charcoal)	40000 ± 1000	Bélanger et al. (2014)
SacA27177	North of Montreal Lake	54.68	-105.50	^{14}C AMS (charcoal)	50100 ± 3300	Bélanger et al. (2014)
SacA27178	North of Montreal Lake	54.68	-105.50	^{14}C AMS (charcoal)	38960 ± 850	Bélanger et al. (2014)
SacA27179	North of Montreal Lake	54.68	-105.50	^{14}C AMS (charcoal)	29030 ± 260	Bélanger et al. (2014)
Beta-342758	Inland Aggregates Pit 48	53.66	-113.28	^{14}C AMS (bone, antler, tooth, tusk)	41460 ± 570	Jass and Beaudoin (2014)
UCIAMS-74417	Anse à la Cabane	47.22	-61.99	^{14}C AMS (wood)	50100 ± 3300	Rémillard et al. (2013)
UCIAMS-84792	Anse à la Cabane	47.22	-61.99	^{14}C AMS (wood)	47100 ± 2300	Rémillard et al. (2013)
UCIAMS-84793	Anse à la Cabane	47.22	-61.99	^{14}C AMS (wood)	47800 ± 2500	Rémillard et al. (2013)
UCIAMS-41189	Anse à la Cabane	47.22	-61.99	^{14}C AMS (wood)	47100 ± 2700	Rémillard et al. (2013)
Beta-100442	Sixmile Creek	42.43	-76.49	^{14}C AMS (plants, seeds)	33950 ± 220	Karig and Miller (2013)
Beta-100443	Sixmile Creek	42.43	-76.49	^{14}C AMS (plants, seeds)	35190 ± 240	Karig and Miller (2013)
CAMS-45917	Sixmile Creek	42.43	-76.49	^{14}C AMS (plants, seeds)	41000 ± 1900	Karig and Miller (2013)
CAMS-45918	Sixmile Creek	42.43	-76.49	^{14}C AMS (plants, seeds)	38790 ± 930	Karig and Miller (2013)
CAMS-45919	Sixmile Creek	42.43	-76.49	^{14}C AMS (plants, seeds)	43000 ± 1600	Karig and Miller (2013)
CAMS-45920	Sixmile Creek	42.43	-76.49	^{14}C AMS (insect)	34510 ± 960	Karig and Miller (2013)
OS-67637	South Fraserdale Lake	49.77	-81.52	^{14}C (wood)	45700 ± 940	Stroup et al. (2013)
OS-67639	South Fraserdale Lake	49.77	-81.52	^{14}C (wood)	42240 ± 370	Stroup et al. (2013)
OS-98037	Sixmile Creek	42.43	-76.49	^{14}C (plants, seeds)	43800 ± 4900	Karig and Miller (2013)
WW-8289	Sixmile Creek	42.43	-76.49	^{14}C (plants, seeds)	42300 ± 1500	Karig and Miller (2013)
WW-8529	Sixmile Creek	42.43	-76.49	^{14}C (plants, seeds)	37200 ± 500	Karig and Miller (2013)
WW-9396	Sixmile Creek	42.43	-76.49	^{14}C (plants, seeds)	40100 ± 630	Karig and Miller (2013)
NOSAMS-79539	Liot Point	73.09	-124.86	^{14}C AMS (carbonate)	34700 ± 200	Lakeman (2012)
NOSAMS-79616	Norway Island	73.70	-124.60	^{14}C AMS (carbonate)	44800 ± 770	Lakeman (2012)
NOSAMS-79535	First Point	73.29	-124.55	^{14}C AMS (carbonate)	49900 ± 550	Lakeman (2012)

Lab code	Site name	Lat	Long	Sample type	Reported age	Reference
NOSAMS-79536	Adam River	73.42	-124.39	^{14}C AMS (carbonate)	30700 ± 140	Lakeman (2012)
UCI-77838	North Bluff IV - Burnett Bay	73.84	-123.90	^{14}C AMS (carbonate)	38540 ± 330	Lakeman (2012)
NOSAMS-79615	North Bluff III - Burnett Bay	73.84	-123.90	^{14}C AMS (carbonate)	35100 ± 220	Lakeman (2012)
NOSAMS-79614	North Bluff II - Burnett Bay	73.84	-123.90	^{14}C AMS (carbonate)	45500 ± 600	Lakeman (2012)
NOSAMS-79613	North Bluff - Burnett Bay	73.84	-123.89	^{14}C AMS (carbonate)	33600 ± 240	Lakeman (2012)
NOSAMS-79612	South Bluff - Burnett Bay	73.83	-123.87	^{14}C AMS (carbonate)	45600 ± 480	Lakeman (2012)
UCI-60258	Jesse Till IV	72.28	-120.32	^{14}C AMS (carbonate)	44000 ± 1000	Lakeman (2012)
UCI-60273	Jesse Till X	72.07	-120.25	^{14}C AMS (carbonate)	32640 ± 260	Lakeman (2012)
UCI-60271	Jesse Till VIII	72.11	-120.20	^{14}C AMS (carbonate)	39610 ± 600	Lakeman (2012)
UCI-60261	Jesse Till V	72.22	-120.19	^{14}C AMS (carbonate)	49700 ± 2100	Lakeman (2012)
UCI-60272	Jesse Till IX	72.19	-120.16	^{14}C AMS (carbonate)	55200 ± 4000	Lakeman (2012)
UCI-60269	Jesse Till VII	72.23	-120.01	^{14}C AMS (carbonate)	32530 ± 250	Lakeman (2012)
UCI-60264	Jesse Till VI	72.25	-120.00	^{14}C AMS (carbonate)	48000 ± 1700	Lakeman (2012)
UCI-50749	Jesse Till III	73.09	-118.94	^{14}C AMS (carbonate)	46100 ± 790	Lakeman (2012)
UCI-50748	Jesse Till II	72.93	-118.39	^{14}C AMS (carbonate)	41490 ± 460	Lakeman (2012)
UCI-50741	Jesse Till	72.87	-118.22	^{14}C AMS (carbonate)	49500 ± 1210	Lakeman (2012)
GSC-728	Taber	49.90	-112.20	^{14}C Conv. (wood)	35980 ± 1060	Jackson et al. (2011)
GSC-578	Evil Smelling Bluff	50.10	-110.66	^{14}C Conv. (wood)	28630 ± 800	Jackson et al. (2011)
GSC-144-1	Galt Island Bluff	50.15	-110.65	^{14}C Conv. (wood)	37700 ± 1100	Jackson et al. (2011)
GSC-144-2	Galt Island Bluff	50.15	-110.65	^{14}C Conv. (wood)	37900 ± 1100	Jackson et al. (2011)
Beta-275124	Pingualuit Crater	61.28	-73.66	^{14}C AMS (organic-rich sediment)	30060 ± 260	Guyard et al. (2011)
Beta-275125	Pingualuit Crater	61.28	-73.66	^{14}C AMS (organic-rich sediment)	27760 ± 210	Guyard et al. (2011)
UCI-177051	Pingualuit Crater	61.28	-73.66	^{14}C AMS (organic-rich sediment)	31200 ± 320	Guyard et al. (2011)
UCI-75731	Pingualuit Crater	61.28	-73.66	^{14}C AMS (organic-rich sediment)	29310 ± 330	Guyard et al. (2011)
UCI-75732	Pingualuit Crater	61.28	-73.66	^{14}C AMS (organic-rich sediment)	31080 ± 420	Guyard et al. (2011)
UCI-75736	Pingualuit Crater	61.28	-73.66	^{14}C AMS (organic-rich sediment)	29550 ± 270	Guyard et al. (2011)
UCI-75737	Pingualuit Crater	61.28	-73.66	^{14}C AMS (organic-rich sediment)	24570 ± 170	Guyard et al. (2011)
UCI-76679	Pingualuit Crater	61.28	-73.66	^{14}C AMS (organic-rich sediment)	26870 ± 220	Guyard et al. (2011)
AA-83058	Cape Grinnell	78.60	-71.57	^{14}C AMS (carbonate)	40000 ± 1200	Mason (2010)
ETH-29215	Hanging Stone Lake (site 401)	56.21	-111.43	^{14}C AMS (wood)	34980 ± 390	Fisher et al. (2009)
ETH-29216	Hanging Stone Lake (site 401)	56.21	-111.43	^{14}C AMS (wood)	42540 ± 780	Fisher et al. (2009)

Lab code	Site name	Lat	Long	Sample type	Reported age	Reference
ETH-32167	Sandy Bog Lake (site 554)	56.32	-111.93	^{14}C AMS (peat)	37820 ± 520	Fisher et al. (2009)
TO-12125	Cape Hay	74.62	-112.18	^{14}C AMS (carbonate)	30190 ± 310	England et al. (2009)
UCIAMS-24771	Cape Hay	74.62	-112.18	^{14}C AMS (carbonate)	48800 ± 1400	England et al. (2009)
UCIAMS-24772	Cape Hay	74.62	-112.18	^{14}C AMS (carbonate)	41870 ± 620	England et al. (2009)
UCIAMS-25402	Cape Hay	74.62	-112.18	^{14}C AMS (carbonate)	50300 ± 3500	England et al. (2009)
TO-11296	Cape Clarendon	74.62	-111.49	^{14}C AMS (carbonate)	27010 ± 200	England et al. (2009)
TO-11300	Cape Clarendon	74.62	-111.49	^{14}C AMS (carbonate)	26510 ± 500	England et al. (2009)
TO-11301	Cape Clarendon	74.62	-111.49	^{14}C AMS (carbonate)	31400 ± 300	England et al. (2009)
TO-11302	Cape Clarendon	74.62	-111.49	^{14}C AMS (carbonate)	30000 ± 260	England et al. (2009)
UCIAMS-24776	Cape Clarendon	74.62	-111.49	^{14}C AMS (carbonate)	36170 ± 310	England et al. (2009)
UCIAMS-24778	Cape Clarendon	74.62	-111.49	^{14}C AMS (carbonate)	42580 ± 680	England et al. (2009)
UCIAMS-24779	Cape Clarendon	74.62	-111.49	^{14}C AMS (carbonate)	41300 ± 570	England et al. (2009)
UCIAMS-24780	Cape Clarendon	74.62	-111.49	^{14}C AMS (carbonate)	31750 ± 190	England et al. (2009)
UCIAMS-24781	Cape Clarendon	74.62	-111.49	^{14}C AMS (carbonate)	30170 ± 150	England et al. (2009)
UCIAMS-24782	Cape Clarendon	74.62	-111.49	^{14}C AMS (carbonate)	34670 ± 260	England et al. (2009)
TO-10636	Table Hills	74.81	-111.02	^{14}C AMS (carbonate)	35630 ± 370	England et al. (2009)
TO-12126	Table Hills	74.81	-111.02	^{14}C AMS (carbonate)	38820 ± 630	England et al. (2009)
TO-12127	Table Hills	74.81	-111.02	^{14}C AMS (carbonate)	45310 ± 1000	England et al. (2009)
TO-12128	Table Hills	74.81	-111.02	^{14}C AMS (carbonate)	29740 ± 260	England et al. (2009)
TO-12129	Table Hills	74.81	-111.02	^{14}C AMS (carbonate)	36070 ± 450	England et al. (2009)
TO-12139	Table Hills	74.81	-111.02	^{14}C AMS (carbonate)	40210 ± 620	England et al. (2009)
UCIAMS-24773	Table Hills	74.81	-111.02	^{14}C AMS (carbonate)	43350 ± 740	England et al. (2009)
UCIAMS-25400	Table Hills	74.81	-111.02	^{14}C AMS (carbonate)	48900 ± 3000	England et al. (2009)
UCIAMS-25404	Table Hills	74.81	-111.02	^{14}C AMS (carbonate)	35980 ± 600	England et al. (2009)
UCIAMS-25405	Table Hills	74.81	-111.02	^{14}C AMS (carbonate)	43800 ± 1600	England et al. (2009)
TO-10626	Cape Phipps	74.72	-110.99	^{14}C AMS (carbonate)	28810 ± 250	England et al. (2009)
TO-10627	Cape Phipps	74.72	-110.99	^{14}C AMS (carbonate)	27860 ± 250	England et al. (2009)
UCIAMS-24789	Cape Phipps	74.72	-110.99	^{14}C AMS (carbonate)	42840 ± 690	England et al. (2009)
UCIAMS-24790	Cape Phipps	74.72	-110.99	^{14}C AMS (carbonate)	38970 ± 430	England et al. (2009)
UCIAMS-25398	Cape Phipps	74.72	-110.99	^{14}C AMS (carbonate)	33930 ± 470	England et al. (2009)
TO-10634	Winter Harbour	74.79	-110.97	^{14}C AMS (carbonate)	29190 ± 220	England et al. (2009)

Lab code	Site name	Lat	Long	Sample type	Reported age	Reference
UCIAMS-24791	Winter Harbour	74.79	-110.97	^{14}C AMS (carbonate)	35560 ± 290	England et al. (2009)
UCIAMS-24792	Winter Harbour	74.79	-110.97	^{14}C AMS (carbonate)	38640 ± 410	England et al. (2009)
UCIAMS-25399	Winter Harbour	74.79	-110.97	^{14}C AMS (carbonate)	38190 ± 780	England et al. (2009)
UCIAMS-26790	Redstone River	63.63	-125.43	^{14}C AMS (wood)	41500 ± 1800	Huntley et al. (2008)
UCIAMS-23866	Dahadinni River	63.84	-124.81	^{14}C AMS (plants, seeds)	45430 ± 7200	Huntley et al. (2008)
UCIAMS-23872	Dahadinni River	63.97	-124.44	^{14}C AMS (plants, seeds)	51600 ± 2600	Huntley et al. (2008)
UCIAMS-23873	Dahadinni River	63.97	-124.44	^{14}C AMS (plants, seeds)	52200 ± 2800	Huntley et al. (2008)
UCIAMS-23884	Ochre River	63.56	-123.55	^{14}C AMS (plants, seeds)	50900 ± 2400	Huntley et al. (2008)
Beta-237891	Great Dantzic Cove	46.98	-55.97	^{14}C AMS (carbonate)	39370 ± 450	Bell et al. (2008)
Beta-237892	Great Dantzic Cove	46.98	-55.97	^{14}C AMS (carbonate)	39810 ± 470	Bell et al. (2008)
Beta-77432	Kidluit Bay	69.50	-133.91	^{14}C AMS (plants, seeds)	31290 ± 350	McNeely (2006)
GSC-5658	Bent Horn Creek	76.35	-103.87	^{14}C Conv. (carbonate)	39000 ± 1480	McNeely (2006)
GSC-6235	Cockscomb Peak	76.22	-97.60	^{14}C Conv. (carbonate)	28600 ± 660	McNeely (2006)
GSC-5666	Buchanan Lake	79.34	-86.35	^{14}C Conv. (carbonate)	33400 ± 790	McNeely (2006)
GSC-5978	Portage-du-Cap	47.24	-61.90	^{14}C Conv. (carbonate)	31000 ± 710	McNeely (2006)
Beta-117277	Buchanan Lake	79.34	-86.35	^{14}C AMS (wood)	49790 ± 1800	McNeely (2006)
AA-42063	18km SW of Elam-DeWitt site	42.81	-77.86	^{14}C AMS (wood)	43300 ± 1800	Young and Burr (2006)
AA-14584	Genesee Valley	42.95	-77.74	^{14}C AMS (wood)	46337 ± 2982	Young and Burr (2006)
AA-30219	Genesee Valley	42.95	-77.74	^{14}C AMS (wood)	41100 ± 1500	Young and Burr (2006)
AA-30220	Genesee Valley	42.95	-77.74	^{14}C AMS (wood)	39900 ± 1200	Young and Burr (2006)
AA-34098	Genesee Valley	42.95	-77.74	^{14}C AMS (wood)	46000 ± 2700	Young and Burr (2006)
AA-34102	Genesee Valley	42.95	-77.74	^{14}C AMS (wood)	36600 ± 910	Young and Burr (2006)
AA-34105	Genesee Valley	42.95	-77.74	^{14}C AMS (wood)	42100 ± 1700	Young and Burr (2006)
AA-34106	Genesee Valley	42.95	-77.74	^{14}C AMS (wood)	40300 ± 1200	Young and Burr (2006)
AA-34107	Genesee Valley	42.95	-77.74	^{14}C AMS (wood)	47300 ± 2900	Young and Burr (2006)
AA-34318	Genesee Valley	42.95	-77.74	^{14}C AMS (wood)	41000 ± 1900	Young and Burr (2006)
AA-57452	Genesee Valley	42.95	-77.74	^{14}C AMS (wood)	45900 ± 2500	Young and Burr (2006)

Lab code	Site name	Lat	Long	Sample type	Reported age	Reference
AA-57454	Genesee Valley	42.95	-77.74	^{14}C AMS (wood)	42100 ± 1600	Young and Burr (2006)
AA-60172	Genesee Valley	42.95	-77.74	^{14}C AMS (wood)	46500 ± 2800	Young and Burr (2006)
AA-60174	Genesee Valley	42.95	-77.74	^{14}C AMS (wood)	43000 ± 1700	Young and Burr (2006)
AA-60176	Genesee Valley	42.95	-77.74	^{14}C AMS (wood)	39400 ± 1200	Young and Burr (2006)
AA-60180	Genesee Valley	42.95	-77.74	^{14}C AMS (wood)	43800 ± 1900	Young and Burr (2006)
AA-60181	Genesee Valley	42.95	-77.74	^{14}C AMS (wood)	44400 ± 2200	Young and Burr (2006)
AA-60183	Genesee Valley	42.95	-77.74	^{14}C AMS (wood)	43900 ± 2000	Young and Burr (2006)
AA-60184	Genesee Valley	42.95	-77.74	^{14}C AMS (wood)	44400 ± 2200	Young and Burr (2006)
AA-60185	Genesee Valley	42.95	-77.74	^{14}C AMS (wood)	39200 ± 1100	Young and Burr (2006)
AA-60186	Genesee Valley	42.95	-77.74	^{14}C AMS (wood)	47200 ± 3000	Young and Burr (2006)
AA-60187	Genesee Valley	42.95	-77.74	^{14}C AMS (wood)	46600 ± 2700	Young and Burr (2006)
AA-60189	Genesee Valley	42.95	-77.74	^{14}C AMS (wood)	43500 ± 1900	Young and Burr (2006)
AA-60190	Genesee Valley	42.95	-77.74	^{14}C AMS (wood)	41600 ± 1600	Young and Burr (2006)
AA-60191	Genesee Valley	42.95	-77.74	^{14}C AMS (wood)	47600 ± 3000	Young and Burr (2006)
AA-60192	Genesee Valley	42.95	-77.74	^{14}C AMS (wood)	40500 ± 1300	Young and Burr (2006)
AA-60193	Genesee Valley	42.95	-77.74	^{14}C AMS (wood)	46400 ± 2700	Young and Burr (2006)
AA-60194	Genesee Valley	42.95	-77.74	^{14}C AMS (wood)	43200 ± 1800	Young and Burr (2006)
AA-34097	Genesee Valley	42.95	-77.74	^{14}C AMS (plants, seeds)	48500 ± 3500	Young and Burr (2006)
AA-34099	Genesee Valley	42.95	-77.74	^{14}C AMS (plants, seeds)	41100 ± 3300	Young and Burr (2006)
AA-34103	Genesee Valley	42.95	-77.74	^{14}C AMS (plants, seeds)	39100 ± 1200	Young and Burr (2006)
AA-34104	Genesee Valley	42.95	-77.74	^{14}C AMS (plants, seeds)	40400 ± 1200	Young and Burr (2006)
AA-34397	Genesee Valley	42.95	-77.74	^{14}C AMS (plants, seeds)	39000 ± 1100	Young and Burr (2006)
AA-42062	Genesee Valley	42.95	-77.74	^{14}C AMS (plants, seeds)	45600 ± 2500	Young and Burr (2006)
AA-57453	Genesee Valley	42.95	-77.74	^{14}C AMS (plants, seeds)	33080 ± 570	Young and Burr (2006)
AA-60173	Genesee Valley	42.95	-77.74	^{14}C AMS (plants, seeds)	40600 ± 1400	Young and Burr (2006)
AA-60178	Genesee Valley	42.95	-77.74	^{14}C AMS (plants, seeds)	43600 ± 1400	Young and Burr (2006)
AA-60179	Genesee Valley	42.95	-77.74	^{14}C AMS (plants, seeds)	41600 ± 1500	Young and Burr (2006)

Lab code	Site name	Lat	Long	Sample type	Reported age	Reference
AA-60188	Genesee Valley	42.95	-77.74	^{14}C AMS (plants, seeds)	43100 ± 1800	Young and Burr (2006)
AA-60195	Genesee Valley	42.95	-77.74	^{14}C AMS (plants, seeds)	40300 ± 1300	Young and Burr (2006)
AA-8638	Genesee Valley	42.95	-77.74	^{14}C AMS (peat)	38400 ± 1200	Young and Burr (2006)
OS-18066	Amarok Lake	66.27	-65.75	^{14}C AMS (other organic material)	47900 ± 780	Fréchette et al. (2006)
OS-18067	Amarok Lake	66.27	-65.75	^{14}C AMS (other organic material)	46000 ± 640	Fréchette et al. (2006)
OS-18064	Brother-of-Fog Lake	66.27	-65.75	^{14}C AMS (other organic material)	60000 ± 1900	Fréchette et al. (2006)
AA-10790	Genesee Valley	42.95	-77.74	^{14}C AMS (organic-rich sediment)	33950 ± 650	Young and Burr (2006)
AA-10791	Genesee Valley	42.95	-77.74	^{14}C AMS (organic-rich sediment)	35350 ± 770	Young and Burr (2006)
AA-10792	Genesee Valley	42.95	-77.74	^{14}C AMS (organic-rich sediment)	35000 ± 740	Young and Burr (2006)
AA-12126	Genesee Valley	42.95	-77.74	^{14}C AMS (organic-rich sediment)	43700 ± 2100	Young and Burr (2006)
AA-34108	Genesee Valley	42.95	-77.74	^{14}C AMS (organic-rich sediment)	40100 ± 1300	Young and Burr (2006)
AA-34317	Genesee Valley	42.95	-77.74	^{14}C AMS (organic-rich sediment)	31100 ± 1000	Young and Burr (2006)
AA-57446	Genesee Valley	42.95	-77.74	^{14}C AMS (organic-rich sediment)	34260 ± 590	Young and Burr (2006)
AA-57447	Genesee Valley	42.95	-77.74	^{14}C AMS (organic-rich sediment)	27680 ± 320	Young and Burr (2006)
AA-57448	Genesee Valley	42.95	-77.74	^{14}C AMS (organic-rich sediment)	30140 ± 380	Young and Burr (2006)
AA-57449	Genesee Valley	42.95	-77.74	^{14}C AMS (organic-rich sediment)	21520 ± 210	Young and Burr (2006)
AA-57450	Genesee Valley	42.95	-77.74	^{14}C AMS (organic-rich sediment)	28350 ± 300	Young and Burr (2006)
AA-8640	Genesee Valley	42.95	-77.74	^{14}C AMS (organic-rich sediment)	26680 ± 300	Young and Burr (2006)
OS-17676	Amarok Lake	66.27	-65.75	^{14}C AMS (organic-rich sediment)	38600 ± 280	Fréchette et al. (2006)
TO-796	Garry Island	69.50	-135.70	^{14}C AMS (carbonate)	43550 ± 470	McNeely (2006)
AA-34316	Genesee Valley	42.95	-77.74	^{14}C AMS (carbonate)	40000 ± 1200	Young and Burr (2006)
Beta-155639	Box Creek	47.79	-106.36	^{14}C AMS (bone, antler, tooth, tusk)	33280 ± 320	Hill (2006)
AA-33146 (1)	Genesee Valley	42.95	-77.74	^{14}C AMS (bone, antler, tooth, tusk)	38490 ± 2600	Young and Burr (2006)
AA-33146 (2)	Genesee Valley	42.95	-77.74	^{14}C AMS (bone, antler, tooth, tusk)	38000 ± 2900	Young and Burr (2006)
AA-8639	Genesee Valley	42.95	-77.74	^{14}C AMS (bone, antler, tooth, tusk)	30285 ± 480	Young and Burr (2006)
CAMS-14611	Genesee Valley	42.95	-77.74	^{14}C AMS (bone, antler, tooth, tusk)	45800 ± 2800	Young and Burr (2006)
IBP02-2a	IBP02-2a	70.22	-69.09	cosmogenic exposure (^{10}Be)	34000 ± 900	Briner et al. (2006)
IBP02-1a (^{10}Be)	IBP02-1a (^{10}Be)	70.21	-69.07	cosmogenic exposure (^{10}Be)	32500 ± 1100	Briner et al. (2006)

Lab code	Site name	Lat	Long	Sample type	Reported age	Reference
CR03-88 (^{10}Be)	CR03-88 (^{10}Be)	69.88	-70.60	cosmogenic exposure (^{10}Be)	47800 ± 1200	Briner et al. (2006)
AL02-11 (^{10}Be)	AL02-11 (^{10}Be)	70.49	-69.66	cosmogenic exposure (^{10}Be)	50000 ± 1200	Briner et al. (2006)
CF02-179 (^{10}Be)	CF02-179 (^{10}Be)	70.44	-68.52	cosmogenic exposure (^{10}Be)	31500 ± 800	Briner et al. (2006)
CAD02-2 (^{10}Be)	CAD02-2 (^{10}Be)	69.89	-67.62	cosmogenic exposure (^{10}Be)	33200 ± 900	Briner et al. (2006)
CR03-13 (^{10}Be)	CR03-13 (^{10}Be)	69.74	-67.15	cosmogenic exposure (^{10}Be)	34200 ± 900	Briner et al. (2006)
IBP02-1a (^{26}Al)	IBP02-1a (^{26}Al)	70.21	-69.07	cosmogenic exposure (^{26}Al)	31800 ± 800	Briner et al. (2006)
CR03-88 (^{26}Al)	CR03-88 (^{26}Al)	69.88	-70.60	cosmogenic exposure (^{26}Al)	42800 ± 1300	Briner et al. (2006)
AL02-11 (^{26}Al)	AL02-11 (^{26}Al)	70.49	-69.66	cosmogenic exposure (^{26}Al)	50300 ± 1700	Briner et al. (2006)
CF02-114 (^{26}Al)	CF02-114 (^{26}Al)	70.35	-68.81	cosmogenic exposure (^{26}Al)	54000 ± 1300	Briner et al. (2006)
CF02-179 (^{26}Al)	CF02-179 (^{26}Al)	70.44	-68.52	cosmogenic exposure (^{26}Al)	30800 ± 1200	Briner et al. (2006)
CR03-26 (^{26}Al)	CR03-26 (^{26}Al)	69.53	-67.65	cosmogenic exposure (^{26}Al)	29500 ± 1200	Briner et al. (2006)
CR03-13 (^{26}Al)	CR03-13 (^{26}Al)	69.74	-67.15	cosmogenic exposure (^{26}Al)	37800 ± 1400	Briner et al. (2006)
Shfd02061	Tuktoyaktuk coastland	69.95	-129.73	luminescence (OSL)	43400 ± 2400	Bateman and Murton (2006)
RIDDL-801	Kendall Island	69.49	-135.28	^{14}C (carbonate)	48200 ± 1100	McNeely (2006)
SR-6086	Box Creek	47.79	-106.36	^{14}C (bone, antler, tooth, tusk)	33660 ± 620	Hill (2006)
TO-10545	Jean Lake	57.47	-113.75	^{14}C AMS (plants, seeds)	32690 ± 340	Paulen et al. (2005)
TO-3561	Brock Island	77.75	-113.80	^{14}C AMS (carbonate)	38270 ± 210	McNeely (2005)
TO-4246	Brock Island	77.75	-113.80	^{14}C AMS (carbonate)	34890 ± 420	McNeely (2005)
CF02-51	Kuvinilk River Basin	70.54	-69.93	cosmogenic exposure (^{10}Be)	30500 ± 1000	Briner et al. (2005)
CF02-88	80-m asl marine limit	70.74	-69.35	cosmogenic exposure (^{10}Be)	40700 ± 1000	Briner et al. (2005)
CF02-92	Eglinton region	70.70	-69.26	cosmogenic exposure (^{10}Be)	38700 ± 1000	Briner et al. (2005)
CF02-77	Eglinton region	70.75	-69.22	cosmogenic exposure (^{10}Be)	52600 ± 1400	Briner et al. (2005)
CF02-82	Eglinton region	70.78	-69.22	cosmogenic exposure (^{10}Be)	38900 ± 1000	Briner et al. (2005)
CF02-67	Eglinton region	70.73	-69.15	cosmogenic exposure (^{10}Be)	50900 ± 2400	Briner et al. (2005)
CF02-40	80-m asl marine limit	70.71	-69.15	cosmogenic exposure (^{10}Be)	40900 ± 1000	Briner et al. (2005)
CF02-163	Kuvinilk River Basin	70.44	-69.01	cosmogenic exposure (^{10}Be)	39300 ± 1000	Briner et al. (2005)
CF02-147	Kuvinilk River Basin	70.42	-68.99	cosmogenic exposure (^{10}Be)	42300 ± 1000	Briner et al. (2005)
CF02-153	Kuvinilk River Basin	70.47	-68.93	cosmogenic exposure (^{10}Be)	53200 ± 1500	Briner et al. (2005)
SIV6-00-2	Kuvinilk River Basin	70.36	-68.92	cosmogenic exposure (^{10}Be)	31800 ± 1000	Briner et al. (2005)

Lab code	Site name	Lat	Long	Sample type	Reported age	Reference
SIV6-00-1	Kuvinilk River Basin	70.36	-68.92	cosmogenic exposure (^{10}Be)	31400 ± 1000	Briner et al. (2005)
CF02-18	Kuvinilk River Basin	70.57	-68.88	cosmogenic exposure (^{10}Be)	44100 ± 1100	Briner et al. (2005)
AL3-01-1	Kuvinilk River Basin	70.52	-68.87	cosmogenic exposure (^{10}Be)	44800 ± 1100	Briner et al. (2005)
CF02-130	Kuvinilk River Basin	70.43	-68.85	cosmogenic exposure (^{10}Be)	38600 ± 1000	Briner et al. (2005)
CF2-01-2	Kuvinilk River Basin	70.53	-68.85	cosmogenic exposure (^{10}Be)	31700 ± 800	Briner et al. (2005)
CF02-115	Uplands adjacent to Patricia Bay	70.35	-68.81	cosmogenic exposure (^{10}Be)	39800 ± 1000	Briner et al. (2005)
CF02-15	Kuvinilk River Basin	70.55	-68.81	cosmogenic exposure (^{10}Be)	43500 ± 1200	Briner et al. (2005)
CF2-01-1	Kuvinilk River Basin	70.51	-68.80	cosmogenic exposure (^{10}Be)	35200 ± 1000	Briner et al. (2005)
CF02-14	Kuvinilk River Basin	70.55	-68.80	cosmogenic exposure (^{10}Be)	32300 ± 900	Briner et al. (2005)
CF02-13	Kuvinilk River Basin	70.55	-68.80	cosmogenic exposure (^{10}Be)	33900 ± 900	Briner et al. (2005)
CF1-01-1	Kuvinilk River Basin	70.56	-68.77	cosmogenic exposure (^{10}Be)	48600 ± 1500	Briner et al. (2005)
CF02-63	Kuvinilk River Basin	70.60	-68.76	cosmogenic exposure (^{10}Be)	42200 ± 1100	Briner et al. (2005)
CF02-22	Kuvinilk River Basin	70.53	-68.70	cosmogenic exposure (^{10}Be)	37700 ± 1000	Briner et al. (2005)
CF02-8	80-m asl marine limit	70.19	-68.61	cosmogenic exposure (^{10}Be)	42600 ± 1200	Briner et al. (2005)
CF02-7	Kuvinilk River Basin	70.55	-68.61	cosmogenic exposure (^{10}Be)	34700 ± 1100	Briner et al. (2005)
GX-28748	VB-01-09	42.26	-86.06	^{14}C (wood)	32480 ± 1850	Kehew et al. (2005)
GX-27991	well near to VB-01-09	42.25	-85.98	^{14}C (wood)	38390 (+2290, -1780)	Kehew et al. (2005)
AECV:1664c	Consolidated Pit 48	53.66	-113.26	^{14}C (bone, antler, tooth, tusk)	40000 ± 3070	Shapiro et al. (2004)
OxA-11613	Consolidated Pit 48	53.66	-113.26	^{14}C (bone, antler, tooth, tusk)	34050 ± 450	Shapiro et al. (2004)
OxA-11620	Consolidated Pit 48	53.66	-113.26	^{14}C (bone, antler, tooth, tusk)	53800 ± 2200	Shapiro et al. (2004)
OxA-12086	Consolidated Pit 48	53.66	-113.26	^{14}C (bone, antler, tooth, tusk)	60400 ± 2900	Shapiro et al. (2004)
AA43172	CR1-00-1	70.48	-69.58	^{14}C AMS (carbonate)	45800 ± 2400	Briner (2003); Dunhill et al. (2004)
AA45384	CI01011	70.29	-69.17	^{14}C AMS (carbonate)	28510 ± 390	Briner (2003); Dunhill et al. (2004)
AA45385	CR01-6a	70.52	-68.65	^{14}C AMS (carbonate)	39200 ± 1200	Briner (2003); Dunhill et al. (2004)
CAMS-66371	North Head of Richards Island	69.57	-134.50	^{14}C AMS (bone, antler, tooth, tusk)	41400 ± 1500	Harington (2003)
CAMS-66370	Near Inuvik	68.00	-134.00	^{14}C AMS (bone, antler, tooth, tusk)	39800 ± 1200	Harington (2003)

Lab code	Site name	Lat	Long	Sample type	Reported age	Reference
TO-2697	Liverpool Bay	69.61	-130.01	^{14}C AMS (bone, antler, tooth, tusk)	40100 ± 680	Harington (2003)
Beta-115201	Near Edmonton	53.60	-113.33	^{14}C AMS (bone, antler, tooth, tusk)	43100 ± 490	Harington (2003)
TO-3714	Riviere Verte	47.77	-69.48	^{14}C AMS (bone, antler, tooth, tusk)	40640 ± 420	Harington (2003)
NSRL13213	CI01-11	70.29	-69.17	^{14}C (carbonate)	34120 ± 170	Briner (2003); Dunhill et al. (2004)
GSC-1475 outer	Kwataboahegan Marine	51.14	-82.12	^{14}C Conv. (carbonate)	38600 ± 2000	McNeely (2002)
TO-1892	Attawapiskat Marine	52.35	-86.25	^{14}C AMS (carbonate)	30790 ± 230	McNeely (2002)
TO-1893	Attawapiskat Marine	52.35	-86.25	^{14}C AMS (carbonate)	33480 ± 310	McNeely (2002)
TO-1894	Attawapiskat Marine	52.35	-86.25	^{14}C AMS (carbonate)	29210 ± 220	McNeely (2002)
TO-2501	Attawapiskat Marine	52.35	-86.25	^{14}C AMS (carbonate)	38530 ± 460	McNeely (2002)
TO-2502	Attawapiskat Marine	52.35	-86.25	^{14}C AMS (carbonate)	35930 ± 460	McNeely (2002)
TO-2503	Kwataboahegan Marine	51.14	-82.12	^{14}C AMS (carbonate)	48260 ± 1090	McNeely (2002)
S-3605	Lancer thrust moraine	50.77	-108.70	^{14}C Conv. (wood)	31300 ± 1400	Morlan et al. (2001)
S-1369	Dalmeny	52.29	-106.71	^{14}C Conv. (wood)	30920 ± 2060	Morlan et al. (2001)
S-96	Outram	49.18	-103.32	^{14}C Conv. (wood)	27750 ± 1200	Morlan et al. (2001)
S-554	Marieval VI	50.58	-102.65	^{14}C Conv. (wood)	28890 ± 310	Morlan et al. (2001)
S-267	Marsden	52.81	-109.82	^{14}C Conv. (peat)	33000 ± 2000	Morlan et al. (2001)
S-251	Wandsworth	52.89	-106.62	^{14}C Conv. (organic-rich sediment)	34000 ± 1800	Morlan et al. (2001)
S-252	Alvena	52.61	-106.05	^{14}C Conv. (organic-rich sediment)	33500 ± 2000	Morlan et al. (2001)
S-423	Fort Qu'Appelle VI	50.77	-103.80	^{14}C Conv. (organic-rich sediment)	28900 ± 1050	Morlan et al. (2001)
S-563	Kahkewistahaw IV	50.53	-102.53	^{14}C Conv. (organic-rich sediment)	28445 ± 1595	Morlan et al. (2001)
S-559	Ochapowace	50.52	-102.30	^{14}C Conv. (organic-rich sediment)	28915 ± 1140	Morlan et al. (2001)
GSC-1342	Runnymede	51.50	-101.70	^{14}C Conv. (organic-rich sediment)	30000 ± 490	Morlan et al. (2001)
CAMS-44450	Fog Lake	67.18	-63.25	^{14}C AMS (organic-rich sediment)	39150 ± 520	Wolfe et al. (2000)
CAMS-44451	Fog Lake	67.18	-63.25	^{14}C AMS (organic-rich sediment)	38600 ± 520	Wolfe et al. (2000)
Beta-111710	Cornwall Island site 11	77.60	-95.87	^{14}C AMS (carbonate)	35750 ± 490	Lamoureux and England (2000)
Beta-111708	Cornwall Island site 10	77.58	-95.18	^{14}C AMS (carbonate)	35820 ± 540	Lamoureux and England (2000)
AA-23580	Cornwall Island site 9	77.67	-94.93	^{14}C AMS (carbonate)	43110 ± 1870	Lamoureux and England (2000)
AA-23577	Cornwall Island site 7	77.75	-94.78	^{14}C AMS (carbonate)	37280 ± 1000	Lamoureux and England (2000)
TO-5616	Cormwall Island site 8	77.70	-94.67	^{14}C AMS (carbonate)	30710 ± 350	Lamoureux and England (2000)

Lab code	Site name	Lat	Long	Sample type	Reported age	Reference
TO-5600	Baumann Fiord	78.15	-87.77	^{14}C AMS (carbonate)	36910 ± 410	Ó'Cofaigh et al. (2000)
TO-5615	Baumann Fiord	78.15	-87.77	^{14}C AMS (carbonate)	36160 ± 430	Ó'Cofaigh et al. (2000)
TO-5602	Bear Corner	78.17	-87.40	^{14}C AMS (carbonate)	35310 ± 400	Ó'Cofaigh et al. (2000)
AA-23585	Stor Island	78.97	-86.28	^{14}C AMS (carbonate)	46850 ± 2800	Ó'Cofaigh et al. (2000)
AA-27489	Stor Island	78.97	-86.28	^{14}C AMS (carbonate)	47790 ± 3500	Ó'Cofaigh et al. (2000)
AA-23607	Bay Fiord 1and2	78.90	-85.00	^{14}C AMS (carbonate)	37130 ± 1000	Ó'Cofaigh et al. (2000)
AA-23608	Bay Fiord 1and2	78.90	-85.00	^{14}C AMS (carbonate)	33030 ± 610	Ó'Cofaigh et al. (2000)
AA-23609	Bay Fiord 1and2	78.90	-85.00	^{14}C AMS (carbonate)	38490 ± 1100	Ó'Cofaigh et al. (2000)
AA-23601	Bay Fiord 4	78.85	-84.55	^{14}C AMS (carbonate)	34830 ± 850	Ó'Cofaigh et al. (2000)
AA-23602	Bay Fiord 4	78.85	-84.55	^{14}C AMS (carbonate)	30930 ± 420	Ó'Cofaigh et al. (2000)
AA-23603	Bay Fiord 4	78.85	-84.55	^{14}C AMS (carbonate)	35510 ± 730	Ó'Cofaigh et al. (2000)
AA-23604	Bay Fiord 4	78.85	-84.55	^{14}C AMS (carbonate)	41690 ± 1700	Ó'Cofaigh et al. (2000)
AA-23605	Bay Fiord 3	78.85	-84.53	^{14}C AMS (carbonate)	27380 ± 360	Ó'Cofaigh et al. (2000)
AA-23606	Bay Fiord 3	78.85	-84.53	^{14}C AMS (carbonate)	37910 ± 960	Ó'Cofaigh et al. (2000)
Beta-119911	Knud Peninsula	79.15	-76.92	^{14}C AMS (carbonate)	33310 ± 400	England et al. (2000)
TO-5607	Thorvald Peninsula	79.02	-76.55	^{14}C AMS (carbonate)	32040 ± 310	England et al. (2000)
TO-5611	Cook Peninsula	79.53	-76.32	^{14}C AMS (carbonate)	33800 ± 410	England et al. (2000)
TO-5614	Copes Bay	79.50	-76.28	^{14}C AMS (carbonate)	36940 ± 460	England et al. (2000)
Beta-119910	Cook Peninsula	79.43	-76.27	^{14}C AMS (carbonate)	43100 ± 910	England et al. (2000)
TO-5593	Cook Peninsula	79.52	-76.27	^{14}C AMS (carbonate)	39060 ± 550	England et al. (2000)
Beta-119909	Koldewey Point	79.10	-75.73	^{14}C AMS (carbonate)	38070 ± 760	England et al. (2000)
Beta-111702	Bache Peninsula	79.02	-74.57	^{14}C AMS (carbonate)	36570 ± 530	England et al. (2000)
GSC-6194	Viks Fiord	75.89	-90.24	^{14}C Conv. (carbonate)	39900 ± 1800	Dyke (1999)
TO-4205	Lake Hazen	81.90	-69.78	^{14}C AMS (plants, seeds)	37260 ± 470	Smith (1999)
TO-3488	Lake Hazen	81.95	-68.92	^{14}C AMS (plants, seeds)	43510 ± 690	Smith (1999)
AA-7591	Robinson Lake	63.40	-64.26	^{14}C AMS (plants, seeds)	29170 ± 420	Miller et al. (1999)
AA-7592	Robinson Lake	63.40	-64.26	^{14}C AMS (plants, seeds)	38050 ± 1100	Miller et al. (1999)
AA-7839	Robinson Lake	63.40	-64.26	^{14}C AMS (plants, seeds)	38000 ± 1100	Miller et al. (1999)
AA-7844	Robinson Lake	63.40	-64.26	^{14}C AMS (plants, seeds)	43140 ± 2000	Miller et al. (1999)
AA-8568	Robinson Lake	63.40	-64.26	^{14}C AMS (plants, seeds)	42700 ± 2000	Miller et al. (1999)
AA-8891	Robinson Lake	63.40	-64.26	^{14}C AMS (plants, seeds)	38540 ± 1200	Miller et al. (1999)
AA-8892	Robinson Lake	63.40	-64.26	^{14}C AMS (other organic material)	30050 ± 435	Miller et al. (1999)
AA-8995	Robinson Lake	63.40	-64.26	^{14}C AMS (other organic material)	43600 ± 1200	Miller et al. (1999)
AA-9009	Robinson Lake	63.40	-64.26	^{14}C AMS (other organic material)	32200 ± 620	Miller et al. (1999)

Lab code	Site name	Lat	Long	Sample type	Reported age	Reference
CAMS-22178	Robinson Lake	63.40	-64.26	^{14}C AMS (other organic material)	43030 ± 1420	Miller et al. (1999)
CAMS-7782	Robinson Lake	63.40	-64.26	^{14}C AMS (other organic material)	37770 ± 1360	Miller et al. (1999)
TO-4879	Croker Bay	74.61	-83.63	^{14}C AMS (carbonate)	27240 ± 270	Dyke (1999)
TO-4196	Franklin Pierce Nay	79.40	-74.83	^{14}C AMS (carbonate)	27270 ± 510	England (1999)
TO-454	Hall Land	81.77	-59.30	^{14}C AMS (carbonate)	30390 ± 300	England (1999)
TO-782	Schowalter	51.55	-112.34	^{14}C AMS (bone, antler, tooth, tusk)	28000 ± 250	Young et al. (1999)
TO-1142	Winter 1	51.57	-112.33	^{14}C AMS (bone, antler, tooth, tusk)	33650 ± 340	Young et al. (1999)
TO-1304	Winter 1	51.57	-112.33	^{14}C AMS (bone, antler, tooth, tusk)	29610 ± 220	Young et al. (1999)
TO-871	Courtney W.	51.52	-112.32	^{14}C AMS (bone, antler, tooth, tusk)	33450 ± 350	Young et al. (1999)
CM24	CM24	65.13	-65.01	cosmogenic exposure (^{10}Be)	36340 ± 2350	Kaplan (1999)
CM13 (^{10}Be)	CM13 (^{10}Be)	65.05	-64.12	cosmogenic exposure (^{10}Be)	54350 ± 3220	Kaplan (1999)
CM40 (^{10}Be)	CM40 (^{10}Be)	65.06	-63.96	cosmogenic exposure (^{10}Be)	38090 ± 2760	Kaplan (1999)
CM66	CM66	65.00	-63.82	cosmogenic exposure (^{10}Be)	44440 ± 2670	Kaplan (1999)
CM13 (^{26}Al)	CM13 (^{26}Al)	65.05	-64.12	cosmogenic exposure (^{26}Al)	45470 ± 3000	Kaplan (1999)
CM40 (^{26}Al)	CM40 (^{26}Al)	65.06	-63.96	cosmogenic exposure (^{26}Al)	34610 ± 2250	Kaplan (1999)
CAMS-30537	Fog Lake	67.18	-63.25	^{14}C AMS (plants, seeds)	32300 ± 470	Steig et al. (1998); Wolfe et al. (2000)
CAMS-28655	Gnarly Lake	67.20	-63.04	^{14}C AMS (plants, seeds)	44600 ± 1500	Steig et al. (1998)
CAMS-30538	Saddle Lake	67.07	-62.70	^{14}C AMS (plants, seeds)	52300 ± 3900	Steig et al. (1998)
CAMS-31807	Fog Lake	67.18	-63.25	^{14}C AMS (organic-rich sediment)	34790 ± 510	Steig et al. (1998); Wolfe et al. (2000)
CAMS-34301	Fog Lake	67.18	-63.25	^{14}C AMS (organic-rich sediment)	36020 ± 450	Steig et al. (1998); Wolfe et al. (2000)
TO-2354	Site 57	80.34	-87.88	^{14}C AMS (carbonate)	36570 ± 430	Bednarski (1998)
TO-2282	Site 56	80.38	-87.62	^{14}C AMS (carbonate)	45040 ± 840	Bednarski (1998)
TO-2283	Site 55	80.38	-87.60	^{14}C AMS (carbonate)	46200 ± 950	Bednarski (1998)
96B1-1 (10Be age)	Mitten Peninsula location 3	67.17	-63.27	cosmogenic exposure (^{10}Be)	35600	Steig et al. (1998)
96B1-2 (10Be age)	Mitten Peninsula location 3	67.17	-63.27	cosmogenic exposure (^{10}Be)	36300	Steig et al. (1998)
96B3-1 (10Be age)	Mitten Peninsula location 4	67.16	-63.16	cosmogenic exposure (^{10}Be)	51900	Steig et al. (1998)
96B1-1 (26Al age)	Mitten Peninsula location 3	67.17	-63.27	Cosmogenic exposure (^{26}Al)	34200	Steig et al. (1998)
96B1-2 (26Al age)	Mitten Peninsula location 3	67.17	-63.27	Cosmogenic exposure (^{26}Al)	36700	Steig et al. (1998)

Lab code	Site name	Lat	Long	Sample type	Reported age	Reference
96B3-1 (26Al age)	Mitten Peninsula location 4	67.16	-63.16	Cosmogenic exposure (^{26}Al)	52100	Steig et al. (1998)
Beta-74434	Richards Island	69.53	-134.00	^{14}C AMS (plants, seeds)	33710 ± 460	Dallimore et al. (1997)
Beta-74433	Richards Island	69.53	-134.00	^{14}C AMS (other organic material)	37400 ± 810	Dallimore et al. (1997)
unknown (not given	Port Huron	43.05	-82.61	luminescence (TL)	57000 ± 900	Karrow et al. (1997)
OS-3468	Lake 9	46.42	-68.05	^{14}C (wood)	41200 ± 1400	Dorion (1997)
GSC-5663	Dobbin Bay	79.78	-74.90	^{14}C Conv. (carbonate)	31400 ± 900	England (1996); McNeely (2006)
GSC-5722	Scoresby Bay	79.88	-71.48	^{14}C Conv. (carbonate)	30900 ± 950	England (1996); McNeely (2006)
CAMS-20185	Titusville	41.62	-79.64	^{14}C AMS (wood)	39070 ± 960	Cong et al. (1996)
TO-3241	Ukalik Lake	66.27	-65.75	^{14}C AMS (plants, seeds)	37990 ± 410	Wolfe and Härting (1996)
TO-3242	Tuligak Lake	66.28	-65.72	^{14}C AMS (plants, seeds)	36120 ± 340	Wolfe and Härting (1996)
CAMS-20895	Titusville	41.62	-79.64	^{14}C AMS (insect)	38900 ± 3200	Cong et al. (1996)
TO-4176	Franklin Pierce Bay	79.40	-74.83	^{14}C AMS (carbonate)	27270 ± 510	England (1996)
TO-4188	Dobbin Bay	79.87	-73.80	^{14}C AMS (carbonate)	42620 ± 660	England (1996)
AA-10232	Wales Island	61.87	-72.07	^{14}C AMS (carbonate)	38700 ± 1200	Manley and Jennings (1996)
TO-4204	Radmore Harbour	80.52	-70.63	^{14}C AMS (carbonate)	28160 ± 970	England (1996)
AA-12606	Ashe Inlet	62.60	-70.54	^{14}C AMS (carbonate)	37760 ± 1050	Manley and Jennings (1996)
AA-12605	Ashe Inlet 2	62.60	-70.54	^{14}C AMS (carbonate)	43750 ± 2100	Manley and Jennings (1996)
AA-7899	Bosanquet Harbour	62.63	-70.48	^{14}C AMS (carbonate)	34790 ± 710	Manley and Jennings (1996)
TO-3476	Kane Basin	80.22	-70.12	^{14}C AMS (carbonate)	39900 ± 530	England (1996)
TO-3768	Kane Basin	80.22	-70.12	^{14}C AMS (carbonate)	34190 ± 350	England (1996)
TO-3478	Kane Basin	80.22	-70.05	^{14}C AMS (carbonate)	38120 ± 450	England (1996)
TO-3479	Kane Basin	80.22	-70.05	^{14}C AMS (carbonate)	37560 ± 430	England (1996)
TO-3480	Kane Basin	80.22	-70.05	^{14}C AMS (carbonate)	44630 ± 800	England (1996)
TO-3481	Kane Basin	80.22	-70.05	^{14}C AMS (carbonate)	49000 ± 1070	England (1996)
Beta-54140	Saguenay	48.14	-69.68	^{14}C AMS (carbonate)	29280 ± 680	Dionne and Occhietti (1996)
TO-3990	Saguenay	48.14	-69.68	^{14}C AMS (carbonate)	34510 ± 380	Dionne and Occhietti (1996)
TO-3483	Rawlings Bay	80.35	-69.58	^{14}C AMS (carbonate)	27030 ± 210	England (1996)
TO-3484	Rawlings Bay	80.35	-69.57	^{14}C AMS (carbonate)	39470 ± 510	England (1996)
AA-10252	Balcom Inlet	62.33	-68.66	^{14}C AMS (carbonate)	30790 ± 450	Manley and Jennings (1996)
TO-2921	Valley D-4	80.70	-68.48	^{14}C AMS (carbonate)	26520 ± 170	England (1996)
AA-11452	Gary Goose Islands	62.26	-68.38	^{14}C AMS (carbonate)	39145 ± 1180	Manley and Jennings (1996)
AA-11453	Wight Inlet 2	62.24	-68.33	^{14}C AMS (carbonate)	40760 ± 1450	Manley and Jennings (1996)
AA-11451	Wight Inlet	62.23	-68.23	^{14}C AMS (carbonate)	35280 ± 760	Manley and Jennings (1996)

Lab code	Site name	Lat	Long	Sample type	Reported age	Reference
AA-12608	Saddleback Island	62.16	-67.95	^{14}C AMS (carbonate)	34820 ± 730	Manley and Jennings (1996)
AA-11450	Bond Inlet site 2	62.21	-67.88	^{14}C AMS (carbonate)	31065 ± 455	Manley and Jennings (1996)
AA-10646	Bond Inlet site	62.17	-67.74	^{14}C AMS (carbonate)	34710 ± 690	Manley and Jennings (1996)
TO-2916	Panikpah River	81.03	-66.67	^{14}C AMS (carbonate)	29010 ± 280	England (1996)
AA-14027	South Reefs	61.91	-66.31	^{14}C AMS (carbonate)	38620 ± 1110	Manley and Jennings (1996)
TO-2912	Daly River	81.23	-65.87	^{14}C AMS (carbonate)	41990 ± 580	England (1996)
PITT-0928	Glendale daycare center, site 41	39.50	-84.57	^{14}C Conv. (wood)	35550 ± 880	Lowell (1995)
PITT-0929	Glendale daycare center, site 41	39.50	-84.57	^{14}C Conv. (wood)	39830 ± 1450	Lowell (1995)
TO-2693	Dinosaur Provincial Park	50.77	-111.48	^{14}C AMS (plants, seeds)	52450 ± 1910	Evans and Campbell (1995)
TO-663	Site 2	80.73	-87.80	^{14}C AMS (carbonate)	37130 ± 430	Bednarski (1995)
TO-420	Site 1	81.07	-87.42	^{14}C AMS (carbonate)	38010 ± 590	Bednarski (1995)
TO-421	Site 1	81.07	-87.42	^{14}C AMS (carbonate)	34800 ± 400	Bednarski (1995)
TO-661	Site 1	81.07	-87.42	^{14}C AMS (carbonate)	35020 ± 640	Bednarski (1995)
TO-4639	Turtle Mountain	49.10	-100.28	^{14}C AMS (bone, antler, tooth, tusk)	33860 ± 330	Fulton (1995)
S-2650	Site 4	81.08	-87.23	^{14}C (carbonate)	30250 ± 1100	Bednarski (1995)
WCSD	Woodbridge	43.76	-79.59	luminescence (TL)	45900 ± 9000	Berger and Eyles (1994)
DVSF-10a	Don Valley Brickyard	43.69	-79.36	luminescence (TL)	59800 ± 8500	Berger and Eyles (1994)
DVSF-10b	Don Valley Brickyard	43.69	-79.36	luminescence (TL)	54100 ± 8200	Berger and Eyles (1994)
SPSD84-1	Sylvan Park	43.73	-79.21	luminescence (TL)	41200 ± 8000	Berger and Eyles (1994)
AECV:1580c	Consolidated Pit 45	53.70	-114.05	^{14}C (wood)	41400 ± 3990	Young et al. (1994)
AECV:1581c	Consolidated Pit 45	53.70	-114.05	^{14}C (wood)	35500 ± 2530	Young et al. (1994)
AECV:1582c	Consolidated Pit 45	53.70	-114.05	^{14}C (wood)	35760 ± 2130	Young et al. (1994)
AECV:1583c	Consolidated Pit 45	53.70	-114.05	^{14}C (wood)	41110 ± 3750	Young et al. (1994)
AECV:1658c	Consolidated Pit 45	53.70	-114.05	^{14}C (wood)	42910 ± 3940	Young et al. (1994)
AECV:1465c	Consolidated Pit 48	53.66	-113.26	^{14}C (wood)	37800 ± 2060	Young et al. (1994)
AECV:920c	Consolidated Pit 48	53.66	-113.26	^{14}C (wood)	40670 ± 4130	Young et al. (1994)
AECV:921c	Consolidated Pit 48	53.66	-113.26	^{14}C (wood)	37500 ± 2650	Young et al. (1994)
AECV:599c	Consolidated Pit 46	53.82	-114.56	^{14}C (bone, antler, tooth, tusk)	27730 ± 1060	Young et al. (1994)
AECV:718c	Consolidated Pit 46	53.82	-114.56	^{14}C (bone, antler, tooth, tusk)	39960 ± 3950	Young et al. (1994)

Lab code	Site name	Lat	Long	Sample type	Reported age	Reference
TO:1828	Consolidated Pit 46	53.82	-114.56	^{14}C (bone, antler, tooth, tusk)	31520 ± 450	Young et al. (1994)
AECV:612c	Apex Pit	53.63	-113.32	^{14}C (bone, antler, tooth, tusk)	28890 ± 960	Young et al. (1994)
AECV:720c	Apex Pit	53.63	-113.32	^{14}C (bone, antler, tooth, tusk)	29380 ± 4970	Young et al. (1994)
AECV:721c	Apex Pit	53.63	-113.32	^{14}C (bone, antler, tooth, tusk)	27860 ± 880	Young et al. (1994)
AECV:1202c	Clover Bar	53.59	-113.32	^{14}C (bone, antler, tooth, tusk)	31220 ± 1260	Young et al. (1994)
AECV:1478c	Consolidated Riverview	53.66	-113.28	^{14}C (bone, antler, tooth, tusk)	36900 ± 2030	Young et al. (1994)
AECV:941c	Consolidated Riverview	53.66	-113.28	^{14}C (bone, antler, tooth, tusk)	31290 ± 1960	Young et al. (1994)
AECV:1102c	Consolidated Pit 48	53.66	-113.26	^{14}C (bone, antler, tooth, tusk)	26750 ± 790	Young et al. (1994)
AECV:934c	Consolidated Pit 48	53.66	-113.26	^{14}C (bone, antler, tooth, tusk)	37120 ± 2370	Young et al. (1994)
AECV:935c	Consolidated Pit 48	53.66	-113.26	^{14}C (bone, antler, tooth, tusk)	38960 ± 3520	Young et al. (1994)
AECV:936c	Consolidated Pit 48	53.66	-113.26	^{14}C (bone, antler, tooth, tusk)	31750 ± 1460	Young et al. (1994)
AECV:937c	Consolidated Pit 48	53.66	-113.26	^{14}C (bone, antler, tooth, tusk)	27520 ± 850	Young et al. (1994)
AECV:938c	Consolidated Pit 48	53.66	-113.26	^{14}C (bone, antler, tooth, tusk)	35840 ± 2370	Young et al. (1994)
AECV:940c	Consolidated Pit 48	53.66	-113.26	^{14}C (bone, antler, tooth, tusk)	36150 ± 2960	Young et al. (1994)
TO-195	Little Bear River	64.13	-126.72	^{14}C AMS (wood)	44420 ± 630	Hughes et al. (1993)
TO-113	Makinson Inlet	77.23	-81.94	^{14}C AMS (wood)	41260 ± 400	Blake (1993)
TO-480	Cape Alfred Ernest	82.38	-85.58	^{14}C AMS (carbonate)	32111 ± 370	Evans and Mott (1993)
GSC-4760	Stuartburn	49.16	-96.72	^{14}C Conv. (wood)	35500 ± 870	McNeely and Jorgensen (1992)
GSC-4710	Lennie Harbour	72.28	-125.64	^{14}C Conv. (carbonate)	34200 ± 1400	McNeely and Jorgensen (1992)
GSC-4793	Nansen Sound	80.70	-90.75	^{14}C Conv. (carbonate)	38500 ± 1320	McNeely and Jorgensen (1992); Bednarski (1998)
GSC-4645	Hall Land	81.77	-59.10	^{14}C Conv. (carbonate)	39200 ± 1450	McNeely and Jorgensen (1992)
TO-1192	Mackenzie River site 19	65.23	-126.93	^{14}C AMS (wood)	27170 ± 250	Smith (1992)
TO-1188	Mackenzie River site 22	64.59	-125.03	^{14}C AMS (wood)	27260 ± 260	Smith (1992)
TO-1187	Mackenzie River site 23	64.56	-124.89	^{14}C AMS (wood)	45570 ± 700	Smith (1992)
TO-1186	Mackenzie River site 24	64.52	-124.89	^{14}C AMS (wood)	52130 ± 1310	Smith (1992)
TO-2242	Black Top Ridge	80.25	-84.65	^{14}C AMS (wood)	44420 ± 840	Bell (1992, 1996)
TO-485	Cape Alfred Ernest	82.38	-85.58	^{14}C AMS (peat)	39270 ± 640	McNeely and Jorgensen (1992)

Lab code	Site name	Lat	Long	Sample type	Reported age	Reference
TO-2206	Worth Point (II)	72.18	-125.66	^{14}C AMS (carbonate)	41090 ± 770	McNeely and Jorgensen (1992); Evans and Mott (1993)
TO-1464	Dinosaur Provincial Park	50.77	-111.48	^{14}C AMS (carbonate)	27420 ± 240	Evans and Campbell (1992)
TO-2228	Iceberg Point lowland	80.25	-86.32	^{14}C AMS (carbonate)	45850 ± 980	Bell (1992)
AA-2224	Bond Inlet	62.22	-67.72	^{14}C AMS (carbonate)	39000 ± 1800	Kaufman and Williams (1992)
AA-2348	Pritzler Harbour	62.08	-67.25	^{14}C AMS (carbonate)	43000 ± 3000	Kaufman and Williams (1992)
AA-6298	Sister Islets	62.02	-66.91	^{14}C AMS (carbonate)	35685 ± 805	Kaufman and Williams (1992)
AA-4244A	Nanook Harbour	61.96	-66.62	^{14}C AMS (carbonate)	37090 ± 1100	Kaufman and Williams (1992)
AA-4244B	Nanook Harbour	61.96	-66.62	^{14}C AMS (carbonate)	40630 ± 1400	Kaufman and Williams (1992)
AA-6304	Inner Cyrus Field Bay	62.97	-65.25	^{14}C AMS (carbonate)	43450 ± 2100	Kaufman and Williams (1992)
AA-7557	Beare Sound	62.50	-64.83	^{14}C AMS (carbonate)	40950 ± 2100	Kaufman and Williams (1992)
TO-2294	Worth Point (III)	72.18	-125.66	^{14}C AMS (bone, antler, tooth, tusk)	41910 ± 800	McNeely and Jorgensen (1992)
AECV-918C	Mackenzie River site 25	64.49	-124.87	^{14}C (wood)	34020 ± 1410	Smith (1992)
AECV-919C	Mackenzie River site 20	64.67	-124.86	^{14}C (wood)	34730 ± 3280	Smith (1992)
TO-2196	Pangnirtung Ice-cored moraine	66.15	-65.72	^{14}C (carbonate)	52460 ± 1430	Kaufman and Williams (1992)
GX-16635	Cyrus Field Lake	63.18	-65.53	^{14}C (carbonate)	30600 ± 1900	Kaufman and Williams (1992)
GSC-3848 HP	Addington Forks	45.57	-62.10	^{14}C Conv. (wood)	36100 ± 520	McNeely and McCuaig (1991)
GSC-4218	Strubel Lake	52.20	-115.00	^{14}C Conv. (organic-rich sediment)	29700 ± 1260	McNeely and McCuaig (1991)
GSC-4640 HP	Millerand	47.22	-61.85	^{14}C Conv. (organic-rich sediment)	39000 ± 500	McNeely and McCuaig (1991); McNeely and Jorgensen (1992)
GSC-4322	Cape Richard	72.92	-102.42	^{14}C Conv. (carbonate)	39300 ± 1900	McNeely and McCuaig (1991)
GSC-4189	Delabarre Bay	59.03	-63.27	^{14}C Conv. (carbonate)	37800 ± 1610	McNeely and McCuaig (1991)
GSC-4204 IF	Delabarre Bay	59.03	-63.27	^{14}C Conv. (carbonate)	40600 ± 1640	McNeely and McCuaig (1991)
GSC-4204 OF	Delabarre Bay	59.03	-63.27	^{14}C Conv. (carbonate)	38900 ± 1420	McNeely and McCuaig (1991)
GSC-4633 HP	Portage-du-Cap	47.23	-61.90	^{14}C Conv. (carbonate)	42900 ± 720	McNeely and McCuaig (1991)
GSC-4563	Fiods Cove	48.51	-58.96	^{14}C Conv. (carbonate)	26600 ± 550	McNeely and McCuaig (1991)
Beta-21591	Ottawa County	42.94	-86.09	^{14}C AMS (unknown)	35520 ± 940	Rieck et al. (1991)

Lab code	Site name	Lat	Long	Sample type	Reported age	Reference
Beta-21590	Newaygo County	43.54	-85.78	^{14}C AMS (unknown)	36120 ± 620	Rieck et al. (1991)
Beta-31046	Newaygo County	43.54	-85.78	^{14}C AMS (unknown)	34340 ± 520	Rieck et al. (1991)
GSC-4635	Canon Fiord	80.20	-81.61	^{14}C Conv. (other organic material)	38200 ± 1510	England (1990); McNeely and Jorgensen (1992)
TO-1198	South Bay	79.55	-81.80	^{14}C AMS (carbonate)	29380 ± 230	Sloan (1990)
TO-1200	South Bay	79.55	-81.80	^{14}C AMS (carbonate)	38100 ± 380	Sloan (1990)
TO-1201	South Bay	79.55	-81.80	^{14}C AMS (carbonate)	34950 ± 340	Sloan (1990)
EKN-3	Leslie Creek	56.42	-94.24	luminescence (TL)	34000 ± 5000	Berger and Nielsen (1990)
EKN-5	Henday	56.46	-94.15	luminescence (TL)	32000 ± 2000	Berger and Nielsen (1990)
EKN-8	Flamborough	57.03	-92.64	luminescence (TL)	46000 ± 4000	Berger and Nielsen (1990)
EKN-7	Port Nelson	57.13	-92.53	luminescence (TL)	38000 ± 3000	Berger and Nielsen (1990)
TO-449	Outer Greely	80.60	-81.92	^{14}C (plants, seeds)	33300 ± 700	England (1990)
TO-1284	Outer Canon	80.17	-82.83	^{14}C (carbonate)	38010 ± 410	England (1990)
TO-1283	Outer Greely	80.37	-81.93	^{14}C (carbonate)	38070 ± 410	England (1990)
WAT-1378	Beaver	55.92	-88.32	^{14}C Conv. (peat)	37400 ± 1600	Wyatt (1989)
UA-2400	Simonette	55.08	-118.17	^{14}C (wood)	37010 ± 2690	Liverman et al. (1989)
UA-2398	Watino	55.72	-117.63	^{14}C (wood)	36220 ± 2520	Liverman et al. (1989)
UA-2399	Watino	55.72	-117.63	^{14}C (wood)	31530 ± 1440	Liverman et al. (1989)
TO-492	Disraeli Fiord	82.60	-73.22	^{14}C (other organic material)	31360 ± 400	Lemmen (1989)
GX-13720	Feachem Lake 3	71.92	-74.40	^{14}C (carbonate)	45600 (+4100, -2700)	Andrews et al. (1989)
TO-500	Disraeli Fiord	82.83	-73.82	^{14}C (carbonate)	30440 ± 330	Lemmen (1989)
GSC-2687	Glacier 7A-45 series (III)	77.83	-84.75	^{14}C Conv. (wood)	32500 ± 1580	Blake (1988)
GSC-3364	Glacier 7A-45 series (III)	77.83	-84.75	^{14}C Conv. (wood)	31100 ± 480	Blake (1988)
GSC-3049	Goodsir Inlet	75.67	-97.68	^{14}C Conv. (organic-rich sediment)	38500 ± 1370	Blake (1988)
GSC-4491 HP	Timmins	48.65	-81.12	^{14}C Conv. (organic-rich sediment)	41400 ± 720	DiLabio et al. (1988); McNeely and McCuaig (1991)
GSC-1409	Cape Storm series (VIII)	76.39	-87.60	^{14}C Conv. (carbonate)	27700 ± 480	Blake (1988)
GSC-1880	Cape Storm series (VIII)	76.39	-87.60	^{14}C Conv. (carbonate)	38300 ± 1360	Blake (1988)
GSC-2310	Cape Storm series (VIII)	76.39	-87.60	^{14}C Conv. (carbonate)	42500 ± 1900	Blake (1988)
GSC-2485 (inner)	Cape Storm series (VIII)	76.39	-87.60	^{14}C Conv. (carbonate)	40500 ± 740	Blake (1988)
GSC-2485 (middle)	Cape Storm series (VIII)	76.39	-87.60	^{14}C Conv. (carbonate)	41400 ± 820	Blake (1988)
GSC-2485 (outer)	Cape Storm series (VIII)	76.39	-87.60	^{14}C Conv. (carbonate)	42400 ± 920	Blake (1988)
GSC-2486	Cape Storm series (VIII)	76.39	-87.60	^{14}C Conv. (carbonate)	31700 ± 540	Blake (1988)

Lab code	Site name	Lat	Long	Sample type	Reported age	Reference
GSC-2800	Cape Storm series (VIII)	76.39	-87.60	^{14}C Conv. (carbonate)	40800 ± 1350	Blake (1988)
GSC-1098	Coburg Island Series	75.88	-79.03	^{14}C Conv. (carbonate)	33600 ± 700	Blake (1988)
GSC-1536 (inner)	Coburg Island Series	75.88	-79.03	^{14}C Conv. (carbonate)	39500 ± 1300	Blake (1988)
GSC-1536 (outer)	Coburg Island Series	75.88	-79.03	^{14}C Conv. (carbonate)	38200 ± 1400	Blake (1988)
GSC-1617 (inner)	Coburg Island Series	75.88	-79.03	^{14}C Conv. (carbonate)	46400 ± 2000	Blake (1988)
GSC-1926 (inner)	Coburg Island Series	75.88	-79.03	^{14}C Conv. (carbonate)	43700 ± 800	Blake (1988)
GSC-1926 (outer)	Coburg Island Series	75.88	-79.03	^{14}C Conv. (carbonate)	41100 ± 600	Blake (1988)
GSC-4310	Cadogan Inlet	78.23	-75.78	^{14}C Conv. (carbonate)	31600 ± 1120	Blake (1988)
GSC-2229	Cape Storm series IX	76.40	-87.57	^{14}C Conv. (bone, antler, tooth, tusk)	28700 ± 1110	Blake (1988)
Beta-9046	Kalkasa	44.73	-85.24	^{14}C (wood)	34200 ± 1320	Winters et al. (1986); Winters et al. (1988); Winters and Rieck (1991)
Beta-9273	Kalkasa	44.73	-85.24	^{14}C (wood)	36300 ± 2450	Winters and Rieck 1991;Winters et al 1986; Winters et al 1988
SI-4519	Upper South Branch Pond	46.08	-68.90	^{14}C (wood)	29200 ± 550	Anderson et al. (1988)
Beta-17891	Kalamazoo	42.25	-85.58	^{14}C (unknown)	33810 ± 750	Winters et al. (1988)
GSC-222-2	Nelson Head	76.14	-122.70	^{14}C Conv. (wood)	47000 ± 1000	Blake (1987)
GSC-3427	Webber Glacier	80.88	-82.25	^{14}C Conv. (wood)	38200 ± 1240	Blake (1987)
GSC-1682	Eskimo Lakes	69.41	-131.99	^{14}C Conv. (plants, seeds)	34500 ± 690	Blake (1987)
GSC-2375-2	Dissection River	73.27	-119.53	^{14}C Conv. (peat)	49100 ± 980	Blake (1987)
GSC-2584	Cape Storm series (VII)	76.40	-87.57	^{14}C Conv. (other organic material)	40300 ± 1550	Blake (1987)
GSC-2584-2	Cape Storm series (VII)	76.40	-87.57	^{14}C Conv. (other organic material)	37600 ± 1200	Blake (1987)
GSC-2584-3	Cape Storm series (VII)	76.40	-87.57	^{14}C Conv. (other organic material)	35800 ± 1080	Blake (1987)
GSC-2780	Banks Island BK Series	71.35	-122.50	^{14}C Conv. (organic-rich sediment)	26900 ± 1560	Blake (1987)
GSC-3819	Banks Island BK Series	71.35	-122.50	^{14}C Conv. (organic-rich sediment)	34100 ± 1060	Blake (1987)
GSC-829	Andersrag Beach	76.42	-87.60	^{14}C Conv. (carbonate)	39700 ± 1300	Blake (1987)
GSC-2786 (inner fraction)	Cape Storm series (VII)	76.40	-87.57	^{14}C Conv. (carbonate)	40500 ± 1660	Blake (1987)
GSC-2786 (outer fraction)	Cape Storm series (VII)	76.40	-87.57	^{14}C Conv. (carbonate)	41500 ± 1460	Blake (1987)
GSC-1055	Cape Norton Shaw	76.53	-78.37	^{14}C Conv. (carbonate)	33900 ± 1360	Blake (1987)
GSC-2367	Carey Oer	76.73	-73.07	^{14}C Conv. (carbonate)	38300 ± 1100	Blake (1987)

Lab code	Site name	Lat	Long	Sample type	Reported age	Reference
GSC-3888	Littleton O	78.36	-72.75	^{14}C Conv. (carbonate)	36700 ± 1990	Blake (1987)
TO-191	Webber Glacier	80.88	-82.25	^{14}C AMS (wood)	46460 ± 520	Blake (1987)
TO-125	Prest Sea Type	50.32	-81.63	^{14}C AMS (carbonate)	40040 ± 400	Andrews (1987)
GSC-2044	Nansen Sound	81.03	-91.63	^{14}C Conv. (carbonate)	28800 ± 1800	Blake (1986)
GSC-4018	Cape George	45.88	-61.92	^{14}C Conv. (carbonate)	35600 ± 990	Blake (1986)
ISGS-772	Nimitz Quarry Section	42.33	-89.00	^{14}C (wood)	47400 ± 1500	Liu et al. (1986)
ISGS-1023	St Francis power plant	42.97	-87.85	^{14}C (wood)	37800 ± 110	Liu et al. (1986)
ISGS-1045	Oak Crest Subdivision	42.33	-88.99	^{14}C (organic-rich sediment)	43100 ± 1100	Liu et al. (1986)
ISGS-1069	Oak Crest Subdivision	42.33	-88.99	^{14}C (organic-rich sediment)	43800 ± 2700	Liu et al. (1986)
ISGS-1073	Oak Crest Subdivision	42.33	-88.99	^{14}C (organic-rich sediment)	37900 ± 1300	Liu et al. (1986)
ISGS-744	Oak Crest Subdivision	42.33	-88.99	^{14}C (organic-rich sediment)	47400 ± 2400	Liu et al. (1986)
ISGS-749	Oak Crest Subdivision	42.33	-88.99	^{14}C (organic-rich sediment)	33220 ± 710	Liu et al. (1986)
ISGS-681	DAA-19	39.49	-88.02	^{14}C (organic-rich sediment)	32620 ± 650	Liu et al. (1986)
ISGS-942	Kokomo	40.55	-86.24	^{14}C (organic-rich sediment)	41600 ± 2200	Liu et al. (1986)
ISGS-726	Bentas Fork #1	39.75	-84.58	^{14}C (organic-rich sediment)	44800 ± 1700	Liu et al. (1986)
GSC-2700	West of Gunnars Island / Bjorne Peninsula	77.48	-85.75	^{14}C Conv. (carbonate)	30100 ± 750	Hodgson (1985); Blake (1986); Ó'Cofaigh et al. (2000)
Gx-9531	Deschaillons	46.55	-72.11	^{14}C Conv. (carbonate)	35100 (+3070, -2420)	Lamothe (1985)
not given	Wadena Till	46.41	-95.14	^{14}C (wood)	36970 ± 950	Meyer (1985)
UQ-406	Pierreville site 96-A	46.07	-72.82	^{14}C (carbonate)	34000 ± 1050	Lamothe (1985)
UQ-698	Pierreville site 96-A	46.07	-72.82	^{14}C (carbonate)	33600 ± 2300	Lamothe (1985)
I-25894	Pierreville site 98-E	46.06	-72.81	^{14}C (carbonate)	37200 ± 2500	Lamothe (1985)
UC-130	Riviere aux vaches 99-C	45.89	-72.50	^{14}C (carbonate)	28000 ± 760	Lamothe (1985)
UC-484	Riviere aux vaches 99-F	45.89	-72.50	^{14}C (carbonate)	26000 ± 2300	Lamothe (1985)
UC-525	Riviere aux vaches 99-F	45.89	-72.50	^{14}C (carbonate)	32500 ± 900	Lamothe (1985)
GSC-2234-2	Cape Collinson	71.24	-122.34	^{14}C Conv. (wood)	53100 ± 1560	Blake (1984)
GSC-1020	Watino	55.72	-117.63	^{14}C Conv. (wood)	43500 ± 620	Jackson and Pawson (1984)
GSC-2409	Minapore	50.91	-114.06	^{14}C Conv. (wood)	49400 ± 1000	Jackson and Pawson (1984)

Lab code	Site name	Lat	Long	Sample type	Reported age	Reference
not given	Waterloo	43.48	-80.54	^{14}C Conv. (wood)	40080 ± 1200	Karrow and Warner (1984)
GSC-3381	Dingwall Series	46.90	-60.45	^{14}C Conv. (wood)	32700 ± 560	Blake (1984)
GSC-3636	Bay St Lawrence	47.01	-60.45	^{14}C Conv. (wood)	44200 ± 820	Blake (1984)
S-206	Carstairs	51.33	-114.17	^{14}C Conv. (peat)	26700 ± 1400	Jackson and Pawson (1984)
S-205	Sharp Hills	51.35	-114.00	^{14}C Conv. (peat)	33500 ± 2000	Jackson and Pawson (1984)
GSC-3206	Big Brook	45.81	-61.22	^{14}C Conv. (organic-rich sediment)	36200 ± 1280	Blake (1984)
GSC-1440	Salmon R	44.06	-66.18	^{14}C Conv. (carbonate)	38600 ± 1300	Blake (1984)
GSC-1440 (inner)	Salmon R	44.06	-66.18	^{14}C Conv. (carbonate)	38600 ± 1300	Blake (1984)
GSC-1440 (outer)	Salmon R	44.06	-66.18	^{14}C Conv. (carbonate)	37500 ± 1300	Blake (1984)
GSC-1408	Grantville	45.64	-61.24	^{14}C Conv. (carbonate)	32100 ± 900	Blake (1984)
GSC-1220	Middle River	46.14	-60.92	^{14}C Conv. (bone, antler, tooth, tusk)	32000 ± 630	Blake (1984)
GSC-1220-2	Middle River	46.14	-60.92	^{14}C Conv. (bone, antler, tooth, tusk)	31300 ± 500	Blake (1984)
U. Thorncliffe	Hi Section	43.71	-79.23	luminescence (TL)	35900 ± 5400	Berger (1984)
GX-102	Twin Cliffs	50.07	-110.63	^{14}C (wood)	29200 (+8100, -4000)	Jackson and Pawson (1984)
I-1878	Irvine	49.92	-110.27	^{14}C (charcoal)	34900 (+2000, -2200)	Jackson and Pawson (1984)
UQ-553	île d'Anticosti site F	49.48	-63.59	^{14}C (carbonate)	36000 ± 3500	Gratton et al. (1984)
UQ-509	île d'Anticosti site H	49.41	-63.57	^{14}C (carbonate)	28100 ± 200	Gratton et al. (1984)
UQ-510	île d'Anticosti site B	49.42	-63.52	^{14}C (carbonate)	29060 ± 1050	Gratton et al. (1984)
UQ-514	île d'Anticosti site B	49.42	-63.52	^{14}C (carbonate)	36000 ± 1200	Gratton et al. (1984)
GSC-2469	Hillsborough	45.91	-64.66	^{14}C Conv. (organic-rich sediment)	37200 ± 1310	Blake (1983)
GSC-2467	Hillsborough	45.91	-64.66	^{14}C Conv. (carbonate)	51500 ± 1270	Blake (1983)
GX-4579	Hooper Island	69.69	-134.92	^{14}C (wood)	35800 (+5400, -3200)	MacKay and Matthews (1983)
UQ-312	Pierreville site 98-E	46.06	-72.81	^{14}C (carbonate)	34000 (+1880, -1470)	Lamothe et al. (1983)
UQ-494	Pierreville site 98-E	46.06	-72.81	^{14}C (carbonate)	38400 (+3000, -2400)	Lamothe et al. (1983)
Beta-3311	Allegan County	42.59	-86.23	^{14}C Conv. (wood)	37150 ± 540	Gephart et al. (1982); Gephart (1983); Monaghan et al. (1986)
Beta-3310	Allegan County	42.59	-86.23	^{14}C Conv. (wood)	38130 ± 740	Gephart et al. (1982); Monaghan et al. (1986)

Lab code	Site name	Lat	Long	Sample type	Reported age	Reference
QL-133	Cowanda hospital interstadial site	42.49	-78.93	^{14}C Conv. (wood)	51600 (+1900, -1500)	Calkin et al. (1982)
QL-134	Cowanda hospital interstadial site	42.49	-78.93	^{14}C Conv. (wood)	47200 ± 800	Calkin et al. (1982)
S-534	Howe Lake	51.61	-103.34	^{14}C (organic-rich sediment)	31710 ± 1420	Christiansen et al. (1982)
S-535	Howe Lake	51.61	-103.34	^{14}C (organic-rich sediment)	32830 ± 1630	Christiansen et al. (1982)
S-536	Howe Lake	51.61	-103.34	^{14}C (organic-rich sediment)	36940 ± 3680	Christiansen et al. (1982)
QC-357	Deschaillons	46.55	-72.11	^{14}C Conv. (carbonate)	37590 (+2300, -1000)	Barrette et al. (1981)
QC-559	Deschaillons	46.55	-72.11	^{14}C Conv. (carbonate)	34900 (+1625, -1350)	Barrette et al. (1981)
W-108	South Haven	42.38	-86.26	^{14}C Conv. (wood)	30000 ± 800	Eschman (1980)
QL-1215	Mill Creek	43.02	-82.58	^{14}C Conv. (wood)	48300 ± 800	Eschman (1980)
GX-3447	North of Avoca	43.08	-82.68	^{14}C Conv. (peat)	36200 (+4400, -2900)	Eschman (1980)
W-3823	GR23	43.04	-85.68	^{14}C (wood)	39500 ± 1000	Rieck and Winters (1980)
QL-1086	Filtaway Lake	70.47	-74.78	^{14}C Conv. (peat)	48700 (+1400, -1000)	Miller (1979)
QL-1087	Filtaway Lake	70.47	-74.78	^{14}C Conv. (peat)	47500 (+1000, -1200)	Miller (1979)
QL-1180	Middle Uivarvluk	68.05	-65.06	^{14}C Conv. (peat)	42400 ± 800	Miller (1979)
QL-1179	Home Bay	68.04	-64.98	^{14}C Conv. (peat)	50700 (+2000, -1600)	Miller (1979)
QU-559	Deschaillons	46.55	-72.11	^{14}C Conv. (carbonate)	34900 (+1625, -1350)	Hillaire-Marcel (1979); Hillaire-Marcel and Page (1980)
QU-279	Deschaillons	46.55	-72.11	^{14}C Conv. (carbonate)	36280 ± 2410	Hillaire-Marcel (1979); Hillaire-Marcel and Page (1980); Barrette et al. (1981)
QU-357	Deschaillons	46.55	-72.11	^{14}C Conv. (carbonate)	37500 (+2300, -1800)	Hillaire-Marcel (1979); Hillaire-Marcel and Page (1980); Barrette et al. (1981)
QL-1181	Quavig/Uivarvluk	66.05	-65.08	^{14}C Conv. (carbonate)	47800 (+1300, -1100)	Miller (1979)
QC-446	Loks Land	62.40	-64.65	^{14}C Conv. (carbonate)	41900 (+7100, -3700)	Miller (1979)

Lab code	Site name	Lat	Long	Sample type	Reported age	Reference
QL-974	Padloping Island	67.55	-63.77	^{14}C Conv. (carbonate)	44400 ± 1000	Miller (1979)
QL-979	Cape Dyer	66.73	-61.45	^{14}C Conv. (carbonate)	37200 ± 800	Miller (1979)
QL-963	Pine River	44.23	-85.88	^{14}C Conv. (wood)	45800 ± 700	Stuiver et al. (1978)
QL-188	Clyde Foreland	70.42	-68.07	^{14}C Conv. (organic-rich sediment)	50400 (+1000, -900)	Miller et al. (1977)
GSC-1656	St. Patrick Bay	81.83	-64.42	^{14}C Conv. (organic-rich sediment)	28100 ± 380	England (1977)
QL-177	Cape Smith	71.11	-70.81	^{14}C Conv. (carbonate)	45200 ± 800	Miller et al. (1977)
QL-184	Clyde Foreland	70.29	-69.17	^{14}C Conv. (carbonate)	40000 ± 300	Miller et al. (1977)
QL-184(2)	Clyde Foreland	70.29	-69.17	^{14}C Conv. (carbonate)	34900 (+2100, -1700)	Miller et al. (1977)
QL-136	Clyde Foreland	70.63	-69.15	^{14}C Conv. (carbonate)	33600 ± 800	Miller et al. (1977)
QL-183	Clyde Foreland	70.72	-69.11	^{14}C Conv. (carbonate)	47700 ± 700	Miller et al. (1977)
QL-186	Clyde Foreland	70.67	-68.83	^{14}C Conv. (carbonate)	40000 ± 1740	Miller et al. (1977)
St.4325	Cape Defrosse	81.25	-65.92	^{14}C Conv. (carbonate)	27950 ± 5400	England (1977)
DIC-517	Near Miriam Lake	59.55	-63.83	^{14}C Conv. (carbonate)	42730 (+6680, -9770)	Ives (1977)
GSC-1442-1	Wascana Creek	50.63	-104.91	^{14}C Conv. (unknown)	37900 ± 1100	Stalker (1976)
GSC-1442-2	Wascana Creek	50.63	-104.91	^{14}C Conv. (unknown)	38700 ± 1100	Stalker (1976)
IGS-256	Schelke Bog	45.28	-89.47	^{14}C Conv. (organic-rich sediment)	40800 ± 2000	Stewart and Mickelson (1976)
GSC-271	Cudia Park	43.72	-79.23	^{14}C Conv. (peat)	38000 ± 1300	Berti (1975)
I-5079	GR-4	42.89	-85.65	^{14}C Conv. (plants, seeds)	28800 ± 1050	Buckley and Willis (1972)
GrN-4468	Elgin	42.05	-88.48	^{14}C Conv. (wood)	41100 ± 1500	Vogel and Waterbolk (1972)
GrN-4408	Elburn	41.87	-88.42	^{14}C Conv. (wood)	32600 ± 520	Vogel and Waterbolk (1972)
I-5078	Grand Rapids	43.02	-85.67	^{14}C Conv. (wood)	33300 ± 1800	Buckley and Willis (1972); Eschman (1980)
GrN-3219	Rocky Fork	40.02	-82.85	^{14}C Conv. (wood)	46600 ± 2200	Vogel and Waterbolk (1972)
GrN-2580	Port Talbot	42.62	-81.38	^{14}C Conv. (wood)	44400 ± 1200	Vogel and Waterbolk (1972)
GrN-4817	Scarborough Bluffs	43.71	-79.24	^{14}C Conv. (wood)	54340 ± 500	Vogel and Waterbolk (1972)
GrN-4397	Port Talbot	42.62	-81.38	^{14}C Conv. (plants, seeds)	33400 ± 500	Vogel and Waterbolk (1972)
GrN-4799	Port Talbot	42.62	-81.38	^{14}C Conv. (plants, seeds)	42700 ± 1200	Vogel and Waterbolk (1972)
GrN-4800	Port Talbot	42.62	-81.38	^{14}C Conv. (plants, seeds)	43400 ± 1300	Vogel and Waterbolk (1972)
GrN-2619	Port Talbot	42.62	-81.38	^{14}C Conv. (peat)	45100 ± 1000	Vogel and Waterbolk (1972)

Lab code	Site name	Lat	Long	Sample type	Reported age	Reference
GrN-4238	St Thomas	42.75	-81.18	^{14}C Conv. (peat)	34000 ± 500	Vogel and Waterbolk (1972)
GrN-4272	St Thomas	42.75	-81.18	^{14}C Conv. (peat)	38000 ± 1500	Vogel and Waterbolk (1972)
GrN-4996	Titusville	41.62	-79.64	^{14}C Conv. (peat)	40500 ± 1000	Vogel and Waterbolk (1972)
GrN-4429	Plum Point	42.60	-81.40	^{14}C Conv. (organic-rich sediment)	45800 ± 1200	Vogel and Waterbolk (1972)
GrN-2570	Port Talbot	42.62	-81.38	^{14}C Conv. (organic-rich sediment)	46700 ± 1400	Vogel and Waterbolk (1972)
GrN-2601	Port Talbot	42.62	-81.38	^{14}C Conv. (organic-rich sediment)	47600 ± 400	Vogel and Waterbolk (1972)
I-1845	Titusville	41.62	-79.64	^{14}C (peat)	39900 (+4900, -2900)	Vogel and Waterbolk (1972)
GSC-1019-2	Freeman Section	54.36	-114.88	^{14}C Conv. (wood)	52200 ± 1760	Lowdon et al. (1971)
GSC-1221	Sunnypoint section	43.72	-79.23	^{14}C Conv. (plants, seeds)	32000 ± 690	Lowdon et al. (1971)
GSC-629-2	Woodbridge	43.76	-79.59	^{14}C Conv. (peat)	40200 ± 480	Lowdon et al. (1971)
GSC-534	Cudia Park	43.72	-79.23	^{14}C Conv. (peat)	48800 ± 1400	Lowdon et al. (1971)
GSC-1181	Woodbridge pit	43.76	-79.59	^{14}C Conv. (organic-rich sediment)	45000 ± 900	Lowdon et al. (1971)
GSC-1082	Hi Section	43.71	-79.23	^{14}C Conv. (organic-rich sediment)	28300 ± 600	Lowdon et al. (1971)
I-1734	South side of Cape Skogn	75.60	-84.50	^{14}C Conv. (carbonate)	31200 ± 1800	Barr (1971)
I-1733	South side of Wolf Hill	75.60	-84.50	^{14}C Conv. (carbonate)	30100 ± 1500	Barr (1971)
GSC-1153	Pond Inlet	72.68	-78.00	^{14}C Conv. (carbonate)	33100 ± 900	Lowdon et al. (1971)
GSC-1041	Kenaston	51.50	-106.31	^{14}C Conv. (wood)	38000 ± 560	Lowdon and Blake (1970); Morlan et al. (2001)
GSC-993-2	Plum Point	42.60	-81.40	^{14}C Conv. (peat)	46400 ± 940	Lowdon and Blake (1970)
I-2581	Sam Fiord	70.98	-70.62	^{14}C Conv. (carbonate)	36250 (+3600, -2000)	Ives and Buckley (1969)
GSC-796	Clyde Foreland	70.63	-68.75	^{14}C Conv. (carbonate)	40000 ± 1740	Ives and Buckley (1969); Lowdon et al. (1971); Miller et al. (1977)
GSC-711	Zelena	51.40	-101.23	^{14}C Conv. (organic-rich sediment)	28220 ± 380	Lowdon and Blake (1968)
GSC-653	Zelena	51.40	-101.23	^{14}C Conv. (charcoal)	37700 ± 1500	Lowdon and Blake (1968)
GSC-667	Winter Harbour Moraine	74.78	-110.87	^{14}C Conv. (carbonate)	27790 ± 480	Lowdon and Blake (1968)
GSC-787	Winter Harbour Moraine	74.64	-110.85	^{14}C Conv. (carbonate)	42400 ± 1900	Lowdon and Blake (1968)
I-4878	Watino	55.72	-117.63	^{14}C (organic-rich sediment)	27400 ± 850	Reimchen (1968)
GSC-111	Location E	79.93	-86.38	^{14}C Conv. (carbonate)	36300 ± 2000	Dyck and Fyles (1964)

Lab code	Site name	Lat	Long	Sample type	Reported age	Reference
GSC-134	Location Y	77.29	-81.81	^{14}C Conv. (carbonate)	29800 ± 220	Dyck and Fyles (1964)
GSC-51	Location F	79.82	-84.61	^{14}C Conv. (carbonate)	28700 ± 600	Dyck and Fyles (1962)
W-747	Hammond	44.93	-92.50	^{14}C Conv. (wood)	29000 ± 1000	Rubin and Alexander (1960)
W-642	Princeton	41.40	-89.47	^{14}C Conv. (wood)	26200 ± 800	Rubin and Alexander (1960)
W-871	Wedron quarry	41.43	-88.78	^{14}C Conv. (wood)	26800 ± 700	Rubin and Alexander (1960)
W-638	Lake Geneva	42.55	-88.50	^{14}C Conv. (wood)	31800 ± 1200	Rubin and Alexander (1960)
L-369B wood lignin	24M	50.31	-82.70	^{14}C Conv. (wood)	40700 ± 4100	Olson and Broecker (1957, 1959)
L-369B peat cellulose	24M	50.31	-82.70	^{14}C Conv. (peat)	39700 ± 2900	Olson and Broecker (1957, 1959)
L-369B wood cellulose	24M	50.31	-82.70	^{14}C Conv. (wood)	40500 ± 3200	Olson and Broecker (1957, 1959)
L-369B peat lignin	24M	50.31	-82.70	^{14}C Conv. (peat)	40600 ± 3000	Olson and Broecker (1957, 1959)